



National Library
of Canada

Bibliothèque nationale
du Canada

Canadian Theses Service Service des thèses canadiennes

Ottawa, Canada
K1A 0N4

NOTICE

The quality of this microform is heavily dependent upon the quality of the original thesis submitted for microfilming. Every effort has been made to ensure the highest quality of reproduction possible.

If pages are missing, contact the university which granted the degree.

Some pages may have indistinct print especially if the original pages were typed with a poor typewriter ribbon or if the university sent us an inferior photocopy.

Reproduction in full or in part of this microform is governed by the Canadian Copyright Act, R.S.C. 1970, c. C-30, and subsequent amendments.

AVIS

La qualité de cette microforme dépend grandement de la qualité de la thèse soumise au microfilmage. Nous avons tout fait pour assurer une qualité supérieure de reproduction.

S'il manque des pages, veuillez communiquer avec l'université qui a conféré le grade.

La qualité d'impression de certaines pages peut laisser à désirer, surtout si les pages originales ont été dactylographiées à l'aide d'un ruban usé ou si l'université nous a fait parvenir une photocopie de qualité inférieure.

La reproduction, même partielle, de cette microforme est soumise à la Loi canadienne sur le droit d'auteur, SRC 1970, c. C-30, et ses amendements subséquents.



National Library
of Canada

Bibliothèque nationale
du Canada

Canadian Theses Service Service des thèses canadiennes

Ottawa, Canada
K1A 0N4

The author has granted an irrevocable non-exclusive licence allowing the National Library of Canada to reproduce, loan, distribute or sell copies of his/her thesis by any means and in any form or format, making this thesis available to interested persons.

The author retains ownership of the copyright in his/her thesis. Neither the thesis nor substantial extracts from it may be printed or otherwise reproduced without his/her permission.

L'auteur a accordé une licence irrévocable et non exclusive permettant à la Bibliothèque nationale du Canada de reproduire, prêter, distribuer ou vendre des copies de sa thèse de quelque manière et sous quelque forme que ce soit pour mettre des exemplaires de cette thèse à la disposition des personnes intéressées.

L'auteur conserve la propriété du droit d'auteur qui protège sa thèse. Ni la thèse ni des extraits substantiels de celle-ci ne doivent être imprimés ou autrement reproduits sans son autorisation.

ISBN 0-315-56414-8

Coal Devolatilization in an Entrained Flow Reactor

By

Laura Anne Gibbs

Ottawa, Ontario. December 1988

A THESIS

PRESENTED TO THE UNIVERSITY OF OTTAWA

IN PARTIAL FULFILLMENT OF THE

REQUIREMENTS FOR THE DEGREE OF

MASTER OF APPLIED SCIENCE

IN

CHEMICAL ENGINEERING

© Laura Anne Gibbs, Ottawa, Canada, 1989.



UNIVERSITÉ D'OTTAWA
UNIVERSITY OF OTTAWA

Abstract

Thermal decomposition, or devolatilization, occurs when coal is heated to elevated temperatures. The moisture present evolves early and as the temperature increases, gases and heavy tarry substances are emitted. The object of this work is to derive reaction rate constants for coal devolatilization from data obtained in a laminar flow test reactor. These constants will ultimately be used in a full model of coal combustion in a furnace.

The devolatilization models presented in the literature were critically evaluated and a competitive two reaction model was selected due to its flexibility and ability to predict the temperature variation of the ultimate yield. A finite difference model of the flow, heat transfer, and particle motion used to predict conditions is expanded to include the effects of particle reaction and mass transfer. The endothermic heat of pyrolysis is also added to the particle energy balance. A procedure is developed for fitting the reaction constants of the model to the experimental data. As a test, this routine was used to fit the reaction constants of the two reaction model to the experimental data of Kobayashi [1]. Tests for the suitability and precision of these parameter estimates indicated that the model adequately described the devolatilization data. The report concludes with recommendations for data acquisition that were determined from experience with the fitting procedure.

Acknowledgement

I would like to express my gratitude to Dr. W.L.H. Hallett for his insight, guidance and assistance throughout the course of this work and to Mr. P. Hughes of CANMET Research Labs for all his help. A hearty thanks to Dr. D. MacLean and Mr. M. Dal Cin for their patience and guidance in helping with the mathematical modelling. I would also like to thank my parents for their support and understanding, which made the rough spots a lot smoother. The financial support of Energy, Mines and Resources is greatly appreciated.

Nomenclature

A_s	particle surface area, m^2
A_o, A_{cs}	ash fraction in original coal, collected sample
B	transfer number, $\exp(\tau_o G/\rho D) - 1$
B, S	constants in Sutherland equation
Bi	Biot number, hr/k
B_m	maximum volatile release rate
C	coal kg
C	correction factor to asymptotic weight loss
c_d, c_{do}	drag coefficient of devolatilizing and non-devolatilizing coal particle respectively
C_i	component i of coal in two component devolatilization model
c_p	heat capacity of the gas, $kJ/(kgK)$
d_p, d	original and swelled particle diameter, m
D	diffusion coefficient, m^2/s
E_i	activation energy of reaction i , $kcal/mol$
E_1	exponential integral
e_u	residual, $y_u - \hat{y}_u$
F	F distribution

$f(E)$	distribution function of activation energies specified in parallel reaction model
$f(x)$	residual function as defined for ZXSSQ
G	mass flux of volatiles, kg/m^2s
$g(x)$	function defining the non-linear model in ZXSSQ
h	convective heat transfer coefficient of coal particle
h_g	enthalpy of escaping volatiles, kJ/kg
h_1	'latent' heat of pyrolysis with process treated as an evaporation process, kJ/kg
ΔH_r	heat of pyrolysis, kJ/kg
k	conductive heat transfer coefficient of particle, $W/(mK)$
k_{oi}	pre-exponential factor, 1/sec
K_u, K_v	adjustable parameters in velocity and temperature expressions in Kobayashi [1] flowfield model
$MAFR$	moisture and ash free fraction of coal particle
p	number of parameters to be fitted in model
Q	$V/(V_o - V_r)$
Q_p	heat flux to particle, W/m^2
q_{rad}	radiative heat transfer, W/m^2
q_{conv}	convective heat transfer, W/m^2
Pr	Prandtl number
r	particle radius, m
R	gas constant, $1.987E-3 kcal/(molK)$
R_i	char formed in reaction i
Re	Reynolds number
$S(\hat{\beta}), S(\beta)$	sum of squares residual at the least squares parameter estimates, and at the parameter estimates defining the 95% confidence region
S_{sw}	ratio of swelled particle diameter to original diameter

t	time, sec
T	temperature, K
T^-, T_p	average particle temperature, K
u	internal energy of coal, kJ/kg
u_p	velocity of particle, m/sec
V, V_{af}	volatile matter or weight loss released based on original ash free coal
V^-	ultimate yield, daf basis
V_i	volatiles formed in reaction i , daf basis
V_o	proximate volatile matter of original coal, daf basis
V_p	particle volume, m^3
V_r	proximate volatile matter of char, daf basis
v_i, v_i'	terminal velocity of particle and of increased swelled diameter particle, m/sec
x	abscissa in integration method
x_n	H/C ratio of volatile n
X_v	fraction of volatiles not yet released
$X(1), X(2)$	initial estimates of parameters in fitting routine
y	ordinate in integration method
y_u	observed or measured response
\hat{y}_u	value of fitted response predicted by model
\bar{y}_u	mean of measured response values at operating conditions u
Y_o, Y_∞	mass fraction of volatiles at particle surface and in ambient gas
Z	difference between the final equilibrium temperature and the initial temperature, K

α_i	yield coefficient of reaction i
β	$12k/(\rho c_p d^2)$, 1/sec
γ	proportionality constant between V_2 and R_2 in two component model
ϵ	emissivity of coal
θ	$\exp(-E/RT^*)$
ϑ	shape factor that correlates K_u and K_v
μ, μ_p	viscosity of the ambient gas and at particle surface, kg/(m s)
ρ	density of gas, kg/m ³
σ	Stefan Boltzmann constant, 5.669E-8 W/(m ² K ⁴)
σ	standard deviation of distribution function
σ^2	estimate of pure error variance
τ	$\rho_p d^2/(18\mu)$

Contents

Abstract	i
Acknowledgement	ii
Nomenclature	iii
1 Introduction	1
2 Literature Survey	4
2.1 Background	4
2.2 Experimental techniques	8
2.2.1 Entrained Flow Reactors	9
2.2.2 Heated Grid	15
2.2.3 Crucible tests	17
2.2.4 Conclusions	19

2.3	Accuracy of the Ash Tracer Technique	21
2.3.1	Crucible Tests	22
2.3.2	Inert Atmosphere Furnace Tests	23
2.3.3	Other Atmosphere Furnace Tests	24
2.3.4	Conclusions	26
3	Model Evaluation	28
3.1	Evaporation model	29
3.1.1	Lockwood et al.	29
3.2	Single first order reaction model	30
3.2.1	Badzioch and Hawksley	30
3.2.2	Scaroni et al.	31
3.2.3	Truelove	32
3.3	Competitive Parallel Reaction Model	32
3.3.1	Kobayashi	32
3.3.2	Ubhayakar et al.	35
3.3.3	Jamaluddin et al.	36
3.3.4	Suzuki et al.	37
3.3.5	Baxter et al.	38

3.4	Two component model	38
3.4.1	Nsakala et al.	39
3.5	Multiple Parallel Reaction Mechanism	40
3.5.1	Anthony and Howard	40
3.5.2	Hashimoto et al.	43
3.5.3	Solomon et al.	43
3.5.4	Suuberg et al.	44
3.5.5	Rizvi	46
3.5.6	Sprouse et al.	46
3.6	Conclusions	47
4	Reactor Model Program	50
4.1	Method of Integration	51
4.2	Effects of mass transfer	55
4.3	Physical properties of coal	59
4.3.1	Specific heat	59
4.4	Heat of Pyrolysis	62
4.4.1	Density and Diameter Behavior	67
5	Fitting Routine	71

5.1	Isothermal fitting procedure	72
5.2	Non-isothermal fitting procedure	74
5.3	Significance tests	78
5.4	Precision of the parameter estimates	79
6	Application of Fitting Procedure	81
6.1	Comparison of Particle Heating Calculations	81
6.2	Isothermal Fitting	86
6.2.1	Determination of Ultimate Yield and Reaction Rate	86
6.2.2	Fitting of the Arrhenius Rate Constants	94
6.3	Non-isothermal Fitting	98
6.3.1	Determination of Low Temperature Parameter Estimates	98
6.3.2	Determination of High Temperature Parameter Estimates	99
6.3.3	Iterative fitting procedure	103
6.4	Precision of the parameter estimates	108
6.5	Significance Tests	118
7	Conclusions and Recommendations	122
7.1	Conclusions	122
7.2	Recommendations	124

List of References	124
A Particle Energy Balance	131
B Effect of Particle Swelling on Particle Heating	133
C Particle Heating Program Listing	136
D Fitting Program Listings	145
E Experimental Data	156

List of Figures

1	Schematic Drawing of Entrained Flow Reactor at Energy, Mines and Resources	2
2	Proposed Model for Molecular Structure of Coal [2]	5
3	Comparison of the composition of devolatilization products [3] of bituminous (a) and lignite (b) coals	7
4	Devolatilization Data Collected by Nsakala [4]	11
5	Weight loss versus residence time as predicted by Anthony and Howard [5,6] model for various temperatures	42
6	Pyrolysis product composition from lignite coal heated to different peak temperatures	45
7	Sample Grid for Laminar Flow Furnace [7]	52
8	Weight Loss Versus Time for Particle Undergoing Exponential Heating . . .	54
9	Effects of Mass Transfer on a Devolatilizing Coal Particle	58
10	Predictions of the Specific Heat of Coal and Coke [8]	60
11	Effect of Heat of Reaction on Internal Temperature Profile [9]	64

12	Effect of heat of pyrolysis on particle temperature	65
13	Weight Loss Versus Time for particle in 1510K furnace	66
14	Typical Temperature-time History of a Coal Particle in a Laminar Flow Furnace	75
15	Weight loss versus residence time for lignite coal	82
16	Weight loss versus residence time for bituminous coal	83
17	Comparison of residence time predictions from present particle heating pro- gram to predictions by Kobayashi[1,10]	84
18	Weight loss versus residence time for 1260K data	88
19	Comparison of the heating history of the lignite and bituminous coals at 1940K	90
20	Weight loss versus residence time for 1740K and 1940K bituminous data . .	91
21	Isothermal fitting of parameter estimates to 1510K bituminous data	93
22	Model Predictions of Two Competitive Reaction Devolatilization Model for Lignite Coal	104
23	Model Predictions of Two Competitive Reaction Devolatilization Model for Bituminous Coal	105
24	Confidence region for parameter estimates of isothermal single reaction model for 1260K lignite data. The point represents the converged parameter estimates.	109
25	Confidence region for parameter estimates of isothermal single reaction model for 1260K bituminous data	110
26	Confidence region for parameter estimates of isothermal single reaction model for 1510K lignite data	111

27	Confidence region for parameter estimates of isothermal single reaction model for 1510K bituminous data	112
28	Confidence Region for Estimates of the Kinetic Rate Constants for the Low Temperature Lignite Data	114
29	Confidence Region for Estimates of the Kinetic Rate Constants for the Low Temperature Bituminous Data	115
30	Confidence Region for Estimates of the Kinetic Rate Constants for Centered Low Temperature Lignite Data	116
31	Confidence Region for Estimates of the Kinetic Rate Constants for Centered Low Temperature Bituminous Data	117
32	Residual Plot for Lignite Data	119
33	Residual Plot for Bituminous Data	120

List of Tables

1	Melting and boiling points of Sodium and Magnesium	27
2	Parameter estimates determined by Kobayashi	49
3	Kobayashi Furnace Dimensions	70
4	Furnace operating conditions	87
5	Ultimate yield and reaction rate predictions	87
6	Low temperature reaction rate constant estimates for isothermal pyrolysis .	96
7	High temperature reaction rate constant estimates for isothermal pyrolysis .	96
8	Heating history and weight loss data of 1260K and 1740K bituminous coal .	96
9	Parameter estimates for non-isothermal single first order reaction model - bituminous coal	100
10	Parameter estimates for non-isothermal single first order reaction model - lignite coal	100
11	Parameter estimates for coal pyrolysis listed in literature	102

12	High temperature parameter estimates for non-isothermal parallel reaction model -bituminous coal	102
13	High temperature parameter estimates for non-isothermal parallel reaction model -lignite coal	102
14	Least squares parameter estimates for lignite and bituminous coals	106
15	Reaction rates for lignite and bituminous coals at 1260K	106
16	Iterative fitting of low temperature parameters to full two reaction model .	106
17	R Test for non-isothermal parallel reaction model	121
18	Low Temperature Experimental Data [1] for Lignite Coal	157
19	High Temperature Experimental Data [1] for Lignite Coal	158
20	High Temperature Experimental Data [1] for Lignite Coal (cont.)	159
21	Low Temperature Experimental Data [1] for Bituminous Coal	160
22	High Temperature Experimental Data [1] for Bituminous Coal	161

Chapter 1

Introduction

Coal is a complex matrix of organic molecules whose chemical composition can change from coal to coal. In order to simplify the complex mechanism of coal combustion, researchers have generally broken the process into three stages: first, devolatilization, also called pyrolysis or thermal decomposition; second, the combustion of the gases released; and third, the combustion of the char particle. In the combustion process, the heating value of the volatile products accounts for up to 50% [11] of the total heating value of the original coal. Since the volatile combustion is approximately 10-15% of the total combustion time, the duration of coal combustion can be estimated from the char combustion process alone. However, this does not diminish the importance of the devolatilization process, as the volatile yield affects the amount of char produced. It is the purpose of this study to devise a means of deriving kinetic rate constants for devolatilization which can then be incorporated into a full combustion model [12].

Energy, Mines and Resources Canada has developed an entrained flow reactor that will be used to examine the combustion of different types of pulverized coal. The first stage of this research, the devolatilization studies, are to be performed in an inert atmosphere to prevent combustion, and therefore simulate the heating undergone by a particle approaching

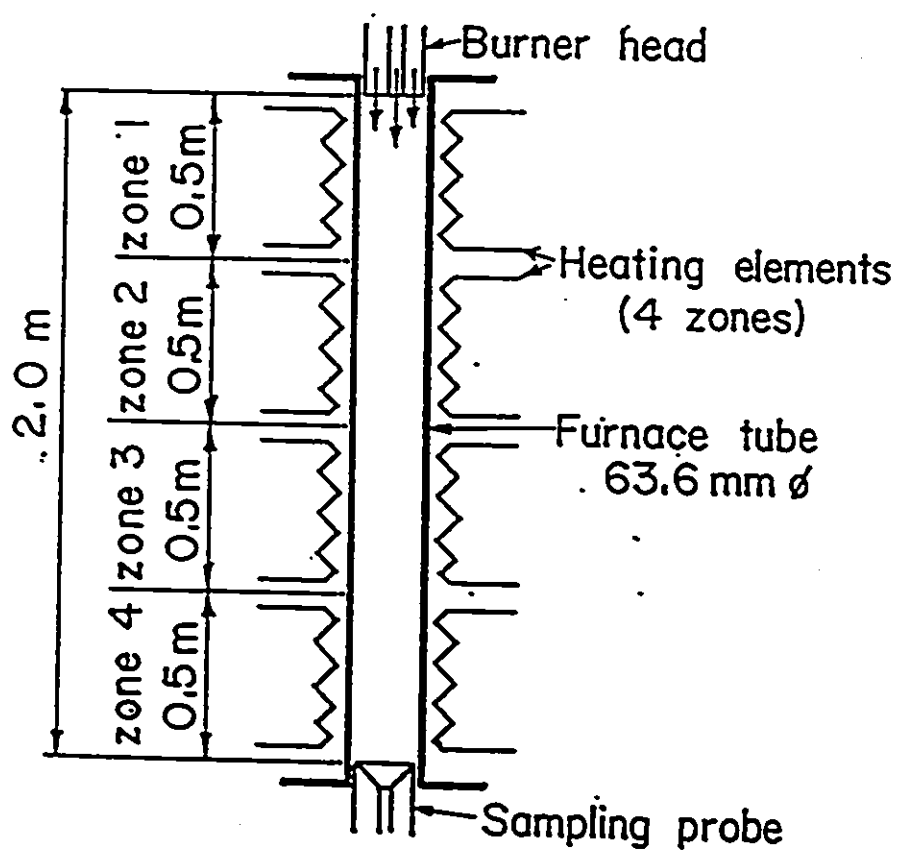


Figure 1: Schematic Drawing of Entrained Flow Reactor at Energy, Mines and Resources

a flame front in a furnace. The entrained flow reactor, figure 1, consists of a long, electrically heated, vertical mullite refractory tube. A dilute coal stream is carried by a water cooled primary gas stream and injected into the center of a preheated laminar secondary gas stream. The particles then flow down the centerline of the laminar flow furnace and are collected by a water cooled sample probe. The char particles are collected isokinetically by the probe and are quenched to prevent further devolatilization. The particle residence time is varied by raising and lowering the sample probe.

In order to interpret the results of the pyrolysis experiments, it is essential to know the particle heating history and residence time. In a previous work [7], a finite difference scheme was developed to predict the gas velocity and temperature within the furnace under different operating conditions, as access to the furnace for local measurements is nearly impossible. The furnace gas velocity and temperature fields were then used to calculate the particle heating rates. The original reactor model [7] assumed that the particles do not react chemically. The present work is concerned with selecting a suitable model for the chemical reactions involved in devolatilization from those available in the literature and implementing it in the existing reactor model. The incorporation of the devolatilization model into the existing computer program required modifications to the convective heat transfer coefficient and drag coefficient as well as the addition of the heat of devolatilization to the energy balance. The second part of this study involved the development of a procedure for fitting the reaction constants for the model to the experimental data. Since experimental data from the EMR reactor is not yet available, as a test this routine was used to fit the reaction constants of the selected model to experimental data of Kobayashi [1] and the suitability and precision of these constants were tested. The results of this test are used to make recommendations for the gathering and treatment of data in experiments.

Chapter 2

Literature Survey

Coal pyrolysis or devolatilization is an important field of study for it enables one to better understand the process of coal combustion. At very high combustion temperatures, up to 70% or more of the reactive coal mass is released as volatiles [2]. Although devolatilization occupies only about 10-15% of the combustion lifetime, the volatiles are important to flame stabilization, and a prediction of the amount of the relatively slower burning char produced is essential. It is the purpose of this chapter to provide some background material about coal and the devolatilization process. A literature review was performed to determine the operational parameters that influence the devolatilization behavior of the coal. This data will be used to critically examine the devolatilization models available in literature.

2.1 Background

Coal is a complex organic matrix, figure 2, whose properties change from coal to coal. Recent devolatilization work [1,5,10,13] has emphasized finely pulverized coal particles at high temperatures. As the raw coal is heated, the moisture present will evolve early as the temperature rises. As the temperature continues to increase, gases and heavy tars are

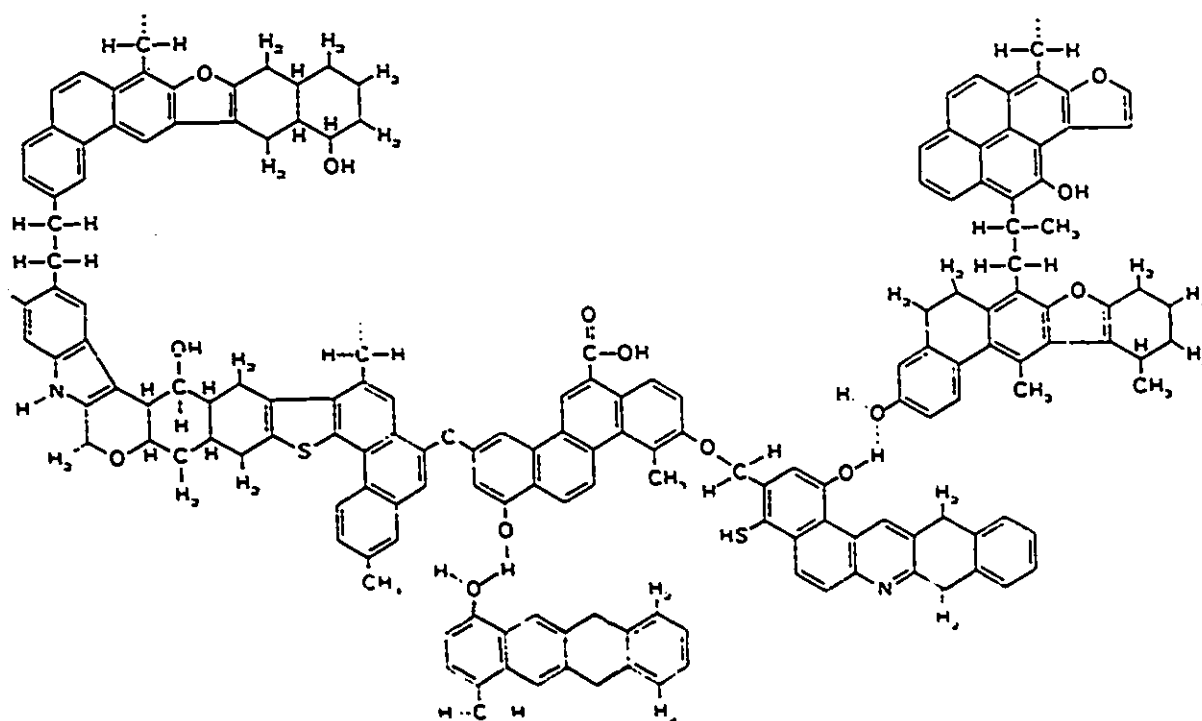


Figure 2: Proposed Model for Molecular Structure of Coal [2]

released. During rapid devolatilization, larger fractions of lower molecular weight species, in addition to tars, are evolved. It has been suggested that these species derive from the rupture of the $-H_2$, $-CH$, $-CH_2$, $-CH_3$, and $-OH$ bonds which appear on the periphery of the coal molecule as well as from a more complete disruption of the weaker cross-link bonds between layers. The proportions of the various products change with temperature as well as with the extent to which the coal devolatilizes, which can vary from a few percent to as much as 70 %. Significantly different pyrolysis behavior between coal types can be seen in figure 3 [3]: much more liquid and hydrocarbons are released by the bituminous coal and more gaseous products are released from the lignite. The volatile matter that escapes from the coal particle can undergo various secondary cracking reactions on the char surface with the possible formation of solid products (soot), which can substantially reduce the overall volatile yield. As the extent and rate of devolatilization increases with increasing temperature, it has been proposed [1] that the variation of the heating rate is a means for varying the temperature range over which the devolatilization takes place.

The analysis of coal is carried out using two ASTM (American Society for Testing and Materials) tests:

- proximate analysis [14] - involves the determination of surface moisture, inherent moisture, volatile matter, fixed carbon and ash. The moisture content is determined by heating the coal sample in an open crucible in an oven preheated to 377-383K for one hour. The moisture content is the difference in weight before and after heating. The volatile matter content is determined by heating the sample in a covered crucible in an oven preheated to $1223 \pm 20K$ for seven minutes. The loss of weight minus moisture equals the volatile matter. The dried coal from the moisture determination is placed in porcelain capsules in a gradually heating furnace. The coal is heated to redness and the process is considered finished once the sample maintains constant weight at a temperature between 973-1023K. The sample is then cooled and weighed to determine the amount of ash. The fixed carbon content in the coal is calculated

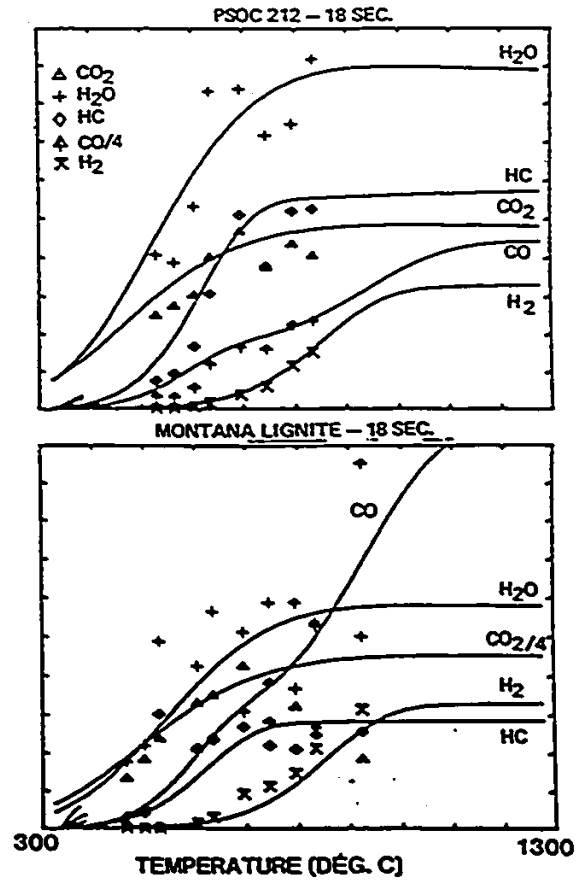


Figure 3: Comparison of the composition of devolatilization products [3] of bituminous (a) and lignite (b) coals

as:

$$\text{Fixed carbon, percent} = 100 - (\text{moisture} + \text{ash} + \text{volatile matter})$$

- ultimate analysis [14] - chemical means of determining the composition of the coal by separating the principal elemental constituents: carbon, hydrogen, nitrogen, sulfur, and oxygen. The method of determining the composition of each of the principal elemental constituents involves rather long procedures which cannot be easily summarized but can be found in reference [14].

These tests are used to characterize the coals for industrial use. However, it has been found that volatile yields significantly larger than the proximate volatile matter have been obtained when the coal is heated rapidly to elevated temperatures [5,6,10,13,15,16]. This is a particularly important finding, since the amount of char to be consumed, the rate controlling step in the combustion of coal particles, is determined by the devolatilization step. Therefore the prediction of the rate of volatile yield under various conditions is indispensable for the proper design of combustion chambers. The requirement for devolatilization studies is an unambiguous reaction history, i.e. rapid heating, an isothermal zone, controlled variation of residence time and temperature and rapid quenching for precise residence times. This section will review some of the experimental techniques and data in the literature so as to determine the operational parameters that were found to influence the devolatilization behavior of the coal.

2.2 Experimental techniques

Pyrolysis has been studied using three different experimental techniques:

- entrained flow reactors
- heated screens

- crucible tests

2.2.1 Entrained Flow Reactors

An entrained flow reactor, figure 1, consists of a vertical tube furnace which is electrically heated and designed for the injection of a dilute coal stream into the center of a preheated gas stream. The flow straightener ensures that the coal passes down the center of the furnace so that the thermal history of each particle is the same. The flow is usually laminar to prevent backmixing and dispersion of the coal. A probe at the bottom of the furnace collects the reacted coal stream and quenches it rapidly. Variation of the reaction time is achieved by raising and lowering the collector probe.

Badzioch and Hawksley [15] used an entrained flow furnace to determine the kinetics of devolatilizing bituminous and semianthracite coal particles at temperatures up to 1273K. The weight loss curves begin at a transit time of about twenty msec. This time delay was attributed to the heating up of the particles, and was subtracted from the transit time to obtain the duration of isothermal decomposition. The weight loss was determined using ash as a tracer; this led to a wide scatter in the results since the majority of the coals had a low ash content. In common with many of the earlier works on coal devolatilization, the model used to calculate the particle residence time and temperature history was crude: the temperature of the particles was assumed to be the same as that of the gas stream, and the velocity profile assumed to be parabolic (fully developed laminar). Flaxman and Hallett [17] have shown that inaccurate models of reactor flow and particle heating can lead to large errors in particle residence times and temperature histories, so that the data presented in this and many other papers must be viewed with mistrust. As the heating history of the particles was simply approximated and the weight loss was not accurately measured, the resulting data are not sufficiently accurate to determine rate constants; however, the trends in the data can be used to learn more about the process of devolatilization. The weight loss of the particles increased with the final temperature attained and the residence time. The

experiments were conducted with particle sizes ranging from 20-60 μm , and no significant effect of particle size on the pyrolysis behavior was found.

Nsakala [4] performed devolatilization experiments to determine the kinetics of pyrolysis at 1081K. The residence time of the particles was determined by the crude method of measuring from the point of entry into the furnace and assuming a uniform velocity at constant temperature for the bulk flow. The weight loss was found to start at a 'false origin' as was the case with Badzioch and Hawksley [15] and this heating period was subtracted out. As there was no temperature variation, the temperature dependence of the weight loss could not be determined. The weight loss curves with a maximum of 40% were below the ASTM volatile matter (47.5%), which was probably due to the experimental temperature being below the temperature at which the ASTM test is conducted. The break in the weight loss data in figure 4 was interpreted as evidence for a two component devolatilization model in which the devolatilization of the first component was particle size dependent while the second component devolatilization was particle size independent. However, this is merely a result of Nsakala's having passed straight lines through the data: if a smooth curve is used instead, the data can be seen to be simply approaching the final weight loss asymptotically as one would expect. The weight loss curves for the particles under 100 μm in figure 4 exhibit similar weight loss behavior, while the curve for the particles over 100 μm is significantly lower, suggesting that the weight loss is a function of particle size for particles over 100 μm .

Tsai and Scaroni [18] investigated the pyrolysis of particles in an entrained flow reactor at 1200K. The particle sizes varied from 74-149 μm to 37-53 μm . The temperatures and residence times of the coal particles were estimated from a mathematical model which incorporated the gas velocities and temperature predictions. The position at which pyrolysis begins in the reactor was found to shift to longer residence times when N_2 replaced He as the primary gas stream. Tsai et al. concluded that as N_2 has a lower thermal diffusivity than He , the devolatilization of a coal particle is affected by the heating rate. An increased heating rate, using He as the primary gas rather than N_2 , enhanced the weight

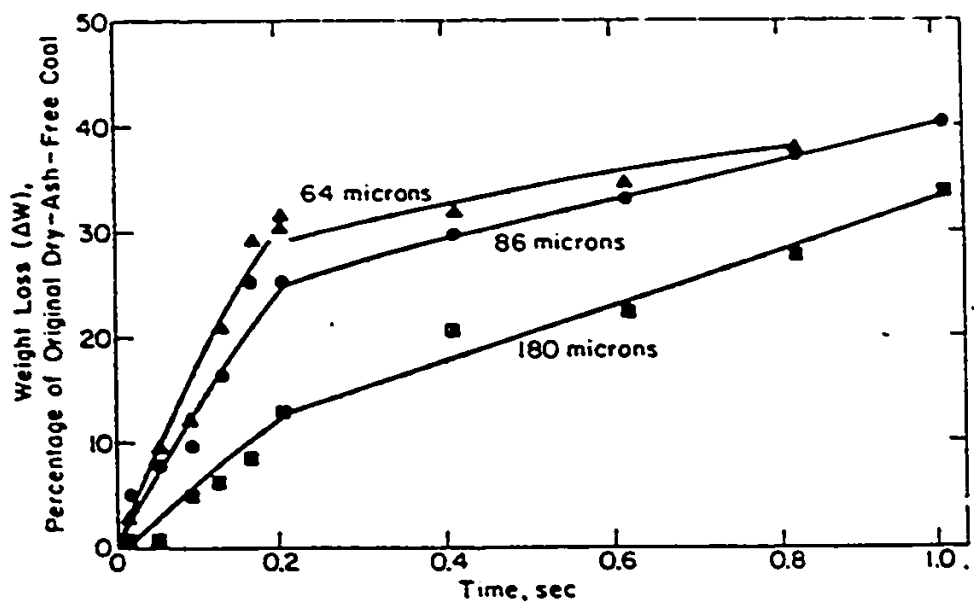


Figure 4: Devolatilization Data Collected by Nsakala [4]

loss; however, as the asymptotic weight loss was not approached in either primary gas experiment, the effect of the heating rate on the ultimate yield could not be examined. The comparison of the asymptotic weight loss of different coals shows that the coals with the higher ASTM volatile matter had higher asymptotic weight losses, which suggests that the chemical composition has an effect on the pyrolysis behavior. An effect of particle size on pyrolysis was noted, which was traced to the fact that the larger particles had higher ASTM volatile matter fractions. This change in volatile yield with particle size indicates segregation of the ash particles in the sample preparation, which probably could be avoided by finer screening of the coal particles. The particle size dependence of the weight loss is contrary to the conclusions of Scaroni, Walker, and Essenhigh [19], who stated that the weight loss was independent of particle size although the particle sizes in these experiments ranged from 41 to 201 μm . In the latter studies no mathematical model of the furnace flow and temperature fields was used; rather the particle velocities were estimated by summing the average gas velocity and particle free-fall velocities. Some of the char in Scaroni, Walker and Essenhigh's experiments bypassed the collector probe, while some adhered to the inner probe surfaces, resulting in collection efficiencies of only 70-80 %. If the flow inside the furnace were laminar, the particles would pass down the furnace in a coherent thin stream directly into the collector. Therefore, the char particles that bypassed the probe could be interpreted as indicative of turbulent flow existing in the furnace, calling the residence time and temperatures even more seriously into question.

Kobayashi et al. [1,10] studied coal devolatilization of lignite and bituminous coals in an entrained flow reactor at temperatures ranging from 1000K to 2100K. The temperature and velocity fields were predicted by numerically solving the fundamental governing equations with several simplifying assumptions which are discussed in a later section. Kobayashi found that the volatile yields at high temperatures were considerably higher than the proximate volatile matter content. The volatile yield of both coals increased significantly with temperature. As the particle size was not varied, the dependence of the weight loss on this factor could not be tested.

Jamaluddin et al. [13] studied the devolatilization of bituminous coals at medium to high heating rates at temperatures ranging from 1073 to 1673K. The coal samples were pulverized to a size range of 53-63 μm . The experiments with high heating rates, $1-5 \times 10^4$ K/sec, were conducted using an entrained flow reactor and the medium heating rate, 250-1000 K/sec, tests with crucibles. The flow fields and particle heating in the laminar flow furnace were modeled by solving the equations of mass, momentum and energy by standard numerical techniques. The heating history of the crucible tests was measured using an empty crucible. As the coal sample was less than 2.5% by weight of the crucible it was assumed that the coal would heat up at the same rate as the empty crucible. A continuous flow of argon was used in the crucible experiments to maintain an inert atmosphere and prevent cracking of the released volatiles; the effectiveness of this is unknown and would be dependent upon the experimental setup. The error bars on the crucible test data indicate that there is quite a spread in the results, in some cases as high as twenty percent, and therefore these results are questionable. The weight loss from both coals in the crucible tests increased with increasing furnace temperatures but did not significantly exceed the proximate volatile matter, which was found with a furnace temperature of 1223K, even at the highest temperature of 1673K. At a furnace temperature of 1673K, the weight loss from the high-volatile coal, with an ASTM volatile matter of 35.2%, was 62% under rapid heating conditions and only 42% under medium heating conditions. The crucible tests are expected to have lower weight loss because of the lower heating rate and the opportunity for cracking reactions. The lower heating rate, as discussed on page 6, results in a greater portion of the devolatilization reaction occurring at a lower temperature where the extent and rate of reaction is lower. There is ample opportunity for cracking reactions in the crucible tests, as the coal particles are closely packed in the crucible and the volatiles being released can easily use the surface of the char particles as sites for secondary reactions. Although these tests are conducted at a much shorter residence time than the ASTM test, attributing the comparatively low yield of the crucible experiments at 1673K solely to the lower heating rate and not to cracking reactions seems questionable. However, Jamaluddin found that the devolatilization of coal particles was increased by both increasing temperature and increasing heating rate.

Maloney and Jenkins [20] performed devolatilization experiments in a laminar flow reactor using two bituminous coals with mean particle diameters of $62 \mu\text{m}$. The furnace temperature was varied from 1073-1273K. All experiments were conducted with N_2 as the secondary gas while some experiments utilized He as the primary gas and were repeated utilizing N_2 as the primary gas. A numerical analysis was performed to estimate the velocity and temperature history of the coal particles. The particle temperature calculations suggested that when $\sim 60 \mu\text{m}$ particles were heated under their experimental conditions, the coal particle temperatures closely tracked that of the surrounding gas. The experimentally determined gas temperature profiles were therefore equated to the coal particle temperatures, although it was admitted that this method overestimated the particle temperatures slightly. These tests were done utilizing He as the primary gas, for which because of the high thermal conductivity of He this method of estimation may be more accurate than in the experiments conducted using N_2 as the primary gas. The weight loss generated in experiments using the two different primary gases illustrated that the increased heating rate associated with the He gas resulted in greater weight losses at smaller residence times. Although the N_2 gas experiment did not have sufficient residence time to clearly approach the asymptotic weight loss, it appears that the carrier gas, and therefore the heating rate, does not have an effect on the ultimate yield.

Kimber and Gray [16] performed devolatilization experiments in a laminar flow reactor with an argon atmosphere. As the flow fields in the furnace were not modeled, the times reported include the heating times of the particle and the temperature refers to the reactor temperature; these data therefore cannot be used to determine rate constants, but can be used to investigate trends in the process of devolatilization. Devolatilization appeared to be a two-stage process: increasing the residence time at 1370K produced no further weight loss, but significant volatile matter was released during subsequent proximate analysis of the char. At higher temperatures (2170K) the evolution of this residual volatile matter was almost complete, indicating a second stage of devolatilization. There was a ten percent increase in weight loss for the $30 \mu\text{m}$ particle as compared to the weight loss of the $50 \mu\text{m}$

particles, which was attributed to the variation in heating rate with particle sizes.

Solomon et al. [21] performed devolatilization experiments in a laminar flow reactor at 1373K using both bituminous and lignite coals with particle size ranging from 44-74 μm . A Fourier Transform Infrared (FT-IR) spectrometer was used for in-situ analysis of gas species and temperature. The relative intensities of hot CO absorption were used for measuring the gas temperature, a technique which was adequate at room temperature but had some problems at high temperatures. The wall profile and input gas temperatures were used to calculate the particle temperatures; however, the major uncertainty in this calculation is the particle velocity, which was assumed to be the average gas velocity. Another experimental technique problem was the lack of a satisfactory method for the quantitative collection of tar and soot, and substantial scatter existed in this data. The functional group changes in the chars were determined, and the exhibition of almost identical changes in relative functional group composition of all the four coals of varying rank indicated that the kinetic rates are independent of coal rank but in fact depend on the functional group distribution of the original coal. However, if this hypothesis were accepted for modelling, it would require that all the functional groups of the coal be determined and the changes modeled, a rather complicated task.

2.2.2 Heated Grid

A heated grid apparatus consists of a folded strip of stainless steel screen into which the coal sample is spread. The screen is then placed between two relatively massive brass electrodes. The heating element and electrodes are enclosed in a vessel capable of operating under a vacuum or at elevated pressures. The reactor is flushed to remove any trace quantities of oxygen and then filled with the desired experimental atmosphere. The external circuitry permits independent control of the heating rate and the final temperature and holding time, limited only by the thermal inertia of the screen. An estimate of temperature-time history of the coal particles is recorded by a thermocouple placed within the sample. As the gaseous

contents remain in the apparatus until purged, there is ample opportunity for secondary cracking reactions.

Suuberg et al. [11] studied the product composition and kinetics of lignite pyrolysis. Experiments were carried out utilizing a Montana lignite in the particle size range of 53-88 μm with 74 μm being the average diameter, and therefore the effect of particle size was not tested. The yield of char, which remains on the screen, was determined gravimetrically. Tars were collected on foil liners within the reactor, on a paper filter at the exit of the reactor, and by washing unlined surfaces. The vapor phase products were collected by purging the reactor vapors through two traps. The coal samples were heated to a maximum temperature of 1273K, at which point the weight loss was slightly exceeding the ASTM volatile matter of the coal. Pyrolysis was found to be a function of the final peak temperature but not a function of the heating rate, which varied from 100-10⁴ K/sec. Tests on the effects of pressure revealed that there is a temperature dependence of the pressure effect on the yield: above 1073K a decrease in pressure was found to increase the total yield and affect the product composition.

Anthony and Howard [5] studied the rapid devolatilization of a lignite and a bituminous coal at temperatures up to 1373K. The heating rate was varied from 10² to 10⁴ K/min, the pressure from .001 to 100 atmospheres, and the particle size from 50-1000 μm . Both coals experienced increased weight loss with increasing temperature and residence time. The weight loss from the lignite was not affected by pressure; however, the weight loss from the bituminous coal decreased substantially with increasing pressure. The devolatilization of the lignite coal was independent of heating rate. The bituminous coal experienced increased weight loss with higher heating rates at pressures of one atmosphere and lower but the effect of the heating rate was negligible at higher pressures. The weight loss was also found to be independent of particle size for the lignite, but increased with decreasing particle size for the bituminous coal.

Jüntgen and Van Heek [22] summarized work in the basic processes and fundamentals of

coal pyrolysis by German researchers. The experiments in which the coals experienced high heating rates, $10^2 - 10^5$ K/min, were conducted in a heated grid apparatus. The rate of gas release at low heating rates, $10^{-3} - 10^2$ K/min, was studied with a captive sample heated at a constant rate in a controlled electric oven. A thermocouple in the sample measured the heating history of the coal particles. The gas produced during this process was carried away by a stream of helium and analyzed. The effect of heating rate on gas formation kinetics was investigated by studying ethane formation at widely differing heating rates; $10^{-2} - 10^4$ K/min. This involved the data of two different sets of apparatus which might have led to variations in pyrolysis behavior due to the different conditions experienced. The temperature range of the experiments was 573-1073K. Increasing rates of heating resulted in a shifting of the emission of ethane towards higher temperatures. Although the method of determining the estimates of the reaction parameters was not discussed, the estimates remained constant within the error limits, indicating that the mechanism of the reaction does not change over the temperature range investigated. The transition from reaction controlled pyrolysis, which is independent of particle size, to diffusion or heat transfer controlled pyrolysis, which is dependent upon the particle size and rate of heating, was calculated and measured using a high volatile coal. Two different curves were determined which separate the two rate determining mechanisms. They show to what degree the particle diameter has to decrease to assure chemical reaction control with rising rates of heating. For example, it shows that at a heating rate of 10^5 K/min or less, the reaction rate controls devolatilization when the particle is smaller than $100 \mu\text{m}$.

2.2.3 Crucible tests

The apparatus of the crucible tests varied from researcher to researcher, and therefore will be described as each study is discussed.

Mahajan et al. [23] studied the pyrolysis of twelve coals of various ranks in a helium atmosphere of 5.6 MPa (gauge). The weight loss in the coal sample was monitored using

a balance in conjunction with a thermal analyzer. A platinum boat containing the coal sample was suspended from the beam of the balance. The thermocouple, which is attached to the balance housing, was placed in close proximity to the sample. The reactor, which was made of a quartz tube with either end acting as inlet and outlet for the reactor gases, was surrounded by a tube furnace. The balance assembly along with the reactor and furnace were mounted in a pressure vessel which was pressurized with nitrogen, and helium was introduced through a pressure flowmeter. The furnace was activated to raise the temperature to 853K at a heating rate of 10K/min. Both the temperature and heating rate are rather low compared to the pyrolysis stage of pulverized coal combustion. Mahajan et al. determined that the variation in pressure from ambient to 5.6 MPa (gauge) had little or no effect on the devolatilization. The weight loss was also determined to be a function of the carbon content: as the carbon content decreases, the weight loss increases. The weight losses in these runs were all well below the ASTM volatile fraction, which was probably due to the experimental temperatures being well below the temperature at which the ASTM test is conducted.

Merrick [8] performed devolatilization tests in tubular pots with heating rates ranging from 3-5 K/min, a rather slow heating rate for devolatilization experiments. The temperature range for these tests was 673 to 823K. The samples of coal were crushed to a maximum particle size range of 3 mm, which is much larger than the pulverized coal used in coal combustors. It was found that the peak rate of release increases with volatile matter content of the coal, but that the temperature at which the peak occurs decreases.

Freihaut [9] used a fluid cooled delivery spoon to drop coal samples into a reactor boat which sat in a preheated, isothermal environment. The operating temperatures varied from 873 to 1173K. The coal particle sizes varied from a 53-106 μm to a 850-1000 μm size range. The differential release of tars was monitored by optical density measurements of the carrier gas stream. The condensate was captured on glass-fiber filters and weighed for estimates of the amount of tar release. The particle size effects on the weight loss were indicated by systematic decreases in the maximum differential mass release and systematic

increases in the reaction time as the particle size increased. This behavior was attributed to the presence of significant temperature gradients in the larger particles. As a result, the variation in particle size leads to in a transition from an isothermal, volumetric pyrolysis process in the case of the smallest particles to a non-isothermal shrinking core type of process in the case of larger particles. In a small particle, the whole volume of the particle devolatilizes uniformly as opposed to concentric 'rings' devolatilizing in a large particle as the temperature of that ring rises to the desired temperature. The effect of the heat of pyrolysis was investigated with a 500 μm particle and was shown to have a pronounced effect on the weight loss, as the endothermic reaction process supports the retention of a temperature gradient in the larger particles.

2.2.4 Conclusions

The experimental techniques of the above researchers were studied to identify the operational parameters that were found to influence the devolatilization behavior of coal. Although there are exceptions, the consensus is that the important operating factors that influence the devolatilization of the coal particle are:

- time
- temperature - increasing temperature results in increased weight loss.
- particle size - if the particle size is small enough that its temperature is nearly uniform, then no effect of particle size should be observed. The criterion for this is the Biot number:

$$Bi = h\tau/k$$

which compares the relative magnitude of the surface convection, h , and the internal conduction resistance to heat transfer, k/τ . A very low value of Bi (< 0.1) means that the internal conduction resistance is negligible in comparison with the surface

convection resistance and therefore implies that the temperature will be nearly uniform throughout the solid [24]. This criterion and experimental evidence shows that devolatilization is independent of size for particles under 100 μm in diameter at rapid heating rates ($10^4 - 10^5$ K/sec).

- heating rate - although most researchers agree that the heating rate is an important factor in determining the devolatilization behavior, there is no agreement on the mechanism of its effect. Two explanations have been offered to the observed increases in volatile yield with heating rate. One is that rapid heating leads to different reaction paths in the coal, and hence to breaking of different bonds and release of different species [10,5]. The other notes that rapid heating is usually found in drop tube reactors, where the coal is widely dispersed, and suggests that dispersion reduces the likelihood of secondary reactions which might decrease the yield [15,19].
- pressure - weight loss was generally found to decrease with increasing pressure.
- chemical composition/rank - an increase in the volatile matter in the original coal increases the asymptotic weight loss.

As pulverized coal combustors require that 65-80% of the coal be less than 74 μm [25], the particle size as a operational parameter will not be required to be taken into account in the devolatilization model. Since coal combustion occurs at ambient pressure, pressure effects will not be required to be included in the model. As the coal's composition can vary greatly from coal to coal, it does not seem reasonable to include this parameter in the model and therefore parameter estimates will be required to be found for the different types of coal used. Thus the parameters that the model must allow for are:

- time
- temperature
- heating rate

2.3 Accuracy of the Ash Tracer Technique

In conducting devolatilization experiments, many experimenters found that the sample collectors were not 100% efficient and therefore direct weight loss measurements could not be used to calculate the amount of volatiles released. As a result, an alternative method, the ash tracer technique, was used to calculate the weight loss of the coal particles during the pyrolysis experiments using:

$$V_{af} = \frac{A_{cs} - A_o}{A_{cs}(1 - A_o)} \quad (2.1)$$

where:

- V_{af} weight loss based on original ash free coal
- A_o ash fraction of original coal
- A_{cs} ash fraction of collected sample

Any uncertainty in the ash tracer technique due to vaporization or loss of ash constituents could affect the results, and therefore many researchers investigated the accuracy of this analytical technique. As the present work was undertaken to develop a procedure for estimating the devolatilization reaction constants for data obtained in a laminar flow test reactor, the data collection side of this problem cannot be ignored, and therefore the accuracy of the ash tracer method is investigated in this section of the literature survey.

In examining the literature, it was found that the experimental conditions under which the ash tracer accuracy was investigated could be divided into three major groups:

- crucible tests
- inert atmosphere furnace tests
- other atmosphere furnace tests

One would expect that the researchers would be in agreement within each group. However, this has not been the case, for there has been disagreement about the accuracy of the ash tracer technique within these groups.

2.3.1 Crucible Tests

Maloney [20] found the ash tracer technique to be an excellent method to determine weight loss in pyrolysis experiments. Samples of each coal were subjected to ASTM tests for volatile matter. The resulting chars were then ashed and the amount of volatile matter released was calculated using the resulting ash yields. The agreement between the ash tracer method and the direct weight loss measurements were found to be excellent at temperatures between 1073-1273K.

Harding [26] performed quite extensive crucible tests on the ash tracer accuracy using a high volatile bituminous coal. His research revealed that there was negligible vaporization of ash below 1500K but there was a significant increase in ash vaporization as the temperature increased up to 2500K. All elements in the ash had a significant degree of vaporization over this temperature range, except for titanium and scandium. Since there was considerably more titanium than scandium, titanium was used as a tracer instead of ash.

Kobayashi et al. [1,10] found that ash vaporization was negligible below 1400K. He also stated that although some of the ash is vaporized at higher temperatures this would be greatly reduced in furnace experiments due to the short residence times experienced. As a result, the errors in using the ash tracer technique would be a fraction of those experienced in crucible tests.

Scaroni et al. [19] found that crucible experiments in ashing furnaces revealed that the use of ash as a tracer consistently underestimated the actual weight losses for the temperature range of 973-1273K. This would suggest that some of the ash was lost in the furnace

experiments. In order to account for this underestimation, an empirical equation was developed. However, this equation is essentially independent of particle size and temperature and therefore is very specific to the data quoted.

2.3.2 Inert Atmosphere Furnace Tests

Sarofim et al. [27] performed tests on the vaporization of mineral matter in a drop tube furnace with a temperature range of 1000-1830K. Negligible amounts of mineral matter were expelled with the volatile matter, although the bituminous coals swelled by a factor of four or more.

Jamaluddin et al. [13] performed devolatilization experiments using a drop tube furnace with an argon atmosphere over a temperature range of 1073-1673K. Since the efficiency of the collector used was essentially 100%, the accuracy of the ash tracer technique was tested by comparison with direct weight loss calculations. The ash tracer technique was found to be a suitable method to estimate the weight loss of a high-volatile bituminous coal but not suitable for a medium volatile bituminous coal. This suggests that the accuracy of the ash tracer depends upon the rank of the coal or more likely on the variation of ash characteristics with the origin of the coal. Jamaluddin postulated that the unsuitability for the medium volatile coal was due to soot and tar from the pyrolysis of the volatiles being deposited on the char particles; however, since such deposition would affect a direct weight loss measurement as well, this argument does not seem valid.

Gat et al. [28] tested the accuracy of the ash tracer technique by laser heating particles carried in an argon gas jet. Although the ash tracer was found to be reliable at low temperatures, it was found to be increasingly unreliable as the temperature was increased. This suggests a temperature dependence of ash vaporization, which was also seen in the findings of some of the crucible tests. At high heating rates and high temperatures (2273-3073K), Gat reported significant losses of both ash and titanium. Ti was thought to be an unreliable

tracer under these conditions because Ti has a high organic affinity. Under rapid heating, the organic structure of the coal is quickly vaporized and there might not be sufficient time for the Ti to separate: it would then be carried out with the hydrocarbons. This contradicts the findings of Sarofim et al. [27], but an analysis of the condensed tars supports this theory. A seed tracer, tungsten carbide powder, was recommended in order to accurately determine the weight loss experienced during coal pyrolysis and combustion.

Badzioch and Hawksley [15] performed devolatilization experiments using a drop-tube furnace with a nitrogen atmosphere and a temperature range of 673-1273K. The ash tracer technique was found to be of poor reproducibility when the ash content is low, for a wide scatter arises from even small analytical errors in the determination of the amount of ash. Another source of scatter is a result of the ash particles being predominately discrete from the coal. They would then tend to segregate upon handling, for example, in vibrating feeders. A correlation was developed between the weight loss calculated by ash tracer and the change in volatile matter found by ASTM tests. One possible explanation for the correlation not passing through the origin was the possibility that there were minute fragments passing through the cyclone collector in the sampling system. These difficulties could be alleviated by closely size-grading the coal samples used, and performing the analysis of the original coal on the sample as fed to the furnace. Any ash tending to segregate into the fine particles would then be eliminated from both the sample and analysis.

2.3.3 Other Atmosphere Furnace Tests

All of the researchers in the literature who performed devolatilization tests in a furnace with an oxidizing atmosphere discovered ash vaporization and therefore found ash to be unsuitable as a tracer. However, it should be noted that these tests were all conducted at very high temperatures.

Ubhayakar et al. [29] performed their devolatilization tests in a turbulent flow entrained

bed gasifier with a hot combustion gas atmosphere with a temperature range of 1800-2250K. The ash vaporization was estimated by analyzing the alumina content of two char samples resulting from high temperature and low temperature runs. Since the ash from a high temperature run had a higher alumina concentration than the low temperature run, it was assumed that some ash vaporization had occurred. Alumina was used as a tracer instead of the ash, since it was the most refractory component in the ash.

Quann et al. [30] performed mineral vaporization tests using a drop tube furnace with a 5-100% oxygen atmosphere with a particle temperature range of 1600-3000K. Quann stated that the submicron particles generated by vaporization and condensation of the ash passed through the impactor and were collected on a back-up membrane filter. The amount and composition of the particles was used to provide a measure of the extent of the ash vaporization during combustion. Through this experimentation, Quann found that the vaporization was dependent on the temperature and the spatial distribution of the mineral matter.

Neville et al. [31] performed ash vaporization experiments in a drop tube furnace with a 30% oxygen in nitrogen atmosphere at 1750K. He found that high temperature and a locally reducing atmosphere promoted ash vaporization. Also, elements such as sodium, which show a small temperature dependence, are vaporized to a large degree during devolatilization. However, elements such as magnesium, which show a strong temperature dependence, are vaporized primarily at a peak temperature encountered after devolatilization is complete. Although the meaning of the temperature dependence was not explained, it is assumed that this refers to the range of temperature between the element's melting and boiling points which are listed in table 1. As sodium melts at a much lower temperature than magnesium, the liquid can be entrained by the escaping volatiles and carried out of the particle. As sodium has a lower boiling point, it vaporizes at a lower temperature and therefore escapes as a gas. Both these effects can result in a greater loss in sodium than magnesium by the devolatilizing coal particle.

2.3.4 Conclusions

From this literature survey, one can see that the vaporization of the mineral matter depends not only on the properties of the coal (i.e. rank, amount of minerals) but also on the conditions (i.e. temperature, atmosphere, heating rate) under which pyrolysis occurs. As a result, it is important to test each coal utilized and to try to duplicate experimental conditions as closely as possible while conducting ash vaporization tests. In examining the literature which reports upon the experiments that most closely duplicate the conditions of the experiments that will be performed (inert atmosphere, approximately 1500K), it seems that the ash tracer method is reliable up to about 1273-1373K, unless the ash has components which vaporize at lower temperatures (e.g. Jamaluddin et al. [13]). In this case, it would be possible to perform supplementary crucible tests over the temperature range of experimentation to determine whether ash vaporization is significant. If no vaporization has occurred then this should be verified by performing drop tube furnace tests to see whether the heating rate or atmospheric conditions have any effect on ash vaporization. It would be important that the sampling equipment be designed so that the weight loss measurements are as accurate as possible. This would enable an accurate comparison between weight loss measurements and the ash tracer method for the furnace experiments.

Table 1: Melting and boiling points of Sodium and Magnesium

	melting point, °C	boiling point
sodium	97.5	880
magnesium	651	1110

Chapter 3

Model Evaluation

The purpose of this chapter is to critically appraise and compare the devolatilization models that are available in the literature, and to select a model which will be suitably accurate in describing the pyrolysis of a coal particle. The model selected is ultimately intended for use in a full model of coal combustion in a furnace, such as that of Lockwood [12]. The role of the devolatilization model in such a model is:

- to predict the mass of char produced for subsequent char combustion
- to predict the rate of volatiles release in the early part of the flame

Of these, the accurate prediction of char mass, i.e. extent of devolatilization, is the most important, as char combustion is the rate-controlling step of coal combustion. Owing to the complexity of a full model of combustion, the devolatilization model selected should be relatively simple and not require substantial computational effort. It is with these factors in mind that the models will be evaluated. Attention will be further confined to models for devolatilization of small coal particles, for which the particle temperature may be assumed uniform. The models presented in literature are quite different, for they range from a simple single first order reaction model to a much more complex and sophisticated multiple parallel

reaction scheme. The reaction schemes to be examined are:

- evaporation model
- single, first order reaction model
- competitive parallel reaction model
- two component model
- multiple parallel reaction mechanism

Each of these models will be examined and their advantages and disadvantages will be listed in an attempt to choose the best model that will serve the requirements listed above.

3.1 Evaporation model

3.1.1 Lockwood et al.

Lockwood et al. [12] developed a model for bituminous coal combustion. Lockwood used a physical model to describe the devolatilization of the coal instead of a reaction model, even though it was acknowledged that pyrolysis is a chemical process. The model used is very simple:

$$- dx_v/dt = \min(Q_p/h_1, B_m) \quad (3.1)$$

where x_v is the mass fraction of volatiles not yet released and h_1 is the 'latent heat' of devolatilization. This treats the evolution of volatiles as an 'evaporation' process. It is assumed that no volatiles were released at temperatures below 600K and that the volatile release rate is linearly dependent upon the heat flux to the particle, Q_p , and limited by a maximum value, B_m . A final assumption is that the total volatile yield is equal to the proximate volatile content. This model cannot describe the experimentally observed

increase of volatile yield with temperature nor the fact that yields above the ASTM value are often obtained [1,10,15,19]. Because it represents a chemical reaction as a physically controlled process, the 'reaction constants', h_1 and B_m , are specific to the temperature range, heating rate and other conditions modeled.

3.2 Single first order reaction model

The single first order model is the simplest reaction model available in literature and therefore is often used in combustion studies. The model is:

$$coal = V^*(volatiles) + (1 - V^*)(char) \quad (3.2)$$

The basic reaction equation for this model is:

$$dV/dt = k(V^* - V) \quad (3.3)$$

where V is the quantity of volatiles evolved up to time t and V^* is the ultimate volatile yield. The reaction constant k is described by an Arrhenius equation:

$$k = k_o \exp(-E/RT) \quad (3.4)$$

This model will be evaluated and discussed by pointing out its advantages and disadvantages.

3.2.1 Badzioch and Hawksley

Badzioch and Hawksley [15] introduced a single first order model which is often used as a standard against which other models are compared. The devolatilization experiments were carried out in a drop tube furnace with a maximum temperature of 1273K.

The model assumes isothermal pyrolysis, and its form is as follows:

$$V = QV_o(1 - C)(1 - \exp(-kt)) \quad (3.5)$$

where V is the weight loss of the coal up to time t , V_o is the ASTM proximate volatile matter of the coal, and Q is the ratio of the weight loss to the change in proximate volatile matter:

$$Q = V/(V_o - V_r) \quad (3.6)$$

where V_r is the proximate volatile matter of the char. C is a correction for the asymptotic weight loss, or the residual volatile matter in the char at infinite time, which allows the increase in yield with temperature to be roughly modelled. Badzioch et al. found C was a function of the swelling factor of the coal: for the non-swelling coals C was a constant while for the swelling coals C was fitted by an exponential function of temperature:

$$C = \exp[-K_1(T - K_2)] \quad (3.7)$$

Badzioch and Hawksley stated that there was a heating period in the furnace and therefore the particles did not experience a completely isothermal residence time. This heating time was subtracted from the residence time to obtain the duration of isothermal decomposition, thus assuming the amount of devolatilization occurring during the heating process was insignificant. This is now known to be a poor assumption [1,5], which limits this model's usefulness. Badzioch and Hawksley [15] stated that this model is not reliable for temperatures above 1273K and that a two reaction model should be used at high temperatures. Both the empirical nature of the temperature variation of the ultimate yield and limitation to temperatures under 1273K also limits this model's usefulness.

3.2.2 Scaroni et al.

Scaroni et al. [19] performed lignite pyrolysis experiments in a drop tube furnace with a temperature range of 973K-1273K. Scaroni included two models, of which the first is strictly an empirical model which is particle size and temperature independent. As a result, this model does not provide any insight into the mechanism of pyrolysis and cannot be applied to other data. The second model is again a simple first order isothermal model:

$$V = V^*(1 - \exp(-kt)) \quad (3.8)$$

where V^* is the maximum potential weight loss. Scaroni states that there is no weight loss during heat up, an assumption that is now considered incorrect [1,5]. It should be noted that in this model the ultimate yield is not a function of temperature.

3.2.3 Truelove

Truelove [32] modeled the combustion of pulverized coal in swirling flow combustors. This model included a simple first order reaction model of the coal devolatilization, this time for non-isothermal conditions:

$$dV/dt = k(V^* - V) \quad (3.9)$$

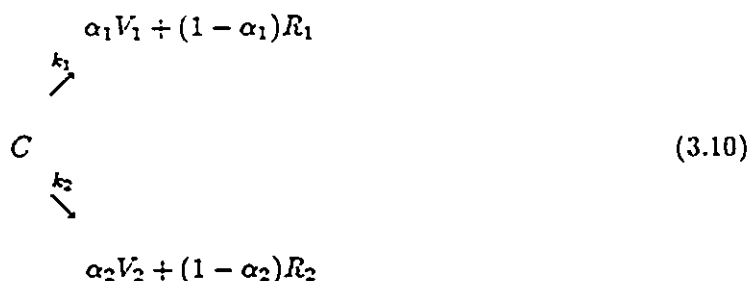
The rate parameters were taken from the work of Badzioch and Hawksley [15].

3.3 Competitive Parallel Reaction Model

It has been suggested that the temperature dependence of volatile yield can be modelled by using two parallel, competing pyrolysis reactions, one dominant at low temperatures and the other at high. This model was initially proposed by Kobayashi [1] but several authors [13,29,33] have used modified versions of this model which will be discussed here.

3.3.1 Kobayashi

Kobayashi proposed the two competitive reaction model since a model was needed that could describe the effects of temperature on volatile yields as well as predict the devolatilization rates at higher temperatures. This model assumes that the original coal substance, C, can decompose to volatiles, V, and char, R via two paths:



where k_i are the reaction rate constants and α_i are the mass stoichiometric constants and

$$k_i = k_{oi} \exp(-E_i/RT) \quad (3.11)$$

The first reaction dominates at low temperatures. At high temperatures, the second reaction is assumed to become faster than the first one, which amounts to requiring E_2 to be larger than E_1 . Kobayashi set α_1 as the proximate analysis volatile yield and α_2 as 1 since all the coal is expected to devolatilize at high temperatures. The mathematical form of this model is:

$$\begin{aligned}
 \frac{dV_1}{dt} &= \alpha_1 k_1 C \\
 \frac{dV_2}{dt} &= \alpha_2 k_2 C
 \end{aligned}$$

so that

$$\begin{aligned}
 \frac{dV}{dt} &= \frac{d}{dt}(V_1 + V_2) \\
 &= (\alpha_1 k_1 + \alpha_2 k_2) C
 \end{aligned} \quad (3.12)$$

where

$$\frac{dC}{dt} = -(k_1 + k_2)C$$

Integrating:

$$C = \exp\left(-\int_0^t (k_1 + k_2) dt\right) \quad (3.13)$$

Substituting equation 3.13 into equation 3.12 yields:

$$V = \int_0^t (\alpha_1 k_1 + \alpha_2 k_2) \exp\left(\int_0^t -(k_1 + k_2) dt\right) dt \quad (3.14)$$

Under isothermal conditions, this equation can be integrated to give:

$$V = [(\alpha_1 k_1 + \alpha_2 k_2)/(k_1 + k_2)][1 - \exp(-(k_1 + k_2)t)] \quad (3.15)$$

As $t \rightarrow \infty$, equation 3.15 reduces to:

$$V^* = (\alpha_1 k_1 + \alpha_2 k_2)/(k_1 + k_2) \quad (3.16)$$

where V^* is the asymptotic weight loss or the maximum possible weight loss. The first reaction dominates at low temperatures, since $k_1 \gg k_2$ and as a result V approaches α_1 , while at high temperatures $k_2 \gg k_1$ and V approaches α_2 . This model can therefore predict the temperature dependence of the asymptotic weight loss as found in the experimental findings of many researchers [1,15,19,10,13]. This model can also be applied to non-isothermal experiments through the numerical integration of equation 3.14 using the temperature-time histories of the coal particles to fit the equation to the experimental weight loss data. However, Kobayashi expended little effort in trying to obtain the best fit. Since the asymptotic weight loss changes from approaching α_1 to approaching α_2 as the temperature increases, one expects that there is a transition temperature interval above which devolatilization becomes increasingly controlled by reaction 2. The transition temperature can be roughly calculated by assuming that k_2 is negligible if it is twenty percent of k_1 :

$$k_2 = .2 \cdot k_1$$

therefore:

$$\begin{aligned} k_{o2} \exp(-E_2/RT) &= .2 \cdot k_{o1} \exp(-E_1/RT) \\ T_{tr} &= (E_2 - E_1)/(R \cdot \ln(k_{o2}/.2k_{o1})) \end{aligned} \quad (3.17)$$

Using the parameter estimates determined by Kobayashi [1,10] listed in table 2, one finds the transition temperature to be approximately 1305K. While the transition temperature found in this example is a function of the parameter values chosen, this temperature is supported by experimental work, since Badzioch and Hawksley [15] found that a second high temperature reaction is required to explain the increase in weight loss if the devolatilization

temperature is above 1273K. The transition temperature is an important 'tool' in determining the type of model that should be utilized. This method can also be used to approximate the temperature at which the first reaction becomes negligible by finding the temperature at which k_1 is twenty percent of k_2 :

$$k_1 = .2 \cdot k_2$$

therefore:

$$k_{01} \exp(-E_1/RT) = .2k_{02} \exp(-E_2/RT)$$

$$T = (E_1 - E_2)/(R \ln(k_{01}/.2k_{02})) \quad (3.18)$$

Using the parameter estimates determined by Kobayashi [1,10] listed in table 2, one finds the temperature at which the first reaction becomes negligible to be approximately 2950K. An interesting feature of this model is that the ultimate yield becomes a function of the temperature-time history of the particle. If the particle is held at a fairly low temperature for a long period of time, the original coal substance, C, will be entirely consumed by reaction 1, producing yield α_1 , so that no further product will be produced by subsequent heating to a temperature at which reaction 2 becomes predominant. Rapid heating to high temperatures, on the other hand, will ensure that most devolatilization occurs by reaction 2, resulting in a higher yield. Thus the Kobayashi model is capable of explaining the observed dependence of yield on the heating rate [13,6,16,20] as well as on temperature.

3.3.2 Ubhayakar et al.

Ubhayakar et al. [29] performed devolatilization experiments in hot combustion gases with temperatures from 1800K to 2250K, which is the temperature range that would require a two reaction model. The model used was in fact the two reaction model presented by Kobayashi with some modifications. Ubhayakar assumed that the stoichiometric mass constants were equal to x/x_n where x_n is equal to the (H/C) ratio of volatile n, n=1,2 and x is equal to the

(H/C) ratio of the coal. As the coal particles were entrained in hot combustion gases, the model used by Ubhayakar incorporates the two reaction model followed by the cracking of the volatiles. The parameters for the two reaction model were fitted using the data provided by Kimber and Gray [16] and Badzioch and Hawksley [15].

From the determination of the stoichiometric constants it appeared that the high temperature process led to higher yields of lower (H/C) volatiles and lower char than the lower temperature process. These observations are derived from the values of α_n :

$$\alpha_1 = 0.3 = x/x_1 \rightarrow x_1 = .194$$

$$\alpha_2 = 0.8 = x/x_2 \rightarrow x_2 = .07275$$

The lower char yield is backed by experimental results [10,15,16] finding increased weight loss with increased temperature. However, as the (H/C) ratios of the volatiles released were unrecorded by Badzioch and Hawksley [15] and Kimber and Gray [16], these results could not be verified. Also, using two sets of experimental data to fit the parameters of the model to be used to fit additional parameters to a third set of data is not advisable as the conditions in the different furnaces can result in very different devolatilization behaviour and therefore parameter estimates are obviously in question.

3.3.3 Jamaluddin et al.

The coal in the experiments of Jamaluddin et al. [13] was devolatilized over a temperature range of 800-1400C, which also supports the use of a two reaction model. Jamaluddin [13] also used the Kobayashi model; however, some slight modifications were made. The low temperature kinetic rate constants were taken as those determined by Badzioch and Hawksley [15] while the high temperature constants were set to those as determined by Ubhayakar et al. [29]. The low temperature mass stoichiometric constant was taken as the proximate analysis volatile matter, which is the definition of α_1 originally given by Kobayashi. However

α_2 was determined from the measured pyrolysis data and was defined by:

$$\alpha_2 = QV_0 \quad (3.19)$$

where $Q = V^*/(V_0 - V_r)$ as defined by Badzioch and Hawksley [15]. As a result, at high temperatures with $k_2 \gg k_1$, the model would reduce down to:

$$V = QV_0(1 - \exp(-k_2t)) \quad (3.20)$$

This model has the same form as the model introduced by Badzioch and Hawksley [15] for low temperature ($< 1273K$) devolatilization, if at the high temperatures the correction factor, C , for the asymptotic weight loss were to be set to zero. The model was found to be accurate for the high volatile bituminous coal but to overpredict the weight loss for the medium volatile coal by up to five percent. One should note that using rate parameters determined by other researchers could compromise the values of α_1 and α_2 determined by fitting the model to the data.

3.3.4 Suzuki et al.

Suzuki et al. [33] performed devolatilization experiments with combustion air as the secondary gas stream with a temperature range up to 1483K. However the furnace had recirculating flow and therefore the temperature-time history of the coal particles is uncertain. Suzuki also used the Kobayashi model; however, α_1 was selected to provide agreement between the experimental data and the predictions while holding all other parameters constant. The values of α_1 were then correlated with the (H/C) ratio and the proximate volatile matter of the coal to provide a means of estimating α_1 . Suzuki found that the extent of devolatilization through the first reaction, α_1 , increases with an increase of the proximate volatile matter and (H/C) ratio of the coal. However, one should note that fixing the other parameters may fix the behaviour of α_1 : i.e. if the values of the other parameters were changed one might find that the behavior of α_1 was changed as well.

3.3.5 Baxter et al.

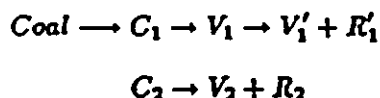
Baxter et al. [34] used statistical routines to fit the parameters of the parallel reaction model to the data obtained by Kobayashi [1]. The temperature, velocity and radiation conditions inside Kobayashi's furnace were calculated with a numerical model of the flow, and were then utilized to determine the temperature of the particle as a function of time. However, the results of this analysis are questionable: at a furnace temperature of 2100K, the particle model developed by Baxter predicts a plateau in the temperature profile at 1400K which is said to be a result of the high rate of mass transfer due to devolatilization of the coal particle. In view of the low value of heat of pyrolysis, it seems unreasonable that the mass flow from the coal particle would maintain the coal particle's temperature 700K below the ambient temperature and still maintain a high rate of mass release. Another difficulty with this model prediction is that it indicates that there is in fact no high temperature devolatilization and would bring to question the temperature profiles of the devolatilizing coal particle at lower temperatures as predicted by this model. The reason for these problems appears to be an incorrect particle energy balance: the enthalpy of the escaping devolatilization gases was included in the energy balance, which can be shown to be in error when the first law of thermodynamics is applied to the pyrolyzing coal particle (Appendix A).

Other researchers [31,35] also have employed the Kobayashi model, using the values of α and k as determined by Kobayashi. As previously stated, Kobayashi expended little effort in optimizing the parameters for the best fit, moreover; his values are specific to his two test coals, so that using his constants without further testing or modifications is not advisable.

3.4 Two component model

The two component model differs from the two competitive reaction model in that instead of having two reactions that come into play at different temperatures, it is assumed that the coal consists of two components. These two components of the coal pyrolyze by independent,

first order reactions which have substantially different rate constants. The mechanism is as follows:



where the first reaction includes a secondary cracking reaction. This model can be simplified by neglecting the secondary cracking stage.

3.4.1 Nsakala et al.

Nsakala [4] studied the kinetics of lignite pyrolysis at 1081K in a drop tube furnace. The model used to describe the devolatilization was the two component hypothesis without the secondary cracking. The evidence cited by Nsakala that dictated the need for this type of model was a 'break' in the weight loss behavior, figure 4, that occurred when the residence time was increased; this was seen to be characteristic of two independent parallel reactions having substantially different rate constants. However, this 'break' could be the result of the weight loss approaching the asymptotic weight loss.

This model requires that the initial concentrations of each component, the proportionality constant, γ , between V_2 and R_2 plus the rate constants to be determined. Nsakala found that the asymptotic weight loss was not a function of temperature, rather

$$V^* = C_1 + C_2/(1 + \gamma) \quad (3.21)$$

The number of parameters to be estimated as well as the asymptotic weight loss not being temperature dependent make this model quite undesirable.

3.5 Multiple Parallel Reaction Mechanism

An alternative model to the two parallel competing reaction model is the multiple parallel reaction model. The premise of this model is that the devolatilization of the coal is a complex phenomenon that should be modelled as a large number of independent parallel reactions. The problem is simplified if it is assumed that the pre-exponentials for each reaction are the same and the reaction rates only differ in activation energies. It is further simplified by assuming that the number of reactions is large enough to permit E to be expressed as a continuous distribution function.

Anthony et al. [5,6] generalized this model to allow for non-isothermal processes. This model was also adapted and modified by several researchers [11,21,36,37].

3.5.1 Anthony and Howard

Anthony and Howard [5,6] performed devolatilization experiments in the temperature range of 673-1373K which is within the single low temperature reaction range. The as yet unreleased volatile fraction for a particular reaction i of the multiple parallel reactions is:

$$V_i^* - V_i = V_i^* \exp\left(-\int_0^t k dt\right) \quad (3.22)$$

V_i^* is a differential part of the total yield V^* and may be written:

$$V_i^* = dV^* \quad (3.23)$$

$$= V^* f(E) dE \quad (3.24)$$

with

$$\int_0^\infty f(E) dE = 1 \quad (3.25)$$

Integrating equation 3.22 over all values of E using equation 3.24 yields;

$$(V^* - V)/V^* = \int_{-\infty}^\infty \exp\left(-\int_0^t k dt\right) f(E) dE \quad (3.26)$$

Anthony and Howard stated that there is negligible numerical effect of altering the lower limit on the left integral from 0 to $-\infty$. The distribution function, $f(E)$, is assumed to be Gaussian with a mean activation energy E_0 and standard deviation σ :

$$f(E) = [\sigma(2\pi)^{0.5}]^{-1} \exp[-(E - E_0)^2/2\sigma^2] \quad (3.27)$$

The model has the $\int_0^t k dt$ term to account for non-isothermal processes.

One difficulty with this model is that it does not predict the variation of yield with temperature at higher temperatures. This can be illustrated by assuming an isothermal process, for which, equation 3.26 becomes:

$$(V^* - V)/V^* = \int_{-\infty}^{\infty} \exp(-kt) f(E) dE \quad (3.28)$$

as $t \rightarrow \infty$,

$$(V^* - V)/V^* = \int_{-\infty}^{\infty} 0 f(E) dE = 0 \quad (3.29)$$

which shows that the asymptotic weight loss is a constant and equal to V^* and therefore independent of temperature. Anthony and Howard state that this model can give the impression of an asymptote being reached by a low temperature decomposition when it is compared with one at high temperatures, but this really amounts to a misinterpretation of the results. The behavior of this model can be illustrated by assuming a uniform rather than a Gaussian distribution of activation energy:

$$\int_{E_a}^{E_b} f(E) dE = 1 \rightarrow f(E) = 1/(E_b - E_a) \quad (3.30)$$

Substituting equation 3.30 into the isothermal equation 3.28, the resulting equation is:

$$V = V^* [1 - RT/(E_a - E_b) [E_1(k_0 t Z_b) - E_1(k_0 t Z_a)]] \quad (3.31)$$

where $E_1(x)$ is the exponential integral:

$$E_1(x) = \int_x^{\infty} \frac{\exp(-t)}{t} dt$$

$$Z_i = \exp(-E_i/RT)$$

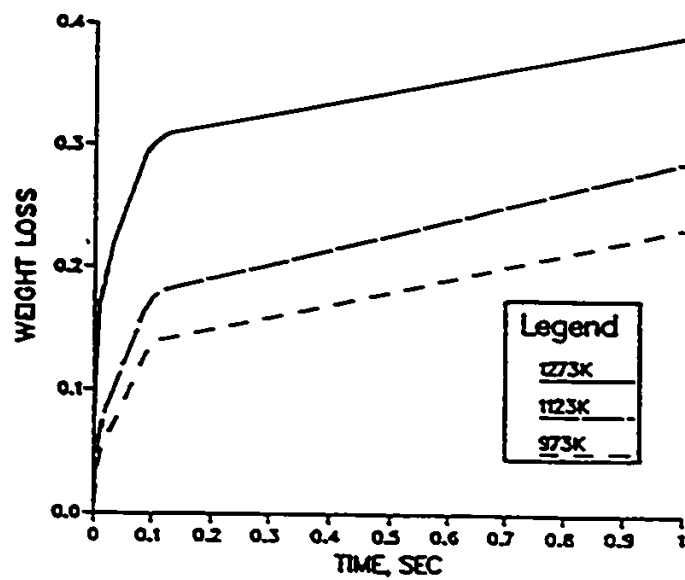
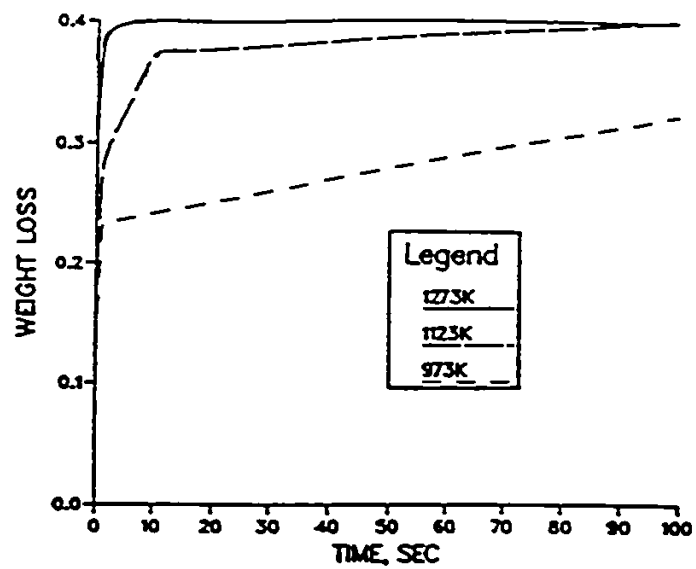


Figure 5: Weight loss versus residence time as predicted by Anthony and Howard [5,6] model for various temperatures

Figure 5 is a graph of the resulting weight loss. It could appear that the low temperature devolatilization had reached an asymptote although in reality it had not. Thus this model does not describe the variation of the asymptotic weight loss with temperature as the Kobayashi model does. A further problem with this model is that k_0 and E are correlated [6,37], since a higher value of k_0 tends to shift the distribution to higher activation energies.

3.5.2 Hashimoto et al.

Hashimoto et al. [37] also used the multiple parallel reaction model to model the thermal regeneration of activated carbons used in wastewater treatment with a temperature range up to 1173K. Hashimoto used Anthony and Howard's non-isothermal model with a modification to correct the dependence of the distribution curve of E on the value of k_0 . This weak point was corrected by approximating k_0 as a function of E :

$$k_0 = \phi \exp(\beta E) \quad (3.32)$$

This modification increases the number of parameters required to be fitted by two and solves the problem of the correlation between k_0 and E . However, this model still has the problem of the ultimate yield not being a function of temperature.

3.5.3 Solomon et al.

Solomon et al. [21] performed pyrolysis experiments in an entrained flow reactor which was designed to operate up to a maximum temperature of 1923K. The model used to describe the pyrolysis of coal was Anthony and Howard's model with a Gaussian distribution for the activation energy. The model, however, was used to describe individual species evolution rather than pyrolysis of the coal as a whole. Solomon justified using a distribution function for the activation energy of individual species by the fact that the quantity of each gas species depends upon the functional group distribution in the original coal. Solomon also

hypothesizes that the functional groups decompose at rates which are insensitive to coal rank to form light gas species. It is for this reason that the model was fitted to the pyrolysis of a lignite in an entrained flow reactor and then applied to a bituminous coal pyrolyzed in a heated grid to test its generality. One difficulty that can be pointed out in this method is that the lignite was only heated to a single temperature (1373 K) while the temperature range of the bituminous coal tests was 673-2073 K. There was a problem in the collection of the tar and soot and therefore substantial scatter existed in the data.

The fit of the model to either coal's devolatilization products is not very good [21]. This might be due to the fact that the parameters were fitted using the functional groups present in the coal. The functional group composition of the coal was then required to be found and the kinetic rate constants of these groups then formed the distribution functions of E. This complicated modeling has a lot of room for error, owing to the many parameters involved.

3.5.4 Suuberg et al.

Suuberg et al. [11] investigated the kinetics of lignite pyrolysis using a heated grid with a constant heating rate and a maximum temperature of 1273K. Suuberg was investigating the applicability of the multiple parallel reaction model to the devolatilization of a lignite by modeling the appearance of several products. Many products are not adequately modeled by a single reaction [11,38] but in fact are the result of different reactions in different temperature intervals. Figure 6 also shows how the various individual reactions form a smooth total weight loss curve. In spite of this evidence, which supports the use of the competitive two reaction model with temperature dependent ultimate yield, Suuberg supports the use of the parallel multiple reaction model, since the distribution function of E is similar to those obtained based on weight loss data [5,6]. Suuberg states that the kinetic parameters obtained by the parallel multiple reaction model are overall properties, in spite of the fact that the species are involved as a result of some combination of two reactions.

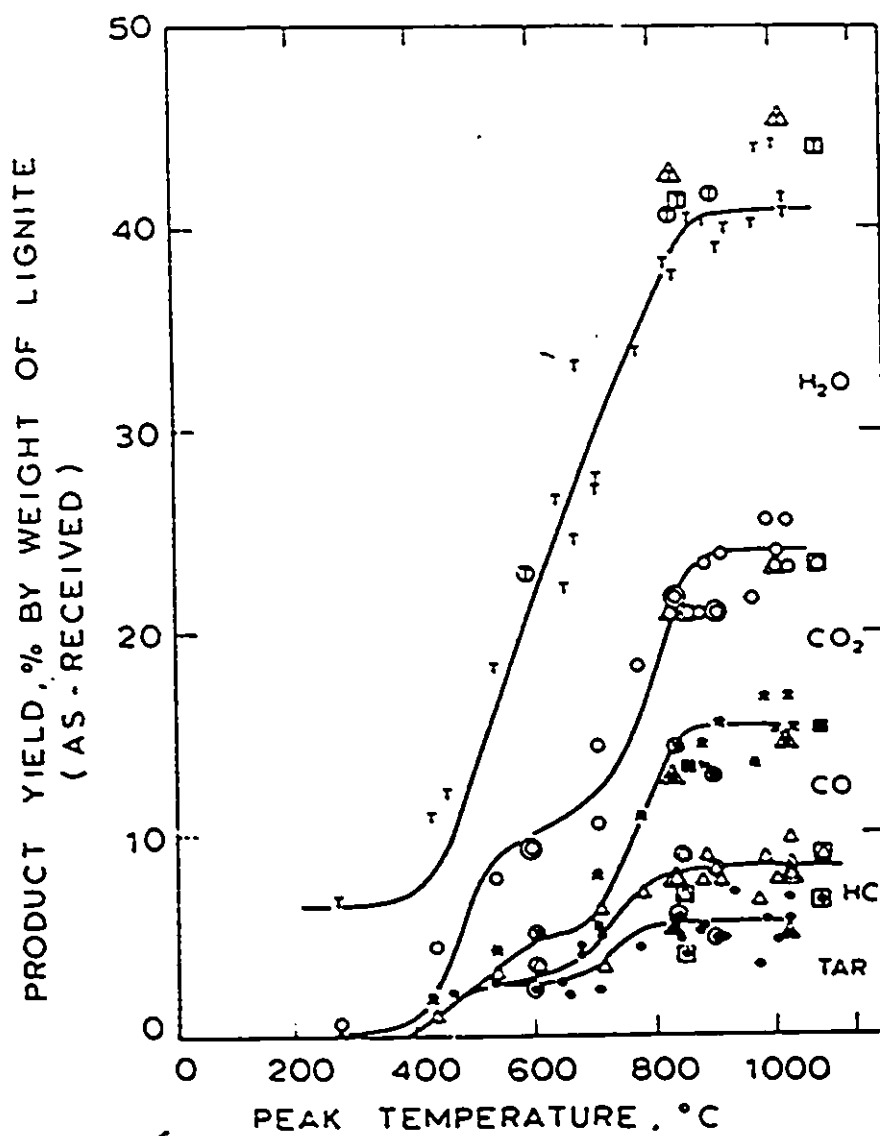


Figure 6: Pyrolysis product composition from lignite coal heated to different peak temperatures

3.5.5 Rizvi

Rizvi [36] modeled the combustion of pulverized coal particles in swirling flow combustors. Rizvi evaluated the performance of the first order reaction, evaporation, two competing reaction and multiple parallel reaction models by comparing the flame behavior that results from the models to the actual flame behavior. Rizvi found that satisfactory predictions of the flame behavior were obtained when either the evaporation or multiple parallel reaction models were utilized while both the two competing reaction and Badzioch and Hawksley's single first order reaction models were found to be less successful. However, it must be stressed that all reaction constants used came from the literature and no attempt was made to fit them for the particular coal being used. Optimization of the constants would probably make all these models more accurate and would certainly be required for a meaningful test. These findings can be seen to be quite questionable, for the two 'acceptable' models are at opposite ends of the spectrum: i.e. one is a purely physical model while the other represents a large number of independent parallel reactions. Another problem with this conclusion is that the analysis is based upon the turbulent flame behavior where any number of unknown factors might come into play apart from the devolatilization process itself.

3.5.6 Sprouse et al.

Sprouse et al. [39] fitted Anthony and Howard's multiple parallel reaction model as well as Kobayashi's two reaction model to the high temperature lignite devolatilization data supplied by Kobayashi [1]. Sprouse performed a non-linear least squares curve-fitting routine on Kobayashi's data, since there was some question whether the Anthony and Howard model, which was previously only applied to low temperature ($< 1200K$) pyrolysis, could adequately handle high temperature devolatilization. Sprouse fitted both models to the Kobayashi data and found that the standard deviation of the Anthony and Howard model was 4.6% while it was 6.1% for the Kobayashi model. This small difference in the standard deviations of the two models is not significant, especially when the char combustion is

the rate controlling step for the complete combustion process. Sprouse also compared the abilities of the two different models to adequately fit devolatilization data by applying the models to the devolatilization of coal during an ASTM test. Although Sprouse found that Anthony and Howard's model described the ASTM devolatilization more accurately than the Kobayashi model, this test cannot be considered a good test due to the long residence time, during which secondary reactions have ample opportunity to effect the devolatilization results.

Sprouse points out that the Anthony and Howard model fits the high temperature data while using fewer parameters. However, k_0 and E are correlated [6,37] and therefore the equation suggested by Hashimoto [37] to correct this model weakness should be added which in turn raised the number of parameters to be fitted. Also, as discussed on page 41, the multiple parallel reaction model only appears to model the change in ultimate yield with temperature, and actually gives a constant ultimate yield.

Sprouse also questions the validity of the Kobayashi model since it cannot predict that a coal heated at low temperature will always devolatilize further when the temperature is raised, while the Anthony and Howard model can predict this behavior. However, a model should suit the purposes of the researcher: since in coal combustion the coal is consumed and therefore any question of reheating to a higher temperature is eliminated, this argument against the Kobayashi model can be considered unimportant for the present purposes.

3.6 Conclusions

The models presented in the literature have been examined and analyzed for their suitability and accuracy in describing the devolatilization of coal. The utility of the evaporation model is confined to the correlation of weight loss data over very narrow ranges of conditions; it is unsuitable as a general model. The one reaction models appear to be suitable for low temperature (below 1300K) pyrolysis and either did not describe the temperature

dependence of the ultimate yield or used some sort of empirical correction [15,19]. The two component hypothesis [4] complicated the pyrolysis model and yet did not address the problems stated above. The multiple parallel reaction model was only used to fit low temperature devolatilization and did not describe the temperature dependence of the ultimate yield at high temperatures. In the form suggested by Anthony and Howard [5,6] a numerical integration of the probability function is required, while other multiple parallel reaction schemes are too complex for the inclusion in a complete model of coal combustion in a furnace.

However, the two competing reaction model illustrated the temperature dependence of the asymptotic weight loss. It is flexible, in that at low temperatures this model reduces down into the simpler one reaction which was found to be acceptable at lower temperatures. This is also the only model which will predict a dependence of the weight loss on the heating rate or temperature history. It is for these reasons that the two competing reaction model has been selected as the best model for the purposes of the present work.

Table 2: Parameter estimates determined by Kobayashi

reaction	k_0	E
low	2E5	25
high	1.3E7	40

Chapter 4

Reactor Model Program

The entrained flow reactor has been designed to provide data under conditions where the particle temperature-time history may be determined and where the heating rate and reaction conditions match a pulverized coal combustor. A particle heating program written by Flaxman [7] models the furnace flow fields as well as the particle motion and heating. This program was modified with the addition of a devolatilization model. The coal loadings are usually kept small to prevent secondary cracking reactions and therefore the effect of the coal particles on the gas velocity and temperature fields is neglected [7,13]. The temperature and velocity fields inside the reactor are determined by numerically solving all fundamental governing equations of energy, momentum and conservation of mass using finite difference techniques. The temperature and velocity fields of the furnace are then used to calculate the coal particle temperature and velocity by numerical solution of the differential equations of particle motion and heating.

As many different designs of entrained flow reactors exist, each with its own geometry, gas flows and particle feed rates, the particle heating program was designed to be flexible so that different furnaces could be modelled by making simple adjustments inside the program. The flexibility of the program is in part achieved by dividing the flow field area into small

control volumes with varying sizes which form a grid pattern. The grid spacing was chosen so that there are many points in the region of large gradients and fewer points as the gradients become smaller. A sample grid for the EMR reactor is shown in figure 7. The nodes for the grid are placed such that the control volume boundaries lie exactly halfway between the adjacent nodes. The nodes can then be adjusted to model the dimensions of the desired entrained flow reactor, for example the Kobayashi furnace [1], with dimensions as shown in table 3.

4.1 Method of Integration

The original particle heating program assumed that the particles do not react chemically. This program was modified by adding the two competitive reaction model selected for coal devolatilization:

$$V = \int_0^t (\alpha_1 k_1 + \alpha_2 k_2) \exp\left(\int_0^t -(k_1 + k_2) dt\right) dt \quad (4.1)$$

As equation 4.1 can not be easily integrated analytically, different methods of numerical integration were investigated to select the simplest method, with regard to consumption of computer time, which can still accurately perform the integration. The accuracy of the methods of integration was tested by making weight loss predictions for a single first order devolatilization reaction in a particle undergoing heating according to:

$$T = Z(1 - \exp(-\beta t)) + T_0 \quad (4.2)$$

where:

- $\beta = 12k/(\rho c_p d^2)$
- Z is the difference between the final equilibrium temperature and the initial temperature, T_0 .

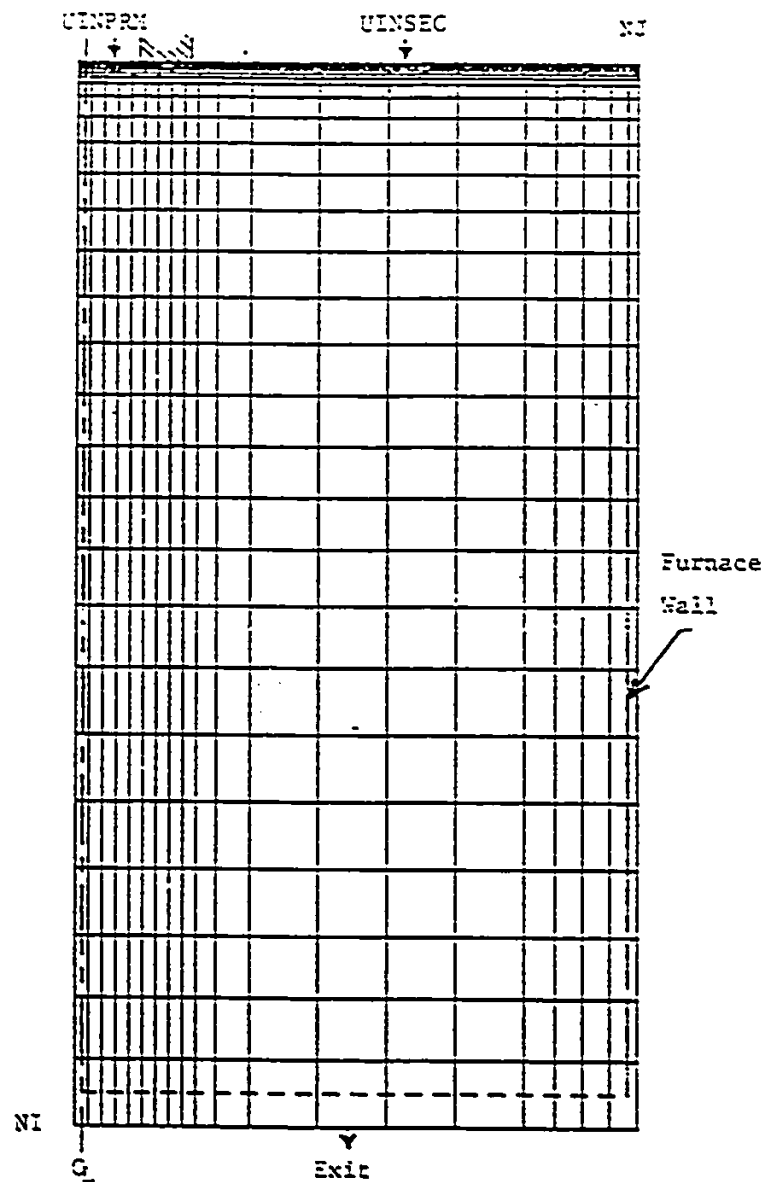


Figure 7: Sample Grid for Laminar Flow Furnace [7]

and comparing these to the analytical solution for this problem. Although the total amount of work involved is not significantly changed, a simpler method with a small step length gives similar accuracy to a more complex method with a larger step length [40]. As the particle heating program already is limited to small step sizes (maximum time step is 5 ms) in the prediction of the particle temperature and velocity, the simpler methods of numerical integration were that investigated are:

- summation - the integration is performed by assuming that the level of the ordinate is constant throughout the step:

$$I = y_1 \cdot (x_2 - x_1) \quad (4.3)$$

where the subscripts 1 and 2 refer to the beginning and end of the integration step respectively.

- trapezoid rule - in trapezoid rule, the value of the integral is the arithmetic average of the two ordinates multiplied by the distance between them:

$$I = \frac{1}{2}(y_1 + y_2)(x_2 - x_1) \quad (4.4)$$

- Simpson's rule - Simpson's rule for three points is based on fitting a quadratic to three equally spaced data points. The resulting equation is:

$$I = \frac{1}{6}(y_1 + 4y_2 + y_3)2h \quad (4.5)$$

In the particle heating program, the maximum temperature step was limited to 5 K, and therefore during particle heatup the magnitude of the time step can vary. This eliminates Simpson's rule, as this method requires equal spacing between the three points used in each integration step.

The exact solution of the first order reaction equation for the weight loss of a particle undergoing exponential heating with a time step of 5 ms is shown in figure 8 with

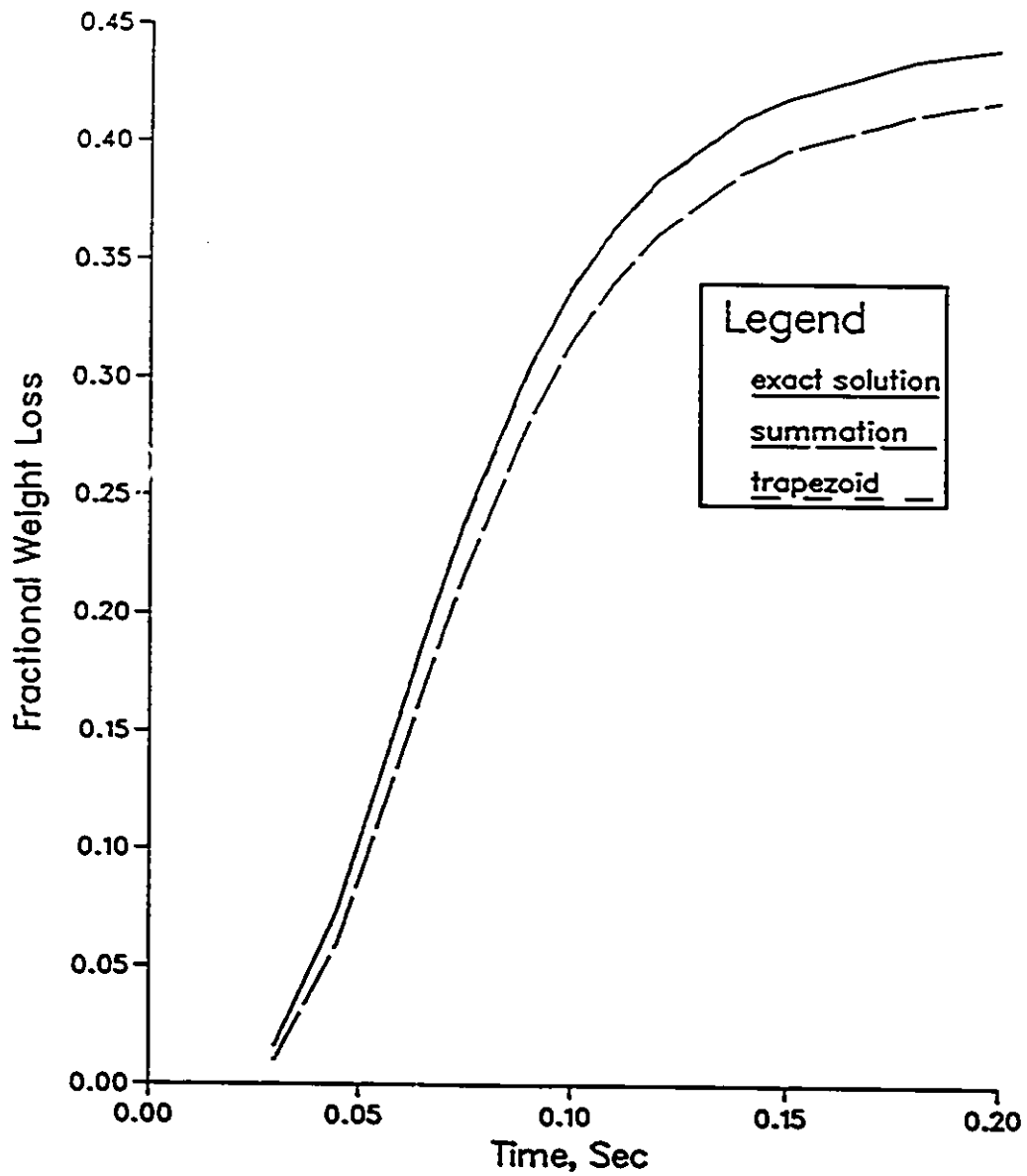


Figure 8: Weight Loss Versus Time for Particle Undergoing Exponential Heating

the predictions of the equation numerically integrated using either the summation or the trapezoidal rule. The results suggest that although the method of summation is inaccurate, the trapezoid rule has sufficient accuracy to very closely approximate the exact solution. The accuracy of the method of numerical integration will have even more importance with the two competing reaction model, equation 4.1, which requires two integrations to be performed in order to solve the equation.

4.2 Effects of mass transfer

The particle heating program solves for the particle velocity and temperature as it passes through the furnace flow field. The acceleration of the particle is given by:

$$\frac{du_p}{dt} = g - \frac{3c_d\rho}{4\rho_p d_p} (u_p - u) |u_p - u| \quad (4.6)$$

For small Reynolds numbers, this equation can be linearized as:

$$\frac{du_p}{dt} = g - A(u_p - u) \quad (4.7)$$

where

$$A = \frac{18\mu}{\rho_p d_p^2} (1 + 0.15Re_o^{0.687})$$

$$Re = \frac{\rho |u_p - u| d_p}{\mu}$$

The bracketed term in A is a correction to Stokes' law for $Re > 1$. With a small time step, Δt , u and Re can be assumed to be constant and this equation can be integrated directly over Δt since A is a constant:

$$u_p = u - \frac{1}{A} [(g - A(u_{p0} - u))e^{-A\Delta t} - g] \quad (4.8)$$

where u_{p0} is the particle velocity at the beginning of Δt . The original expression for particle heat transfer was:

$$\frac{dT}{dt} = \frac{6}{\rho_p c_{pp} d_p} (q_{rad} - q_{conv}) \quad (4.9)$$

As stated earlier, the value of Δt must be selected so that u , Re , and the gas temperature can be assumed constant. Equation 4.9 can also be integrated analytically in a fashion similar to equation 4.6 if these values are assumed constant over the time step, Δt . The value of Δt was selected by arbitrarily choosing a maximum temperature step, ΔT_{max} , of 5K and therefore

$$\Delta t \approx \frac{\rho_p c_{pp} d_p \Delta T_{max}}{6(q_{rado} - q_{convo})} \quad (4.10)$$

where q_{rado} and q_{convo} are from the previous time step. This results in a small time step initially where the heating is rapid, which gradually increases. A maximum time step of 5 ms was chosen to ensure the gas velocity is nearly constant over the time step.

When the devolatilization model was added to the particle heating program, several modifications were incorporated. Corrections to the convective heat transfer coefficient and drag coefficient are required to allow for the effects of mass transfer from the pyrolyzing coal particle. This can be corrected for by means of the transfer number, B , which is defined as:

$$B = (Y_o - Y_{\infty}) / (1 - Y_o) \quad (4.11)$$

where Y_o and Y_{∞} are the particle surface and ambient mass fractions of volatiles respectively. From simple droplet evaporation theory, this is related to the volatiles mass flux G by:

$$B = \exp(r_o G / \rho D) - 1 \quad (4.12)$$

where r_o is the particle radius, G the mass flux of volatiles, ρ the gas density and D the diffusion coefficient. The drag coefficient is then [41]:

$$c_d = c_{d_o} / (1 + B) \quad (4.13)$$

where c_{d_o} is the drag coefficient of the non-pyrolyzing coal particle:

$$c_{d_o} = \frac{24}{Re} (1 + 0.15 Re^{0.687}) \quad (4.14)$$

$$Re = \frac{\rho |u_p - u| d_p}{\mu}$$

The net effect is that the drag coefficient is decreased by the transfer because the boundary layer thickness is increased, lowering the skin friction, and the wake region is filled, leading to a reduction in form drag. The heat transfer coefficient becomes [41]:

$$h = h_o \ln(1 + B)/B \quad (4.15)$$

where h_o refers to the convective heat transfer coefficient in the absence of mass transfer [24]:

$$h = [2.0 + (0.4Re^{0.5} + 0.6Re^{0.66})(Pr^{0.25})(\frac{\mu}{\mu_p})^{0.25}] \frac{\mu c_p}{Pr d_p} \quad (4.16)$$

At small mass transfer rates, equation 4.15 reduces to h being equal to h_o , since $\ln(1 + B) \sim B$ for small B . Mass transfer decreases the values of the convective heat transfer coefficient, again because of the increased thickness of the boundary layer. The thermal conductivity of the gas in equation 4.16 is substituted using the definition of the Prandtl number:

$$Pr = \frac{c_p \mu}{k} \quad (4.17)$$

so that

$$k = \frac{c_p \mu}{Pr} \quad (4.18)$$

where the heat capacity of the gas is estimated using correlations from Reid, Prausnitz, and Sherwood [42], and the gas viscosity is fitted by the Sutherland equation [17]:

$$\mu = \frac{BT^{1.5}}{T + S}$$

where B and S are constants. The mass transfer from a devolatilizing coal particle (using parameter estimates determined by Kobayashi [1]) can be seen in figure 9 to have a negligible effect on the particle temperature.

The original particle energy balance was modified by including the heat of pyrolysis term:

$$\frac{dT}{dt} = \frac{6}{\rho_p c_{pp} d_p} [q_{rad} - q_{conv} - GH_T] \quad (4.19)$$

where G is the instantaneous mass flux from the particle surface and is equal to:

$$G = (\Delta V \cdot \rho_p \cdot V_p) / (A_s \cdot \Delta t)$$

where:

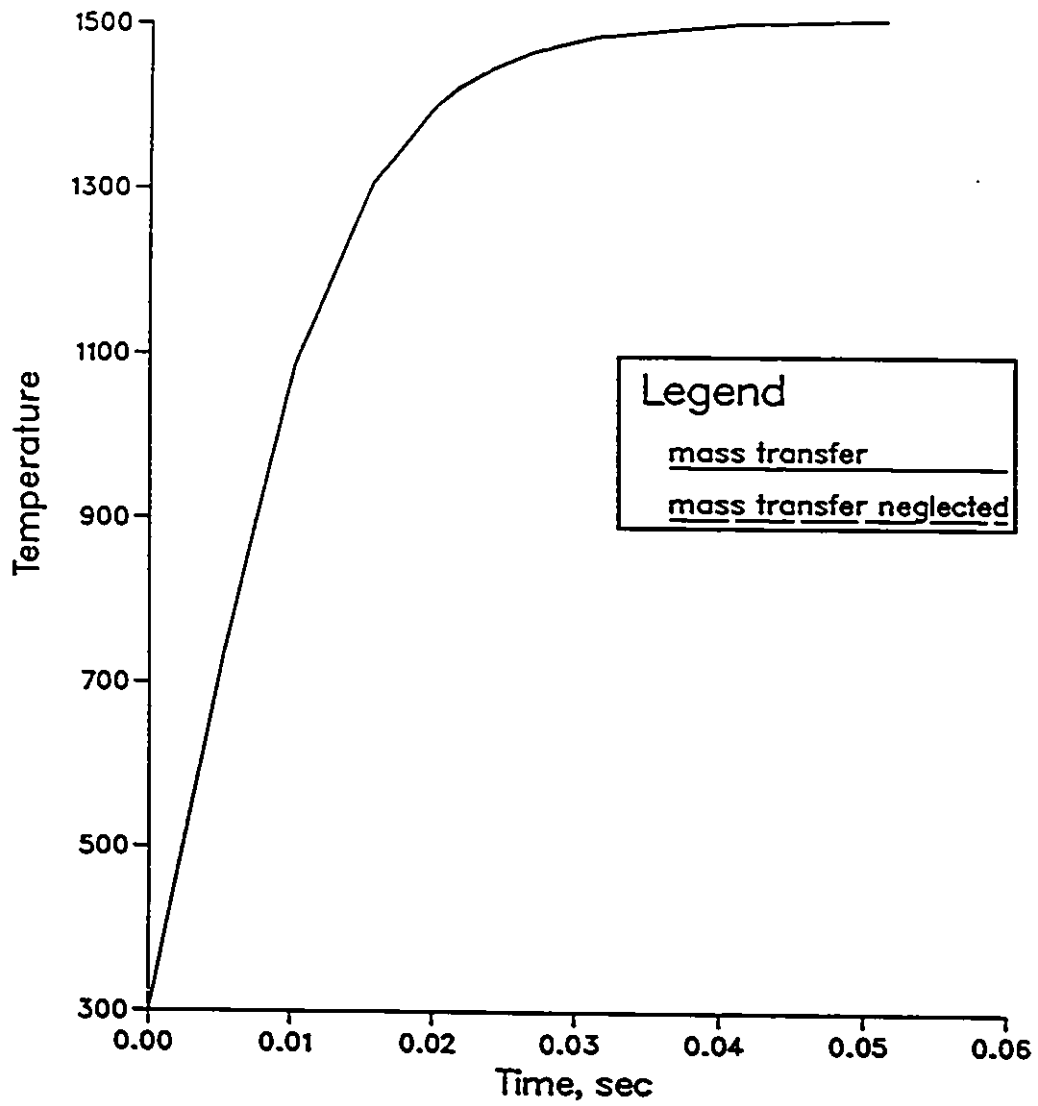


Figure 9: Effects of Mass Transfer on a Devolatilizing Coal Particle

- ΔV - the change in weight loss during the time step
- V_p - the particle volume
- A_s - the particle surface area

4.3 Physical properties of coal

Modeling of coal pyrolysis requires data for physical properties of coal such as the specific heat, density and emissivity. There is little variation in the estimates of the coal emissivity which is generally listed [24,25] as:

$$\epsilon = 0.8 \quad (4.20)$$

Unfortunately, there is a basic lack of specific heat and density data, so estimates of these properties of coal have been used in this study. These estimates for a substance like coal, which changes both chemically and physically when heated, are questionable. The estimates of these properties are even questionable for unheated coal because of the difficulty in accounting for the strong effects of coal rank, mineral matter and moisture content. The method of selection of estimates by other experimenters will be reviewed.

4.3.1 Specific heat

Merrick [8] found that the specific heat of coal usually increases with temperature and volatile matter. The specific heat of coal and coke was modelled based on atoms oscillating in the solid matrix. It was postulated that as the coal devolatilizes, the loss of hydrogen content results in the specific heat approaching the lower curve for coke. Figure 10 also shows that the specific heat generally could be considered to remain constant at a value of 2000 J/kg K in the temperature range of interest. However, it should be noted that this model predicts the specific heat for coals heated at lower heating rates and lower temperatures than a coal particle would experience upon entering a combustor. The dependence of the

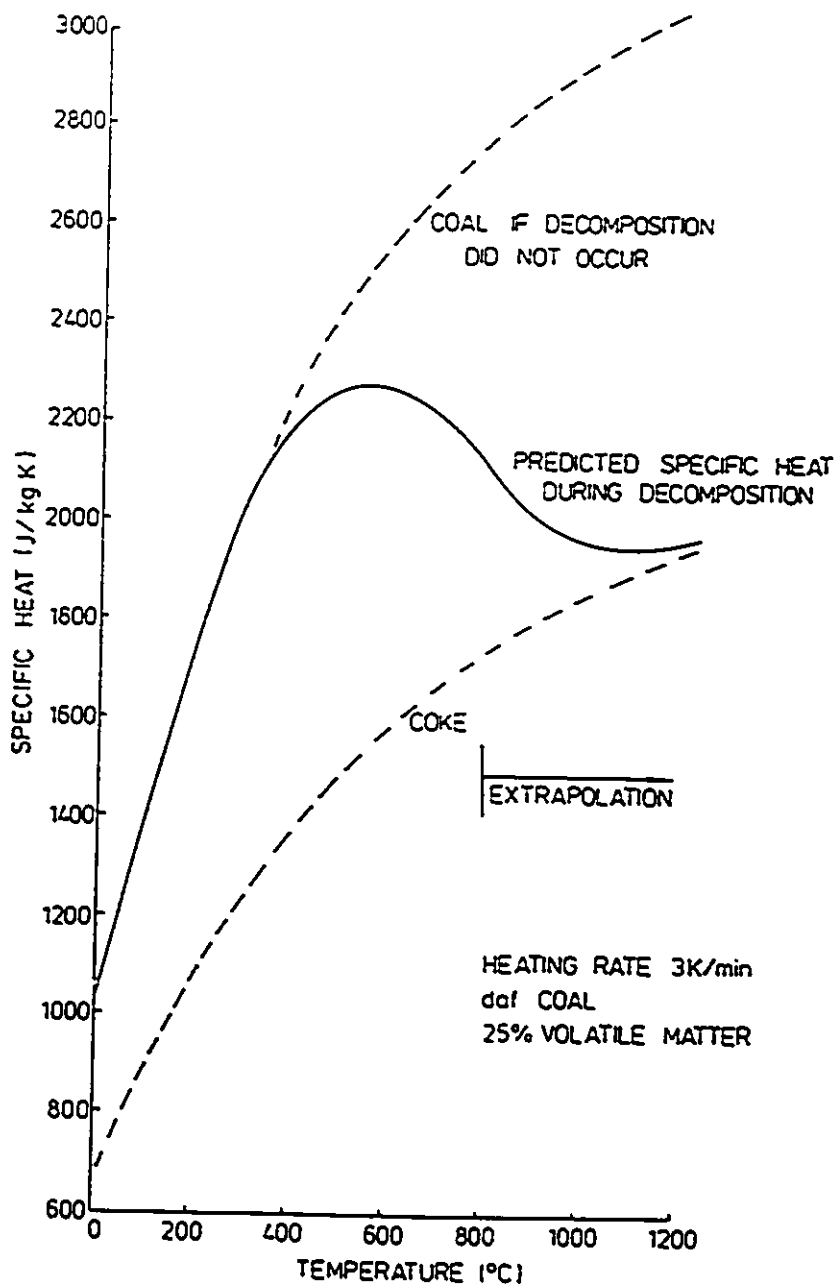


Figure 10: Predictions of the Specific Heat of Coal and Coke [8]

specific heat on devolatilization would suggest that specific heat could also depend on the heating history. Merrick stated that this comparatively high specific heat included the endothermic heat of pyrolysis.

Kobayashi [1] found that the specific heat of raw coal increases with increasing volatile matter and moisture content but decreases with increasing ash content. Coals with volatile matter in the range of forty percent were found to have specific heats around 1255 J/kg K. The specific heat was also found to be affected by the physical and chemical changes of the coal during heating. It was found that for a given heating rate, the position of the specific heat maximum is displaced towards higher temperatures as the volatile matter of the coal decreases. Chars produced from coals with volatile matter in the range of thirty to forty percent would be expected to have a specific heat value of 1380 J/kg K.

Eisermann et al. [43] presented a method of estimating the specific heat of coal and char. This method is based on the summation of specific heats weighed by the respective mass fractions of the different components: moisture, primary volatile matter, secondary volatile matter, fixed carbon, and ash. The evaluation of the original fraction of volatile matter in the coal or char is found by a correlation which utilizes the composition of the coal or char as determined by ultimate analysis. The secondary volatile matter is taken to be ten percent if the total volatile matter content is greater than ten percent and equals the total volatile matter if the amount is less than or equal to ten percent. The primary volatile matter is taken to be the amount in excess of ten percent. It should be noted that this seemingly arbitrary categorization of the volatile matters, as well as the evaluation of the amount of original volatile matter, is highly questionable. The specific heat of each component is then estimated using correlations with the devolatilization temperature as the only variable. The specific heat of coal and char is determined by a weighted summation of the different components. The difference between the specific heats of coal and char is determined mainly by their different compositions. There are two main problems with this method: first, the correlations that determine the specific heat of each component are based solely on temperature and therefore are highly specific; secondly, the use of broad categories

as 'primary volatile matter' results in the model not being able to account for the variations in composition of these mixtures [38].

The majority of researchers did not list the physical properties used for coal. Of the researchers that did, the estimate that was used in calculations was merely stated with little or no discussion. The specific heat estimates used by these researchers [44,20,45,28] varied from 1255-4187 J/kg K.

The specific heat of coal is not well documented and there is much uncertainty in the values listed, particularly as it is difficult experimentally to separate the specific heat and the heat of pyrolysis. These two must be separated, however, since the devolatilization process depends on the temperature and heating history. Hence Merrick's data [8] is unusable. As Kobayashi's devolatilization data was to be used in determining rate constant estimates, it was decided that to be consistent it would be best to use the specific heat estimate for char listed by Kobayashi (1380 J/kg K), as it is also an 'intermediate' value of all the specific heat estimates listed. A realistic value could be expected to lie between the specific heat of pure carbon (750 J/(kg K) at room temperature [25]) and those of typical liquid hydrocarbons (roughly 2000 J/(kg K)); this rules out the larger values reported in the literature.

4.4 Heat of Pyrolysis

A complete energy balance on a devolatilizing coal particle must include the endothermic heat of coal devolatilization. Heats of reaction in the range of $10^5 - 10^6$ J/kg are not unreasonable when considering thermal bond breaking processes such as:



However, the heat of pyrolysis, which theoretically could be calculated from the heats of formation of reactants and products, is in practice unknown.

Maloney and Jenkins [20] listed the heat of reaction to be in the range of 2.1E5 to

4.2E5 J/kg coal. Stickler et al. [45] included the heat of pyrolysis for each reaction in a two competitive reaction scheme as 1.675E6 and 8.37E5 J/kg for the low and high temperature reactions respectively. Tsai and Scaroni [46] predicted a temperature drop of 5-25 K for a heat of pyrolysis of 1.67E6 J/kg. It should be noted that these researchers listed the values of the heat of pyrolysis with little or no discussion. For the sake of comparison, the heat of combustion of coal ranges from 20E6 to 35 E6 J/kg and a typical hydrocarbon from 40E6 to 45E6 J/kg.

Mahajan et al. [23] tested the heat of pyrolysis at temperatures up to 853K using a thermal analytical technique called differential scanning calorimetry, in which the heat flow between the sample and reference material is measured. The heat of pyrolysis varied from -1.2E5 to 2.8E5 J/kg and was an irregular function of carbon content that had a maximum in exothermicity and endothermicity around 71% and 81% carbon respectively. It should be noted that there was some question about the results, since after correction for weight changes, the exothermic effects observed in uncorrected curves became either entirely or partly endothermic.

Freihaut [9] tested the effect of the heat of reaction, which was varied from 0-4.2E6 J/kg, upon the predicted temperature internal profiles of a 100 μm particle. From figure 11, it can be seen that the maximum temperature difference predicted inside the particle is 150K.

This survey shows that there is wide disagreement as to the value of the heat of pyrolysis: it is very difficult to measure, and will almost certainly vary with coal rank and ultimate yield. In performing measurements of the heat of pyrolysis, it is easy to confuse it with evaporation of moisture or the variation of specific heat with temperature. In view of this, an intermediate value of the heat of pyrolysis, 8.37E5 J/kg, was arbitrarily selected for the model. The sensitivity of the model to the value chosen was tested by making sample calculations for the Kobayashi furnace [1]. The heat of pyrolysis can be seen in figure 12 to have but a slight effect upon the particle temperature: the comparison of the temperature variation due to the heat of pyrolysis to the weight loss versus time history

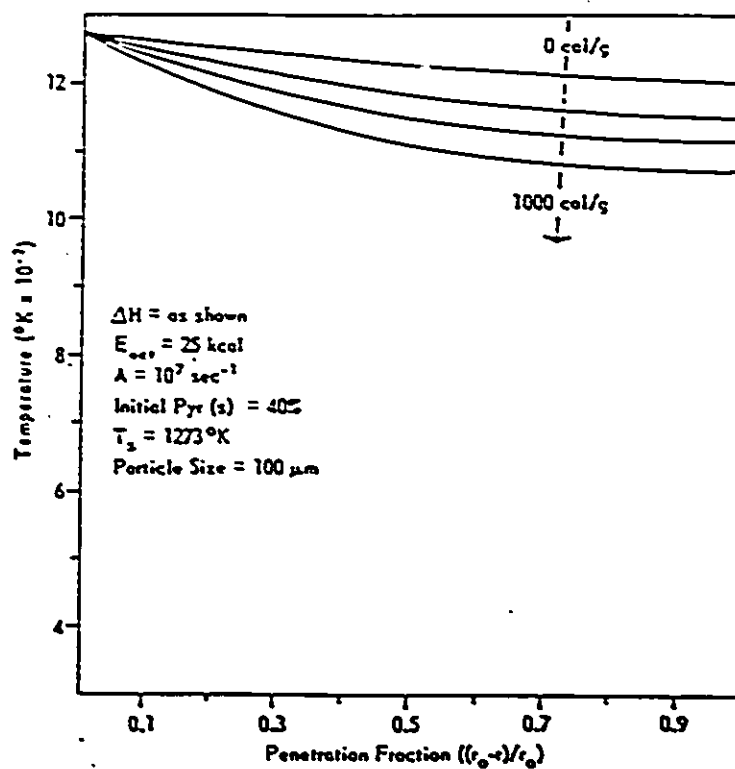


Figure 11: Effect of Heat of Reaction on Internal Temperature Profile [9]

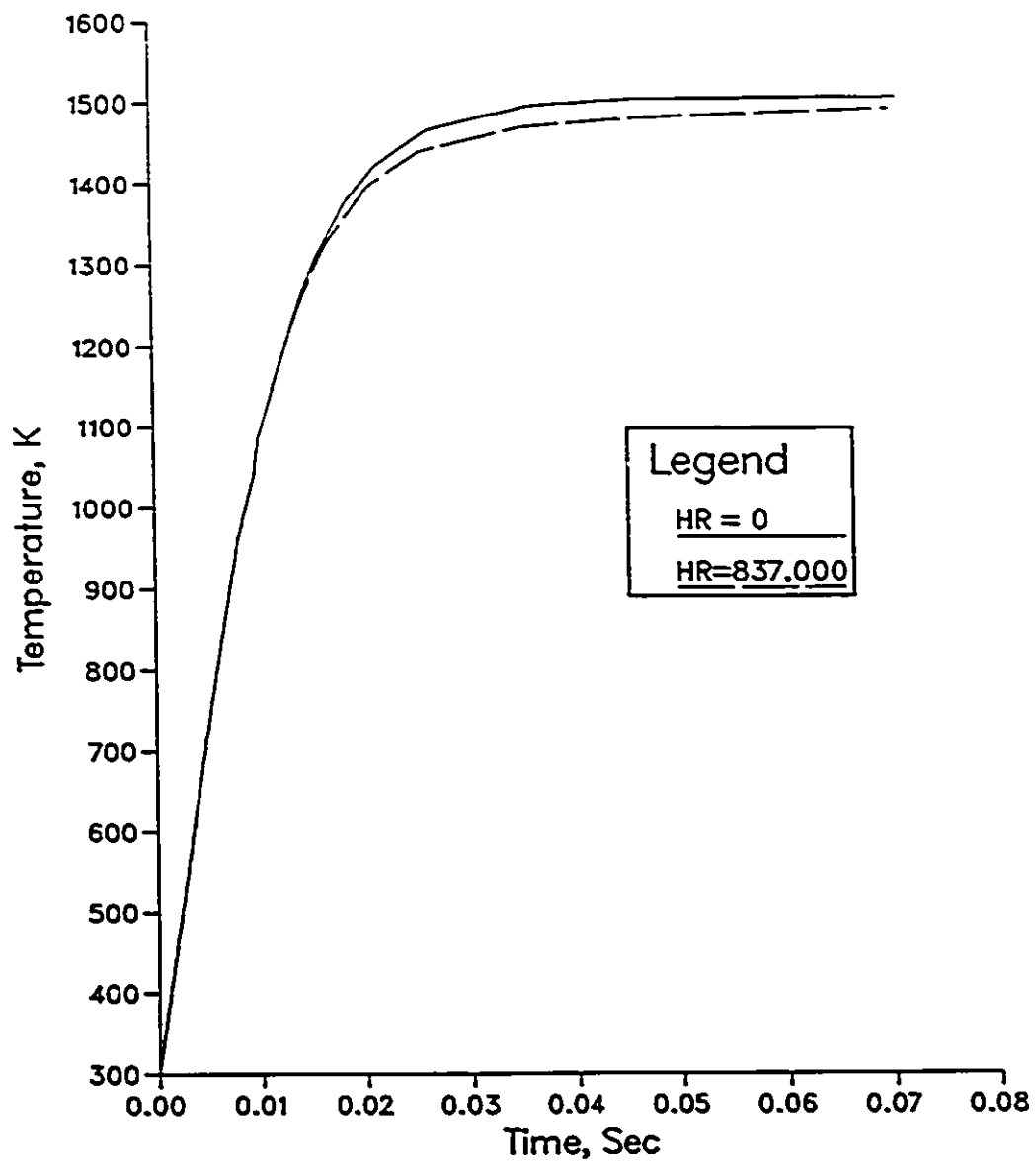


Figure 12: Effect of heat of pyrolysis on particle temperature

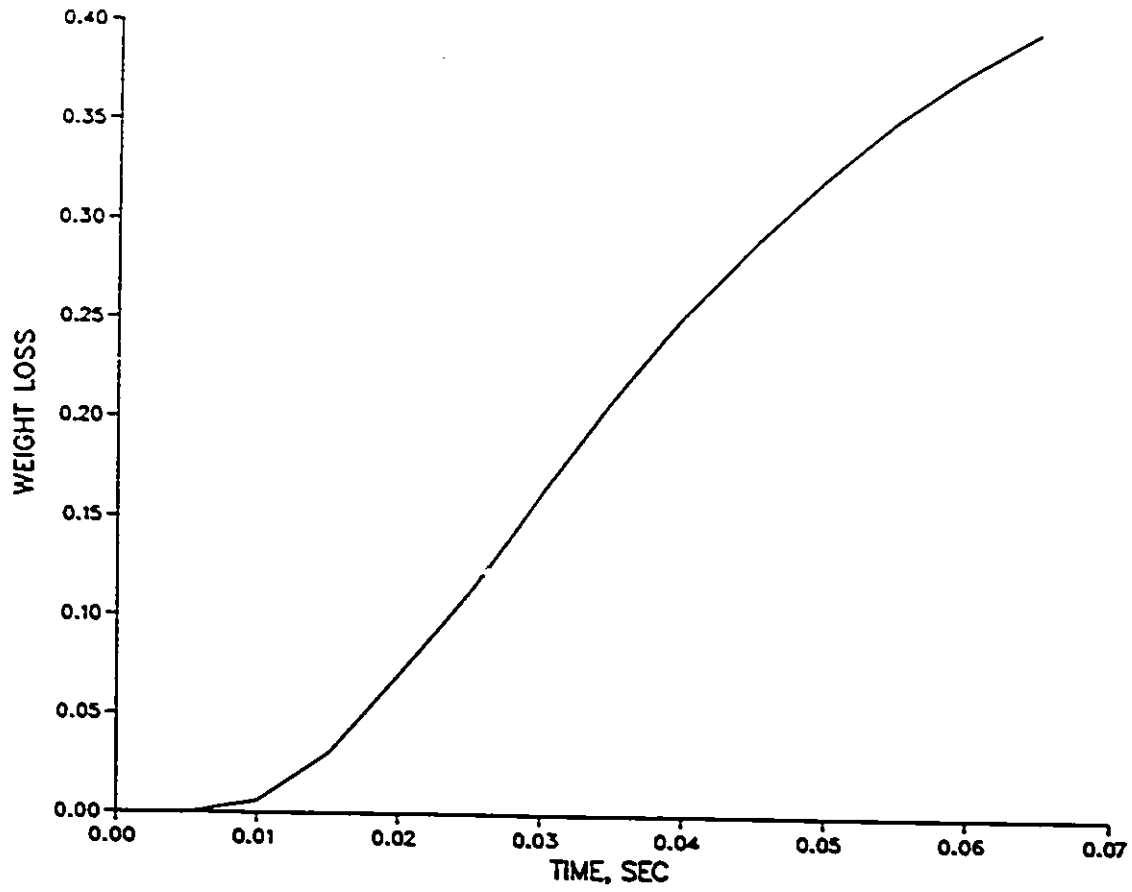


Figure 13: Weight Loss Versus Time for particle in 1510K furnace

shown in figure 13 shows that the effect on the particle temperature becomes the most significant, as expected, in the later stages of the devolatilization once a significant portion of the particle has devolatilized. These results suggest that little attention needs to be devoted to accurate evaluation of the heat of pyrolysis.

4.4.1 Density and Diameter Behavior

Coal undergoes considerable physical change upon heating. One of these changes is swelling, which is of particular interest as it could result in clogging of experimental or industrial equipment. Researchers have identified two different types of behavior during devolatilization:

- particle diameter remains relatively constant but density decreases as devolatilization proceeds. This behavior has been verified by visual observation of lignite coal particles after devolatilization experiments [1,4,27,47].
- particle diameter increases and density decreases as well. This behavior also has been substantiated by visual observation [15,27,47,48,49,50,51] of bituminous coals.

The ASTM free swelling index measures the tendency of coal to swell when burned or gasified in a fixed or fluidized bed; however, it is not recommended as a method of determining the expansion of coal in coke ovens [14]. Swelling coals are generally medium to high volatile bituminous coals which become plastic on heating.

Constant particle diameter

The changing density of a constant volume particle can be calculated as:

$$\rho = \rho_o MAFR(1 - V) + (1 - MAFR)\rho_o \quad (4.21)$$

where

- MAFR represents the moisture and ash free fraction of the coal
- ρ_o is the original density of the coal particle
- V is the fractional weight loss of coal on a moisture and ash free basis

The second term corresponds to the ash in the coal particle which is assumed to remain constant. The first term corresponds to the devolatilizing mass of coal. Equation 4.21 can be further reduced to:

$$\rho = \rho_o(1 - MAFR \cdot V) \quad (4.22)$$

Changing particle diameter and density

Several researchers [48,36] have addressed the problem of changing particle diameter by using a swelling factor. Coal particles have been observed to swell by as little as ten percent to as much as ten times the original particle diameter. A suggested model for changing particle diameter [48,36] is as follows:

$$d = d_p(1 + (S_{sw} - 1)(1 - X_v)) \quad (4.23)$$

where

- d_p - original particle diameter
- S_{sw} - ratio of swelled particle diameter to original diameter
- X_v - fraction of volatiles not yet released

One serious problem with this method is that it requires an estimate of the ultimate yield, which however is a function of temperature and heating history and is not known until the devolatilization is complete. An alternative method of predicting the particle diameter would therefore be desirable, but no other expression has been devised as yet.

The density of the particle is linked with the changing particle diameter by the following equation:

$$\rho = \rho_o(1 - MAFR \cdot V) \cdot \frac{d_p^3}{d^3} \quad (4.24)$$

where

- d_p - initial particle diameter
- d - current particle diameter

Calculations in appendix B show that if the particle diameter increases, the heat transfer by convection increases as d/d_p , while the heat transfer by radiation could increase as $(d/d_p)^2$. Although Kobayashi [1] did not record the diameter of the devolatilizing coal particles during the devolatilization experiments, additional experiments were conducted in which the changing diameter of the coal undergoing pyrolysis was recorded. The determination of the particle temperature at the point of the last observation at which there is minimal particle size change indicates that the particle is essentially heated up to furnace temperature before any significant particle size change occurs, thereby minimizing any change in heat transfer due to particle size. The effect of particle size on particle motion is also checked in appendix B, which indicates that there is no significant change in velocity associated with the increased size of the particle. Because of this, and because of the problems associated with modelling the swelling of the particles, only the constant particle diameter equation has been incorporated into the computer program in the present work. Although the particles in this study reached furnace temperature before significant swelling occurred, this might not be true for other furnaces and the change in heat transfer rates could seriously effect the accuracy of the particle heating program and therefore this problem should be investigated and a more acceptable equation to describe changing particle diameter should be developed.

Table 3: Kobayashi Furnace Dimensions

	size, inches
burner	.047 ID 3/16 OD
reactor tube	2 ID

Chapter 5

Fitting Routine

A part of the object of this study is devising a procedure for fitting devolatilization reaction constants to experimental data. This chapter describes a trial fitting procedure, which in the following chapter will be applied to the data of Kobayashi [1] to test its utility. Future work with this procedure may result in further modifications; in particular, experience may allow for elimination of some of the steps used to get initial estimates of the parameters.

The two reaction model:

$$V = \int_0^t (\alpha_1 k_1 + \alpha_2 k_2) c dt \quad (5.1)$$

where

$$c = \exp \int_0^t -(k_1 + k_2) dt$$

is to be fitted to the experimental data with the following parameters to be estimated for each of the reactions:

- α_i - the ultimate yield
- k_{oi} - the pre-exponential constant in the Arrhenius rate expression

- E_i - the activation energy of each reaction path

A two part procedure was required for fitting. The model is intrinsically nonlinear and therefore a non-linear regression routine is required. However, as the convergence of the non-linear routine to a solution proved to be greatly dependent upon the quality of the initial estimates, an approximate model using isothermal devolatilization and linear regression was first used to get initial estimates. The first part therefore assumed that devolatilization occurred isothermally, while the second part incorporated the full heating history of the particle and therefore involved non-isothermal devolatilization. Each part of the analysis had several steps which will be listed in full.

5.1 Isothermal fitting procedure

The isothermal analysis was performed by assuming the particle temperature was constant and equal to that of the furnace. The heating histories of the particles were examined and any data obtained at a temperature deviating from the furnace temperature by more than about twenty percent were omitted from this section of the analysis. The isothermal fitting of the data was performed using SAS [52], which is an acronym for Statistical Analysis System. The first SAS procedure used is the REG procedure which is used to fit least squares estimates to linear regression models. Least squares estimates of the parameters of non-linear models are produced using the SAS procedure called NLIN. Non-linear models are more difficult to specify and estimate than linear models, for linear models require simply the independent and dependent variables to be listed, while for non-linear models one must write the regression expression, guess starting values and specify derivatives of the model with respect to the parameters.

The isothermal fitting procedure is broken down into several steps to produce initial estimates for the non-isothermal fitting procedure. In the first step, the single first order

reaction model

$$V = \alpha_1(1 - \exp(-kt)) \quad (5.2)$$

$$k = k_o \exp E/RT$$

with the parameters α_1 , the ultimate yield at temperature T , and k , the reaction rate constant, for all of the temperature runs was fitted to the isothermal weight loss data using NLIN. The process of selecting starting values for the parameter estimates that are required by NLIN is simplified since α , the ultimate yield, can only logically vary between 0 and 1.

The second stage of the isothermal fitting routine is to produce initial estimates of the pre-exponential constants and activation energies of each reaction. With estimates of k at several different temperature levels, the Arrhenius equation is linearized to the form

$$\ln k = \ln k_o - E/RT \quad (5.3)$$

This linearized equation is fitted to the data with the SAS linear regression procedure called REG by fitting $\ln k$ versus $1/T$. In the use of least squares, one of the assumptions made about the pure error of the data is that its variance is constant over the region of the operating variables used to collect the data. The logarithmic transformation used to convert the rate expression from a non-linear to a linear expression can lead to a violation of this assumption. Therefore, this procedure is used to get initial estimates of k_o and E from the slope and intercept of the fitted line, which are then to be used in the non-linear fitting routine. This leads to the third step of the isothermal fitting routine in which the reaction rate constants, k_o and E , are fitted non-linearly

$$k = k_o \exp E/RT \quad (5.4)$$

with the linear estimates input as the required initial estimates. The last step in the isothermal fitting is fitting

$$V = \alpha(1 - \exp(-k_o \exp(-E/RT)t)) \quad (5.5)$$

non-linearly using the isothermal data. The value of α was set to the least squares estimate found during the first step of the fitting routine. This step is important, for the parameter estimates determined in this step are not dependent on the values of k produced in step one as the parameter estimates found in the previous two steps are. The results of the non-linear fitting of the rate constant parameters are used as initial estimates of the parameters for the non-isothermal fitting routine. Although not all the values of the parameter estimates from this step are required as initial estimates of the parameters in the non-isothermal procedure, they are all included to verify that this procedure converges to a single solution regardless of the initial starting values.

5.2 Non-isothermal fitting procedure

The second part of the fitting procedure incorporates the full heating history of a particle at a given furnace temperature. The full heating history of the particle is important to the devolatilization process, since the longer the heat-up time is the greater the effect the first reaction has on the pyrolysis of a particle heated to elevated temperatures. The fitting routine used in this procedure is an IMSL routine [53] called ZXSSQ. IMSL is a system of Fortran subroutines for mathematics and statistics, in which ZXSSQ is a derivative-free routine that finds the local minimum of the sum of squares of non-linear equations. One of the major advantages to ZXSSQ is that it eliminates the need for explicit derivatives. This is a very important consideration since the full model:

$$V = \int_0^t (\alpha_1 k_1 + \alpha_2 k_2) \exp\left(\int_0^t -(k_1 + k_2) dt\right) dt \quad (5.6)$$

cannot be easily integrated analytically. As the pyrolysis is non-isothermal, the temperature change with time must be incorporated into the integral. An examination of a typical temperature-time profile, figure 14, shows that the best function to describe its behavior is an exponential function as used by Badzioch and Hawksley [15]. However the first integration results in exponential integrals which in turn need to be integrated. These problems

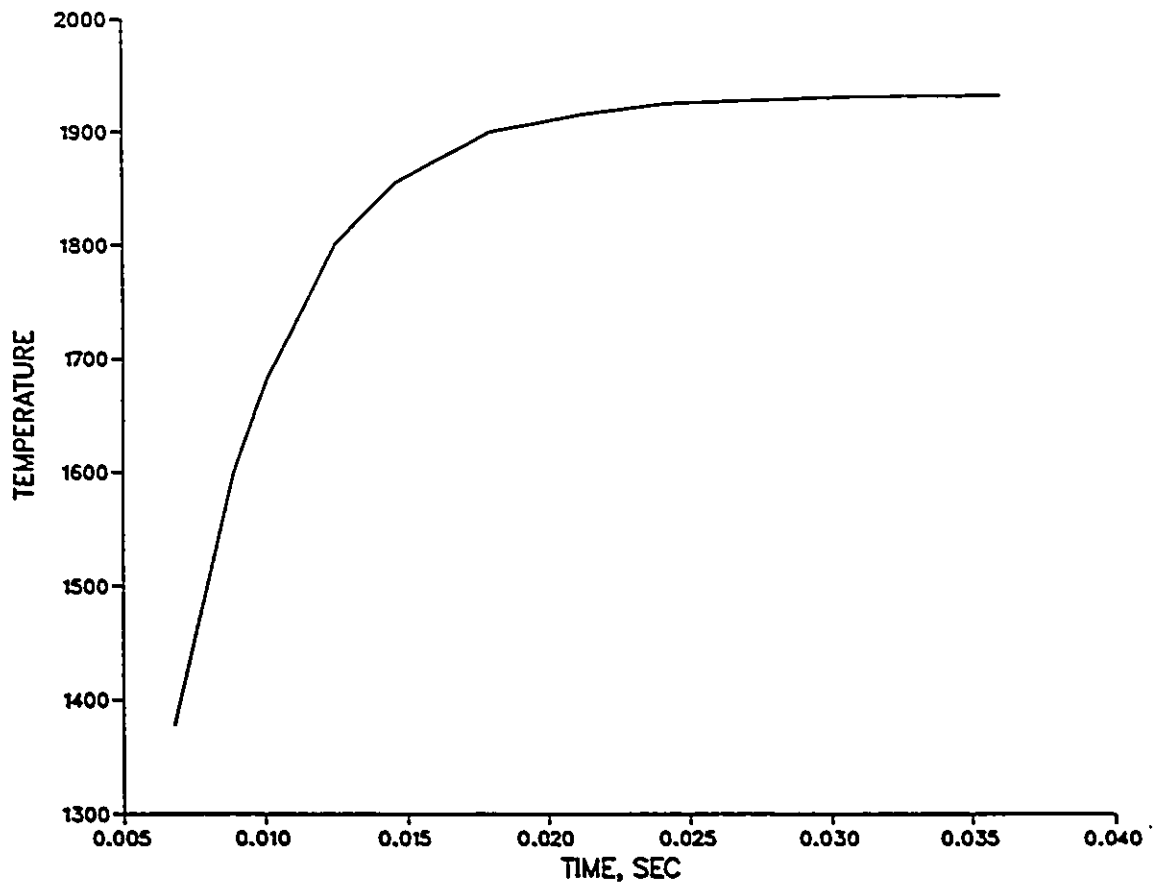


Figure 14: Typical Temperature-time History of a Coal Particle in a Laminar Flow Furnace

make an analytical integration of this model very difficult and therefore explicit derivatives could not be found. ZXSSQ was used as the explicit derivatives were not required and the integration could be performed numerically using the trapezoid rule. ZXSSQ requires that the residuals be supplied by the user:

$$f(x) = y_u - g(x) \quad (5.7)$$

where:

- y_u - observed response, which in these experiments is the weight loss of the coal particle to time t
- $g(x)$ - function defining the non-linear model, equation 5.6

Being a non-linear least squares routine, ZXSSQ requires initial estimates and these were taken from the isothermal fitting routine described above.

In integrating equation 5.6 to determine $g(x)$, the time step was taken as the spacing between the data points. As this could require rather large steps to be taken in this procedure as compared to the particle heating routine, the results can still only be approximate, depending upon the spacing of the data. The particle temperatures were taken from the particle heating program using the parameter estimates determined by Kobayashi [1,10] for the two competitive reaction model. Although it would seem inconsistent to use these particle temperatures to fit new parameter estimates, the heat of reaction and mass transfer from the devolatilizing particle can be seen in figures 9 and 12 to have a negligible effect on the temperature of the particle. The accuracy of the integration would of course be improved by using the smaller time step of the particle heating program; however, this would give calculated points in between the data points an equal weight in the fitting routine as the calculated points that correspond to the data points. This rather crude integration scheme proved capable of producing parameter estimates that fitted the data well, as will be shown in Chapter 6.

ZXSSQ has three convergence criteria [53]. The first criterion is satisfied if on two successive iterations, the parameter estimates agree to a specified number of significant digits. In this study, the number of significant digits was set to six. The second convergence criterion is satisfied if on two successive iterations, the residual sum of squares estimates have a relative difference less than or equal to a second value specified by the user which was set to $1E - 8$. The last criterion is satisfied if the norm of the gradient is less than or equal to a third value, which was set to $1E - 8$ in this study. Convergence is assumed if any one of these criteria is met.

Each set of parameters was fitted by using a representative temperature in each of the groups of high and low temperature runs. At low temperatures, it is assumed that the second reaction has a minimal role in devolatilization, so the first step of the non-isothermal fitting routine is fitting the low temperature estimates using the non-isothermal single first order reaction model. However, this can not be done with the high temperature parameters, since the temperature at which the first reaction has a minimal effect is usually beyond the range of experimental data. This procedure is used to get better estimates of the low temperature constants.

The second step of the non-isothermal fitting routine is fitting the high temperature parameters using the full two reaction model. This was accomplished by fixing the low temperature parameters and fitting the second set of parameters to a suitable run of non-isothermal pyrolysis data. The equation being fit is:

$$V = \int_0^t (\alpha_1 k_1 + \alpha_2 k_2) \exp(-\int_0^t (k_1 + k_2) dt) dt \quad (5.8)$$

where:

- $k_1 = k_{o1} \exp(-E_1/RT)$, where k_{o1} and E_1 are set
- $k_2 = k_{o2} \exp(-E_2/RT)$, where k_{o2} and E_2 are the parameters being fit to the data.

The low temperature parameters utilized were those determined in the first step of the non-isothermal fitting routine. In order to best fit the second set of parameters, it is important that during the second stage of the non-isothermal fitting procedure, the temperature run that is used is high enough that the first reaction has a reduced effect in the devolatilization process.

A technique used to increase the efficiency of the non-linear estimation routine is to center the data about its mean temperature, T^* . The following equivalent Arrhenius expression is then used:

$$k = \theta \exp(-E/R(1/T - 1/T^*)) \quad (5.9)$$

where

$$\theta = k_0 \exp(-E/RT^*) \quad (5.10)$$

The fitting procedure, therefore, searches for the least squares estimates of θ and E , which can then be converted to values of k_0 and E .

5.3 Significance tests

The suitability of the estimated parameters was then tested using residual plots and the R ratio test. In order to explain the R test, some background theory [54] should first be explained. When performing a regression procedure the aim is to reduce the sum of squares of residuals:

$$\begin{aligned} \Sigma e_u^2 &= \Sigma (y_u - \hat{y}_u)^2 \\ &= \Sigma (y_u - \bar{y}_u)^2 + \Sigma (\bar{y}_u - \hat{y}_u)^2 \end{aligned} \quad (5.11)$$

- \hat{y}_u - value of fitted response
- y_u - measured response value
- \bar{y}_u - mean of measured response values at operating conditions u

The first term in equation 5.11 represents pure error or the scatter in the experimental data as determined from replicates in the data. The second term denotes the lack of fit of the model in representing the experimental data. The purpose of the R test is to determine whether the variance of the lack of fit of the model in describing the data is smaller than the variance of the data itself. The R test, which is the ratio of the lack of fit variance to the variance of the data, is compared to the F probability function. The F distribution function has two numbers of degrees of freedom which are the degrees of freedom associated with the two independent variance estimates [54] and therefore the F function is used to determine whether the two variances are the same at the desired probability level. If R is less than F, it suggests that any inadequacy in the fitted model is not significantly larger at the specified significance level of the F function than the experimental error. The sensitivity of this test decreases sharply with the number of degrees of freedom, and thus unless the data contains several replicates this procedure will detect only gross inadequacies in the fitted model.

The second test of significance for the fitted model is the residual plot. A residual plot consists of the residual, the difference between the predicted and measured response value, plotted against the predicted response value. The plots should be examined to detect any unusual behavior, for the residual plot from an adequately fitted model should behave randomly. Any trends in the residual plots would indicate that the model is not accurately describing the experimental data and that some unknown variable is affecting the data.

5.4 Precision of the parameter estimates

The precision of parameter estimates can be described by joint confidence regions which show the degree to which the least squares estimate of one of the parameters depends upon the value of the other parameter. A $100(1 - \alpha)$ confidence region contains the values of the parameters, β , that satisfy the inequality:

$$S(\beta) - S(\hat{\beta}) \leq p\sigma^2 F_{p,\nu,\alpha} \quad (5.12)$$

where

- $S(\hat{\beta})$ - sum of squares at the least squares estimates of the parameters
- p - number of parameters estimated
- σ^2 - estimate of pure error variance with ν degrees of freedom
- F - F distribution having p and ν degrees of freedom

As there are more than two parameters being fitted in this study, the confidence regions will be dealing with two parameters at a time with the other parameters being set to their least squares estimates. As a result, the confidence regions shown in this study are actually conditional confidence regions.

Chapter 6

Application of Fitting Procedure

In this chapter the fitting procedure outlined previously will be tried out on the data of Kobayashi [1]. The furnace used by Kobayashi for data collection was a laminar flow furnace in which the coal samples were entrained in a argon primary gas flow and injected into the center of a preheated argon secondary gas flow. The data were collected at six different furnace temperature levels for two different coals, a lignite and a high volatile bituminous coal, and are shown in figures 15 and 16.

6.1 Comparison of Particle Heating Calculations

The first step of the analysis is the determination of the heating history of the coal particles. In collecting data, Kobayashi recorded the distance between the injector and the collector, the coal mass flowrates, and the primary and secondary gas flowrates. Table 4 contains the operating conditions of the furnace heated to different temperatures for the two coals. The particle heating program [17], suitably modified to represent Kobayashi's reactor as described in chapter 4, was then run to determine the residence times and temperatures of the particles at the injector distances specified.

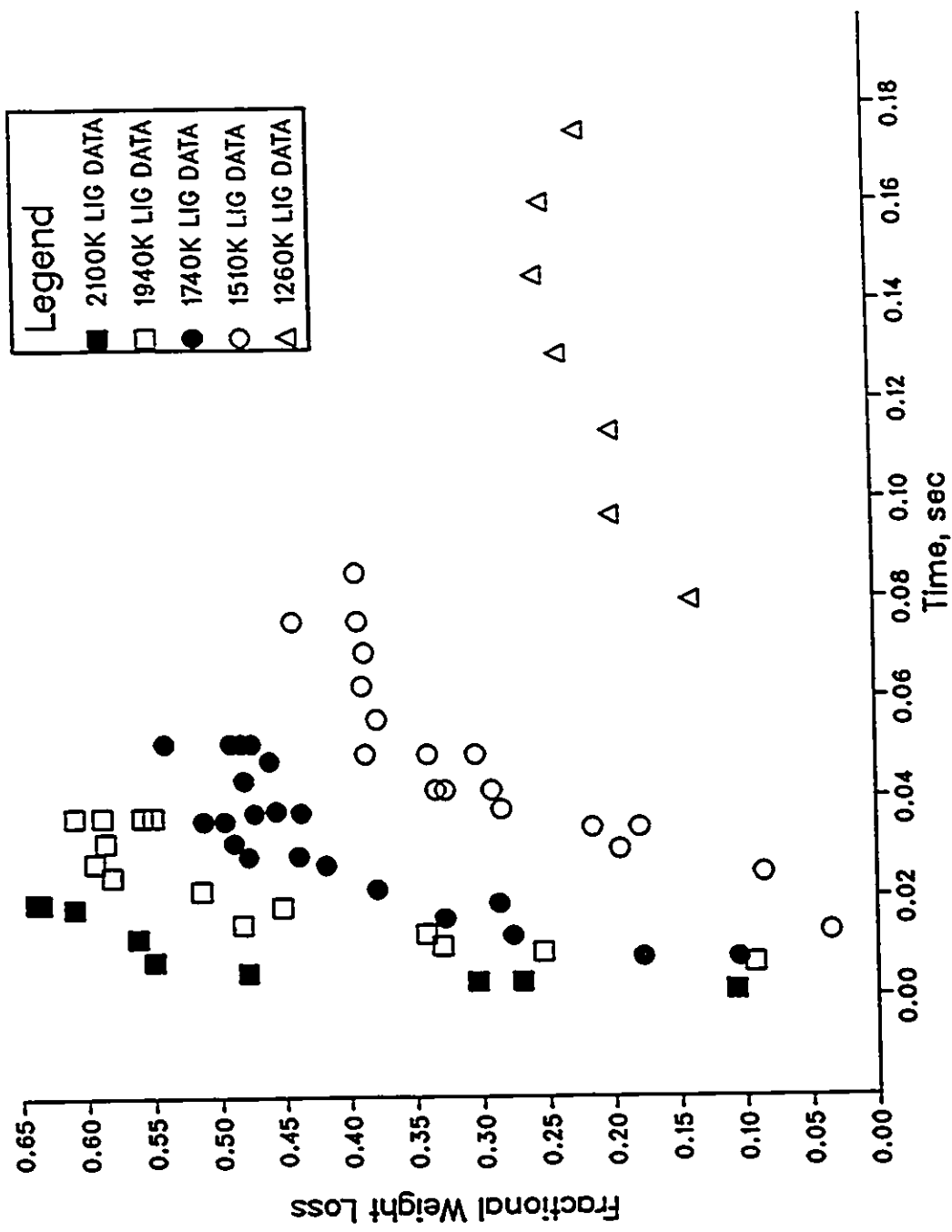


Figure 15: Weight loss versus residence time for lignite coal

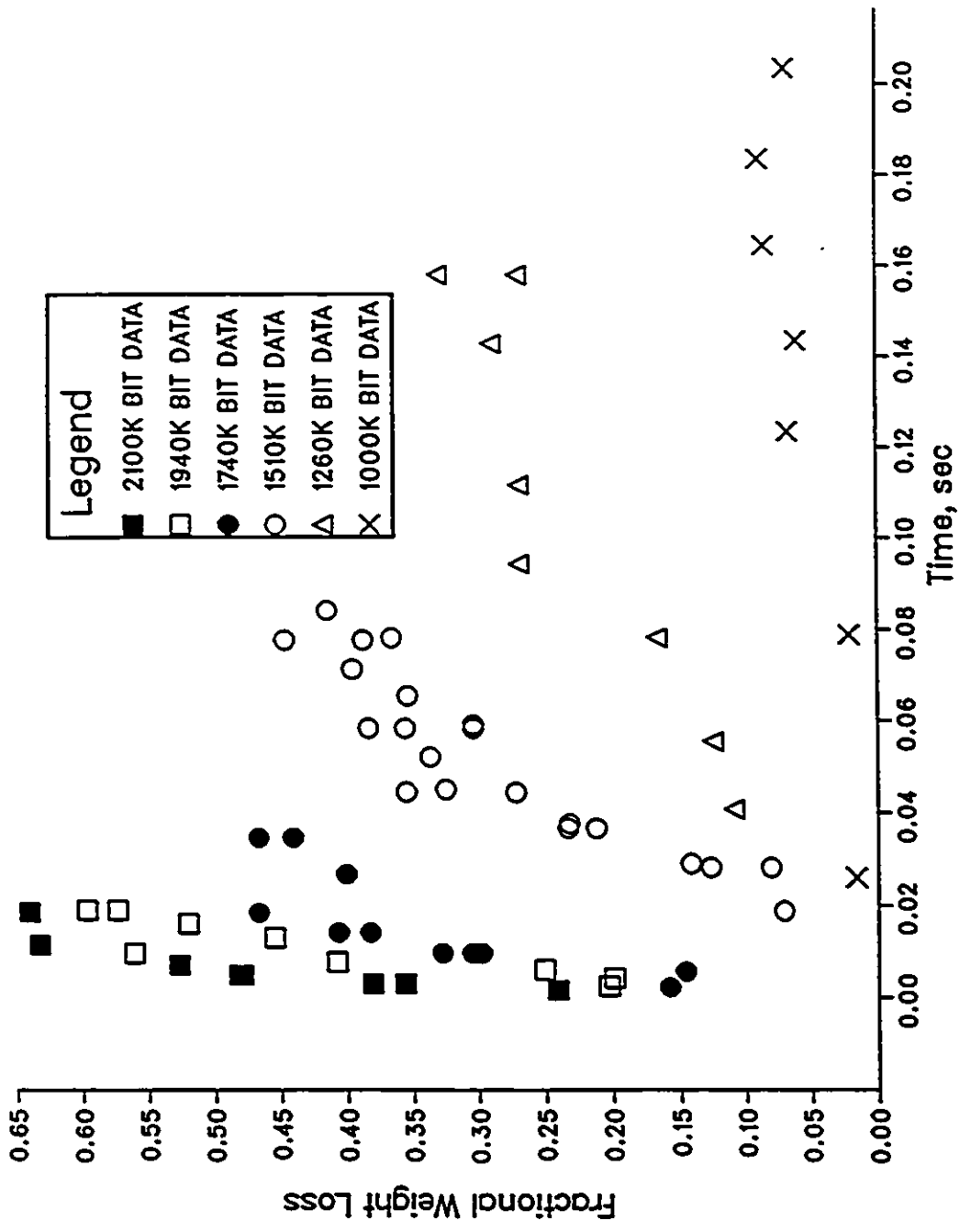


Figure 16: Weight loss versus residence time for bituminous coal

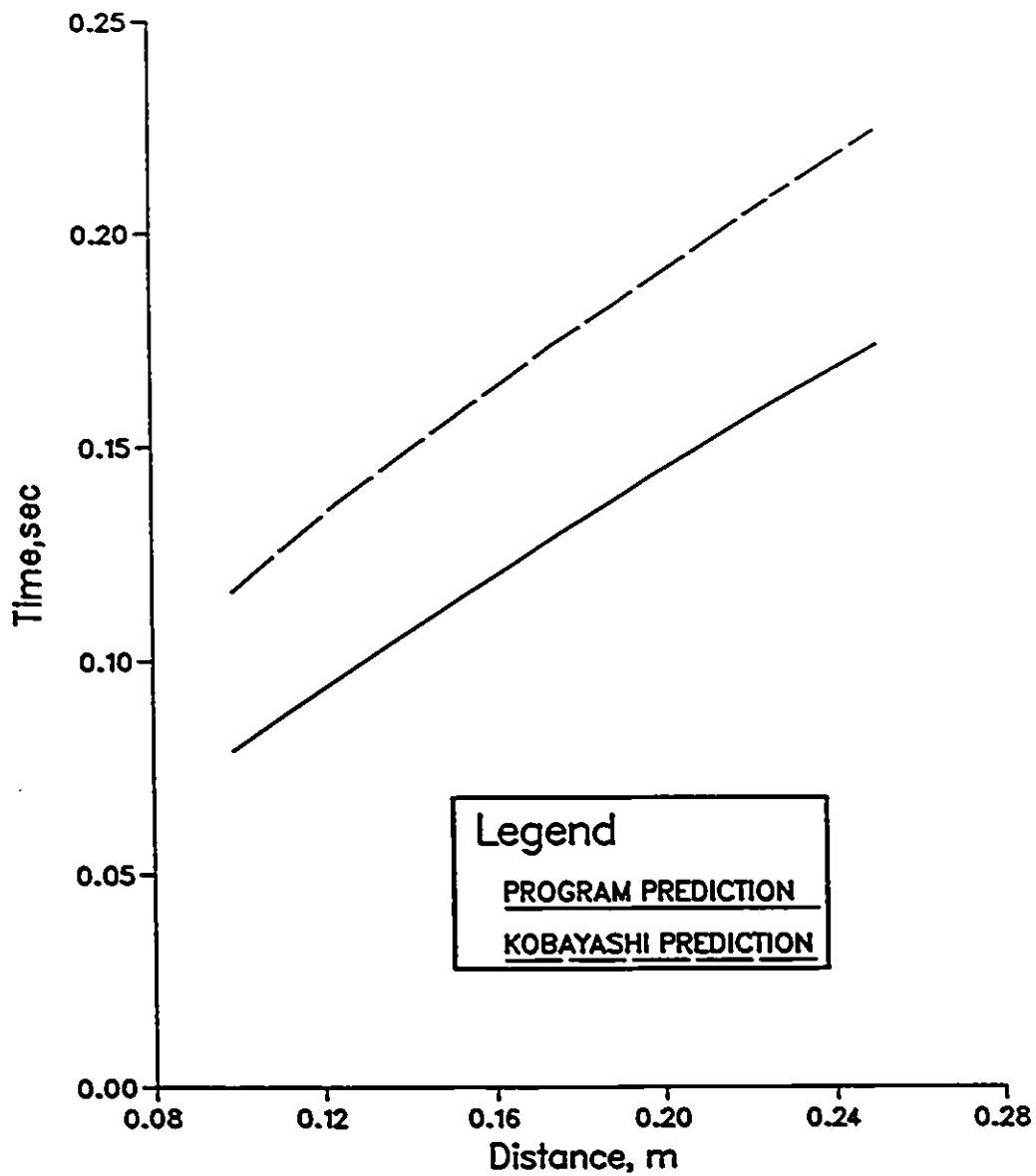


Figure 17: Comparison of residence time predictions from present particle heating program to predictions by Kobayashi[1,10]

Figure 17 shows an example of the residence times of the particles as predicted by the particle heating program and those as predicted by Kobayashi. This comparison reveals a rather large discrepancy between the two residence time predictions. Kobayashi determined the temperature and velocity fields inside the furnace by making several simplifying assumptions, the chief one being that the temperature and velocity profiles of the main gas and carrier gas flows are flat and the gradients at the interfaces are approximated with equations with adjustable parameters, K_u and K_v . A momentum integral method analysis was then used to predict the development of the velocity profiles with distance along the reactor. Kobayashi also assumed that there is no particle slip, so that particles and gas move at the same velocity. This enabled the parameter for the velocity expression, K_u , to be found experimentally from the results of laser velocity measurements of the coal particles. As the radiation from the sides of the furnace made the measurement of the particle temperature impossible, the two parameters were related using a shape factor, ϑ :

$$K_v = \vartheta * K_u \quad (6.1)$$

where K_v is the parameter for the temperature profile, and an indirect method of choosing θ was used based on the observed weight losses at different temperatures. In comparison, the program written by Flaxman [7] numerically solves all the fundamental governing equations using finite difference techniques. The temperature and velocity fields of the furnace are then used to calculate the coal particle temperature and velocity by numerical solution of the differential equations of particle motion and heating. When the devolatilization model was added to the particle heating program, several modifications were also included which are discussed in chapter 4. As the particle heating program in the present work is much more rigorous, it was taken to be much more accurate than Kobayashi's model.

6.2 Isothermal Fitting

The isothermal fitting procedure is used to produce initial estimates for the non-isothermal fitting routine. The isothermal analysis was performed by assuming the particle temperature was constant and equal to that of the furnace. As stated previously, any data taken at a temperature deviation from that of the furnace of greater than twenty percent were omitted from this section of the analysis.

6.2.1 Determination of Ultimate Yield and Reaction Rate

The first stage of the fitting routine is the non-linear regression fitting of the isothermal first order reaction model

$$V = \alpha(1 - \exp(-kt)) \quad (6.2)$$

to the data for each individual temperature run. It should be noted that the parameters could not be fitted to the lignite coal run at 1000K because a major portion of these data recorded a negative weight loss. These data are clearly unacceptable and the elimination of these data resulted in insufficient data for fitting the parameters in this run. The parameters were then fitted to the remainder of the temperature runs and the results are listed in table 5.

Table 5 reveals that the fitted ultimate yields of both coals at 1260K are very close to their proximate volatile matter yields, which are .362 and .407 for the lignite and bituminous coals respectively. Any discrepancy might be due to the fact that neither coal at 1260K has experienced sufficient residence time to approach its asymptotic weight loss. This can be clearly seen in figure 18. The residence time is insufficient as well at 1000K for the bituminous coal. However, as the proximate analysis test is performed at 950K, it is believed that if given sufficient time the coals devolatilized at 1000K would have achieved an asymptotic weight loss approximately equal to their proximate volatile yield. Therefore it is evident that the lower temperature maximum weight loss is roughly equal to the proximate volatile yield. It is for this reason that α_1 , the low temperature reaction ultimate

Table 4: Furnace operating conditions

temperature K	primary gas flowrate l/sec	secondary gas flowrate l/sec	suction flowrate l/sec
1000	6.67E-4	0.49	0.25
1510	2.50E-4	1.16	0.50
1740 (lig)	5.83E-4	1.72	0.86
1740 (bit)	5.55E-3	1.72	0.86
1940 (lig)	5.83E-4	2.50	0.86
1940 (bit)	5.00E-3	2.50	0.86
2100	1.01E-2	2.50	0.86

Table 5: Ultimate yield and reaction rate predictions

temperature K	ultimate yield	reaction rate 1/sec
lignite		
1260	.3062	9.8331
1510	.4595	28.3637
1740	.5239	61.8103
1940	.6014	99.7716
2100	.6665	153.917
bituminous		
1000	.2263	2.3321
1260	.4538	7.1982
1510	.4739	23.183
1740	.4467	167.525
1940	.9984	46.920
2100	.6416	377.008

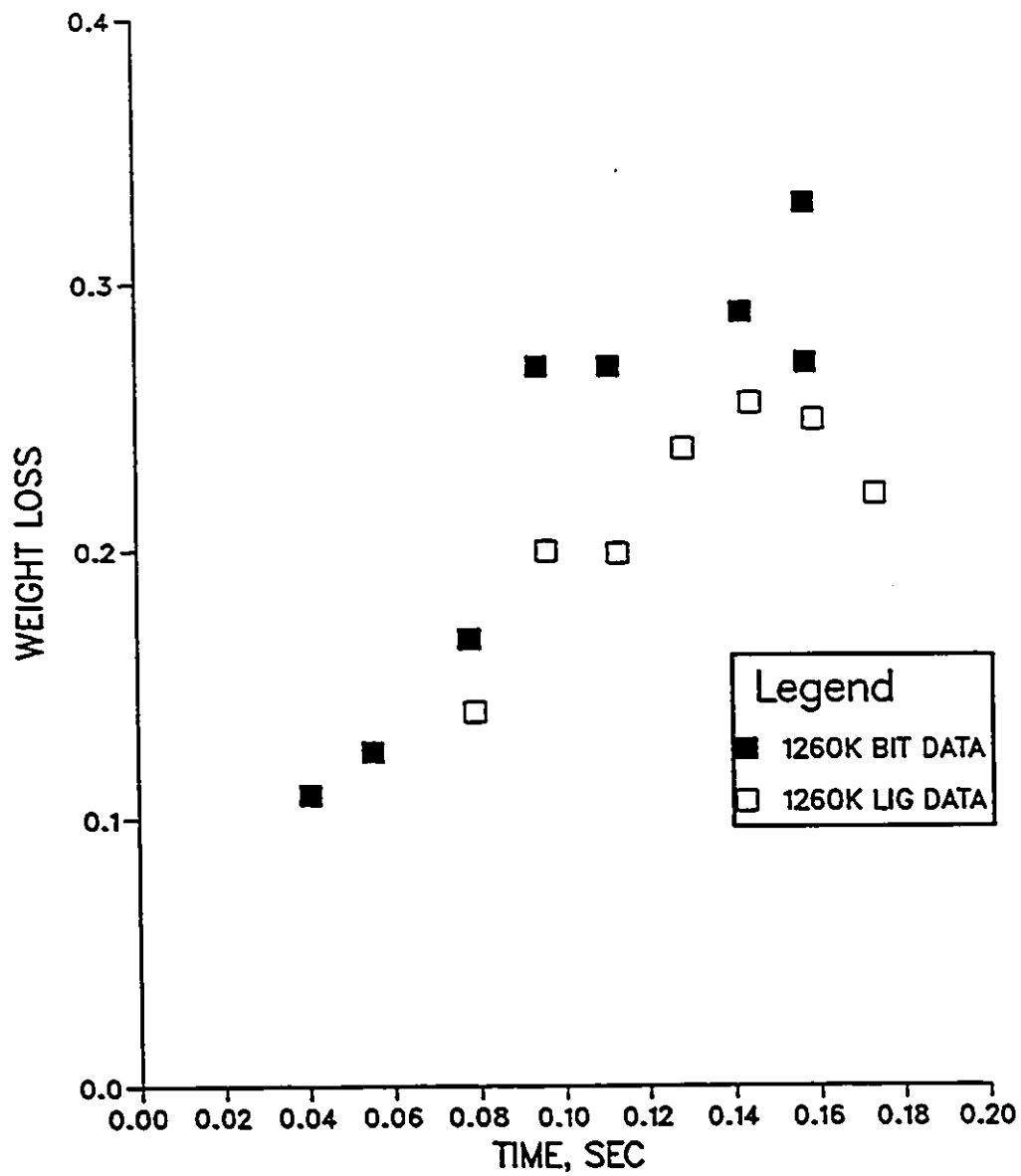


Figure 18: Weight loss versus residence time for 1260K data

yield of each coal, will henceforth be set to its fitted ultimate yield at 1260K. Although Kobayashi [1,10], Ubhayakar [29], and Jamaluddin [13] set the low temperature ultimate yield to the proximate volatile matter yield of the coal, this would 'pull' the fitting routine off the line of best fit and affect the least squares parameter estimates. If the number of data points collected per run is increased in future experiments, it is expected that the fitted ultimate yield at 1260K will more closely approach the proximate volatile matter yield.

An examination of table 5 reveals that the parameter estimates for the 1740K and 1940K bituminous runs do not fit into the general trend of increased ultimate yield and reaction rate constant with increased temperature. The fitting of the 1740K bituminous run results in a reaction rate that seems to be excessively high along with an ultimate yield that is too low in comparison to the values predicted for the 1510K bituminous run. As stated previously, the data obtained at a temperature twenty percent or more below the furnace temperature were omitted from the isothermal section of the analysis. In table 4, it can be seen that the gas flow rates are the same for both coals at a given temperature except at 1740K and 1940K. At these two temperature runs, the primary gas mass flowrates for the bituminous coal are approximately ten times the flowrates for the lignite runs. Figure 19 shows that while the lignite coal quickly comes up to temperature, the bituminous coal does not approach the furnace temperature until the end of the furnace. This resulted in the rejection of most of the data points in the 1740K and 1940K bituminous runs for the isothermal section of the regression analysis. Only four data points and two replicates were used in this fitting procedure for the 1740K bituminous run. As the weight loss data included in this procedure was leveling off to the asymptotic weight loss, it was the reaction rate that was adversely affected by the reduction in data. Conversely, for the 1940K bituminous run, the ultimate yield is obviously overestimated. This is a result of the residence time being too short to clearly approach the asymptotic weight loss, as can be seen in figure 20. This weakness is compounded by the effects of having only three different experimental data points and one replicate. As a result, the fitting routine wildly overshoots the true ultimate yield. This emphasizes the importance of having more than the minimum data to

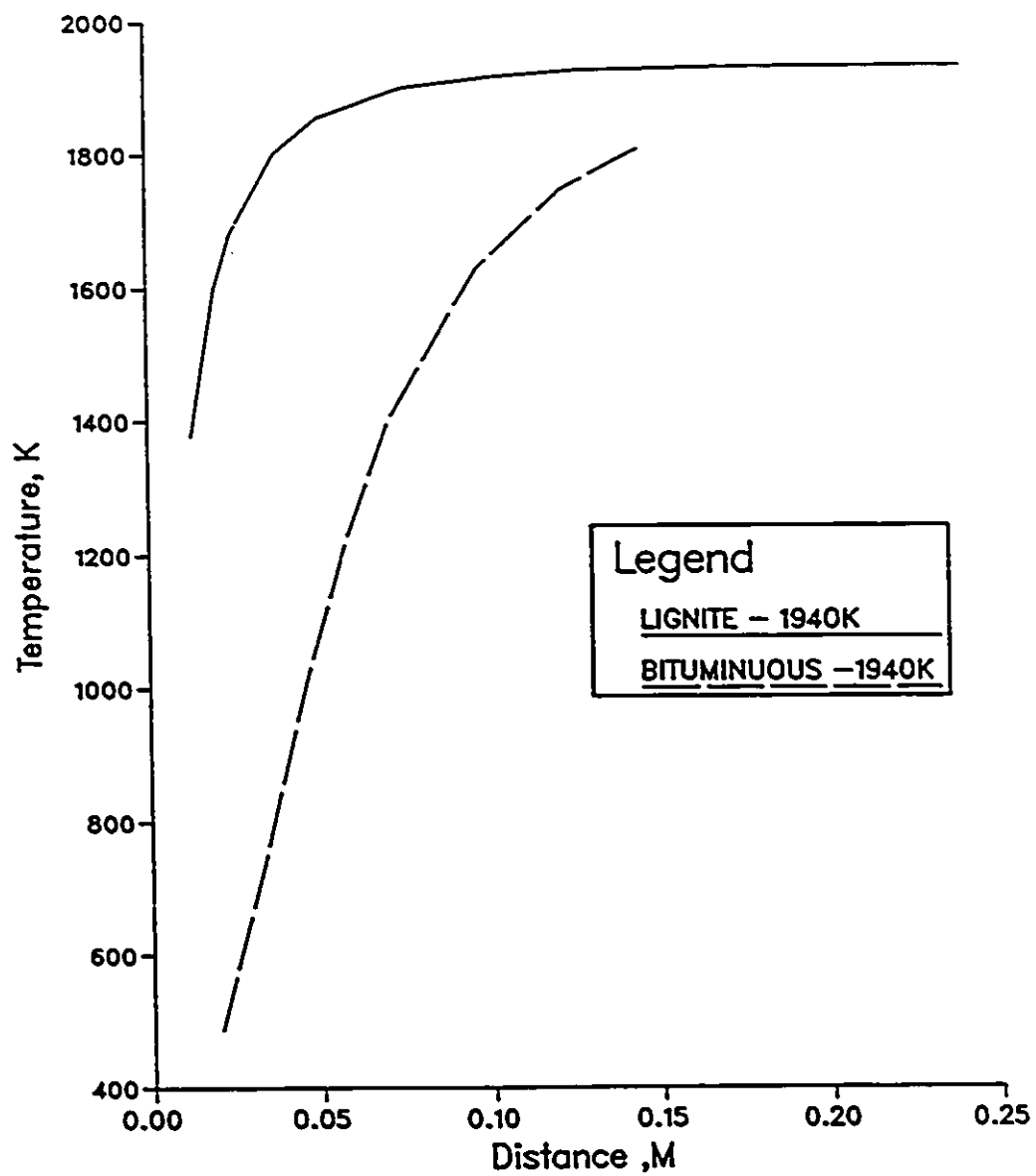


Figure 19: Comparison of the heating history of the lignite and bituminous coals at 1940K

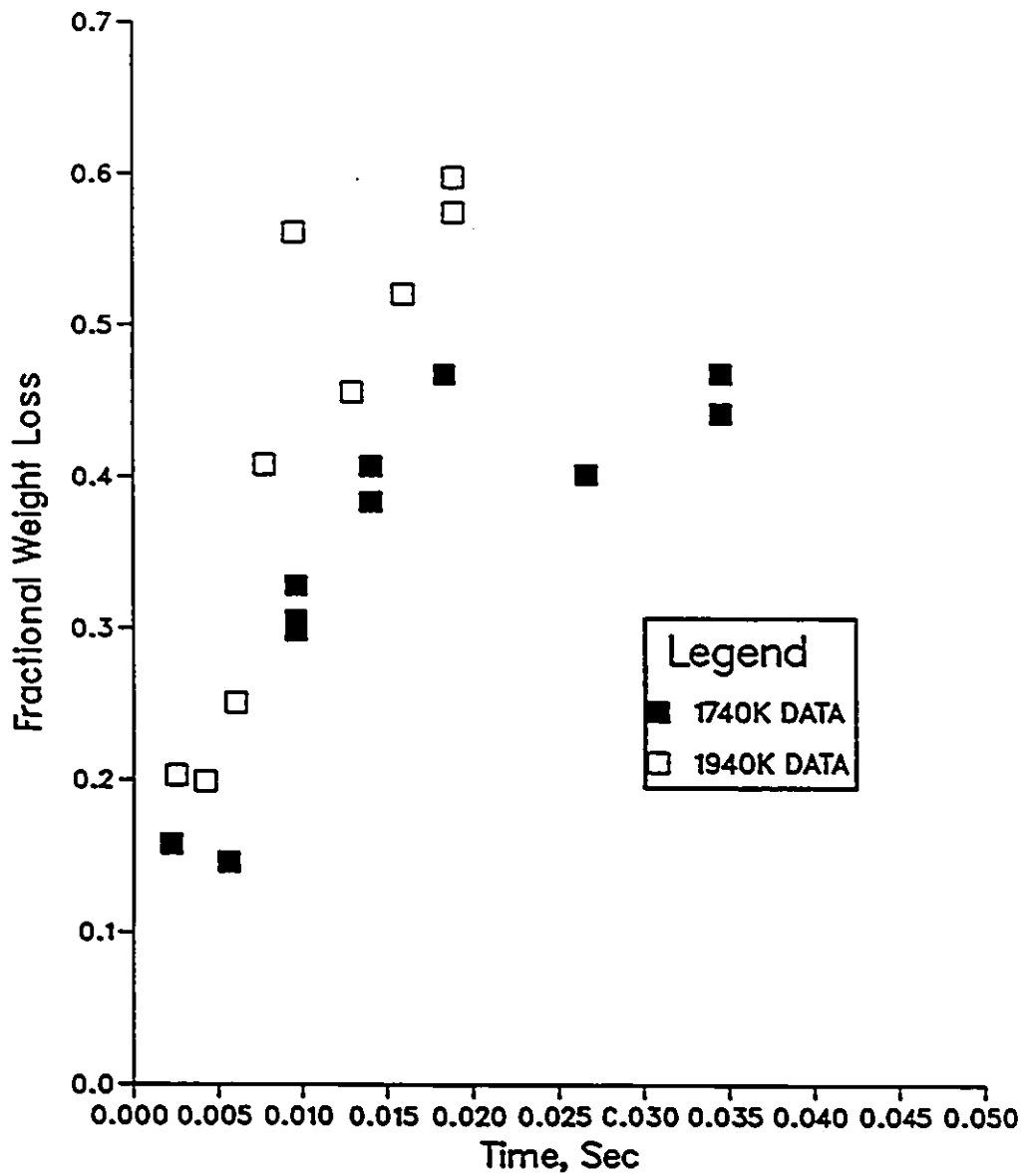


Figure 20: Weight loss versus residence time for 1740K and 1940K bituminous data.

fit the parameters as well as the importance of the asymptotic weight loss being reached in the experiments.

It may be argued that these problems might solely be the effects of using too little data. However, this argument was effectively dismissed in the fitting of the parameters to the 1510K bituminous data. In this fitting procedure not all the data that fell within twenty percent of the final temperature were included. When all the data were included, the fitting procedure overestimated the ultimate yield because the weight loss data approaches an asymptote but does not extend far into the asymptotic weight loss region. Figure 21 shows that when all the points are included the asymptotic weight loss line is ignored, and SAS fits a steep straight line. When fewer points are included the curve of the asymptote is emphasized more and SAS fits a more realistic curve. This behavior can also be seen in figure 21. It can be concluded that it is most important to extend the residence time so that the asymptotic weight loss is clearly reached and to have a number of data points in this region.

One problem with omitting the data collected at twenty percent below the furnace temperature is that it masks the effects of the heating history of the coal, which is more significant for the bituminous coal heated to the higher temperatures. Figure 19 compares the heating histories of the two coals at 1940K. Since the bituminous coal heats up more slowly, the first reaction has a larger effect and the devolatilization is affected by this. This effect can be seen in the following equation for the two reaction model:

$$V = \int_0^t (\alpha_1 k_1 + \alpha_2 k_2) C dt \quad (6.3)$$

where

$$C = \exp \int_0^t -(k_1 + k_2) dt$$

In the above equation, C is the mass of coal not yet devolatilized. With a relatively slower heating rate, the first reaction has a significant role in the devolatilization and therefore

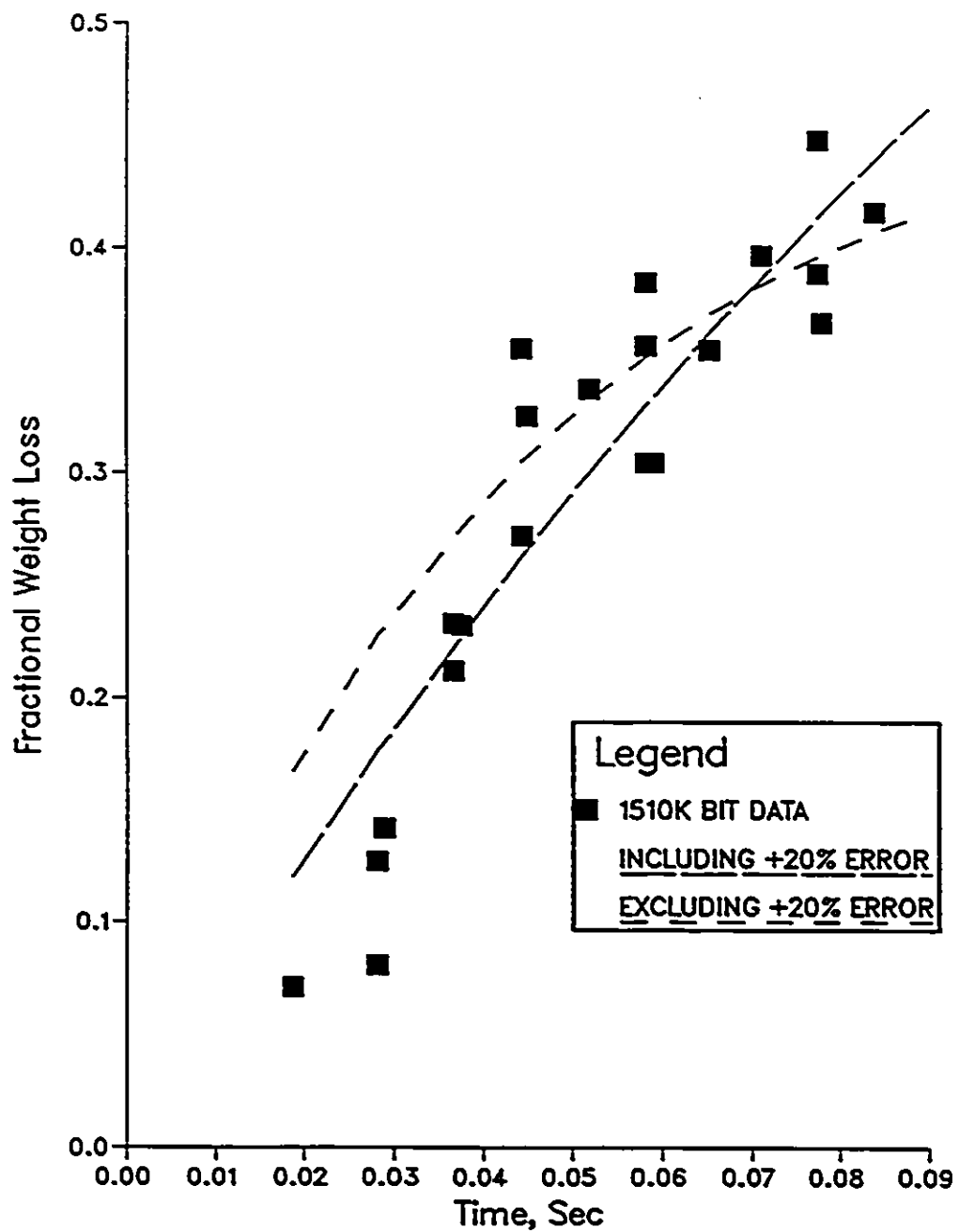


Figure 21: Isothermal fitting of parameter estimates to 1510K bituminous data

reduces the mass of coal that is available to be devolatilized by the second high temperature reaction. It is in this manner that the heating rate affects the devolatilization of the coal.

6.2.2 Fitting of the Arrhenius Rate Constants

The next stage of the fitting routine is to estimate the Arrhenius rate constants using the isothermal data. The fitting of the parameters was performed by splitting the data into two sections, low and high temperature data. The low temperature data includes the 1000K, 1260K and 1510K data, with the remaining runs being included in the high temperature runs. The parameter estimates for each coal are found by fitting the model to each set of data. As the data for the lignite coal at 1000K were eliminated, attempts to fit the low temperature parameters for the lignite coal were conducted using two different methods: first, using only the 1260K and 1510K data; and secondly, using the 1000K bituminous data along with the 1260K and 1510K lignite data. Although it would seem inconsistent to use the data of the two coals to determine parameter estimates, it should be noted that the isothermal fitting procedure is used only to determine initial estimates of the parameters. This will not be done in the non-isothermal procedure which is the final stage in the fitting procedure. The high temperature parameter estimates were fitted using the appropriate temperature runs.

The first step of this procedure is to use the k at each of the temperature runs to fit the equation:

$$\ln k = \ln k_0 - E/RT \quad (6.4)$$

to the isothermal data. This fitting will give initial estimates of k_0 and E for the high and low temperature reactions. The results are listed in tables 6 and 7. The next step is to use these values as initial estimates in the non-linear regression of:

$$k = k_0 \exp(-E/RT) \quad (6.5)$$

These results are also listed in tables 6 and 7. The last step in the isothermal regression is

to fit:

$$V = \alpha(1 - \exp(-k_0 \exp(-E/RT)t)) \quad (6.6)$$

As this last step utilizes a non-linear regression routine, the parameter estimates from the previous step are used as initial estimates for this routine. The results of this regression are also included in tables 6 and 7. Each of these steps represents an increase in the accuracy of the parameter estimates. Although the regression using equations 6.5 and 6.6 could possibly be omitted from this procedure, the steps are included in order to have several different parameter estimates to use to test and ensure the convergence of the non-isothermal regression routine that is used in a later step.

An analysis of the parameter estimates found through the regression of isothermal data reveals that although this operation was successful in that the routine converged, the high temperature parameter estimates seem questionable, since the values of the activation energies are lower than expected (Table 11). However, it should be noted that since a single equation devolatilization model is being used at this point, these values represent the effective E and k_0 of the two equation system. In the temperature range used to determine estimates of the high temperature reaction constants, it is expected that the first reaction will still have a significant role in the devolatilization of the coal. As a result, the parameter estimates in this procedure would be expected to be lower than the estimates to be determined in the non-isothermal procedure where the first reaction equation is included in the model. However, the high temperature parameter estimates are even lower than expected since they are in fact only slightly higher than those of the low temperature reaction path. The high temperature parameter estimates were not found for the bituminous coal since the estimates of k for 1740K and 1940K are clearly in error.

The low estimates of the activation energy of the high temperature reaction causes some concern and a further examination of the devolatilization data. The weight loss data for high temperature devolatilization show unrealistic weight losses at short residence times. Table 8 lists the weight loss and heating history of the bituminous coal at 1200K and 1740K.

Table 6: Low temperature reaction rate constant estimates for isothermal pyrolysis

routine	bituminous		lignite		lignite + 1000K bit	
	k_o	E	k_o	E	k_o	E
linear k equation	1746	13.29	5909.1	16.02	3583	14.62
nonlinear k equation	5730	16.57	5909.2	16.02	5327	15.71
nonlinear full model	4637	15.97	5919.6	16.02	4406	15.16

Table 7: High temperature reaction rate constant estimates for isothermal pyrolysis

routine	lignite	
	k_o	E
linear k equation	9295	18.21
nonlinear k equation	15120	19.19
nonlinear full model	12504	17.67

Table 8: Heating history and weight loss data of 1260K and 1740K bituminous coal

1260K bituminous			1740 bituminous		
time sec	temperature K	wtloss	time sec	temperature K	wtloss
.041	1220	.109	.002	426	.158
.055	1239	.125	.006	789	.146
.078	1245	.167	.010	1168	.328
.094	1248	.269	.010	1168	.298
.111	1250	.269	.010	1168	.305
.143	1252	.289	.014	1422	.383
.158	1254	.270	.014	1422	.407
.158	1254	.330	.018	1552	.467
			.027	1655	.401
			.035	1688	.467
			.035	1688	.441

Comparing the first few data points of these two experimental runs, the coal entering the furnace heated to 1740K experienced a greater weight loss although the residence time and temperature was much lower. This behavior is also evident in the lignite data, and is clearly unrealistic. One possible cause of the overprediction of the weight loss could be recirculation of the primary gas stream. This would result in much greater residence times than predicted and higher weight losses than expected.

Kobayashi was made aware of these discrepancies while performing collection efficiency tests of the bronze filter [1] used to catch the coal particles after pyrolysis. The collection efficiency tests were conducted using coal particles at room temperature and using alumina particles at experimental temperatures. Recoveries of greater than ninety eight percent were found for the lignite coal. However, it was found that about five percent by weight of the original bituminous coal was lost under simulated experimental conditions at room temperature. This loss could be attributed to the use of water jets for quenching, which forced some of the fine particles to escape through the pores of the filter. These tests for the collection efficiencies for the two coals were conducted with the collector just below the injector at room temperature. Kobayashi explained that the smaller samples and higher main gas flows at high temperatures were responsible for the increased particle loss, which was detected from comparisons of the direct weight loss to the weight loss determined from ash tracer. As the flowrates are higher at higher temperatures, it is likely that the velocity at which the particles hit the filter increases. This increases the chance that fragments are broken off the particles which could be forced through the filter and result in a higher weight loss being recorded than actually occurred. Kobayashi also proposed that the weight loss at the high temperatures and longer residence times is underestimated for the bituminous coal, because bituminous coal tends to produce a lot of soot during devolatilization [1,13,55]. As the coal is collected on the filter the pores become clogged and more soot is collected on the filter, resulting in an underestimation of the weight loss. The rapid clogging of the filter was detected by Kobayashi by rapid increases in the pressure drop across the filter.

6.3 Non-isothermal Fitting

It was explained on page 92 that the particle heating history can have a significant effect upon the devolatilization process of a coal particle, and therefore the heating history of the particle was incorporated into the second part of the fitting routine. As stated previously the overestimation of the weight loss for the coals at high temperature required that these data be omitted from the fitting routine, as factors other than the devolatilization of the coal particle are affecting the data. These factors would affect the validity of the parameter estimates. This elimination of the high temperature data requires an alteration to the non-isothermal fitting procedure. Instead of fitting the high temperature parameters using a high temperature run, they must be fitted to the 1510K temperature run, which appears to be the highest temperature at which reliable data are available. This may affect the parameter estimation, since the role of the second reaction at 1510K is not as pronounced as it would be at a higher temperature.

6.3.1 Determination of Low Temperature Parameter Estimates

The first part of the non-isothermal fitting routine is to fit the low temperature parameter estimates to the 1260K temperature run. It is assumed that the second reaction has a minimal role in the pyrolysis of the coal particle at the temperatures at which the first reaction parameter estimates are being fitted, so the single first order reaction equation

$$V = \alpha(1 - \exp(-\theta \exp(-\frac{E}{R}(1/T - 1/T^*))dt)) \quad (6.7)$$

where:

$$\theta = k_0 \exp(-E/(RT^*))$$

is used in this section of the fitting routine. As stated on page 86, the low temperature mass fraction, α , is set to the fitted ultimate yield at 1260K. The initial estimates used are those found in the previous fitting procedures. Several different initial estimates were

used to ensure that the fitting program had converged to a single solution. The parameter estimates found for the bituminous coal are listed in table 9, where $X(1)$ and $X(2)$ are initial estimates for α and E and SSR denotes the sum of squares residuals, while the estimates for the lignite coal are listed in table 10.

The parameter estimates for both coals show fairly consistent results regardless of the initial estimates given within the range attempted. This indicates that the routine is converging to a single solution. However, the parameter estimates for the lignite coal are slightly less consistent than the bituminous coal, which is to be expected since the temperature range for this data is only some ten degrees. This, coupled with the effects of only having seven experimental data points, leads to a lowering of expectations for the accuracy that can be achieved in the parameter estimates. The parameter estimates for the bituminous coal are in fact surprisingly consistent, since the number of data points used in the fitting procedure is just eight. The estimates of E obtained are similar to those of other workers which can be seen in table 11, hence appear reasonable.

6.3.2 Determination of High Temperature Parameter Estimates

With the low temperature estimates fitted, the next step in the non-isothermal procedure is to fit the high temperature constants using the full two reaction model:

$$V = \int_0^t (\alpha_1 k_1 + \alpha_2 k_2) \exp\left(-\int_0^t (k_1 + k_2) dt\right) dt \quad (6.8)$$

As stated earlier, α_1 was set to the value of the fitted ultimate yield at 1260K, which therefore leaves α_2 , the high temperature ultimate yield, to be set before the process of determining the high temperature parameters can be started. Jamaluddin et al. [13] used the following expression to describe α_2 :

$$\alpha_2 = QV_0 \quad (6.9)$$

where $Q = V^*/(V_0 - V_r)$ as defined by Badzioch and Hawksley [15]. This method removes the temperature dependence of the ultimate yield, as an estimate of the ultimate yield,

Table 9: Parameter estimates for non-isothermal single first order reaction model -bituminous coal

X(1)	X(2)	θ	E	k_0	SSR
7.1385	16.57	7.58761	14.6224	2798	.560758E-2
8.1164	13.29	7.58783	14.6238	2798	.560758E-2
17.719	25.21	7.58760	14.6225	2797	.560758E-2
5.1907	40.26	7.58801	14.6159	2790	.560758E-2
9.1170	16.02	7.58801	14.6159	2790	.560758E-2

Table 10: Parameter estimates for non-isothermal single first order reaction model -lignite coal

X(1)	X(2)	θ	E	k_0	SSR
7.1385	16.57	10.0219	14.5102	3446	.264955E-2
8.1164	13.29	10.0213	14.4221	3323	.264954E-2
9.3438	16.02	10.0215	14.4015	3296	.264954E-2
9.5401	15.71	10.0216	14.4093	3310	.264954E-2
5.1907	40.26	10.0214	14.4703	3390	.264954E-2

V^* , is required in the determination of Q ; it is therefore undesirable. Ubhayakar et al. [29] determined that α_2 was equal to 0.8 by fitting the data of two separate researchers [15,16] who used different coals. This seems questionable, as the coals used in the two different furnaces most likely experienced different conditions, which would affect the devolatilization behavior. Both these methods of determining α_2 seem questionable, and yet α_2 would almost be impossible to determine experimentally, since the furnace temperature would have to be high enough so that the first reaction has a negligible effect. The required temperature can be roughly calculated by assuming that k_1 is negligible if it is twenty percent of k_2 :

$$T = (E_1 - E_2)/(R \ln(k_{o1}/.2k_{o2})) \quad (6.10)$$

Using the parameter estimates determined by Kobayashi [1,10], it was shown in section 3.3.1 that the furnace temperature required is approximately 2950K, which is an extremely high temperature for performing devolatilization experiments. Also, as no experiments have been performed at this temperature, one does not even have an estimate to start with. The simplest argument to date is that of Kobayashi [1]: he set the high temperature ultimate yield to 1, stating that as the temperature gets high enough all the coal will be transformed to volatiles. This is supported by the idea that as the temperature increases, more of the bonds in the coal structure will break, leading to smaller and more volatile units as the products. It is for this reason that α_2 for both coals will henceforth be set to 1. As there were serious doubts about the validity of the high temperature data, the high temperature parameters were fitted using the 1510K data. The low temperature parameter estimates were fixed to the values found in the non-isothermal single reaction model procedure. The data was again centered around the mean temperature, T^* , for accelerated convergence. The high temperature parameter estimates for the bituminous coal are listed in table 12 while the estimates for the lignite coal are listed in table 13, where $X(1)$ and $X(2)$ are initial estimates for θ and E_2 respectively. In spite of the fitting routine being given very different initial estimates, the resulting parameter estimates are very similar for both coals, which indicates the routine is converging. Although it is difficult to say whether the values of E_2 are physically reasonable or not, they do appear to be somewhat higher than those listed

Table 11: Parameter estimates for coal pyrolysis listed in literature

researcher	coal type	temperature, K	k_0	E
One Reaction Models				
Badzioch and Hawksley [15]	bituminous	923-1273	$\sim 5E5$	17.7
Scaroni et al. [19]	lignite	973-1273	0.6E3	10.8
Two Reaction Models				
Kobayashi [1,10]	bituminous and lignite	1000-2100	2E5	25
			1.3E7	40
Baxter et al. [34]	bituminous	673-1373	2.91E9	36.89
	lignite	1000-2100	5.78E2	11.8
			6.6E7	48.8
	bituminous	1000-2100	1.94E4	21.6
			9.65E9	73.9
Ubhayakar [29]	bituminous	1000-2170	3.7E5	17.6
			1.46E13	60.0

Table 12: High temperature parameter estimates for non-isothermal parallel reaction model -bituminous coal

X(1)	X(2)	θ	E	k_0	SSR
5.191	40.26	3.8731	89.661	5.27E13	.27894E-1
17.72	25.21	3.8731	89.676	5.29E13	.27894E-1
23.13	19.19	3.8731	89.684	5.31E13	.27894E-1
19.98	18.21	3.8728	89.600	5.29E13	.27894E-1

Table 13: High temperature parameter estimates for non-isothermal parallel reaction model -lignite coal

X(1)	X(2)	θ	E	k_0	SSR
5.1907	40.26	11.117	63.896	2.63E10	.17508E-1
17.719	25.21	11.117	63.895	2.63E10	.17508E-1
23.132	19.19	11.117	63.901	2.64E10	.17508E-1
79.362	40.28	11.117	63.891	2.63E10	.17508E-1

in table 11.

The final values of the parameter estimates are listed in table 14. These were used to produce the model predictions shown in figures 22 and 23. The model predictions seem quite good for each coal except for the 1510K lignite run at large weight losses and the 1000K bituminous run. The 1510K lignite data does not extend far enough into the asymptotic weight loss region to be accurately predicted by the model. The model prediction for the 1000K bituminous run overpredicts the devolatilization data. It should be noted that the validity of this data is in question since the first few data points in this run recorded negative weight losses. The assumption made during the fitting procedure that the second reaction is unimportant at 1260K can be checked by calculating the reaction rates for each coal using the fitted parameter estimates. From the reaction rates and ratios for each coal listed in table 15, one can see that the second reaction does not play a significant role in the devolatilization procedure and this assumption has been verified.

6.3.3 Iterative fitting procedure

As the assumption that the second reaction has only a small effect was verified, attempts to iterate back to refit k_{o1} and E_1 to the full two reaction model with k_{o2} and E_2 set using the 1260K runs were performed. The results of this iteration listed in table 16 indicate that this procedure was not successful, as the parameter estimates from this procedure are considerably different from those determined previously. The values of E obtained are clearly unreasonable: those for bituminous coal are too low, while those for lignite are two orders of magnitude too great.

The low temperature reaction rate predicted using the parameter estimates from the iteration step for the bituminous coal is calculated as:

$$\begin{aligned} k_1 &= 87.83 \exp(-5.84/(1.987E - 3 * 1260)) \\ &= 8.52 \end{aligned}$$

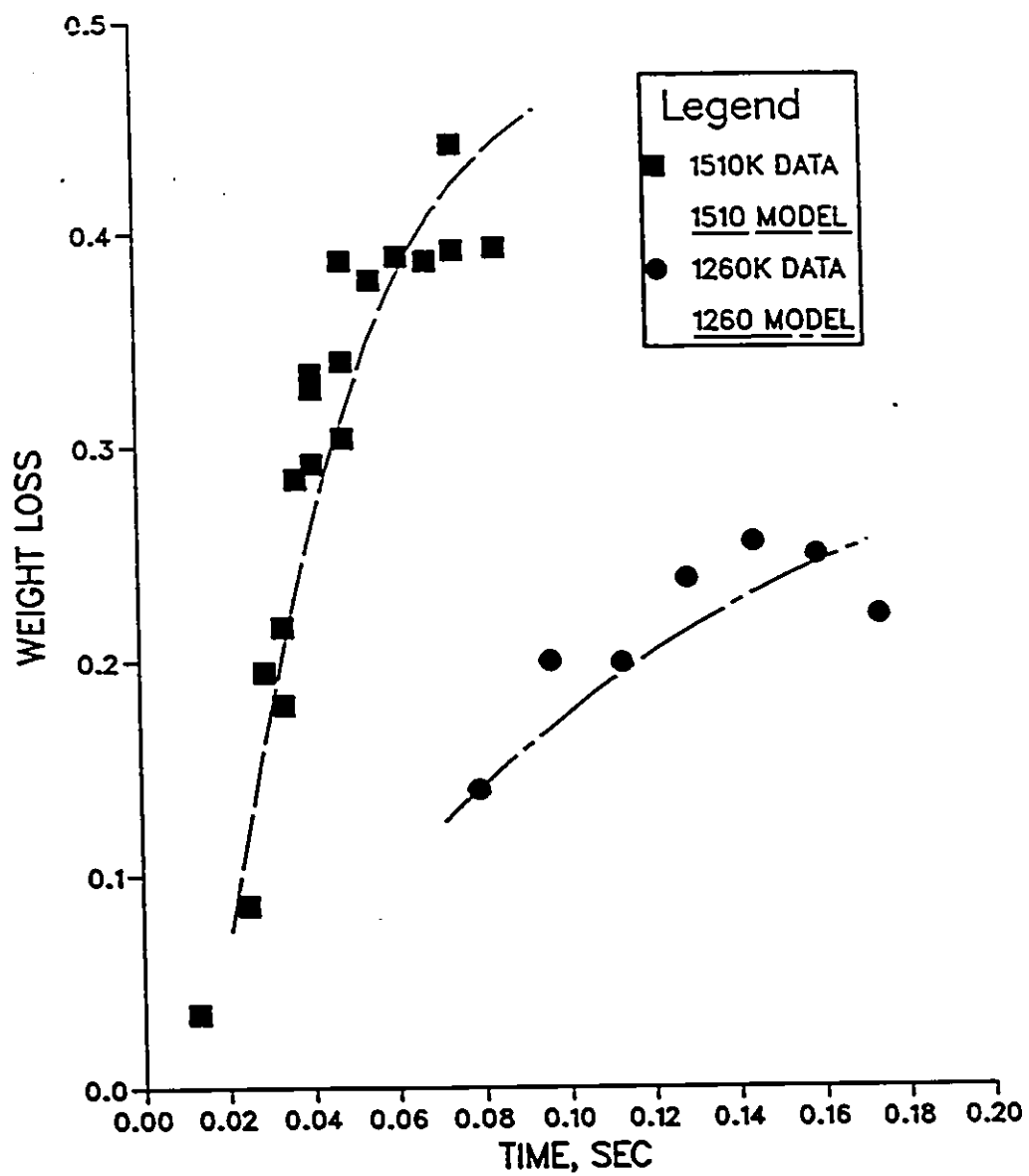


Figure 22: Model Predictions of Two Competitive Reaction Devolatilization Model for Lignite Coal

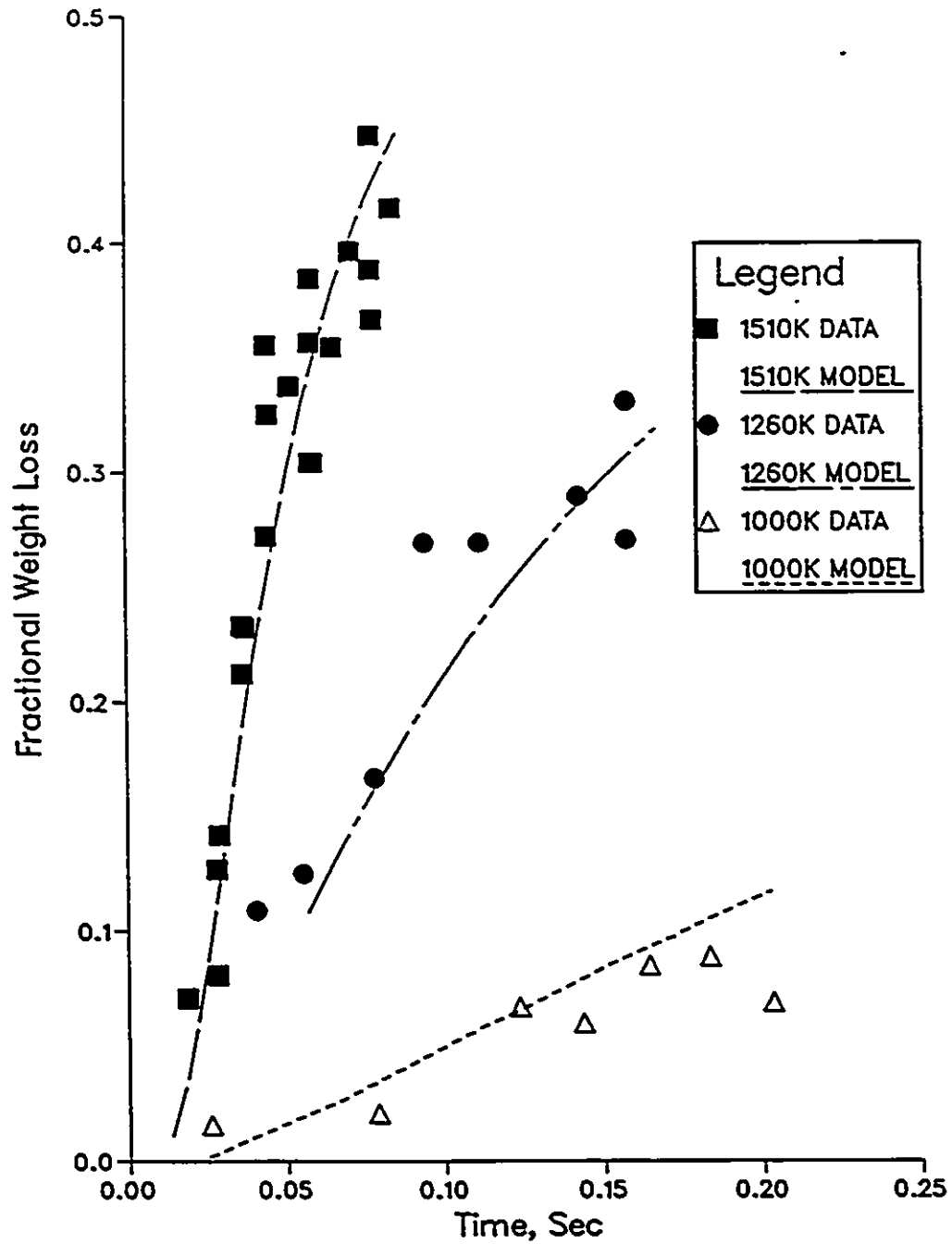


Figure 23: Model Predictions of Two Competitive Reaction Devolatilization Model for Pituminous Coal

Table 14: Least squares parameter estimates for lignite and bituminous coals

	bituminous	lignite
α_1	.4538	.3062
α_2	1.0	1.0
k_{o1}	3000	3320
E_1	14.6	14.42
k_{o2}	5.27E13	2.63E10
E_2	89.7	63.9

Table 15: Reaction rates for lignite and bituminous coals at 1260K

	k_1	k_2	k_2/k_1
bituminous	8.801	1.452E-2	1.65E-3
lignite	10.47	2.165E-1	2.07E-2

Table 16: Iterative fitting of low temperature parameters to full two reaction model

X(1)	X(2)	θ	E	k_o	SSR
bituminous					
7.1385	16.57	8.2896	5.8403	87.83	.54506E-2
7.309	15.99	8.2896	5.8405	87.83	.54506E-2
8.1164	13.29	8.2895	5.8407	87.84	.54506E-2
lignite					
7.1385	16.57	208.47	1753.5	****	.26355E-2
9.3438	16.02	208.47	1753.4	****	.26355E-2
8.1164	13.29	208.92	1754.8	****	.26355E-2

Comparing this value to the value of the reaction rate using the previously fitted parameters, listed in table 15, shows that the value of the predicted reaction rate at 1260K has only changed by 3% this iteration step. Rather, it is the values of the estimated parameters that have changed during this procedure; this is not so surprising, considering that the number of data points and the particle temperature range in the 1260K run were quite limited. The residual plots, which are discussed in the next section, show the 95% confidence region for these parameters. These plots show that there are many different values of k_0 and E that can be considered to be the least squares parameter estimates for the same reaction rate, and therefore it should not be surprising that the routine converges to different estimates of the parameters. The change in the low temperature reaction rate, while small, is still an order of magnitude larger than the ratio of high to low temperature rates, k_2/k_1 , listed in table 15. The low temperature rate is therefore quite sensitive to the high temperature parameters, and it can be postulated that this is a result of the fact that the high temperature reaction also affects the yield as well as the reaction rate. Because of the small temperature range and very large scatter of the data, these small changes exert an unreasonably large influence on E_1 . Once again the need for a consistent body of data spread over the whole devolatilization history in order to establish E_1 is highlighted. A further consideration is that even at 1510K the rate of the second reaction is a subordinate one: k_2/k_1 is .237 for bituminous and .545 for lignite at 1510K. The second reaction thus contributes a small portion to the overall devolatilization process, and the fitted E_2 can then not be expected to be very accurate.

The iteration step for the lignite coal was much less successful. In the fitting routine, the data was centered around the mean temperature, T^* , and the rate constant was predicted using the following equation:

$$k = \theta \exp\left(-\frac{E}{R}(1/T - 1/T^*)\right) \quad (6.11)$$

where θ and E are the parameter estimates to be determined. Since

$$\theta = k_0 \exp(-E/RT^*) \quad (6.12)$$

k_0 is calculated by:

$$k_0 = \theta / \exp(-E/RT^*) \quad (6.13)$$

However, with the very high estimate of activation energy

$$\begin{aligned} \exp(-E/RT^*) &= \exp(-1750.6/(1.987E - 3 * 1250.4)) \\ &\simeq 0 \end{aligned}$$

which is why attempts to calculate k_0 led to exponent overflow. The ratio k_2/k_1 is higher for the lignite, table 15, which when using the arguments in the previous paragraph suggests a much stronger influence of the second reaction. The temperature range for the 1260K lignite run is only 9K, which is obviously too small to be used to predict constants for as complicated a model as the two reaction devolatilization model. Of course, this iteration procedure brings forward the question of the precision of the parameter estimates which will be discussed in the next section.

6.4 Precision of the parameter estimates

The precision of parameter estimates can be described by joint confidence regions which show the degree to which the least squares estimate of one of the parameters depends upon the value of the other parameter. The confidence regions consist of the values of the parameters β which satisfy equation 5.12, which were found using a computer program written by Dal Cin [56]. As this program requires analytical derivatives of the model with respect to the parameters, the 95% confidence regions could only be found for the isothermal fitting of the model. The isothermal confidence regions are used as a rough estimate of the parameter precision. As the confidence regions are found for two parameters at a time the other parameters were set to their least squares estimates. The confidence regions for α_1 and k are shown in figures 24 to 27. The confidence regions of both coals at 1260K can be seen in figures 24 and 25. Both these plots show that the estimates of α_1 and k are highly correlated, meaning that the least squares estimate of one parameter has a dramatic effect

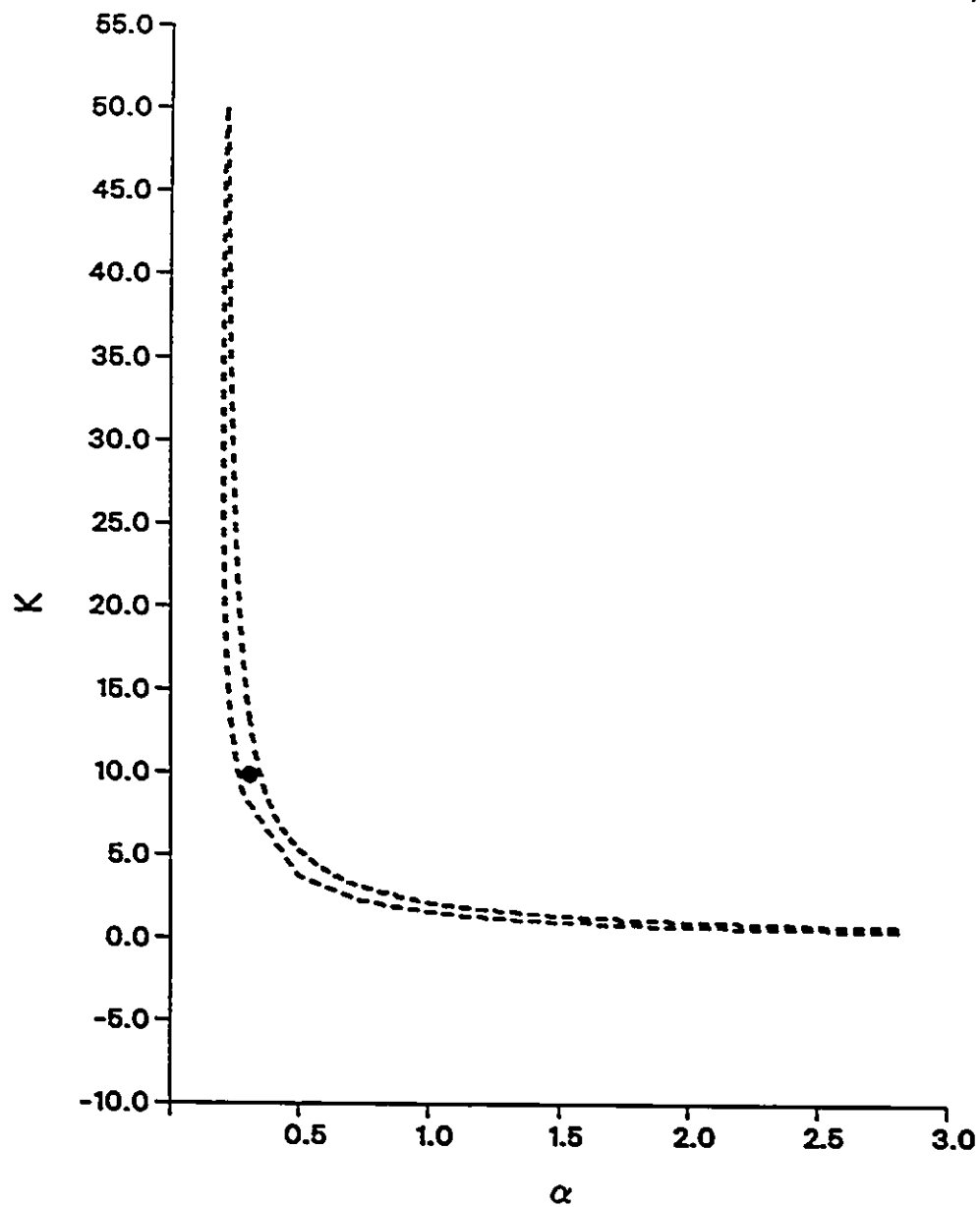


Figure 24: Confidence region for parameter estimates of isothermal single reaction model for 1260K lignite data. The point represents the converged parameter estimates.

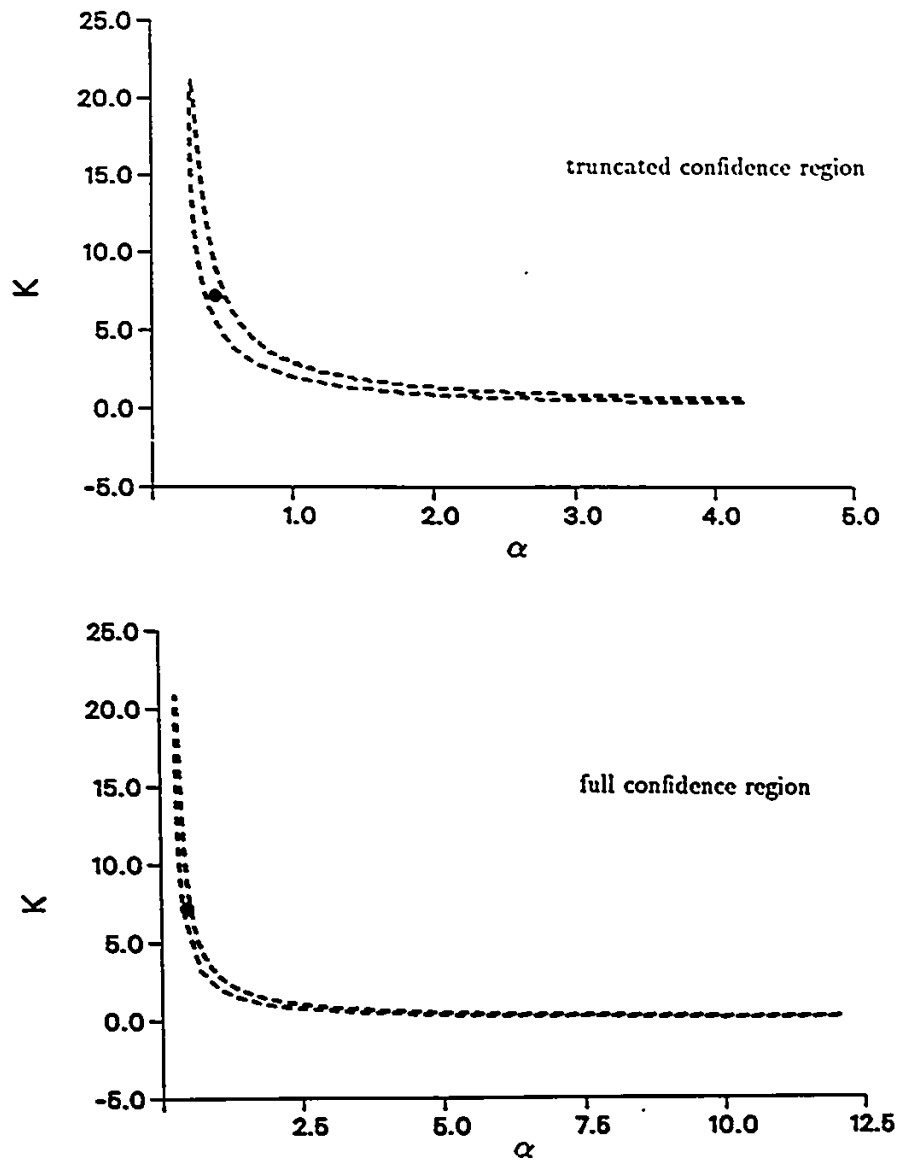


Figure 25: Confidence region for parameter estimates of isothermal single reaction model for 1260K bituminous data

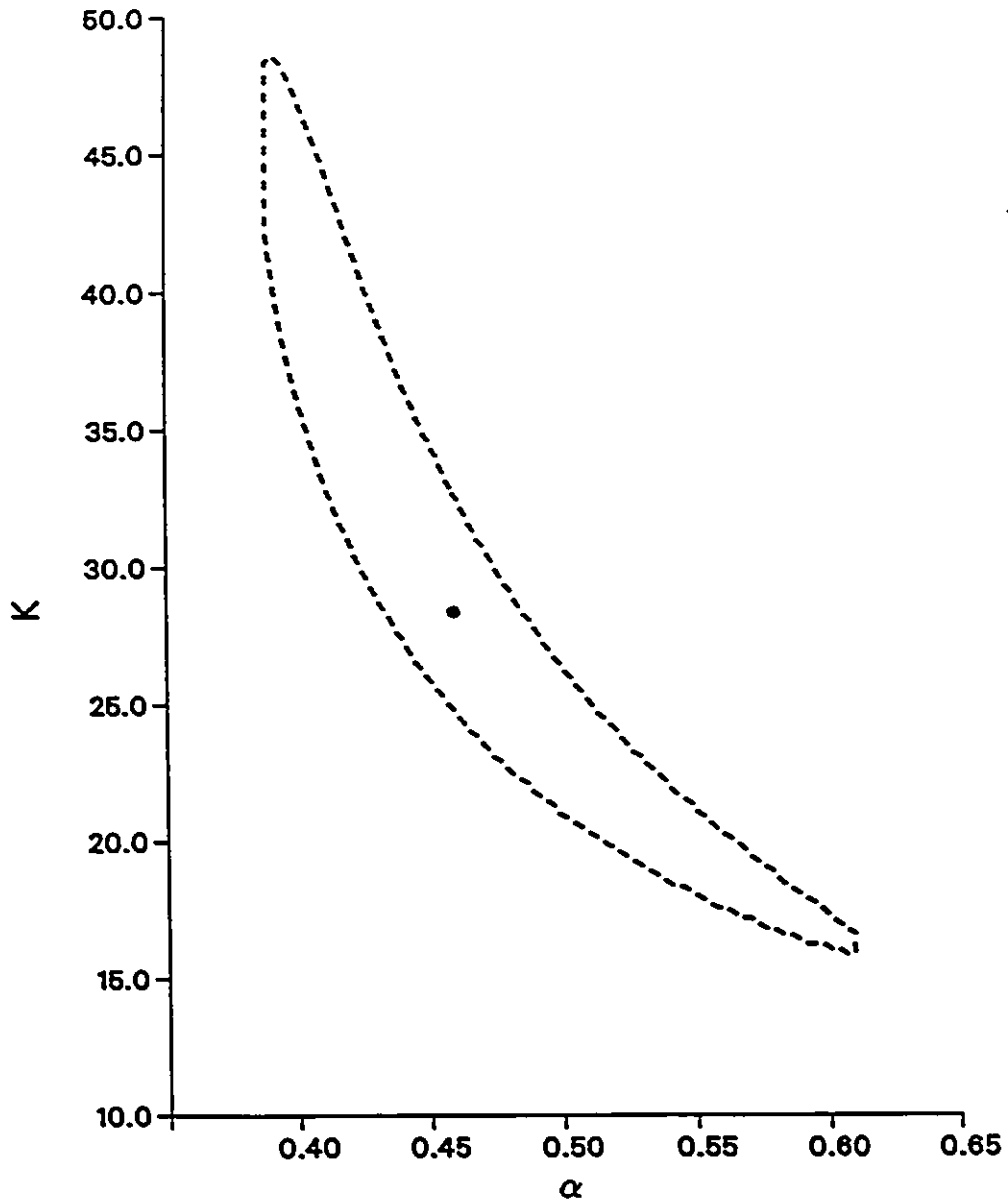


Figure 26: Confidence region for parameter estimates of isothermal single reaction model for 1510K lignite data

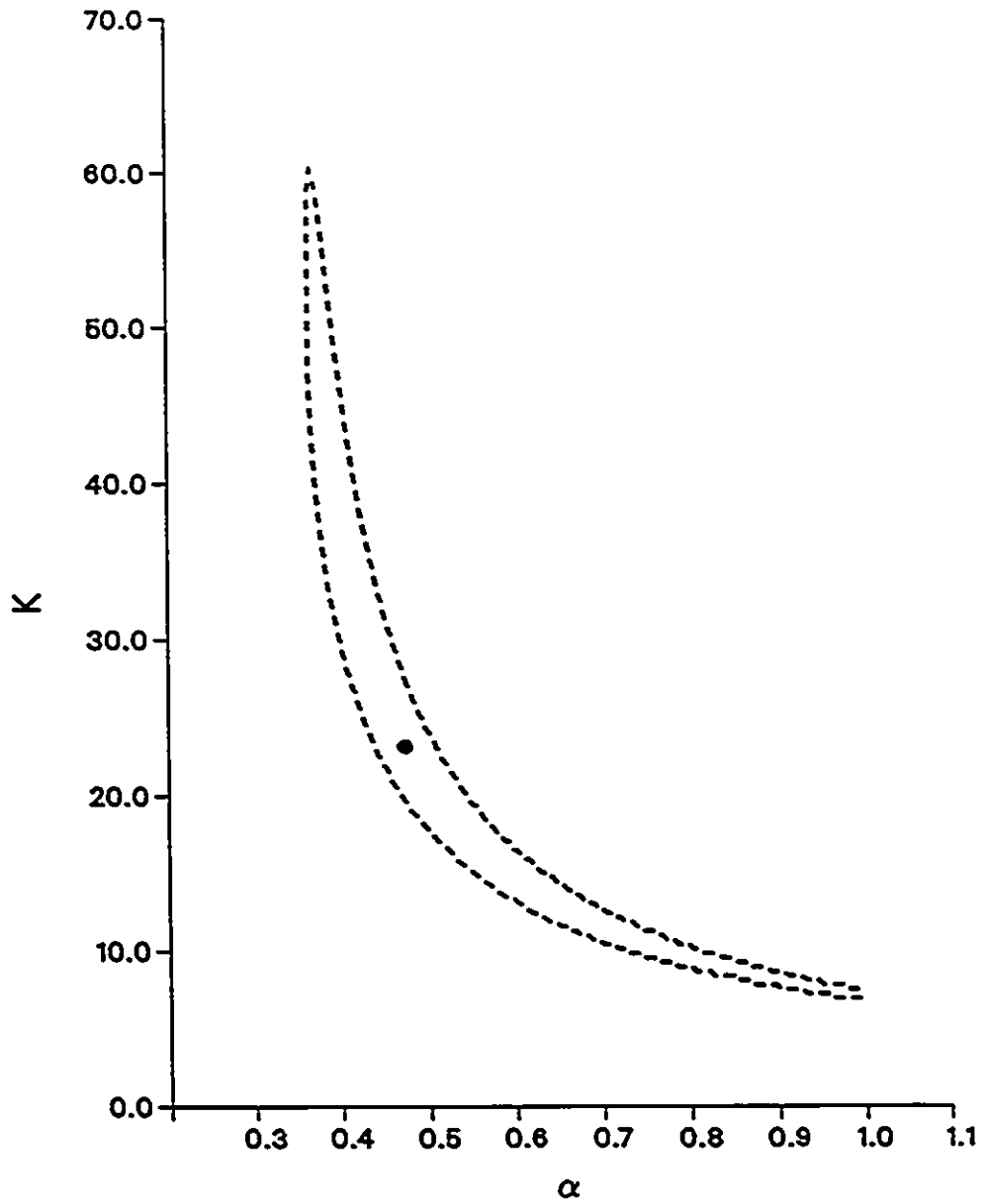


Figure 27: Confidence region for parameter estimates of isothermal single reaction model for 1510K bituminous data

on the value of the other parameter. The interval of the region on each axis represents the relative uncertainty of their estimates. Comparing the relative uncertainty of the value of α for the coals at 1510K and 1260K, one can see that the precision of this parameter estimate is greater at 1510K for both coals than at 1260K. This result is in fact not surprising since the residence time at 1260K was insufficient to approach the asymptotic weight loss. Although the confidence region for α at 1260K is quite large, it should be noted that since α represents mass fractions, any values greater than one are physically impossible, while values substantially different from the ASTM volatile fraction are highly unlikely. As the range of 'possible' values is in fact quite narrow, the uncertainty in these values is considerably reduced. The effect of not extending fully into the asymptotic weight loss can also be seen in figure 27 for the 1510K bituminous coal, as the range of values of α is larger than the corresponding range for 1510K lignite.

Figures 28 to 29 show the confidence regions for the fitting of the low temperature Arrhenius rate constants using equation 6.6 with α_1 set to the least squares estimates. Figures 28 and 29 show that the confidence region of k_0 and E for both coals is long and attenuated, and therefore it is quite understandable that a least squares fitting routine would converge slowly to the least squares estimates and that the quality of the initial estimates would be quite important. Figures 30 and 31 show the confidence region obtained by centering the data about the mean temperature. As the confidence region is not elongated, accelerated convergence in the parameter estimation routine is achieved. However, these plots show that the uncertainty in E , which is certainly significantly lower than that of k_0 , is still quite large. As mentioned earlier, this points up the need for more data points in the heating up part of the devolatilization history so as to increase the temperature range of the data.

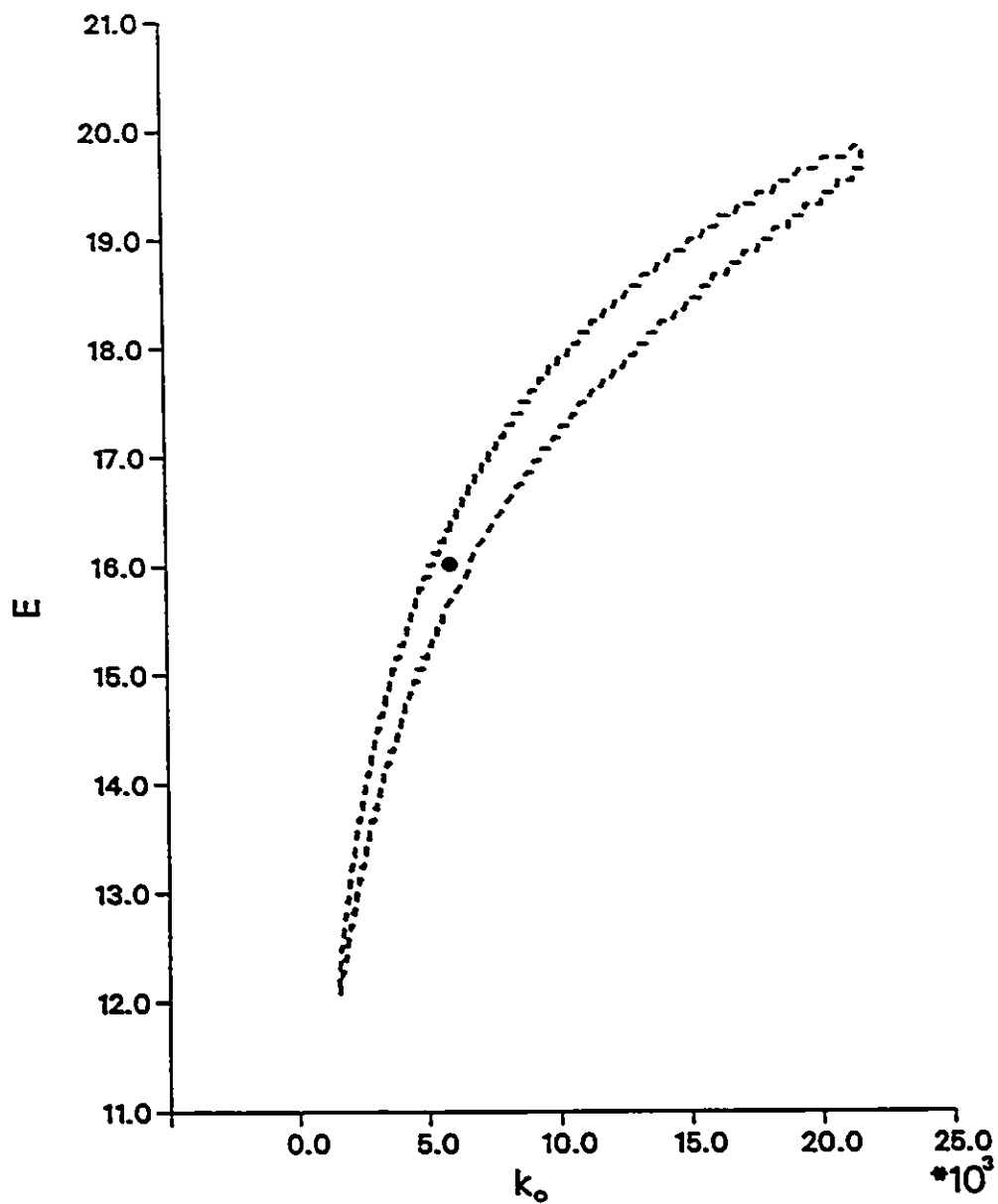


Figure 28: Confidence Region for Estimates of the Kinetic Rate Constants for the Low Temperature Lignite Data

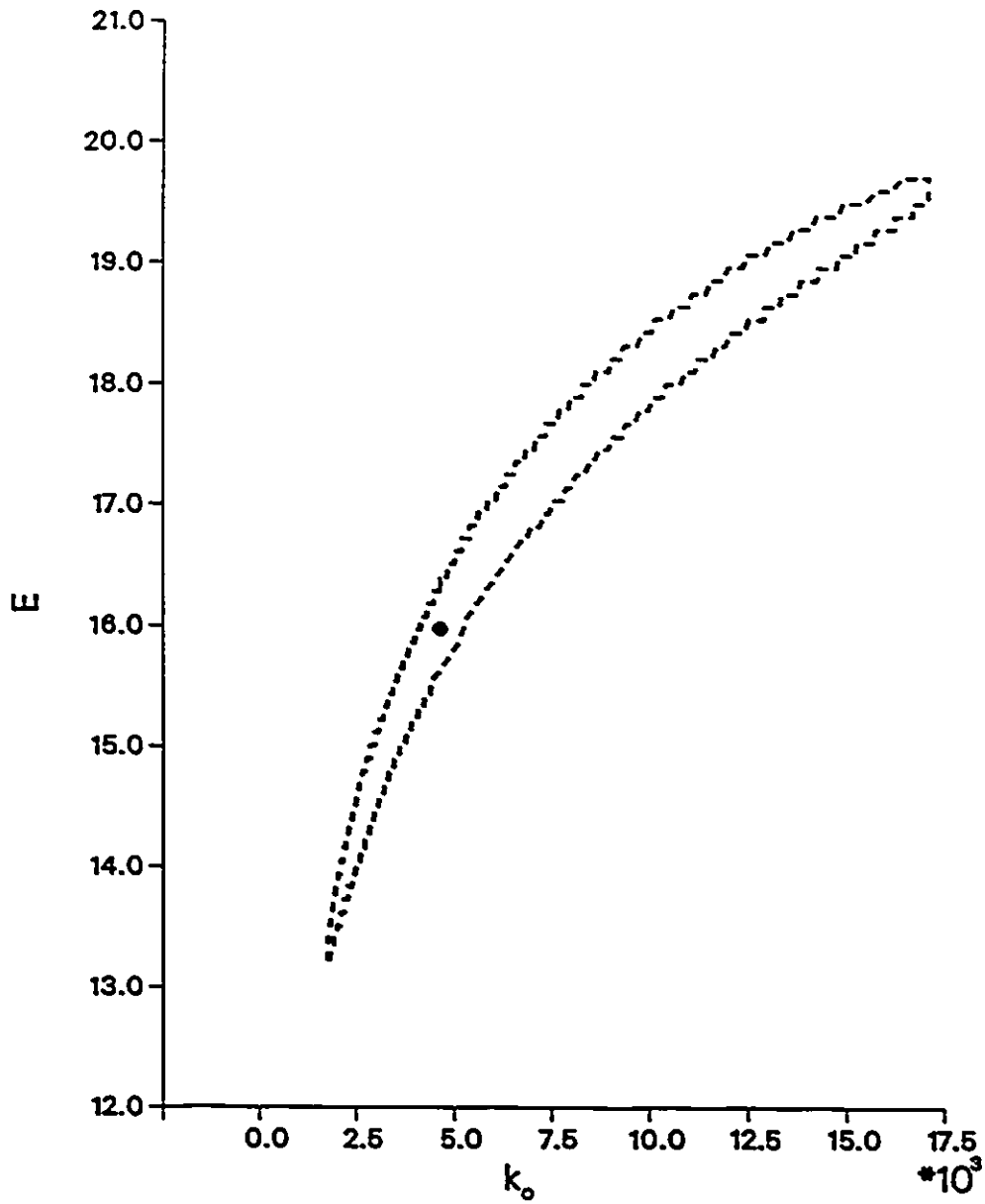


Figure 29: Confidence Region for Estimates of the Kinetic Rate Constants for the Low Temperature Bituminous Data

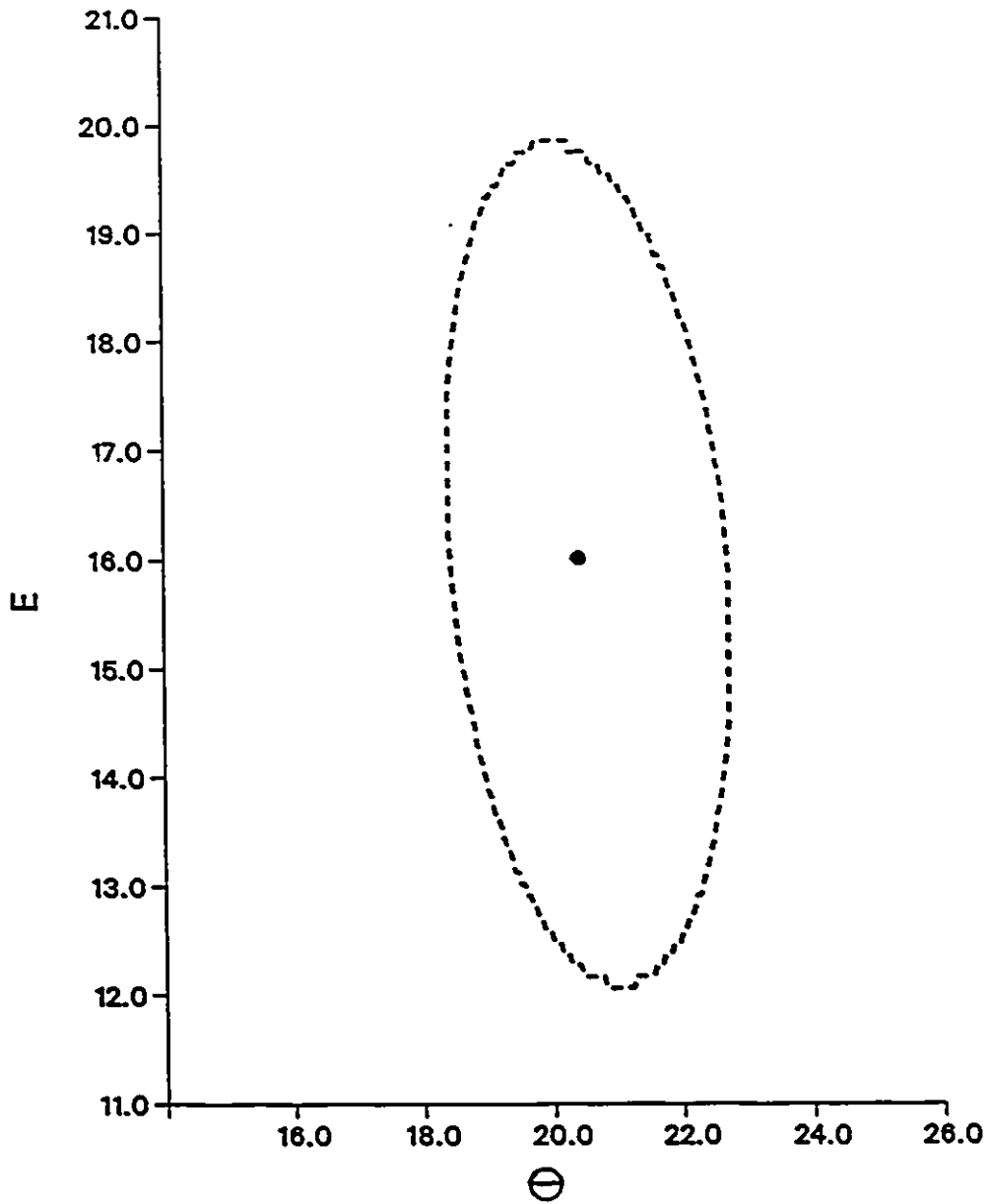


Figure 30: Confidence Region for Estimates of the Kinetic Rate Constants for Centered Low Temperature Lignite Data

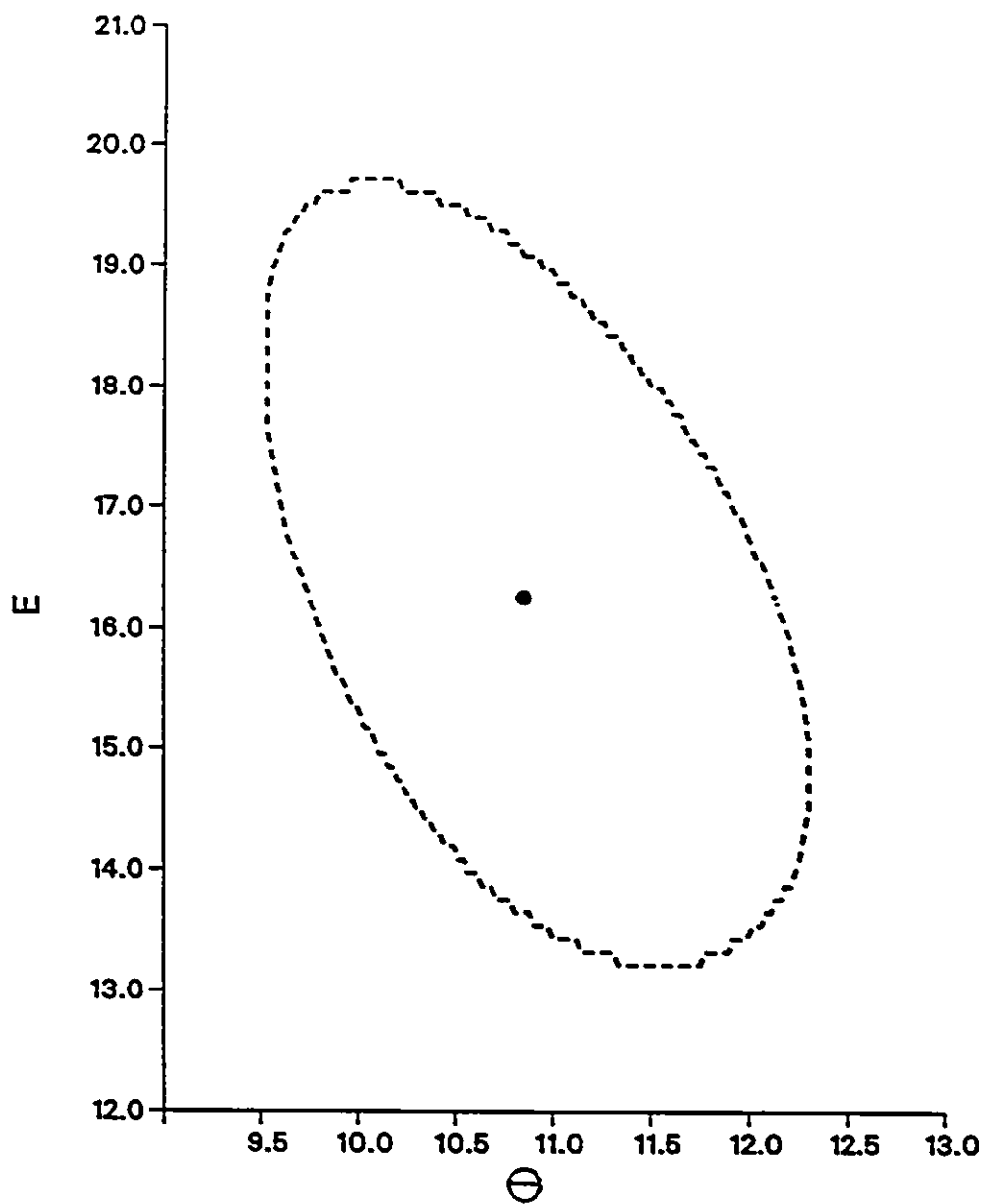


Figure 31: Confidence Region for Estimates of the Kinetic Rate Constants for Centered Low Temperature Bituminous Data

6.5 Significance Tests

The suitability of the estimated parameters are tested using two significance tests, first the residual plots and secondly the R test. The residual plots and R test were performed for each coal for the parameter estimates (without iteration) of the model. The results of the R test for each coal are listed in table 17. The R test verifies whether the variance of the error of the model in describing the data is less than the pure error or scatter in the experimental data. This test suggests that the model is adequate if the ratio of the model error variance to the pure error variance is less than the corresponding F probability function at the desired probability level. Table 17 shows that the R ratio is in fact less than F function at the ninety-five percent probability level, which suggests that the model adequately represents the data. The second test of significance for the model is the residual plots, which can be seen in figures 32 and 33 for the lignite and bituminous coals respectively. The residual plot for the bituminous coal is a scatter plot indicating that the model is accurately describing the experimental data. The residual plot for the lignite coal is also a scatter plot except for a slight trend in the 1510K data at high weight losses. This appears to be caused by the data not extending far enough into the asymptotic weight loss region to be accurately predicted by the model. As this can not be avoided without the collection of further data, the model for the lignite coal is considered suitably accurate in describing the experimental data.

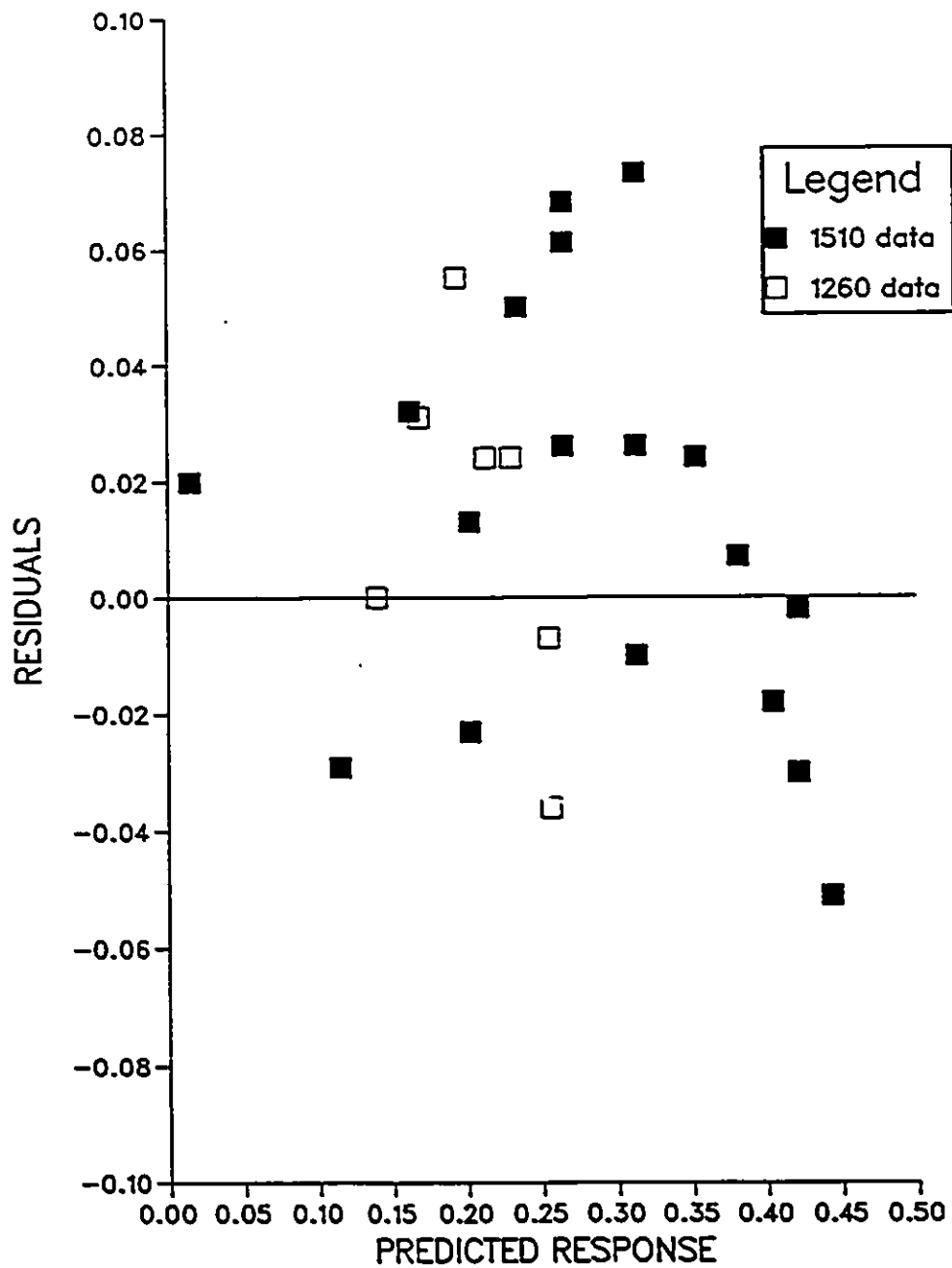


Figure 32: Residual Plot for Lignite Data

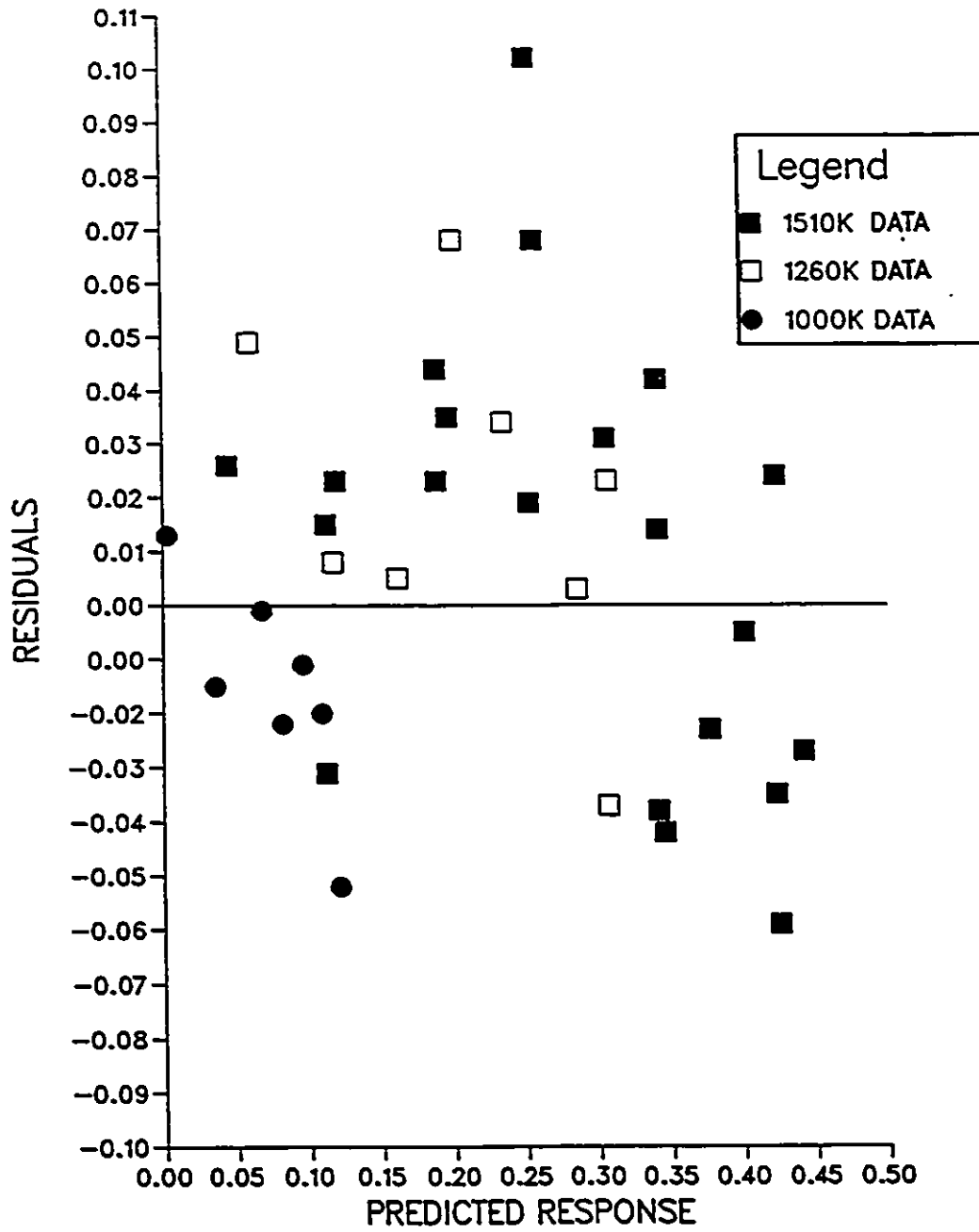


Figure 33: Residual Plot for Bituminous Data

Table 17: R Test for non-isothermal parallel reaction model

coal	R	F
lignite	1.577	3.94
bituminous	0.913	3.405

Chapter 7

Conclusions and Recommendations

The objective of this study was to recommend a model and to determine estimates of the kinetic rate constants for the devolatilization of a coal particle from experiments in a laminar flow reactor which can then be incorporated into a full coal combustion model.

7.1 Conclusions

The first stage of this study involved the selection of a suitable devolatilization model from the models now available in literature. The different models were critically appraised to select a model which is relatively simple so as to not require substantial computational effort, yet is physically realistic. The model selected was the two competitive reaction model which was first proposed by Kobayashi [1,10]:

$$V = \int_0^t (\alpha_1 k_1 + \alpha_2 k_2) \exp\left(\int_0^t -(k_1 + k_2) dt\right) dt \quad (7.1)$$

where:

$$k = k_0 \exp(E/RT)$$

and the α_i are the yield coefficients which determine the volatile yield. Subscripts 1 and 2 refer to the reactions which dominate at low and at high temperatures respectively. This model is the only model that can predict the temperature dependence of the ultimate yield. It is also quite flexible, in that at low temperatures this model reduces down into the simpler one reaction model which was found to be acceptable at lower temperatures.

The addition of devolatilization to the existing model [7] for flow and particle heating in a laminar flow reactor required modifications to the convective heat transfer and drag coefficients to allow for the effects of mass transfer from the pyrolyzing coal particle, which increases the thickness of the boundary layer. The original particle energy balance was modified by including a heat of pyrolysis term. As the heat of pyrolysis is very difficult to measure, there was great variation in the values listed. In view of this, an intermediate value was arbitrarily selected, and was found to have but a slight effect upon the particle temperature.

The physical changes of coal upon heating are of considerable interest. The behavior of non-swelling coals with changing particle density as devolatilization proceeds was modelled and incorporated into the particle heating program. The effects of swelling on particle heating were estimated to be small under typical reactor conditions, as most swelling is likely to occur after the particle has approached its final temperature. Swelling also had no significant effect on the particle velocity. Hence the particle swelling was neglected.

The next step was developing a method by which the estimates of the kinetic rate constants can be determined from experimental data. Since experimental data is not yet available from the Energy, Mines and Resources reactor, the experimental data of Kobayashi [1] was used as a test of the fitting routine. A two part procedure was developed for the fitting routine. First an isothermal procedure was used to get first estimates of the yield coefficient, α , and reaction rate, k , for a simple one-step reaction model. The low temperature yield

coefficient, α_1 , of the two reaction model was set to the fitted ultimate yield for each coal at 1260K while the high temperature yield coefficient, α_2 , was set to 1. Estimates of the pre-exponential, k_0 , and the activation energy, E , were found for the isothermal one reaction model and were used as initial estimates of the parameters for the non-isothermal fitting routine incorporating the full heating history of a particle at a given furnace temperature. These initial fitting steps were used merely to get good trial values of parameters for the final fitting process, and can be eliminated if other sources of physically reasonable trial values are available. The estimates of the low temperature reaction rate constants that were used in the full two reaction model were then fitted to the 1260K furnace data using a one reaction non-isothermal model. The estimates of the high temperature reaction constants in the full two reaction model were then fitted to the high temperature furnace data. As there was doubt about the validity of the 1740K, 1940K, and 2100K data, the 1510K data was used for this procedure. The fitted parameters at this stage had physically reasonable values, and reproduced the experimental data for each temperature well. The extent of reaction due to the second reaction was found to be only a few percent at low temperature (1260K), justifying the use of the single-step reaction fitting procedure in fitting the low temperature parameters. Attempts to improve the estimates of the low temperature reaction constants by refitting the 1260K data with the high temperature parameters held constant were unsuccessful, leading to unrealistic values of E_1 . These difficulties are believed due to the small number of available data points as well as the small temperature range of the collected data, leading to large uncertainties in the fitted parameters.

The precision of the parameter estimates was investigated in the next stage of the fitting procedure. The estimates of α and k determined for each furnace temperature in the isothermal procedure were found to be highly correlated, in that the least squares estimate of one parameter was highly dependent upon the value of the other; however, for physically reasonable values of α , which are between 0 and 1, the correlation and the associated uncertainty in the fitted parameters are both considerably reduced. The uncertainty of the pre-exponential, k_0 , and the activation energy, E , was found to be quite large as well,

due mainly to the small number and poor quality of the available data. The uncertainty in both these sets of parameter estimates highlights the need to collect more data during the heating of the coal particle and the asymptotic weight loss region so as to increase the accuracy of the parameter estimates. The suitability of the parameter estimates was tested using two significance tests: residual plots and the R test. Both these tests suggested that the model adequately represented the data. The fitting procedure was quite successful as the parameter estimates used to produce the model predictions shown in figures 22 and 23 represent the weight loss data well.

7.2 Recommendations

- As the contribution of the second reaction to the total weight loss increases as the temperature rises, experiments should be run at as high a temperature as possible in order to increase the accuracy of the estimates of the high temperature reaction constants. Conversely, for reliable fitting of low temperature reaction parameters, data should be collected at a temperature sufficiently low so that the second reaction is negligible. A temperature of 1100-1200K is suggested for this purpose.
- Difficulties in the fitting routine lead to the recommendation that the data must be collected over the full 'range' of devolatilization. It is important to collect devolatilization data during particle heating so that the effect of both reactions during heating can be determined in the non-isothermal procedure. It is equally important to collect data well into the asymptotic weight loss region so that the asymptotic weight loss can be accurately predicted.
- The accuracy of the fitting procedure is greatly affected by the number of data points collected and therefore the maximum number of data points possible should be collected in these regions.

List of References

- [1] H. Kobayashi. *Devolatilization of Pulverized Coal at High Temperatures*. PhD thesis, M.I.T., 1976.
- [2] L.D. Smoot and P.J. Smith. *Coal Combustion and Gasification*. Plenum Press, 1985.
- [3] P.R. Solomon and M.B. Colket. Coal devolatilization. *17th Symposium (Int.) on Combustion*, 131, 1978.
- [4] N.Y. Nsakala, R.H. Essenhigh, and P.L. Walker Jr. Characteristics of chars produced from lignites by pyrolysis at 808°C following rapid heating. *Fuel*, 57:605-611, 1978.
- [5] D.B. Anthony and J.B. Howard. Coal devolatilization and hydrogasification. *AIChE Journal*, 22:625-656, 1976.
- [6] D.B. Anthony, J.B. Howard, H.C. Hottel, and H.P. Meissner. Rapid devolatilization of pulverized coal. *15th Symposium (Int.) on Combustion*, 1303-1317, 1975.
- [7] R.J. Flaxman. *A Study of Flow and Particle Heating in a Drop Tube Furnace*. MAsC thesis, University of Ottawa, 1986.
- [8] D. Merrick. The thermal decomposition of coal: mathematical models of the chemical and physical changes. In A. Volborth, editor, *Coal Science and Chemistry*, pages 1435-1443, Elsevier Science Publishers, 1984.
- [9] J.D. Freihaut. *A Numerical and Experimental Investigation of Rapid Coal Pyrolysis*. PhD thesis, Pennsylvania State University, 1980.

- [10] H. Kobayashi, J.B. Howard, and A.F. Sarofim. Coal devolatilization at high temperatures. *16th Symposium (Int.) on Combustion*, 411-425, 1976.
- [11] E.M. Sunberg, W.A. Peters, and J.B. Howard. Product composition and kinetics of lignite pyrolysis. *Ind. Eng. Chem. Process Des. Dev.*, 17:37-46, 1978.
- [12] F.C. Lockwood, S.M.A. Rizvi, G.K. Lee, and H. Whaley. Coal combustion model validation using cylindrical furnace data. *20th Symposium (Int.) on Combustion*, 513-522, 1984.
- [13] A.S. Jamaluddin, J.S. Truelove, and T.F. Wall. Devolatilization of bituminous coals at medium to high heating rates. *Combustion and Flame*, 63:329-337, 1986.
- [14] *1970 Annual Book of ASTM Standards*. American Society for Testing and Materials. Part 19.
- [15] S. Badzioch and P. Hawksley. Kinetics of thermal decomposition of pulverized coal particles. *Ind. Eng. Chem. Process Des. Develop.*, 9:521-530, 1970.
- [16] G.M. Kimber and M.D. Gray. Rapid devolatilization of small coal particles. *Combustion and Flame*, 11:360-362, 1967.
- [17] R.J. Flaxman and W.L.H. Hallett. Flow and particle heating in an entrained flow reactor. *Fuel*, 66:607-611, 1986.
- [18] C. Tsai and A.W. Scaroni. Pyrolysis and combustion of bituminous coal fractions in an entrained-flow reactor. *Energy and Fuels*, 1:263-269, 1987.
- [19] A.W. Scaroni, P.L. Walker, and R.H. Essenhigh. Kinetics of lignite pyrolysis in an entrained-flow, isothermal furnace. *Fuel*, 60:71-76, 1981.
- [20] D.J. Maloney and R.G. Jenkins. Coupled heat and mass transport and chemical rate limitations during coal rapid pyrolysis. *20th Symposium (Int.) on Combustion*, 1435-1443, 1984.

- [21] P.R. Solomon, D.G. Hamblen, R.M. Carangelo, and J.L. Krause. Coal thermal decomposition in an entrained flow reactor: experiments and theory. *19th Symposium (Int.) on Combustion*, 1139-1149, 1982.
- [22] H. Juntgen and K.H. van Heek. An update of german non-isothermal coal pyrolysis work. *Fuel Processing Technology*, 2:261-293, 1979.
- [23] O.P. Mahajan, A. Tomita, and P.L. Walker Jr. Differential scanning calorimetry studies on coal: 1. pyrolysis in an inert atmosphere. *Fuel*, 55:63-69, 1976.
- [24] J.P. Holman. *Heat Transfer*. McGraw-Hill, 5th edition, 1981.
- [25] R.H. Perry and D. Green. *Perry's Chemical Engineers Handbook*. McGraw-Hill, 5th edition, 1984.
- [26] N.S. Harding. *Effects of Secondary Swirl and Other Burner Parameters on Nitrogen Pollution Formation in a Pulverized Coal Combustor*. PhD thesis, Brigham Young U., 1980.
- [27] A.F. Sarofim, J.B. Howard, and A.S. Padia. The physical transformation of the mineral matter in pulverized coal under simulated combustion conditions. *Combustion Science and Technology*, 16:187-204, 1977.
- [28] N. Gat. On internal temperature gradients in a pyrolysing coal particle. *Combustion Science and Technology*, 49:297-303, 1986.
- [29] S.K. Ubhayakar, D.B. Stickler, C.W. Von Rosenberg Jr., and R.E. Gannon. Rapid devolatilization of pulverized coal in hot combustion gases. *16th Symposium (Int.) on Combustion*, 427-436, 1976.
- [30] R.J. Quann, M. Neville, M. Janghorbani, C.A. Mims, and A.F. Sarofim. Mineral matter and trace-element vaporization in a laboratory- pulverized coal combustion system. *Environ. Sci. Technol.*, 16:776-781, 1982.

- [31] M. Neville, J.M. Beer, and A.F. Sarofim. Effect of coal particle temperature on ash vaporization. International Flame Research Foundation Conference, 1978.
- [32] J.S. Truelove. The modelling of flow and combustion in swirled, pulverized-coal combustion. *20th Symposium (Int.) on Combustion*, 523-530, 1984.
- [33] T. Suzuki, L.D. Smoot, T.H. Fletcher, and P.J. Smith. Prediction of high intensity pulverized coal combustion. Report.
- [34] L. Baxter, P.J. Smith, and L.D. Smoot. Optimization of coal devolatilization model parameters for comprehensive gasification and combustion models. Combustion Inst. Canadian/Western States Sections Spring Technical Meeting, 1986.
- [35] L.D. Smoot. Pulverized coal diffusion flames: a perspective through modeling. *18th Symposium (Int.) on Combustion*, 1185-1202, 1981.
- [36] S.M.A. Rizvi. *Prediction of Flow, Combustion and Heat Transfer in Pulverized Coal Flames*. PhD thesis, University of London, 1985.
- [37] K. Hashimoto, K. Miura, and T. Watanabe. Kinetics of thermal regeneration reaction of activated carbons used in waste water treatment. *AIChE Journal*, 28:737-746, 1982.
- [38] E.M. Suuberg, W.A. Peters, and J.B. Howard. Product compositions and formation kinetics in rapid pyrolysis of pulverized coal-implications for combustion. *17th Symposium (Int.) on Combustion*, 117-130, 1978.
- [39] K.M. Sprouse and M.D. Schuman. Predicting lignite devolatilization with the multiple parallel and two-competing reaction models. *Combustion and Flame*, 265-271, 1981.
- [40] V.G. Jenson and G.V. Jeffreys. *Mathematical Methods in Chemical Engineering*. Academic Press, 2nd edition, 1977.
- [41] L.D. Smoot and D.T. Pratt. *Pulverized-Coal Combustion and Gasification: Theory and Application for Continuous Flow Processes*. Plenum Press, 1979.

- [42] R.C. Reid, J.M. Prausnitz, and Sherwood T.K. *Properties of Gases and Liquids*. McGraw-Hill, 3rd edition, 1977.
- [43] W. Eisermann, P. Johnson, and W.L. Conger. Estimating thermodynamic properties of coal, char, tar and ash. *Fuel Processing Technology*, 3:39-53, 1980.
- [44] W. Fu, Y. Zhang, H. Han, and Y. Duan. A study on devolatilization of large coal particles. *Combustion and Flame*, 70:253-266, 1987.
- [45] D.B. Stickler, F.E. Becker, and S.K. Ubhayakar. Combustion of pulverized coal in high temperature preheated air. 17th Aerospace Sciences Meeting, 1979.
- [46] C. Tsai and A.W. Scaroni. Pyrolysis during the initial stages of pulverized-coal combustion. *20th Symposium (Int.) on Combustion*, 1455-1462, 1981.
- [47] G.A. Simons. Coal pyrolysis II: species transport theory. *Combustion and Flame*, 55:181-194, 1984.
- [48] M.M. Baum and P.J. Street. Predicting the combustion behaviour of coal particles. *Combustion Science and Technology*, 3:231-243, 1971.
- [49] S. Niksa and A.R. Kerstein. On the role of macromolecular configuration in rapid coal devolatilization. *Fuel*, 66:1389-1399, 1987.
- [50] A.S. Jamaluddin, T.F. Wall, and J.S. Truelove. Modelling of high intensity combustion of pulverized coal in a tubular combustor. *Combustion Science and Technology*, 55:89-113, 1987.
- [51] W.R. Seeker, G.S. Samuelsen, M.P. Heap, and J.D. Trolinger. The thermal decomposition of pulverized coal particles. *18th Symposium (Int.) on Combustion*, 1213-1226, 1981.
- [52] *SAS User's Guide: Statistics*. SAS Institute Inc., 1982 edition, 1982.
- [53] *IMSL Library: FORTRAN Subroutines for Mathematics and Statistics*. IMSL Problem-Solving Software Systems, 1984.

- [54] D.W. Bacon. *Collection and Interpretation of Industrial Data*. Department of Chemical Engineering, Queen's University.
- [55] R.D. Neuniger, J.B. Howard, and A.P. Sarofim. Sooting potentials of coals. *Journal of Coal Science*, 521-524, 1983.
- [56] M. Dal Cin. *Nonlinearities in Catalytic Rate Modelling*. MSc thesis, University of Ottawa, 1988.
- [57] G.J. Van Wylen and R.E. Sonntag. *Fundamentals of Classical Thermodynamics*. John Wiley and Sons, 3rd edition, 1985.

Appendix A

Particle Energy Balance

There was some question about the validity of the energy balance used by Baxter [34] in which the enthalpy of the escaping devolatilization gases was included. This was tested by applying the first law of thermodynamics to a pyrolyzing coal particle. This first law for the particle is:

$$Q = \dot{m}_v h_g + \frac{dm_p u}{dt} \quad (\text{A.1})$$

where:

- $\frac{dm_p}{dt} = \dot{m} - \dot{m}_v$
- \dot{m}_v - mass of volatiles released during time step
- m_p - mass of particle
- h_g - enthalpy of released volatiles
- u - internal energy of particle

Assuming constant temperature inside the time step:

$$Q = \dot{m}_v h_g + \frac{dm_p}{dt} u + m_p \frac{du}{dt}$$

since $\dot{m}_v = -\frac{dm_p}{dt}$

$$Q = \dot{m}_v(h_g - u) + m_p \frac{du}{dt}$$

For an incompressible solid $u_p = h_p$ [57], and $h_g - u$ is simply the heat of pyrolysis per unit mass volatiles, ΔH_v . Therefore:

$$Q = \dot{m}_v \Delta H_v + m_p \frac{du}{dt}$$

and no explicit inclusion of the enthalpy of the escaping volatiles is needed.

Appendix B

Effect of Particle Swelling on Particle Heating

Swelling coals are generally medium to high volatile bituminous coals which become plastic upon heating. This swelling is generally of concern as it could result in clogging of experimental or industrial equipment. However, the interest in this study is on the effects of swelling on particle motion and heating.

In order to simplify this discussion, it is assumed that the slip velocity of the particle relative to the gas is equal to the terminal velocity:

$$v_t = \tau g \quad (\text{B.1})$$

where, assuming Stokes' law to be valid,

$$\tau = \frac{\rho_p d_p^2}{18\mu}$$

For a constant diameter particle, it was shown in chapter 3 that

$$\rho_p = \rho_o(1 - V \cdot MAFR) \quad (\text{B.2})$$

substitution into equation B.2 yields:

$$\tau = \frac{\rho_o d_o^2 (1 - V \cdot MAFR)}{18\mu} \quad (\text{B.3})$$

For a swelling particle,

$$\rho'_p = \rho_o (1 - V \cdot MAFR) \frac{d_p^3}{d^3} \quad (\text{B.4})$$

therefore:

$$\tau' = (\rho_o (1 - V \cdot MAFR) \frac{d_p^3}{d^3}) / 18\mu \quad (\text{B.5})$$

The ratio of terminal velocities is therefore:

$$\frac{v'_t}{v_t} = \frac{\tau'}{\tau} \quad (\text{B.6})$$

$$= \frac{d_p}{d} \quad (\text{B.7})$$

so that the slip velocity varies as the diameter. However, since the slip velocity is generally an order of magnitude less than the gas velocity [17], the effect of swelling on particle motion is small.

$$\frac{Re'}{Re} = \frac{v'_t d'}{v d_p} \quad (\text{B.8})$$

$$= 1 \quad (\text{B.9})$$

This indicates that the increased particle size has no effect upon the particle Reynolds number.

The effect of swelling on particle heating is investigated by determining the effect of the increased diameter has on the convection and radiation heat transfer.

$$q_{conv} = hA(T_p - T_{\infty}) \quad (\text{B.10})$$

where

$$h = \frac{kNu}{d}$$

$$Nu = 2 + (0.4Re^{0.5} + 0.6Re^{.66}) Pr^{0.4} \frac{\mu_{\infty}}{\mu_p}$$

since $Re' = Re$ then $Nu' = Nu$ and

$$\frac{q_{conv}}{q'_{conv}} = \frac{d}{d_o} \quad (\text{B.11})$$

For radiation,

$$q_{rad} = \epsilon F \sigma A (T_w - T_p) \quad (\text{B.12})$$

where:

- ϵ - emissivity of coal
- F - view factor
- σ - Stefan-Boltzmann constant
- A - surface area of particle

therefore

$$\frac{q'_{rad}}{q_{rad}} = \frac{d^2}{d_o^2} \quad (\text{B.13})$$

This indicates that both the convective and radiation heating processes are affected by the increased particle size. However, as the particles [1] were heated nearly to furnace temperature before any significant devolatilization occurred, the effect of particle swelling on the heating is minimized.

Appendix C

Particle Heating Program Listing

The particle heating program with the modifications to the drag coefficient, convective heat transfer coefficient and energy balance equation included is listed below:

```
C  SET UP FOR LIG - TO CHANGE MUST CHANGE DP ,NAFR AND ALPHA1
C  SET UP WITH VARIABLE DENPAR
    DIMENSION DIST(500),UP(500),TP(500),WLOSS(500),G(500)
    DIMENSION X(32),XU(32),RV(32),U(30),T(30),TW(30),DEN(30),VIS(30)
    DIMENSION KSUN(500),DENPAR(500),C(500),K1(500),K2(500)
    DIMENSION KSUN1P(500),KSUN1(500),KSUN2P(500)
    DIMENSION TIME(500),H(500),KK1(500)
    REAL KSUN1,K1P,K2P,KK1P,K1,K2,KK1,KK2P,K12P,K22P,NAFR,KSUN1P
    REAL KSUN2P,KSUN
C
    NI=28
    NJ=21
    NINI=NI-1
    DO 191 N=3,3
C
    IF(N.EQ.1)DIAPAR=0.000010
    IF(N.EQ.2)DIAPAR=0.0000675
    IF(N.EQ.3)DIAPAR=0.0000476
    IF(N.EQ.4)DIAPAR=0.0000604
C
    IF(N.EQ.5)DIAPAR=0.000200
C
    IF(N.EQ.6)DIAPAR=0.000250
```

```

C
  WRITE(6,11) DIAPAR
11  FORMAT(///,'DIA M',E10.2,3X,'TIME S',3X,'VEL M/S',5X,'DIST M',7X,
  * 'RE',7X,'E W/M2C',2X,'GRAD W/M2',3X,'QCON W/M2',4X,'TEMP K'
  * ',5X,'WLOSS',5X,'COAL FRAC',/)
C
C-----COAL PROPERTIES
C
  RR=208.13
  PATH=101325
  CONST=RR/PATH
  CPPAR=1300.0
C  CPPAR=2000.0
  EPS=0.9
  DENPAR(1)=1250.0
C  DENPAR=1300.0
C
C-----INITIAL VALUES
C
  DO 100 I=1,NI
    READ(5,020) X(I),XU(I),U(I),T(I),TW(I)
020  FORMAT(F6.3,2X,F6.4,2X,F5.3,2X,F6.1,2X,F6.1)
    DEN(I)=101325.0/(208.13*T(I))
    VIS(I)=1.91E-6*T(I)**1.5/(136.9*T(I))
100  CONTINUE
    RV(IJ)=0.0264
    RV(7)=0.0024
    UU=U(2)
    VSC=VIS(1)
    THP=T(1)
    TWL=TW(2)
    TP(1)=T(1)
    TIEPRM=T(1)
    TIESEC=TW(2)
    TEKIT=TIEPRM
    DST=DEN(1)
    DIST(1)=0.0
C
C-----TEMPERATURE INCREMENT
  DELTDP=25.0
C

```

```

GRAVITY=9.806
SIG=5.669E-8
C
C-----THIS GIVES INITIAL DISTANCE TRAVELLED
C
UP(1)=UU+(SQRT((576.0*VSC**2)/(DIAPAR**4*DENPAR(1)**2)+(32.0*DST*
* GRAVITY)/(3.0*DENPAR(1)*DIAPAR))-24.0*VSC/(DIAPAR**2
* DENPAR(1)))*(DENPAR(1)*DIAPAR)/(4.0*DST)
C
VFPE=0.5*(1.0-1.0/SQRT(1.0+RV(NJ)**2/KU(WI)**2))
VFPW=1.0-VFPE-0.5
QRAD=SIG*EPS*VFPW*(TVL**4-TP(1)**4)
RELC=0.0
HTC=0.0
QCDEV=0.0
TIME(1)=0.0
C
C MAFR - MOISTURE AND ASH FREE FRACTION OF ORIGINAL COAL
C HR - ENDOTHERMIC HEAT OF PYROLYSIS HEAT OF PYROLYSIS, J/KG
C
MAFR=.786
C MAFR=.87
HR=637*1000
C HR=0.0
PRANDL=.66
PATH=101325.0
RR=208.13
RG=1.967E-3
WTLOSS(1)=0
C
C BI - PRE-EXPONENTIAL FACTOR, 1/S
C EI - ACTIVATION ENERGY, KCAL/GMOL
C ALPHA1 - MASS FRACTION VOLATILE I IN 2 PARALLEL REACTION
C MODEL
C
ALPHA1=0.3065
ALPHA2=1.0
B1=1629.0
B2=4.5888
E1=12.66
E2=52.0

```

```

FACTOR=.1
G(1)=0
DELT=DEMPAR(1)*CPPAR*DIAPAR*DELTHP/(6.0*ABS(QRAD-QCONV-ER*G(1)
*))
C(1)=1.0
SAREA=3.142*DIAPAR**2
VP=3.142*DIAPAR**3/6
K=2
L=2
C
200 CONTINUE
LL=1
DELT=DEMPAR(K-1)*CPPAR*DIAPAR*DELTHP/(6.0*ABS(QRAD-QCONV-ER*G(K-1)
C DELT=DEMPAR(1)*CPPAR*DIAPAR*DELTHP/(6.0*ABS(QRAD-QCONV-ER*G(K-1)
*))
IF(DELT.GT.0.005) DELT=0.005
TIME(K)=TIME(K-1)+DELT
DIST(K)=DIST(K-1)+UP(K-1)*DELT
C WRITE(6,96) TIME(K-1),UP(K-1),DIST(K-1),RELC,ETC,QRAD,QCONV,
C *TP(K-1),WLOSS(K-1),C(K-1)
C 95 FORMAT(17X,F7.5,2X,E10.3,1X,E10.3,2X,E10.3,2X,F8.2,2X,E11.4,2X,
C * E10.4,2X,F7.1,2X,E11.4,2X,E11.4)
WRITE(6,96) TIME(K-1),UP(K-1),DIST(K-1),TP(K-1),WLOSS(K-1)
95 FORMAT(17X,F7.5,2X,E10.3,2X,E10.3,2X,F7.1,2X,E11.4)
IF(DIST(K).GE.XU(WI)) THEN
WRITE(6,9)
9 FORMAT('PARTICLE EXITED FURNACE')
GO TO 300
ENDIF
J=L
C
DO 90 I=J,NI
IF((DIST(K).LE.X(I)).AND.(DIST(K).GT.X(I-1))) L=I
90 CONTINUE
C
C BLOCK 1
C THIS CALCULATES THE TEMPERATURE OF THE NON-PYROLYZING PARTICLE
C
CST=(DIST(K)-X(L-1))/(X(L)-X(L-1))
VSC=VIS(L-1)+(VIS(L)-VIS(L-1))*CST
DST=DEH(L-1)+(DEH(L)-DEH(L-1))*CST

```

```

TMP=T(L-1)+(T(L)-T(L-1))*CST
TWL=TW(L-1)+(TW(L)-TW(L-1))*CST
IF(DIST(K).LT.XU(L)) UU=U(L-1)+(U(L)-U(L-1))*(DIST
• (K)-XU(L-1))/(XU(L)-XU(L-1))
IF(DIST(K).GE.XU(L)) UU=U(L)+(U(L+1)-U(L))*(DIST(K)
• -XU(L))/(XU(L+1)-XU(L))
C
C-----THIS CALCULATES FILM TEMPERATURE PROPERTIES
C
TAVER=(TMP+TP(K-1))/2
VSCF=1.91E-6*TAVER**1.5/(TAVER+136.9)
DSTF=(1.0/(CONST*TP(K-1))+DST)/2.0
C
C-----CALCULATE PARTICLE VELOCITY
C
RELC=ABS(UP(K-1)-UU)*DIAPAR*DSTF/VSCF
AUP=18.0*VSCF*(1.0+0.15*RELC**0.687)/(DENPAR(K-1)*DIAPAR**2)
C AUP=18.0*VSCF*(1.0+0.15*RELC**0.687)/(DENPAR(1)*DIAPAR**2)
UP(K)=UU-((GRAVITY-AUP*(UP(K-1)-UU))*EXP(-AUP*DELTA)-GRAVITY)/AUP
C
C-----CALCULATE PARTICLE TEMPERATURE
C
CPP=(TMP-350.0)*0.212+1000.0
CPP=(4.969-.767E-5*TMP+1.234E-8*TMP**2)*104.598
VFPP=0.5*(1.0-1.0/SQRT(1.0+RV(7)**2/DIST(K)**2))
VFPS=0.5*(1.0-1.0/SQRT(1.0+RV(NJ)**2/DIST(K)**2))-VFPP
VFPE=0.5*(1.0-1.0/SQRT(1.0+RV(NJ)**2/(XU(NJ)-DIST(K)**2))
VFPW=1.0-VFPP-VFPS-VFPE
VSCP=1.91E-6*TP(K-1)**1.5/(136.9*TP(K-1))
HTC=(2.0*(0.4*RELC**(1/2)+0.06*RELC**(2/3))*(PRANDL**0.4
• )*(VSC/VSCP)**0.25)*VSC*CPP/(PRANDL*DIAPAR)
HPP=SIG*EPS*VFPP*(TINPM+TP(K-1))*(TINPM**2+TP(K-1)**2)
HPS=SIG*EPS*VFPS*(TINSEC+TP(K-1))*(TINSEC**2+TP(K-1)**2)
HPE=SIG*EPS*VFPE*(TEKIT+TP(K-1))*(TEKIT**2+TP(K-1)**2)
HPW=SIG*EPS*VFPW*(TML+TP(K-1))*(TML**2+TP(K-1)**2)
ATP=6.0*(HPP+HPS+HPE+HPW+HTC)/(DENPAR(K-1)*CPPAR*DIAPAR)
C ATP=6.0*(HPP+HPS+HPE+HPW+HTC)/(DENPAR(1)*CPPAR*DIAPAR)
BTP=6.0*(HPP+TINPM+HPS+TINSEC+HPE+TEKIT+HPW+TML+HTC+TMP)/
• (DENPAR(K-1)*CPPAR*DIAPAR)
C • (DENPAR(1)*CPPAR*DIAPAR)
TP(K)=(BTP+(ATP*TP(K-1)-BTP)*EXP(-ATP*DELTA))/ATP

```

```

C
C
C
C THIS CALCULATES THE WEIGHT LOSS EXPERIENCED BASED ON THE
C NON-PYROLYZING TEMPERATURE CALCUATION
C
KSUM1(1)=0
KSUM2P(1)=0
K1(K-1)=B1*EXP(-1*E1/(RG*TP(K-1)))
K2(K-1)=B2*EXP(-1*E2/(RG*TP(K-1)))
KK1(K-1)=K1(K-1)+K2(K-1)
H(K-1)=DELT
KSUM1(K)=KSUM1(K-1)+(-1*KK1(K-1))*H(K-1)
ALK=ALPHA1*K1(K-1)+ALPHA2*K2(K-1)
WLOSS1=WLOSS(K-1)+H(K-1)*ALK*EXP(KSUM1(K))
C1=EXP(KSUM1(K))

C-----BLOCK 2
C THIS LOOP CAUSES THE PROGRAM TO BE EXITED IF THE WLOSS IS
C EQUAL TO OR GREATER THAN 1 OR CALCULATES THE PARTICLE DENSITY
C BASED ON THE WEIGHT LOSS EXPERIENCED
C
IF(C1.LE.1E-2) THEN
DENP1=(1-NAFR)*DENPAR(1)
DENPAR(K)=DENP1
C(K)=C1
WLOSS(K)=WLOSS1
GO TO 799
ELSE
DENP1=DENPAR(1)*(1-WLOSS1)+NAFR*(1-NAFR)*DENPAR(1)
ENDIF
TP1=TP(K)

C
C THIS SECTION CALCULATES THE PARTICLE TEMPERATURE OF THE
C PYROLYZING PARTICLE AND ITERATES UNTIL CONVERGING
C
C
C CALCULATE B HERE - BASED ON TP1
C -B - CORRECTION OF VELOCITY AND TEMP FIELDS DUE TO
C MASS TRANSFER
C

```

```

G1=(WTLOS1-WTLOSS(K-1))*DENP1*VP/(SAREA*DELT)
G1=(WTLOS1-WTLOSS(K-1))*DENPAR(1)*VP/(SAREA*DELT)
GAMMA=VSCF/PRAEHL
Z=DIAPAR*G1/(2*GAMMA)
B=EXP(Z)-1
C   B=0.0
C
C
560 CONTINUE
C
C   THIS SECTION INDICATES WHETHER THE MODEL IS BEING USED
C
C   IF(B.EQ.0.0) THEN
C     VALUE =1
C   ELSE
C     VALUE=LOG(1+B)/B
C   ENDDIF
C
C   AUP=18.0*VSCF*(1.0+0.15*RELC**0.687)/((1+B)*DENP1*DIAPAR**2)
C   AUP=18.0*VSCF*(1.0+0.15*RELC**0.687)/((1+B)*DENPAR(1)*DIAPAR**2)
C   UP(K)=UU-((GRAVITY-AUP*(UP(K-1)-UU))*EXP(-AUP*DELT)-GRAVITY)/AUP
C   HTC=VALUE*(2.0*(0.4*RELC**(1/2)+0.06*RELC**(2/3))*(PRAEHL**
C     0.4)*(VSC/VSCP)**0.25)+VSC*CPP/(PRAEHL*DIAPAR)
C
C   ATP=6.0*(HPP*HPS+HPE*HPW+HTC)/(DENP1*CPPAR*DIAPAR)
C   ATP=6.0*(HPP*HPS+HPE*HPW+HTC)/(DENPAR(1)*CPPAR*DIAPAR)
C   BTP=6.0*(HPP*TIJPM+HPS*TIJSEC+HPE*TKKIT+HPW*TWL+HTC
C     *THP-HR*G1)/(DENP1*CPPAR*DIAPAR)
C   *THP-HR*G1)/(DENPAR(1)*CPPAR*DIAPAR)
C   TP2=(BTP+(ATP*TP(K-1)-BTP)*EXP(-ATP*DELT))/ATP
C   K12P=B1*EXP(-1*K1/(RG*TP2))
C   K22P=B2*EXP(-1*K2/(RG*TP2))
C   KK2P=K12P+K22P
C   KSUR2P(K)=KSUR2P(K-1)+(H(K-1)/2)*(-1*(KK1(K-1)+KK2P))
C   ALKP2=ALPHA1*K12P+ALPHA2*K22P
C   WTLOS2=WTLOSS(K-1)+(H(K-1)/2)*(ALK*EXP(KSUR1(K-1))+ALKP2*
C     EXP(KSUR2P(K)))
C   C2=EXP(KSUR2P(K))
C
C
C   THIS EXITS THE PROGRAM IF DEVOLATILATION IS COMPLETE
C
C

```

```

IF(C2.LE.1E-2) THEN
DENP2=(1-MAFR)*DENPAR(1)
DENPAR(K)=DENP2
C(K)=C2
WLOSS(K)=WLOSS2
GO TO 799
ELSE
DENP2=DENPAR(1)*(1-WLOSS2)*MAFR+(1-MAFR)*DENPAR(1)
ENDIF
C
IF(ABS(TP2-TP1).LE.FACTOR) THEN
GO TO 550
ELSE
LL=LL+1
C WRITE(6,561) TNP,TP1,TP2,LL
C561 FORMAT(E12.5,2X,E12.5,2X,E12.5,I3)
TP1=TP2
WLOSS1=WLOSS2
GO TO 560
ENDIF
550 CONTINUE
TP(K)=TP2
C(K)=C2
C KSUM(K)=KSUM2
WLOSS(K)=WLOSS2
DENPAR(K)=DENP2
G(K)=(WLOSS(K)-WLOSS(K-1))*DENPAR(K)*VP/(SAREA*DELT)
C G(K)=(WLOSS(K)-WLOSS(K-1))*DENPAR(1)*VP/(SAREA*DELT)
QRAD=SIG*EPS*(VFPP*(TIMEP**4-TP(K)**4)+VFPS*(TIMSEC**4-TP(K)**4)
* +VFPE*(TEKIT**4-TP(K)**4)+VFPN*(TUL**4-TP(K)**4))
QCONV=HTC*(TP(K)-TNP)
K=K+1
GO TO 200
799 CONTINUE
WRITE(6,798)
798 FORMAT(2X,'PARTICLE HAS COMPLETELY DEVOLATILIZED')
WRITE(6,960) TIME(K),UP(K),DIST(K),RELC,HTC,QRAD,QCONV,
*TP(K),WLOSS(K),C(K)
950 FORMAT(17X,F7.5,2X,E10.3,1X,E11.4,2X,E10.3,2X,F8.2,2X,E11.4,2X,
* E10.4,2X,F7.1,2X,E11.4,2X,E11.4)
300 CONTINUE

```

191 CONTINUE

STOP

END

Appendix D

Fitting Program Listings

This is a SAS program that finds the least squares parameter estimates of the yield coefficient, α , and the reaction rate, k of the isothermal one reaction model:

$$V = \alpha(1 - \exp kt) \quad (D.1)$$

```
DATA BIT;
INPUT T II W;
LABEL T=TEMPERATURE
      II=TIME
      W=WEIGHT LOSS;
CARDS;
      1260 .05544 .125
      1260 .07812 .167
      1260 .09432 .269
      1260 .11146 .269
      1260 .14274 .289
      1260 .15782 .270
      1260 .15782 .330
:
DATA LIG;
INPUT T II W;
LABEL T=TEMPERATURE
      II=TIME
```

```
W=WEIGHT LOSS;
CARDS;
    1260 .07944 .140
    1260 .09640 .200
    1260 .11327 .199
    1260 .12890 .238
    1260 .14466 .255
    1260 .15952 .249
    1260 .17410 .221
;
PROC PRINT DATA=lig;
PROC NLIN DATA=lig BEST=10 METHOD=MARQUARDT;
    PARS ALPHA= .2 TO .8 BY .1
        AK= 3;
    BOUNDS ALPHA<1;
    EX=EXP(-AK*TI);
    Y=ALPHA*(1-EX);
MODEL W=Y;
    DER.ALPHA=(1-EX);
    DER.AK=ALPHA*TI*EX;
OUTPUT OUT=KOB1 P=YHAT R=RESID L95=L96 U95=U96;
PROC PLOT DATA=KOB1;
    PLOT RESID=YHAT/VREF=0 VPOS=25 HPOS=50;
    PLOT RESID=TI/VREF=0 VPOS=25 HPOS=50;
```

This is a SAS program that determines the least squares parameter estimates of the pre-exponential, k_0 , and the activation energy, E , for the linearized Arrhenius rate equation:

$$\ln k = -E/RT + \ln k_0 \quad (D.2)$$

with the data normalized for unbiased estimates.

```

DATA LAURA;
  INPUT T K RUMORD;
  LABEL T=TEMP
        K=REACTION RATE CONSTANT;
  C=LOG(K);
  I=1/T;
  IA=.5*(1/1740+1/2100);
  IH=.5*(1/1740-1/2100);
  IO=(I-IA)/IH;
  CARDS;
  1740  61.8103  1
  1940  99.7716  2
  2100  153.9167  3
;
PROC PRINT DATA=LAURA;
PROC REG ALL DATA=LAURA;
  MODEL C=IO /P R CLI CLM;
  OUTPUT OUT=D P=YHAT R =RESID L95=L95 U95=U95 COOED=COOED;
PROC PRINT DATA=D;
PROC PLOT DATA=D;
  PLOT C=IO='Y' YHAT=IO='P' U95=IO='U' L95=IO='L'
        /OVERLAY VPOS=18 HPOS=50;
  PLOT RESID=IO/VPOS=20 HPOS=50;
  PLOT RESID=YHAT/VPOS=20 HPOS=50;

```

This is a SAS program that determines the least squares parameter estimates of the pre-exponential, k_0 , and the activation energy, E , for the Arrhenius rate equation:

$$k = k_0 \exp(-E/RT) \quad (D.3)$$

using estimates of the reaction rate, k , determined for each temperature run.

```

DATA ONE;
  INPUT T K;
  LABEL T=TEMP
        K=REACTION RATE CONSTANT;
  CARDS;
    1740  61.810
    1940  99.772
    2100 153.917
  ;
PROC PRINT DATA=ONE;
PROC NLIN BEST=10 METHOD=MARQUARDT;
  PARAMS KO=.5E4
        E=20 TO 40 BY 5;
  R=1.987E-3;
  TP=(1740+1940+2100)/3;
  EXP=EXP(-E/(R*TP));
  DT=(1/T-1/TP);
  EKS=EXP(-E*DT/R);
MODEL K=KO*EXP+EKS;
DER.KO=EXP+EKS;
DER.E=KO*EXP*(-1)*DT+EKS/R+EKS*(-1)*KO/(R*TP)*EXP;
OUTPUT OUT=LAU P=YHAT R=RESID L95=L95 U95=U95;
PROC PLOT DATA=LAU;
  PLOT RESID=YHAT/VREF=0 VPOS=25 HPOS=50;
  PLOT RESID=T/VREF=0 VPOS=25 HPOS=50;
  PLOT YHAT=T='P' K=T='Y' L95=T='L' U95=T='U'
        /OVERLAY VPOS=25 HPOS=50;

```

This is a SAS program that determines the least squares parameter estimates of the pre-exponential, k_0 , and the activation energy, E , for the isothermal, one reaction model:

$$V = \alpha(1 - \exp(-k_0 \exp(-E/R * (1/T - 1/T_p)))) \quad (D.4)$$

with the data centered around the mean temperature, T_p .

```

DATA BIT;
  INPUT T TI W AL;
  LABEL T=TEMP
        TI=TIME
        W=WT LOSS
        AL=ALPHA;
  CARDS:
    1000 .07878 .021 .2263
    1000 .12341 .067 .2263
    1000 .14341 .060 .2263
    1000 .16425 .085 .2263
    1000 .18341 .089 .2263
    1000 .20329 .069 .2263
    1260 .04040 .109 .4538
    1260 .05554 .125 .4538
    1260 .07813 .167 .4538
    1260 .09499 .269 .4538
    1260 .11151 .269 .4538
    1260 .14276 .289 .4538
    1260 .15768 .270 .4538
    1260 .15768 .330 .4538
    1510 .04439 .355 .4738
    1510 .04439 .272 .4738
    1510 .04498 .325 .4738
    1510 .06200 .337 .4738
    1510 .06828 .384 .4738
    1510 .06828 .356 .4738
    1510 .06828 .304 .4738
    1510 .06907 .304 .4738
    1510 .06544 .354 .4738
    1510 .07119 .396 .4738
    1510 .07763 .388 .4738
    1510 .07763 .447 .4738

```

1510 .07811 .366 .4738
 1510 .08406 .415 .4738

:

DATA LIG;

INPUT T TI W AL;

LABEL T=TEMP

TI=TIME

W=WT LOSS

AL=ALPHA;

CARDS;

1000	.07878	.021	.2263
1000	.12341	.067	.2263
1000	.14341	.060	.2263
1000	.16425	.085	.2263
1000	.18341	.089	.2263
1000	.20329	.069	.2263
1260	.07944	.140	.3062
1260	.09640	.200	.3062
1260	.11327	.199	.3062
1260	.12890	.238	.3062
1260	.14466	.255	.3062
1260	.15952	.249	.3062
1260	.17410	.221	.3062
1510	.03750	.285	.4595
1510	.04141	.334	.4595
1510	.04141	.292	.4595
1510	.04141	.327	.4595
1510	.04857	.304	.4595
1510	.04857	.340	.4595
1510	.04857	.387	.4595
1510	.05554	.378	.4595
1510	.06212	.389	.4595
1510	.06880	.387	.4595
1510	.07506	.392	.4595
1510	.07506	.442	.4595
1510	.08485	.393	.4595

:

PROC PRINT DATA=LIG;

PROC NLIN DATA=LIG BEST=15 METHOD=MARQUARDT;

PARMS E0=00000

E=15 TO 25 BY 1;

```
R=1.987E-3;
TP=(1000+1260+1510)/3;
EXP=EXP(-1.*E/(R*TP));
DT=(1/T-1/TP);
EKS=EXP(-E*DT/R);
MODEL W=AL*(1-EXP(-K0*EXP*EKS*TI));
DER.K0=EXP*EKS*TI*AL*EXP(-K0*EXP*EKS*TI);
DER.E=AL*TI*EXP(-K0*EXP*EKS*TI)*(K0*EXP*(-1)
      *DT*EKS/R-EKS*K0*EXP/(R*TP));
OUTPUT OUT=K0B1 P=YHAT R=RESID L95=L95 U95=U95;
PROC PLOT DATA=K0B1;
  PLOT RESID=YHAT/VREF=0 VPOS=25 HPOS=50;
  PLOT RESID=TI/VREF=0 VPOS=25 HPOS=50;
  PLOT YHAT=TI='P' W=TI='W' L95=TI='L' U95=TI='U'
      /OVERLAY VPOS=25 HPOS=50;
```

This program utilizes the IMSL subroutine ZXSSQ to fit the non-isothermal one reaction model to the experimental data centered around the mean temperature T_p . Subroutine model performs the numerical integration of this model as well as calculates the residuals required by ZXSSQ.

```

EXTERNAL MODEL
INTEGER N,B,ILJAC,NSIG,MAXFB,IOPT,I,INFER,IER
REAL*8 PARM(4),X(3),F(37),XJAC(37,3),XJTJ(3),WORK(80),EPS,
*SGH,SSQ,Y(37),DT(37),TE(37),AL(37),KSUM(37),WTLOS(37),
*DELTA
COMMON
*/ZSQ/Y,DT,TE,AL,WTLOS
N=7
B=2
ILJAC=7
NSIG=5
EPS=1E-8
DELTA=1E-8
MAXFB=450
IOPT=1
X(1)=7.1385
X(2)=16.57
WRITE(6,222) X(1),X(2)
222 FORMAT(F7.4,2X,F7.3)
DO 44 I=1,N
  READ(5,22) TE(I),DT(I),Y(I),AL(I)
22 FORMAT(11X,F6.1,1X,F6.5,1X,F4.3,2X,F5.4)
  WRITE(6,26) TE(I),DT(I),Y(I),AL(I)
26 FORMAT(11X,F6.1,1X,F6.5,1X,F4.3,2X,F5.4)
44 CONTINUE
CALL ZXSSQ(MODEL,N,B,NSIG,EPS,DELTA,MAXFB,IOPT,PARM,X,SSQ,F,
*      XJAC,ILJAC,XJTJ,WORK,INFER,IER)
WRITE(6,19) X(1),X(2),SSQ
19 FORMAT(E13.6,2X,E13.6,2X,E13.6)
DO 9 I=1,N
  WRITE(6,20) F(I),DT(I),Y(I),WTLOS(I),TE(I)
20 FORMAT(E11.4,2X,F6.5,2X,F4.3,2X,F4.3,2X,F6.1)
9 CONTINUE
WRITE(6,21) INFER,IER
21 FORMAT(I2,2X,I3)
WRITE(6,221) WORK(1),WORK(2),WORK(3)

```

```

221 FORMAT(E11.4,2X,E11.4,2X,E11.4)
STOP
END
C
C
SUBROUTINE MODEL(X,M,N,F)
INTEGER M,N,I
REAL*8 I(3),F(37),Y(37),DT(37),K1(37),TE(37),AL(37),W(37)
REAL*8 K2(37),KSUM(40),WILOS(37),TP
COMMON
* /ZSQ/Y,DT,TE,AL,WILOS
R=1.967E-3
TP=1250.4
DO 15 I=1,M
K1(I)=X(1)*DEXP(-I(2)/R*(1/TE(I)-1/TP))
IF(I.EQ.1) THEN
KSUM(I)=(-1)*K1(I)*DT(I)
ELSE
IF(DT(I).EQ.DT(I-1))THEN
KSUM(I)=KSUM(I-1)
ELSE
KSUM(I)=KSUM(I-1)+(-1)*(K1(I)+K1(I-1))
* DT(I)/2
ENDIF
ENDIF
WILOS(I)=AL(I)*(1-DEXP(KSUM(I)))
F(I)=Y(I)-WILOS(I)
15 CONTINUE
RETURN
END

```

This program utilizes the IMSL subroutine ZXSSQ to fit the non-isothermal two reaction model:

$$V = \int_0^t (\alpha_1 k_1 + \alpha_2 k_2) \exp(-\int_0^t (k_1 + k_2) dt) dt \quad (D.5)$$

to the experimental data centered around the mean temperature T_p . ZXSSQ calls the subroutine model which performs the numerical integration of this model as well as calculates the residuals required by ZXSSQ.

```

EXTERNAL MODEL
INTEGER N,N,IXJAC,NSIG,MAXFN,IOP,T,I,INFER,IER
REAL*8 PARM(4),X(3),F(37),XJAC(37,3),XJTJ(3),WORK(90),EPS,
•   SQN,SSQ,Y(37),DT(37),TE(37),AL(37),RESUM(37),
•   WTLOSS(37),DELTA
COMMON
•/ZSQ/Y,DT,TE,AL,WTLOSS
N=7
N=2
IXJAC=7
NSIG=6
EPS=1E-8
DELTA=1E-8
MAXFN=1000
IOP=1
X(1)=8.1164
X(2)=13.29
WRITE(6,444) X(1),X(2)
444 FORMAT(F7.4,2X,F7.4)
DO 44 I=1,N
  READ(5,22) TE(I),DT(I),Y(I),AL(I)
22  FORMAT(11X,F6.1,1X,F6.5,1X,F4.3,2X,F6.4)
  WRITE(6,26) TE(I),DT(I),Y(I),AL(I)
26  FORMAT(11X,F6.1,1X,F6.5,1X,F4.3,2X,F6.4)
44  CONTINUE
CALL ZXSSQ(MODEL,N,N,NSIG,EPS,DELTA,MAXFN,IOP,PARM,X,SSQ,F,
•   XJAC,IXJAC,XJTJ,WORK,INFER,IER)
WRITE(6,19) X(1),X(2),    SSQ
19  FORMAT(E12.5,2X,E12.5,2X,    E12.5)
DO 9 I=1,N
  WRITE(6,20) F(I),DT(I),Y(I),WTLOSS(I),TE(I)

```

```

20  FORMAT(E11.4,2X,F6.5,2X,F4.3,2X,F4.3,2X,F6.1)
9   CONTINUE
    WRITE(6,21) INFER,IER
21  FORMAT(I2,2X,I3)
    WRITE(6,99) WORK(1),WORK(2),WORK(3),WORK(4)
99  FORMAT(E12.5,2X,E12.5,2X,E12.5,2X,E12.5)
    STOP
    END

C
SUBROUTINE MODEL(X,M,N,F)
INTEGER N,M,I
REAL*8  I(3),F(37),Y(37),DT(37),K1(37),TE(37),AL(37),W(37),
*      K2(37),WLOSS(40),KK(40),AKSUM(40),KSUM(40)
COMMON
*/ZSQ/Y,DT,TE,AL,WLOSS
R=1.987E-3
DO 15 I=1,M
TP=1250.4
K2(I)=2.63E10*DEXP(-63.90/(R*TE(I)))
K1(I)=X(1)*DEXP(-X(2)/R*(1/TE(I)-1/TP))
KK(I)=K1(I)+K2(I)
AKSUM(I)=.3062*K1(I)+1.0*K2(I)
IF(I.EQ.1) THEN
    KSUM(I)=(-1)*KK(I)*DT(I)
    WLOSS(I)=AKSUM(I)*DEXP(KSUM(I))*DT(I)
ELSE
    IF(DT(I).NE.DT(I-1))THEN
        KSUM(I)=KSUM(I-1)+(-1)*(KK(I)+KK(I-1))
        *      *DT(I)/2
        WLOSS(I)=WLOSS(I-1)+(AKSUM(I)*DEXP(KSUM(I))+
        *      AKSUM(I-1)*DEXP(KSUM(I-1)))*DT(I)/2
    ELSE
        KSUM(I)=KSUM(I-1)
        WLOSS(I)=WLOSS(I-1)
    ENDIF
ENDIF
    F(I)=Y(I)-WLOSS(I)
15  CONTINUE
    RETURN
    END

```

Appendix E

Experimental Data

The following are tables of the experimental data of Kobayashi [1] with the residence time and temperature predicted by the reactor model program.

Table 18: Low Temperature Experimental Data [1] for Lignite Coal

Furnace temperature	Particle temperature	Residence time	Weight loss
1260	1245	.07944	.140
	1248	.09640	.200
	1250	.11327	.199
	1251	.12890	.238
	1252	.14466	.255
	1253	.15952	.249
	1254	.17410	.221
	1510	1310	.01300
1476		.02477	.086
1490		.02946	.195
1496		.03375	.180
1496		.03375	.216
1499		.03750	.285
1501		.04141	.334
1501		.04141	.292
1501		.04141	.327
1503		.04857	.304
1503		.04857	.340
1503		.04857	.387
1504		.05554	.378
1505		.06212	.389
1506		.06880	.387
1507		.07505	.392
1507		.07505	.442
1507		.08485	.393

Table 19: High Temperature Experimental Data [1] for Lignite Coal

Furnace temperature	Particle temperature	Residence time	Weight loss
1740	1259	.00778	.173
	1259	.00778	.105
	1547	.01216	.277
	1650	.01569	.328
	1693	.01871	.287
	1713	.02145	.379
	1724	.02635	.418
	1726	.02818	.439
	1726	.02818	.478
	1728	.03086	.489
	1730	.03526	.512
	1730	.03526	.496
	1731	.03693	.437
	1731	.03693	.473
	1732	.03725	.456
	1735	.04349	.481
	1738	.04737	.461
	1739	.05086	.491
	1739	.05086	.541
	1739	.05086	.475
1940	1739	.05086	.483
	1378	.00681	.093
	1599	.00890	.254
	1683	.01006	.330
	1801	.01254	.342
	1855	.01461	.483
	1900	.01805	.452
	1916	.02127	.514
	1925	.02424	.581
	1928	.02695	.594
	1932	.03104	.586
	1933	.03607	.609
	1933	.03607	.558
1933	.03607	.588	
1933	.03607	.550	

Table 20: High Temperature Experimental Data [1] for Lignite Coal (cont.)

Furnace temperature	Particle temperature	Residence time	Weight loss
2100	404	.00124	.107
	677	.00297	.304
	677	.00297	.270
	1075	.00491	.479
	1444	.00720	.550
	1831	.01192	.562
	1983	.01788	.610
	1994	.01903	.639
	1994	.01903	.635

Table 21: Low Temperature Experimental Data [1] for Bituminous Coal

Furnace temperature	Particle temperature	Residence time	Weight loss
1000	890	.02591	.016
	985	.07878	.021
	991	.12341	.067
	993	.14341	.060
	994	.16425	.085
	995	.18341	.089
	995	.20329	.069
	1260	1220	.04066
1239		.05544	.125
1245		.07812	.167
1248		.09432	.269
1250		.11146	.269
1252		.14274	.289
1254		.15782	.270
1254		.15782	.330
1510	1375	.01870	.071
	1470	.02809	.081
	1470	.02809	.127
	1473	.02881	.142
	1494	.03649	.212
	1494	.03649	.233
	1494	.03750	.232
	1501	.04423	.355
	1501	.04423	.272
	1501	.04480	.325
	1504	.05179	.337
	1505	.05807	.384
	1505	.05807	.356
	1505	.05807	.304
	1505	.05885	.304
	1506	.06521	.354
	1506	.07096	.396
	1507	.07739	.388
1507	.07739	.447	
1507	.07786	.366	
1507	.08382	.415	

Table 22: High Temperature Experimental Data [1] for Bituminous Coal

Furnace temperature	Particle temperature	Residence time	Weight loss	
1740	426	.00222	.158	
	789	.00564	.146	
	1168	.00960	.328	
	1168	.00960	.298	
	1168	.00960	.305	
	1422	.01401	.383	
	1422	.01401	.407	
	1552	.01834	.467	
	1655	.02658	.401	
	1688	.03449	.467	
	1788	.03449	.441	
	1940	487	.00246	.203
		734	.00422	.199
		1008	.00605	.251
1221		.00774	.408	
1390		.00951	.561	
1615		.01287	.455	
1747		.01588	.520	
1807		.01877	.574	
1807		.01877	.597	
2100		387	.00156	.241
	600	.00293	.356	
	600	.00293	.381	
	914	.00477	.479	
	914	.00477	.482	
	1243	.00691	.527	
	1697	.01144	.633	
	1960	.01853	.641	

END

05/12/90

FIN

Contents

Abstract	i
Acknowledgement	ii
Nomenclature	iii
1 Introduction	1
2 Literature Survey	4
2.1 Background	4
2.2 Experimental techniques	8
2.2.1 Entrained Flow Reactors	9
2.2.2 Heated Grid	15
2.2.3 Crucible tests	17
2.2.4 Conclusions	19

2.3	Accuracy of the Ash Tracer Technique	21
2.3.1	Crucible Tests	22
2.3.2	Inert Atmosphere Furnace Tests	23
2.3.3	Other Atmosphere Furnace Tests	24
2.3.4	Conclusions	26
3	Model Evaluation	28
3.1	Evaporation model	29
3.1.1	Lockwood et al.	29
3.2	Single first order reaction model	30
3.2.1	Badzioch and Hawksley	30
3.2.2	Scaroni et al.	31
3.2.3	Truelove	32
3.3	Competitive Parallel Reaction Model	32
3.3.1	Kobayashi	32
3.3.2	Ubhayakar et al.	35
3.3.3	Jamaluddin et al.	36
3.3.4	Suzuki et al.	37
3.3.5	Baxter et al.	38

3.4	Two component model	38
3.4.1	Nsakala et al.	39
3.5	Multiple Parallel Reaction Mechanism	40
3.5.1	Anthony and Howard	40
3.5.2	Hashimoto et al.	43
3.5.3	Solomon et al.	43
3.5.4	Suuberg et al.	44
3.5.5	Rizvi	46
3.5.6	Sprouse et al.	46
3.6	Conclusions	47
4	Reactor Model Program	50
4.1	Method of Integration	51
4.2	Effects of mass transfer	55
4.3	Physical properties of coal	59
4.3.1	Specific heat	59
4.4	Heat of Pyrolysis	62
4.4.1	Density and Diameter Behavior	67
5	Fitting Routine	71

5.1	Isothermal fitting procedure	72
5.2	Non-isothermal fitting procedure	74
5.3	Significance tests	78
5.4	Precision of the parameter estimates	79
6	Application of Fitting Procedure	81
6.1	Comparison of Particle Heating Calculations	81
6.2	Isothermal Fitting	86
6.2.1	Determination of Ultimate Yield and Reaction Rate	86
6.2.2	Fitting of the Arrhenius Rate Constants	94
6.3	Non-isothermal Fitting	98
6.3.1	Determination of Low Temperature Parameter Estimates	98
6.3.2	Determination of High Temperature Parameter Estimates	99
6.3.3	Iterative fitting procedure	103
6.4	Precision of the parameter estimates	108
6.5	Significance Tests	118
7	Conclusions and Recommendations	122
7.1	Conclusions	122
7.2	Recommendations	124

List of References	124
A Particle Energy Balance	131
B Effect of Particle Swelling on Particle Heating	133
C Particle Heating Program Listing	136
D Fitting Program Listings	145
E Experimental Data	156

List of Figures

1	Schematic Drawing of Entrained Flow Reactor at Energy, Mines and Resources	2
2	Proposed Model for Molecular Structure of Coal [2]	5
3	Comparison of the composition of devolatilization products [3] of bituminous (a) and lignite (b) coals	7
4	Devolatilization Data Collected by Nsakala [4]	11
5	Weight loss versus residence time as predicted by Anthony and Howard [5,6] model for various temperatures	42
6	Pyrolysis product composition from lignite coal heated to different peak temperatures	45
7	Sample Grid for Laminar Flow Furnace [7]	52
8	Weight Loss Versus Time for Particle Undergoing Exponential Heating . . .	54
9	Effects of Mass Transfer on a Devolatilizing Coal Particle	58
10	Predictions of the Specific Heat of Coal and Coke [8]	60
11	Effect of Heat of Reaction on Internal Temperature Profile [9]	64

12	Effect of heat of pyrolysis on particle temperature	65
13	Weight Loss Versus Time for particle in 1510K furnace	66
14	Typical Temperature-time History of a Coal Particle in a Laminar Flow Furnace	75
15	Weight loss versus residence time for lignite coal	82
16	Weight loss versus residence time for bituminous coal	83
17	Comparison of residence time predictions from present particle heating pro- gram to predictions by Kobayashi[1,10]	84
18	Weight loss versus residence time for 1260K data	88
19	Comparison of the heating history of the lignite and bituminous coals at 1940K	90
20	Weight loss versus residence time for 1740K and 1940K bituminous data . .	91
21	Isothermal fitting of parameter estimates to 1510K bituminous data	93
22	Model Predictions of Two Competitive Reaction Devolatilization Model for Lignite Coal	104
23	Model Predictions of Two Competitive Reaction Devolatilization Model for Bituminous Coal	105
24	Confidence region for parameter estimates of isothermal single reaction model for 1260K lignite data. The point represents the converged parameter estimates.	109
25	Confidence region for parameter estimates of isothermal single reaction model for 1260K bituminous data	110
26	Confidence region for parameter estimates of isothermal single reaction model for 1510K lignite data	111

27	Confidence region for parameter estimates of isothermal single reaction model for 1510K bituminous data	112
28	Confidence Region for Estimates of the Kinetic Rate Constants for the Low Temperature Lignite Data	114
29	Confidence Region for Estimates of the Kinetic Rate Constants for the Low Temperature Bituminous Data	115
30	Confidence Region for Estimates of the Kinetic Rate Constants for Centered Low Temperature Lignite Data	116
31	Confidence Region for Estimates of the Kinetic Rate Constants for Centered Low Temperature Bituminous Data	117
32	Residual Plot for Lignite Data	119
33	Residual Plot for Bituminous Data	120

List of Tables

1	Melting and boiling points of Sodium and Magnesium	27
2	Parameter estimates determined by Kobayashi	49
3	Kobayashi Furnace Dimensions	70
4	Furnace operating conditions	87
5	Ultimate yield and reaction rate predictions	87
6	Low temperature reaction rate constant estimates for isothermal pyrolysis .	96
7	High temperature reaction rate constant estimates for isothermal pyrolysis .	96
8	Heating history and weight loss data of 1260K and 1740K bituminous coal .	96
9	Parameter estimates for non-isothermal single first order reaction model - bituminous coal	100
10	Parameter estimates for non-isothermal single first order reaction model - lignite coal	100
11	Parameter estimates for coal pyrolysis listed in literature	102

12	High temperature parameter estimates for non-isothermal parallel reaction model -bituminous coal	102
13	High temperature parameter estimates for non-isothermal parallel reaction model -lignite coal	102
14	Least squares parameter estimates for lignite and bituminous coals	106
15	Reaction rates for lignite and bituminous coals at 1260K	106
16	Iterative fitting of low temperature parameters to full two reaction model .	106
17	R Test for non-isothermal parallel reaction model	121
18	Low Temperature Experimental Data [1] for Lignite Coal	157
19	High Temperature Experimental Data [1] for Lignite Coal	158
20	High Temperature Experimental Data [1] for Lignite Coal (cont.)	159
21	Low Temperature Experimental Data [1] for Bituminous Coal	160
22	High Temperature Experimental Data [1] for Bituminous Coal	161

Chapter 1

Introduction

Coal is a complex matrix of organic molecules whose chemical composition can change from coal to coal. In order to simplify the complex mechanism of coal combustion, researchers have generally broken the process into three stages: first, devolatilization, also called pyrolysis or thermal decomposition; second, the combustion of the gases released; and third, the combustion of the char particle. In the combustion process, the heating value of the volatile products accounts for up to 50% [11] of the total heating value of the original coal. Since the volatile combustion is approximately 10-15% of the total combustion time, the duration of coal combustion can be estimated from the char combustion process alone. However, this does not diminish the importance of the devolatilization process, as the volatile yield affects the amount of char produced. It is the purpose of this study to devise a means of deriving kinetic rate constants for devolatilization which can then be incorporated into a full combustion model [12].

Energy, Mines and Resources Canada has developed an entrained flow reactor that will be used to examine the combustion of different types of pulverized coal. The first stage of this research, the devolatilization studies, are to be performed in an inert atmosphere to prevent combustion, and therefore simulate the heating undergone by a particle approaching

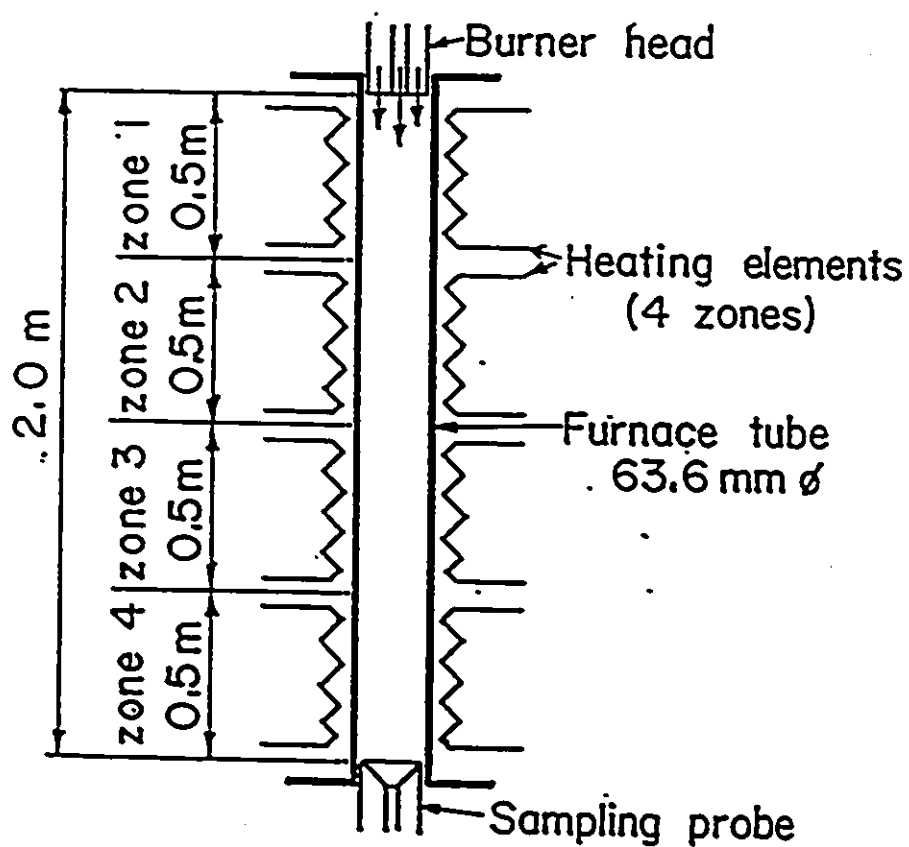


Figure 1: Schematic Drawing of Entrained Flow Reactor at Energy, Mines and Resources

a flame front in a furnace. The entrained flow reactor, figure 1, consists of a long, electrically heated, vertical mullite refractory tube. A dilute coal stream is carried by a water cooled primary gas stream and injected into the center of a preheated laminar secondary gas stream. The particles then flow down the centerline of the laminar flow furnace and are collected by a water cooled sample probe. The char particles are collected isokinetically by the probe and are quenched to prevent further devolatilization. The particle residence time is varied by raising and lowering the sample probe.

In order to interpret the results of the pyrolysis experiments, it is essential to know the particle heating history and residence time. In a previous work [7], a finite difference scheme was developed to predict the gas velocity and temperature within the furnace under different operating conditions, as access to the furnace for local measurements is nearly impossible. The furnace gas velocity and temperature fields were then used to calculate the particle heating rates. The original reactor model [7] assumed that the particles do not react chemically. The present work is concerned with selecting a suitable model for the chemical reactions involved in devolatilization from those available in the literature and implementing it in the existing reactor model. The incorporation of the devolatilization model into the existing computer program required modifications to the convective heat transfer coefficient and drag coefficient as well as the addition of the heat of devolatilization to the energy balance. The second part of this study involved the development of a procedure for fitting the reaction constants for the model to the experimental data. Since experimental data from the EMR reactor is not yet available, as a test this routine was used to fit the reaction constants of the selected model to experimental data of Kobayashi [1] and the suitability and precision of these constants were tested. The results of this test are used to make recommendations for the gathering and treatment of data in experiments.

Chapter 2

Literature Survey

Coal pyrolysis or devolatilization is an important field of study for it enables one to better understand the process of coal combustion. At very high combustion temperatures, up to 70% or more of the reactive coal mass is released as volatiles [2]. Although devolatilization occupies only about 10-15% of the combustion lifetime, the volatiles are important to flame stabilization, and a prediction of the amount of the relatively slower burning char produced is essential. It is the purpose of this chapter to provide some background material about coal and the devolatilization process. A literature review was performed to determine the operational parameters that influence the devolatilization behavior of the coal. This data will be used to critically examine the devolatilization models available in literature.

2.1 Background

Coal is a complex organic matrix, figure 2, whose properties change from coal to coal. Recent devolatilization work [1,5,10,13] has emphasized finely pulverized coal particles at high temperatures. As the raw coal is heated, the moisture present will evolve early as the temperature rises. As the temperature continues to increase, gases and heavy tars are

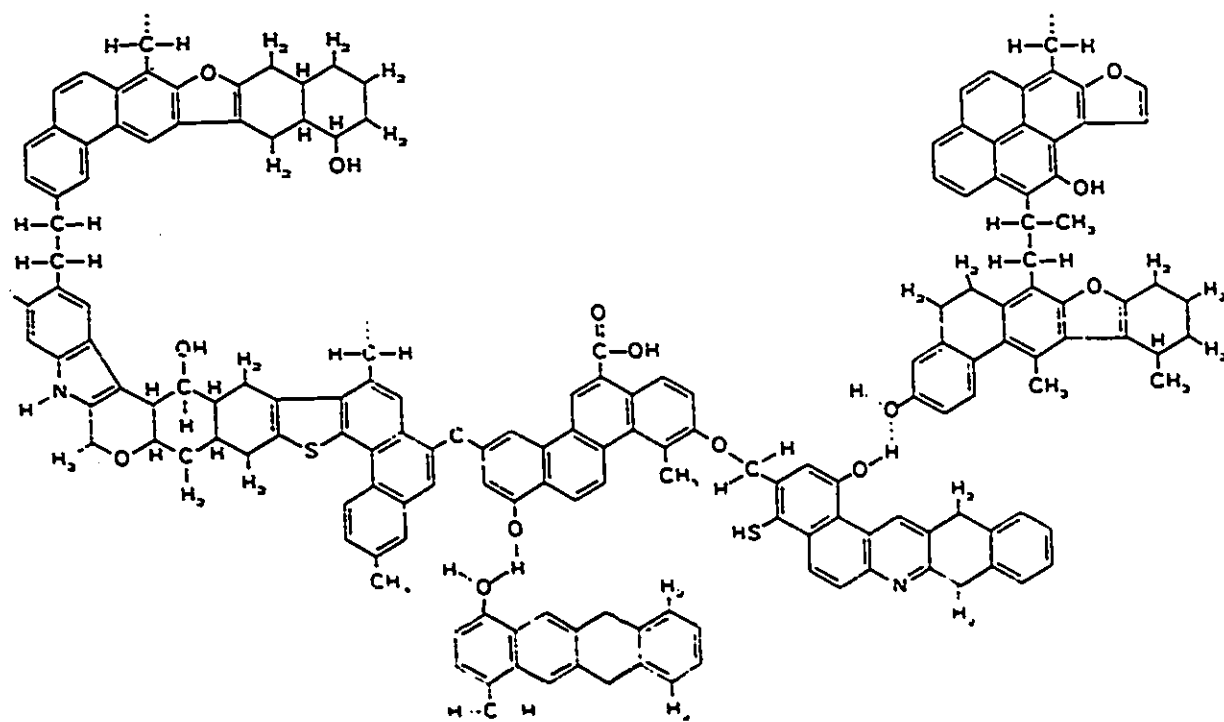


Figure 2: Proposed Model for Molecular Structure of Coal [2]

released. During rapid devolatilization, larger fractions of lower molecular weight species, in addition to tars, are evolved. It has been suggested that these species derive from the rupture of the $-H_2$, $-CH$, $-CH_2$, $-CH_3$, and $-OH$ bonds which appear on the periphery of the coal molecule as well as from a more complete disruption of the weaker cross-link bonds between layers. The proportions of the various products change with temperature as well as with the extent to which the coal devolatilizes, which can vary from a few percent to as much as 70 %. Significantly different pyrolysis behavior between coal types can be seen in figure 3 [3]: much more liquid and hydrocarbons are released by the bituminous coal and more gaseous products are released from the lignite. The volatile matter that escapes from the coal particle can undergo various secondary cracking reactions on the char surface with the possible formation of solid products (soot), which can substantially reduce the overall volatile yield. As the extent and rate of devolatilization increases with increasing temperature, it has been proposed [1] that the variation of the heating rate is a means for varying the temperature range over which the devolatilization takes place.

The analysis of coal is carried out using two ASTM (American Society for Testing and Materials) tests:

- proximate analysis [14] - involves the determination of surface moisture, inherent moisture, volatile matter, fixed carbon and ash. The moisture content is determined by heating the coal sample in an open crucible in an oven preheated to 377-383K for one hour. The moisture content is the difference in weight before and after heating. The volatile matter content is determined by heating the sample in a covered crucible in an oven preheated to $1223 \pm 20K$ for seven minutes. The loss of weight minus moisture equals the volatile matter. The dried coal from the moisture determination is placed in porcelain capsules in a gradually heating furnace. The coal is heated to redness and the process is considered finished once the sample maintains constant weight at a temperature between 973-1023K. The sample is then cooled and weighed to determine the amount of ash. The fixed carbon content in the coal is calculated

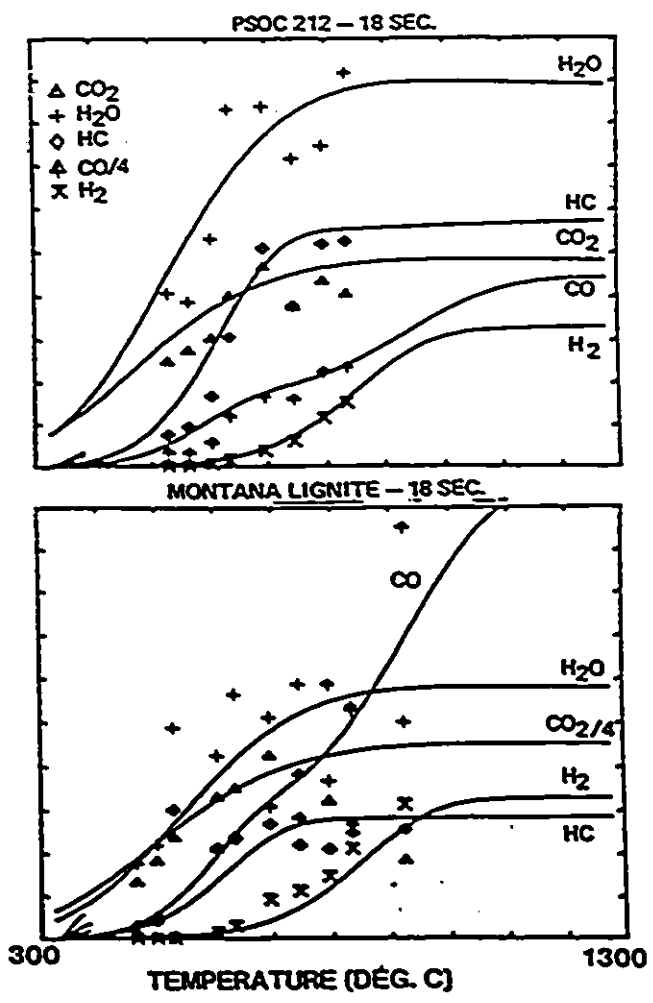


Figure 3: Comparison of the composition of devolatilization products [3] of bituminous (a) and lignite (b) coals

as:

$$\text{Fixed carbon, percent} = 100 - (\text{moisture} + \text{ash} + \text{volatile matter})$$

- ultimate analysis [14] - chemical means of determining the composition of the coal by separating the principal elemental constituents: carbon, hydrogen, nitrogen, sulfur, and oxygen. The method of determining the composition of each of the principal elemental constituents involves rather long procedures which cannot be easily summarized but can be found in reference [14].

These tests are used to characterize the coals for industrial use. However, it has been found that volatile yields significantly larger than the proximate volatile matter have been obtained when the coal is heated rapidly to elevated temperatures [5,6,10,13,15,16]. This is a particularly important finding, since the amount of char to be consumed, the rate controlling step in the combustion of coal particles, is determined by the devolatilization step. Therefore the prediction of the rate of volatile yield under various conditions is indispensable for the proper design of combustion chambers. The requirement for devolatilization studies is an unambiguous reaction history, i.e. rapid heating, an isothermal zone, controlled variation of residence time and temperature and rapid quenching for precise residence times. This section will review some of the experimental techniques and data in the literature so as to determine the operational parameters that were found to influence the devolatilization behavior of the coal.

2.2 Experimental techniques

Pyrolysis has been studied using three different experimental techniques:

- entrained flow reactors
- heated screens

- crucible tests

2.2.1 Entrained Flow Reactors

An entrained flow reactor, figure 1, consists of a vertical tube furnace which is electrically heated and designed for the injection of a dilute coal stream into the center of a preheated gas stream. The flow straightener ensures that the coal passes down the center of the furnace so that the thermal history of each particle is the same. The flow is usually laminar to prevent backmixing and dispersion of the coal. A probe at the bottom of the furnace collects the reacted coal stream and quenches it rapidly. Variation of the reaction time is achieved by raising and lowering the collector probe.

Badzioch and Hawksley [15] used an entrained flow furnace to determine the kinetics of devolatilizing bituminous and semianthracite coal particles at temperatures up to 1273K. The weight loss curves begin at a transit time of about twenty msec. This time delay was attributed to the heating up of the particles, and was subtracted from the transit time to obtain the duration of isothermal decomposition. The weight loss was determined using ash as a tracer; this led to a wide scatter in the results since the majority of the coals had a low ash content. In common with many of the earlier works on coal devolatilization, the model used to calculate the particle residence time and temperature history was crude: the temperature of the particles was assumed to be the same as that of the gas stream, and the velocity profile assumed to be parabolic (fully developed laminar). Flaxman and Hallett [17] have shown that inaccurate models of reactor flow and particle heating can lead to large errors in particle residence times and temperature histories, so that the data presented in this and many other papers must be viewed with mistrust. As the heating history of the particles was simply approximated and the weight loss was not accurately measured, the resulting data are not sufficiently accurate to determine rate constants; however, the trends in the data can be used to learn more about the process of devolatilization. The weight loss of the particles increased with the final temperature attained and the residence time. The

experiments were conducted with particle sizes ranging from 20-60 μm , and no significant effect of particle size on the pyrolysis behavior was found.

Nsakala [4] performed devolatilization experiments to determine the kinetics of pyrolysis at 1081K. The residence time of the particles was determined by the crude method of measuring from the point of entry into the furnace and assuming a uniform velocity at constant temperature for the bulk flow. The weight loss was found to start at a 'false origin' as was the case with Badzioch and Hawksley [15] and this heating period was subtracted out. As there was no temperature variation, the temperature dependence of the weight loss could not be determined. The weight loss curves with a maximum of 40% were below the ASTM volatile matter (47.5%), which was probably due to the experimental temperature being below the temperature at which the ASTM test is conducted. The break in the weight loss data in figure 4 was interpreted as evidence for a two component devolatilization model in which the devolatilization of the first component was particle size dependent while the second component devolatilization was particle size independent. However, this is merely a result of Nsakala's having passed straight lines through the data: if a smooth curve is used instead, the data can be seen to be simply approaching the final weight loss asymptotically as one would expect. The weight loss curves for the particles under 100 μm in figure 4 exhibit similar weight loss behavior, while the curve for the particles over 100 μm is significantly lower, suggesting that the weight loss is a function of particle size for particles over 100 μm .

Tsai and Scaroni [18] investigated the pyrolysis of particles in an entrained flow reactor at 1200K. The particle sizes varied from 74-149 μm to 37-53 μm . The temperatures and residence times of the coal particles were estimated from a mathematical model which incorporated the gas velocities and temperature predictions. The position at which pyrolysis begins in the reactor was found to shift to longer residence times when N_2 replaced He as the primary gas stream. Tsai et al. concluded that as N_2 has a lower thermal diffusivity than He , the devolatilization of a coal particle is affected by the heating rate. An increased heating rate, using He as the primary gas rather than N_2 , enhanced the weight

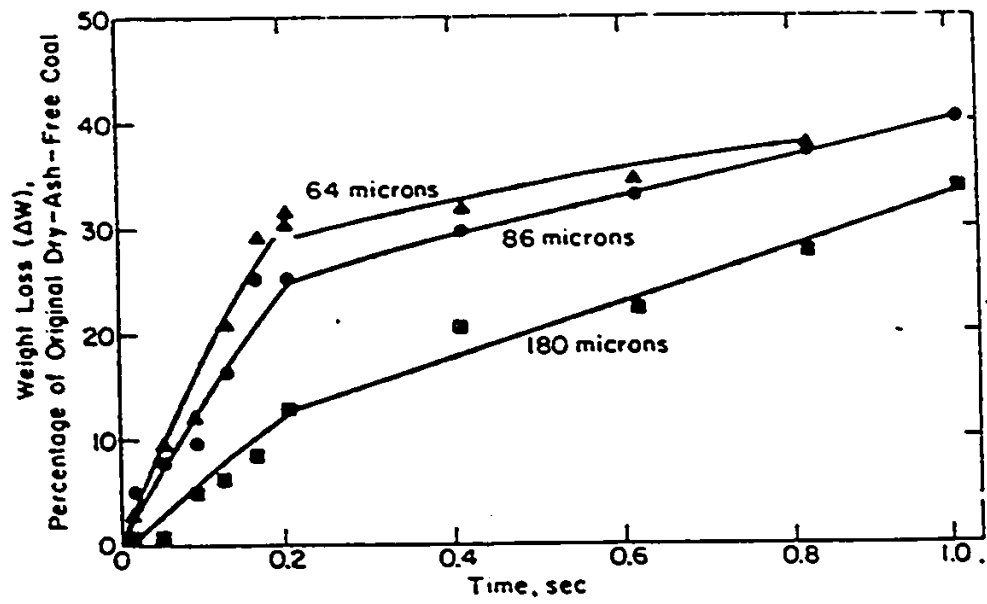


Figure 4: Devolatilization Data Collected by Nsakala [4]

loss; however, as the asymptotic weight loss was not approached in either primary gas experiment, the effect of the heating rate on the ultimate yield could not be examined. The comparison of the asymptotic weight loss of different coals shows that the coals with the higher ASTM volatile matter had higher asymptotic weight losses, which suggests that the chemical composition has an effect on the pyrolysis behavior. An effect of particle size on pyrolysis was noted, which was traced to the fact that the larger particles had higher ASTM volatile matter fractions. This change in volatile yield with particle size indicates segregation of the ash particles in the sample preparation, which probably could be avoided by finer screening of the coal particles. The particle size dependence of the weight loss is contrary to the conclusions of Scaroni, Walker, and Essenhigh [19], who stated that the weight loss was independent of particle size although the particle sizes in these experiments ranged from 41 to 201 μm . In the latter studies no mathematical model of the furnace flow and temperature fields was used; rather the particle velocities were estimated by summing the average gas velocity and particle free-fall velocities. Some of the char in Scaroni, Walker and Essenhigh's experiments bypassed the collector probe, while some adhered to the inner probe surfaces, resulting in collection efficiencies of only 70-80 %. If the flow inside the furnace were laminar, the particles would pass down the furnace in a coherent thin stream directly into the collector. Therefore, the char particles that bypassed the probe could be interpreted as indicative of turbulent flow existing in the furnace, calling the residence time and temperatures even more seriously into question.

Kobayashi et al. [1,10] studied coal devolatilization of lignite and bituminous coals in an entrained flow reactor at temperatures ranging from 1000K to 2100K. The temperature and velocity fields were predicted by numerically solving the fundamental governing equations with several simplifying assumptions which are discussed in a later section. Kobayashi found that the volatile yields at high temperatures were considerably higher than the proximate volatile matter content. The volatile yield of both coals increased significantly with temperature. As the particle size was not varied, the dependence of the weight loss on this factor could not be tested.

Jamaluddin et al. [13] studied the devolatilization of bituminous coals at medium to high heating rates at temperatures ranging from 1073 to 1673K. The coal samples were pulverized to a size range of 53-63 μm . The experiments with high heating rates, 1.5×10^4 K/sec, were conducted using an entrained flow reactor and the medium heating rate, 250-1000 K/sec, tests with crucibles. The flow fields and particle heating in the laminar flow furnace were modeled by solving the equations of mass, momentum and energy by standard numerical techniques. The heating history of the crucible tests was measured using an empty crucible. As the coal sample was less than 2.5% by weight of the crucible it was assumed that the coal would heat up at the same rate as the empty crucible. A continuous flow of argon was used in the crucible experiments to maintain an inert atmosphere and prevent cracking of the released volatiles; the effectiveness of this is unknown and would be dependent upon the experimental setup. The error bars on the crucible test data indicate that there is quite a spread in the results, in some cases as high as twenty percent, and therefore these results are questionable. The weight loss from both coals in the crucible tests increased with increasing furnace temperatures but did not significantly exceed the proximate volatile matter, which was found with a furnace temperature of 1223K, even at the highest temperature of 1673K. At a furnace temperature of 1673K, the weight loss from the high-volatile coal, with an ASTM volatile matter of 35.2%, was 62% under rapid heating conditions and only 42% under medium heating conditions. The crucible tests are expected to have lower weight loss because of the lower heating rate and the opportunity for cracking reactions. The lower heating rate, as discussed on page 6, results in a greater portion of the devolatilization reaction occurring at a lower temperature where the extent and rate of reaction is lower. There is ample opportunity for cracking reactions in the crucible tests, as the coal particles are closely packed in the crucible and the volatiles being released can easily use the surface of the char particles as sites for secondary reactions. Although these tests are conducted at a much shorter residence time than the ASTM test, attributing the comparatively low yield of the crucible experiments at 1673K solely to the lower heating rate and not to cracking reactions seems questionable. However, Jamaluddin found that the devolatilization of coal particles was increased by both increasing temperature and increasing heating rate.

Maloney and Jenkins [20] performed devolatilization experiments in a laminar flow reactor using two bituminous coals with mean particle diameters of $62 \mu\text{m}$. The furnace temperature was varied from 1073-1273K. All experiments were conducted with N_2 as the secondary gas while some experiments utilized He as the primary gas and were repeated utilizing N_2 as the primary gas. A numerical analysis was performed to estimate the velocity and temperature history of the coal particles. The particle temperature calculations suggested that when $\sim 60 \mu\text{m}$ particles were heated under their experimental conditions, the coal particle temperatures closely tracked that of the surrounding gas. The experimentally determined gas temperature profiles were therefore equated to the coal particle temperatures, although it was admitted that this method overestimated the particle temperatures slightly. These tests were done utilizing He as the primary gas, for which because of the high thermal conductivity of He this method of estimation may be more accurate than in the experiments conducted using N_2 as the primary gas. The weight loss generated in experiments using the two different primary gases illustrated that the increased heating rate associated with the He gas resulted in greater weight losses at smaller residence times. Although the N_2 gas experiment did not have sufficient residence time to clearly approach the asymptotic weight loss, it appears that the carrier gas, and therefore the heating rate, does not have an effect on the ultimate yield.

Kimber and Gray [16] performed devolatilization experiments in a laminar flow reactor with an argon atmosphere. As the flow fields in the furnace were not modeled, the times reported include the heating times of the particle and the temperature refers to the reactor temperature; these data therefore cannot be used to determine rate constants, but can be used to investigate trends in the process of devolatilization. Devolatilization appeared to be a two-stage process: increasing the residence time at 1370K produced no further weight loss, but significant volatile matter was released during subsequent proximate analysis of the char. At higher temperatures (2170K) the evolution of this residual volatile matter was almost complete, indicating a second stage of devolatilization. There was a ten percent increase in weight loss for the $30 \mu\text{m}$ particle as compared to the weight loss of the $50 \mu\text{m}$

particles, which was attributed to the variation in heating rate with particle sizes.

Solomon et al. [21] performed devolatilization experiments in a laminar flow reactor at 1373K using both bituminous and lignite coals with particle size ranging from 44-74 μm . A Fourier Transform Infrared (FT-IR) spectrometer was used for in-situ analysis of gas species and temperature. The relative intensities of hot CO absorption were used for measuring the gas temperature, a technique which was adequate at room temperature but had some problems at high temperatures. The wall profile and input gas temperatures were used to calculate the particle temperatures; however, the major uncertainty in this calculation is the particle velocity, which was assumed to be the average gas velocity. Another experimental technique problem was the lack of a satisfactory method for the quantitative collection of tar and soot, and substantial scatter existed in this data. The functional group changes in the chars were determined, and the exhibition of almost identical changes in relative functional group composition of all the four coals of varying rank indicated that the kinetic rates are independent of coal rank but in fact depend on the functional group distribution of the original coal. However, if this hypothesis were accepted for modelling, it would require that all the functional groups of the coal be determined and the changes modeled, a rather complicated task.

2.2.2 Heated Grid

A heated grid apparatus consists of a folded strip of stainless steel screen into which the coal sample is spread. The screen is then placed between two relatively massive brass electrodes. The heating element and electrodes are enclosed in a vessel capable of operating under a vacuum or at elevated pressures. The reactor is flushed to remove any trace quantities of oxygen and then filled with the desired experimental atmosphere. The external circuitry permits independent control of the heating rate and the final temperature and holding time, limited only by the thermal inertia of the screen. An estimate of temperature-time history of the coal particles is recorded by a thermocouple placed within the sample. As the gaseous

contents remain in the apparatus until purged, there is ample opportunity for secondary cracking reactions.

Suuberg et al. [11] studied the product composition and kinetics of lignite pyrolysis. Experiments were carried out utilizing a Montana lignite in the particle size range of 53-88 μm with 74 μm being the average diameter, and therefore the effect of particle size was not tested. The yield of char, which remains on the screen, was determined gravimetrically. Tars were collected on foil liners within the reactor, on a paper filter at the exit of the reactor, and by washing unlined surfaces. The vapor phase products were collected by purging the reactor vapors through two traps. The coal samples were heated to a maximum temperature of 1273K, at which point the weight loss was slightly exceeding the ASTM volatile matter of the coal. Pyrolysis was found to be a function of the final peak temperature but not a function of the heating rate, which varied from 100-10⁴ K/sec. Tests on the effects of pressure revealed that there is a temperature dependence of the pressure effect on the yield: above 1073K a decrease in pressure was found to increase the total yield and affect the product composition.

Anthony and Howard [5] studied the rapid devolatilization of a lignite and a bituminous coal at temperatures up to 1373K. The heating rate was varied from 10² to 10⁴ K/min, the pressure from .001 to 100 atmospheres, and the particle size from 50-1000 μm . Both coals experienced increased weight loss with increasing temperature and residence time. The weight loss from the lignite was not affected by pressure; however, the weight loss from the bituminous coal decreased substantially with increasing pressure. The devolatilization of the lignite coal was independent of heating rate. The bituminous coal experienced increased weight loss with higher heating rates at pressures of one atmosphere and lower but the effect of the heating rate was negligible at higher pressures. The weight loss was also found to be independent of particle size for the lignite, but increased with decreasing particle size for the bituminous coal.

Jüntgen and Van Heek [22] summarized work in the basic processes and fundamentals of

coal pyrolysis by German researchers. The experiments in which the coals experienced high heating rates, $10^2 - 10^5$ K/min, were conducted in a heated grid apparatus. The rate of gas release at low heating rates, $10^{-3} - 10^2$ K/min, was studied with a captive sample heated at a constant rate in a controlled electric oven. A thermocouple in the sample measured the heating history of the coal particles. The gas produced during this process was carried away by a stream of helium and analyzed. The effect of heating rate on gas formation kinetics was investigated by studying ethane formation at widely differing heating rates: $10^{-2} - 10^4$ K/min. This involved the data of two different sets of apparatus which might have led to variations in pyrolysis behavior due to the different conditions experienced. The temperature range of the experiments was 573-1073K. Increasing rates of heating resulted in a shifting of the emission of ethane towards higher temperatures. Although the method of determining the estimates of the reaction parameters was not discussed, the estimates remained constant within the error limits, indicating that the mechanism of the reaction does not change over the temperature range investigated. The transition from reaction controlled pyrolysis, which is independent of particle size, to diffusion or heat transfer controlled pyrolysis, which is dependent upon the particle size and rate of heating, was calculated and measured using a high volatile coal. Two different curves were determined which separate the two rate determining mechanisms. They show to what degree the particle diameter has to decrease to assure chemical reaction control with rising rates of heating. For example, it shows that at a heating rate of 10^5 K/min or less, the reaction rate controls devolatilization when the particle is smaller than $100 \mu\text{m}$.

2.2.3 Crucible tests

The apparatus of the crucible tests varied from researcher to researcher, and therefore will be described as each study is discussed.

Mahajan et al. [23] studied the pyrolysis of twelve coals of various ranks in a helium atmosphere of 5.6 MPa (gauge). The weight loss in the coal sample was monitored using

a balance in conjunction with a thermal analyzer. A platinum boat containing the coal sample was suspended from the beam of the balance. The thermocouple, which is attached to the balance housing, was placed in close proximity to the sample. The reactor, which was made of a quartz tube with either end acting as inlet and outlet for the reactor gases, was surrounded by a tube furnace. The balance assembly along with the reactor and furnace were mounted in a pressure vessel which was pressurized with nitrogen, and helium was introduced through a pressure flowmeter. The furnace was activated to raise the temperature to 853K at a heating rate of 10K/min. Both the temperature and heating rate are rather low compared to the pyrolysis stage of pulverized coal combustion. Mahajan et al. determined that the variation in pressure from ambient to 5.6 MPa (gauge) had little or no effect on the devolatilization. The weight loss was also determined to be a function of the carbon content: as the carbon content decreases, the weight loss increases. The weight losses in these runs were all well below the ASTM volatile fraction, which was probably due to the experimental temperatures being well below the temperature at which the ASTM test is conducted.

Merrick [8] performed devolatilization tests in tubular pots with heating rates ranging from 3-5 K/min, a rather slow heating rate for devolatilization experiments. The temperature range for these tests was 673 to 823K. The samples of coal were crushed to a maximum particle size range of 3 mm, which is much larger than the pulverized coal used in coal combustors. It was found that the peak rate of release increases with volatile matter content of the coal, but that the temperature at which the peak occurs decreases.

Freihaut [9] used a fluid cooled delivery spoon to drop coal samples into a reactor boat which sat in a preheated, isothermal environment. The operating temperatures varied from 873 to 1173K. The coal particle sizes varied from a 53-106 μm to a 850-1000 μm size range. The differential release of tars was monitored by optical density measurements of the carrier gas stream. The condensate was captured on glass-fiber filters and weighed for estimates of the amount of tar release. The particle size effects on the weight loss were indicated by systematic decreases in the maximum differential mass release and systematic

increases in the reaction time as the particle size increased. This behavior was attributed to the presence of significant temperature gradients in the larger particles. As a result, the variation in particle size leads to in a transition from an isothermal, volumetric pyrolysis process in the case of the smallest particles to a non-isothermal shrinking core type of process in the case of larger particles. In a small particle, the whole volume of the particle devolatilizes uniformly as opposed to concentric 'rings' devolatilizing in a large particle as the temperature of that ring rises to the desired temperature. The effect of the heat of pyrolysis was investigated with a 500 μm particle and was shown to have a pronounced effect on the weight loss, as the endothermic reaction process supports the retention of a temperature gradient in the larger particles.

2.2.4 Conclusions

The experimental techniques of the above researchers were studied to identify the operational parameters that were found to influence the devolatilization behavior of coal. Although there are exceptions, the consensus is that the important operating factors that influence the devolatilization of the coal particle are:

- time
- temperature - increasing temperature results in increased weight loss.
- particle size - if the particle size is small enough that its temperature is nearly uniform, then no effect of particle size should be observed. The criterion for this is the Biot number:

$$Bi = hr/k$$

which compares the relative magnitude of the surface convection, h , and the internal conduction resistance to heat transfer, k/r . A very low value of Bi (< 0.1) means that the internal conduction resistance is negligible in comparison with the surface

convection resistance and therefore implies that the temperature will be nearly uniform throughout the solid [24]. This criterion and experimental evidence shows that devolatilization is independent of size for particles under 100 μm in diameter at rapid heating rates ($10^4 - 10^5$ K/sec).

- heating rate - although most researchers agree that the heating rate is an important factor in determining the devolatilization behavior, there is no agreement on the mechanism of its effect. Two explanations have been offered to the observed increases in volatile yield with heating rate. One is that rapid heating leads to different reaction paths in the coal, and hence to breaking of different bonds and release of different species [10,5]. The other notes that rapid heating is usually found in drop tube reactors, where the coal is widely dispersed, and suggests that dispersion reduces the likelihood of secondary reactions which might decrease the yield [15,19].
- pressure - weight loss was generally found to decrease with increasing pressure.
- chemical composition/rank - an increase in the volatile matter in the original coal increases the asymptotic weight loss.

As pulverized coal combustors require that 65-80% of the coal be less than 74 μm [25], the particle size as a operational parameter will not be required to be taken into account in the devolatilization model. Since coal combustion occurs at ambient pressure, pressure effects will not be required to be included in the model. As the coal's composition can vary greatly from coal to coal, it does not seem reasonable to include this parameter in the model and therefore parameter estimates will be required to be found for the different types of coal used. Thus the parameters that the model must allow for are:

- time
- temperature
- heating rate

2.3 Accuracy of the Ash Tracer Technique

In conducting devolatilization experiments, many experimenters found that the sample collectors were not 100% efficient and therefore direct weight loss measurements could not be used to calculate the amount of volatiles released. As a result, an alternative method, the ash tracer technique, was used to calculate the weight loss of the coal particles during the pyrolysis experiments using:

$$V_{af} = \frac{A_{cs} - A_o}{A_{cs}(1 - A_o)} \quad (2.1)$$

where:

- V_{af} weight loss based on original ash free coal
- A_o ash fraction of original coal
- A_{cs} ash fraction of collected sample

Any uncertainty in the ash tracer technique due to vaporization or loss of ash constituents could affect the results, and therefore many researchers investigated the accuracy of this analytical technique. As the present work was undertaken to develop a procedure for estimating the devolatilization reaction constants for data obtained in a laminar flow test reactor, the data collection side of this problem cannot be ignored, and therefore the accuracy of the ash tracer method is investigated in this section of the literature survey.

In examining the literature, it was found that the experimental conditions under which the ash tracer accuracy was investigated could be divided into three major groups:

- crucible tests
- inert atmosphere furnace tests
- other atmosphere furnace tests

One would expect that the researchers would be in agreement within each group. However, this has not been the case, for there has been disagreement about the accuracy of the ash tracer technique within these groups.

2.3.1 Crucible Tests

Maloney [20] found the ash tracer technique to be an excellent method to determine weight loss in pyrolysis experiments. Samples of each coal were subjected to ASTM tests for volatile matter. The resulting chars were then ashed and the amount of volatile matter released was calculated using the resulting ash yields. The agreement between the ash tracer method and the direct weight loss measurements were found to be excellent at temperatures between 1073-1273K.

Harding [26] performed quite extensive crucible tests on the ash tracer accuracy using a high volatile bituminous coal. His research revealed that there was negligible vaporization of ash below 1500K but there was a significant increase in ash vaporization as the temperature increased up to 2500K. All elements in the ash had a significant degree of vaporization over this temperature range, except for titanium and scandium. Since there was considerably more titanium than scandium, titanium was used as a tracer instead of ash.

Kobayashi et al. [1,10] found that ash vaporization was negligible below 1400K. He also stated that although some of the ash is vaporized at higher temperatures this would be greatly reduced in furnace experiments due to the short residence times experienced. As a result, the errors in using the ash tracer technique would be a fraction of those experienced in crucible tests.

Scaroni et al. [19] found that crucible experiments in ashing furnaces revealed that the use of ash as a tracer consistently underestimated the actual weight losses for the temperature range of 973-1273K. This would suggest that some of the ash was lost in the furnace

experiments. In order to account for this underestimation, an empirical equation was developed. However, this equation is essentially independent of particle size and temperature and therefore is very specific to the data quoted.

2.3.2 Inert Atmosphere Furnace Tests

Sarofim et al. [27] performed tests on the vaporization of mineral matter in a drop tube furnace with a temperature range of 1000-1830K. Negligible amounts of mineral matter were expelled with the volatile matter, although the bituminous coals swelled by a factor of four or more.

Jamaluddin et al. [13] performed devolatilization experiments using a drop tube furnace with an argon atmosphere over a temperature range of 1073-1673K. Since the efficiency of the collector used was essentially 100%, the accuracy of the ash tracer technique was tested by comparison with direct weight loss calculations. The ash tracer technique was found to be a suitable method to estimate the weight loss of a high-volatile bituminous coal but not suitable for a medium volatile bituminous coal. This suggests that the accuracy of the ash tracer depends upon the rank of the coal or more likely on the variation of ash characteristics with the origin of the coal. Jamaluddin postulated that the unsuitability for the medium volatile coal was due to soot and tar from the pyrolysis of the volatiles being deposited on the char particles; however, since such deposition would affect a direct weight loss measurement as well, this argument does not seem valid.

Gat et al. [28] tested the accuracy of the ash tracer technique by laser heating particles carried in an argon gas jet. Although the ash tracer was found to be reliable at low temperatures, it was found to be increasingly unreliable as the temperature was increased. This suggests a temperature dependence of ash vaporization, which was also seen in the findings of some of the crucible tests. At high heating rates and high temperatures (2273-3073K), Gat reported significant losses of both ash and titanium. Ti was thought to be an unreliable

tracer under these conditions because Ti has a high organic affinity. Under rapid heating, the organic structure of the coal is quickly vaporized and there might not be sufficient time for the Ti to separate: it would then be carried out with the hydrocarbons. This contradicts the findings of Sarofim et al. [27], but an analysis of the condensed tars supports this theory. A seed tracer, tungsten carbide powder, was recommended in order to accurately determine the weight loss experienced during coal pyrolysis and combustion.

Badzioch and Hawksley [15] performed devolatilization experiments using a drop-tube furnace with a nitrogen atmosphere and a temperature range of 673-1273K. The ash tracer technique was found to be of poor reproducibility when the ash content is low, for a wide scatter arises from even small analytical errors in the determination of the amount of ash. Another source of scatter is a result of the ash particles being predominately discrete from the coal. They would then tend to segregate upon handling, for example, in vibrating feeders. A correlation was developed between the weight loss calculated by ash tracer and the change in volatile matter found by ASTM tests. One possible explanation for the correlation not passing through the origin was the possibility that there were minute fragments passing through the cyclone collector in the sampling system. These difficulties could be alleviated by closely size-grading the coal samples used, and performing the analysis of the original coal on the sample as fed to the furnace. Any ash tending to segregate into the fine particles would then be eliminated from both the sample and analysis.

2.3.3 Other Atmosphere Furnace Tests

All of the researchers in the literature who performed devolatilization tests in a furnace with an oxidizing atmosphere discovered ash vaporization and therefore found ash to be unsuitable as a tracer. However, it should be noted that these tests were all conducted at very high temperatures.

Ubhayakar et al. [29] performed their devolatilization tests in a turbulent flow entrained

bed gasifier with a hot combustion gas atmosphere with a temperature range of 1800-2250K. The ash vaporization was estimated by analyzing the alumina content of two char samples resulting from high temperature and low temperature runs. Since the ash from a high temperature run had a higher alumina concentration than the low temperature run, it was assumed that some ash vaporization had occurred. Alumina was used as a tracer instead of the ash, since it was the most refractory component in the ash.

Quann et al. [30] performed mineral vaporization tests using a drop tube furnace with a 5-100% oxygen atmosphere with a particle temperature range of 1600-3000K. Quann stated that the submicron particles generated by vaporization and condensation of the ash passed through the impactor and were collected on a back-up membrane filter. The amount and composition of the particles was used to provide a measure of the extent of the ash vaporization during combustion. Through this experimentation, Quann found that the vaporization was dependent on the temperature and the spatial distribution of the mineral matter.

Neville et al. [31] performed ash vaporization experiments in a drop tube furnace with a 30% oxygen in nitrogen atmosphere at 1750K. He found that high temperature and a locally reducing atmosphere promoted ash vaporization. Also, elements such as sodium, which show a small temperature dependence, are vaporized to a large degree during devolatilization. However, elements such as magnesium, which show a strong temperature dependence, are vaporized primarily at a peak temperature encountered after devolatilization is complete. Although the meaning of the temperature dependence was not explained, it is assumed that this refers to the range of temperature between the element's melting and boiling points which are listed in table 1. As sodium melts at a much lower temperature than magnesium, the liquid can be entrained by the escaping volatiles and carried out of the particle. As sodium has a lower boiling point, it vaporizes at a lower temperature and therefore escapes as a gas. Both these effects can result in a greater loss in sodium than magnesium by the devolatilizing coal particle.

2.3.4 Conclusions

From this literature survey, one can see that the vaporization of the mineral matter depends not only on the properties of the coal (i.e. rank, amount of minerals) but also on the conditions (i.e. temperature, atmosphere, heating rate) under which pyrolysis occurs. As a result, it is important to test each coal utilized and to try to duplicate experimental conditions as closely as possible while conducting ash vaporization tests. In examining the literature which reports upon the experiments that most closely duplicate the conditions of the experiments that will be performed (inert atmosphere, approximately 1500K), it seems that the ash tracer method is reliable up to about 1273-1373K, unless the ash has components which vaporize at lower temperatures (e.g. Jamaluddin et al. [13]). In this case, it would be possible to perform supplementary crucible tests over the temperature range of experimentation to determine whether ash vaporization is significant. If no vaporization has occurred then this should be verified by performing drop tube furnace tests to see whether the heating rate or atmospheric conditions have any effect on ash vaporization. It would be important that the sampling equipment be designed so that the weight loss measurements are as accurate as possible. This would enable an accurate comparison between weight loss measurements and the ash tracer method for the furnace experiments.

Table 1: Melting and boiling points of Sodium and Magnesium

	melting point, °C	boiling point
sodium	97.5	880
magnesium	651	1110

Chapter 3

Model Evaluation

The purpose of this chapter is to critically appraise and compare the devolatilization models that are available in the literature, and to select a model which will be suitably accurate in describing the pyrolysis of a coal particle. The model selected is ultimately intended for use in a full model of coal combustion in a furnace, such as that of Lockwood [12]. The role of the devolatilization model in such a model is:

- to predict the mass of char produced for subsequent char combustion
- to predict the rate of volatiles release in the early part of the flame

Of these, the accurate prediction of char mass, i.e. extent of devolatilization, is the most important, as char combustion is the rate-controlling step of coal combustion. Owing to the complexity of a full model of combustion, the devolatilization model selected should be relatively simple and not require substantial computational effort. It is with these factors in mind that the models will be evaluated. Attention will be further confined to models for devolatilization of small coal particles, for which the particle temperature may be assumed uniform. The models presented in literature are quite different, for they range from a simple single first order reaction model to a much more complex and sophisticated multiple parallel

reaction scheme. The reaction schemes to be examined are:

- evaporation model
- single, first order reaction model
- competitive parallel reaction model
- two component model
- multiple parallel reaction mechanism

Each of these models will be examined and their advantages and disadvantages will be listed in an attempt to choose the best model that will serve the requirements listed above.

3.1 Evaporation model

3.1.1 Lockwood et al.

Lockwood et al. [12] developed a model for bituminous coal combustion. Lockwood used a physical model to describe the devolatilization of the coal instead of a reaction model, even though it was acknowledged that pyrolysis is a chemical process. The model used is very simple:

$$- dx_v/dt = \min(Q_p/h_1, B_m) \quad (3.1)$$

where x_v is the mass fraction of volatiles not yet released and h_1 is the 'latent heat' of devolatilization. This treats the evolution of volatiles as an 'evaporation' process. It is assumed that no volatiles were released at temperatures below 600K and that the volatile release rate is linearly dependent upon the heat flux to the particle, Q_p , and limited by a maximum value, B_m . A final assumption is that the total volatile yield is equal to the proximate volatile content. This model cannot describe the experimentally observed

increase of volatile yield with temperature nor the fact that yields above the ASTM value are often obtained [1,10,15,19]. Because it represents a chemical reaction as a physically controlled process, the 'reaction constants', h_1 and B_m , are specific to the temperature range, heating rate and other conditions modeled.

3.2 Single first order reaction model

The single first order model is the simplest reaction model available in literature and therefore is often used in combustion studies. The model is:

$$coal = V^*(volatiles) + (1 - V^*)(char) \quad (3.2)$$

The basic reaction equation for this model is:

$$dV/dt = k(V^* - V) \quad (3.3)$$

where V is the quantity of volatiles evolved up to time t and V^* is the ultimate volatile yield. The reaction constant k is described by an Arrhenius equation:

$$k = k_o \exp(-E/RT) \quad (3.4)$$

This model will be evaluated and discussed by pointing out its advantages and disadvantages.

3.2.1 Badzioch and Hawksley

Badzioch and Hawksley [15] introduced a single first order model which is often used as a standard against which other models are compared. The devolatilization experiments were carried out in a drop tube furnace with a maximum temperature of 1273K.

The model assumes isothermal pyrolysis, and its form is as follows:

$$V = QV_o(1 - C)(1 - \exp(-kt)) \quad (3.5)$$

where V is the weight loss of the coal up to time t , V_o is the ASTM proximate volatile matter of the coal, and Q is the ratio of the weight loss to the change in proximate volatile matter:

$$Q = V/(V_o - V_r) \quad (3.6)$$

where V_r is the proximate volatile matter of the char. C is a correction for the asymptotic weight loss, or the residual volatile matter in the char at infinite time, which allows the increase in yield with temperature to be roughly modelled. Badzioch et al. found C was a function of the swelling factor of the coal: for the non-swelling coals C was a constant while for the swelling coals C was fitted by an exponential function of temperature:

$$C = \exp[-K_1(T - K_2)] \quad (3.7)$$

Badzioch and Hawksley stated that there was a heating period in the furnace and therefore the particles did not experience a completely isothermal residence time. This heating time was subtracted from the residence time to obtain the duration of isothermal decomposition, thus assuming the amount of devolatilization occurring during the heating process was insignificant. This is now known to be a poor assumption [1,5], which limits this model's usefulness. Badzioch and Hawksley [15] stated that this model is not reliable for temperatures above 1273K and that a two reaction model should be used at high temperatures. Both the empirical nature of the temperature variation of the ultimate yield and limitation to temperatures under 1273K also limits this model's usefulness.

3.2.2 Scaroni et al.

Scaroni et al. [19] performed lignite pyrolysis experiments in a drop tube furnace with a temperature range of 973K-1273K. Scaroni included two models, of which the first is strictly an empirical model which is particle size and temperature independent. As a result, this model does not provide any insight into the mechanism of pyrolysis and cannot be applied to other data. The second model is again a simple first order isothermal model:

$$V = V^*(1 - \exp(-kt)) \quad (3.8)$$

where V^* is the maximum potential weight loss. Scaroni states that there is no weight loss during heat up, an assumption that is now considered incorrect [1,5]. It should be noted that in this model the ultimate yield is not a function of temperature.

3.2.3 Truelove

Truelove [32] modeled the combustion of pulverized coal in swirling flow combustors. This model included a simple first order reaction model of the coal devolatilization, this time for non-isothermal conditions:

$$dV/dt = k(V^* - V) \quad (3.9)$$

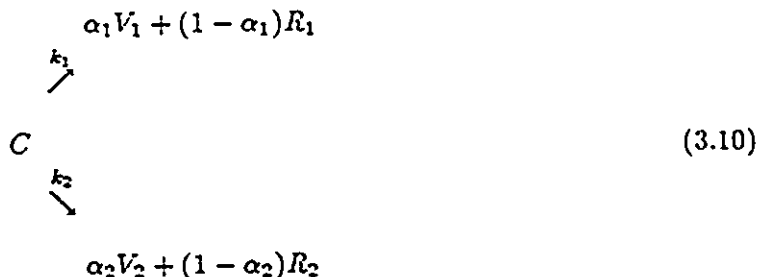
The rate parameters were taken from the work of Badzioch and Hawksley [15].

3.3 Competitive Parallel Reaction Model

It has been suggested that the temperature dependence of volatile yield can be modelled by using two parallel, competing pyrolysis reactions, one dominant at low temperatures and the other at high. This model was initially proposed by Kobayashi [1] but several authors [13,29,33] have used modified versions of this model which will be discussed here.

3.3.1 Kobayashi

Kobayashi proposed the two competitive reaction model since a model was needed that could describe the effects of temperature on volatile yields as well as predict the devolatilization rates at higher temperatures. This model assumes that the original coal substance, C, can decompose to volatiles, V, and char, R via two paths:



where k_i are the reaction rate constants and α_i are the mass stoichiometric constants and

$$k_i = k_{oi} \exp(-E_i/RT) \quad (3.11)$$

The first reaction dominates at low temperatures. At high temperatures, the second reaction is assumed to become faster than the first one, which amounts to requiring E_2 to be larger than E_1 . Kobayashi set α_1 as the proximate analysis volatile yield and α_2 as 1 since all the coal is expected to devolatilize at high temperatures. The mathematical form of this model is:

$$\begin{aligned}
 \frac{dV_1}{dt} &= \alpha_1 k_1 C \\
 \frac{dV_2}{dt} &= \alpha_2 k_2 C
 \end{aligned}$$

so that

$$\begin{aligned}
 \frac{dV}{dt} &= \frac{d}{dt}(V_1 + V_2) \\
 &= (\alpha_1 k_1 + \alpha_2 k_2) C
 \end{aligned} \quad (3.12)$$

where

$$\frac{dC}{dt} = -(k_1 + k_2)C$$

Integrating:

$$C = \exp\left(-\int_0^t (k_1 + k_2) dt\right) \quad (3.13)$$

Substituting equation 3.13 into equation 3.12 yields:

$$V = \int_0^t (\alpha_1 k_1 + \alpha_2 k_2) \exp\left(\int_0^t -(k_1 + k_2) dt\right) dt \quad (3.14)$$

Under isothermal conditions, this equation can be integrated to give:

$$V = [(\alpha_1 k_1 + \alpha_2 k_2)/(k_1 + k_2)][1 - \exp(-(k_1 + k_2)t)] \quad (3.15)$$

As $t \rightarrow \infty$, equation 3.15 reduces to:

$$V^* = (\alpha_1 k_1 + \alpha_2 k_2)/(k_1 + k_2) \quad (3.16)$$

where V^* is the asymptotic weight loss or the maximum possible weight loss. The first reaction dominates at low temperatures, since $k_1 \gg k_2$ and as a result V approaches α_1 , while at high temperatures $k_2 \gg k_1$ and V approaches α_2 . This model can therefore predict the temperature dependence of the asymptotic weight loss as found in the experimental findings of many researchers [1,15,19,10,13]. This model can also be applied to non-isothermal experiments through the numerical integration of equation 3.14 using the temperature-time histories of the coal particles to fit the equation to the experimental weight loss data. However, Kobayashi expended little effort in trying to obtain the best fit. Since the asymptotic weight loss changes from approaching α_1 to approaching α_2 as the temperature increases, one expects that there is a transition temperature interval above which devolatilization becomes increasingly controlled by reaction 2. The transition temperature can be roughly calculated by assuming that k_2 is negligible if it is twenty percent of k_1 :

$$k_2 = .2 \cdot k_1$$

therefore:

$$\begin{aligned} k_{o2} \exp(-E_2/RT) &= .2 \cdot k_{o1} \exp(-E_1/RT) \\ T_{tr} &= (E_2 - E_1)/(R \cdot \ln(k_{o2}/.2k_{o1})) \end{aligned} \quad (3.17)$$

Using the parameter estimates determined by Kobayashi [1,10] listed in table 2, one finds the transition temperature to be approximately 1305K. While the transition temperature found in this example is a function of the parameter values chosen, this temperature is supported by experimental work, since Badzioch and Hawksley [15] found that a second high temperature reaction is required to explain the increase in weight loss if the devolatilization

temperature is above 1273K. The transition temperature is an important 'tool' in determining the type of model that should be utilized. This method can also be used to approximate the temperature at which the first reaction becomes negligible by finding the temperature at which k_1 is twenty percent of k_2 :

$$k_1 = .2 \cdot k_2$$

therefore:

$$k_{01} \exp(-E_1/RT) = .2k_{02} \exp(-E_2/RT)$$

$$T = (E_1 - E_2)/(R \ln(k_{01}/.2k_{02})) \quad (3.18)$$

Using the parameter estimates determined by Kobayashi [1,10] listed in table 2, one finds the temperature at which the first reaction becomes negligible to be approximately 2950K. An interesting feature of this model is that the ultimate yield becomes a function of the temperature-time history of the particle. If the particle is held at a fairly low temperature for a long period of time, the original coal substance, C, will be entirely consumed by reaction 1, producing yield α_1 , so that no further product will be produced by subsequent heating to a temperature at which reaction 2 becomes predominant. Rapid heating to high temperatures, on the other hand, will ensure that most devolatilization occurs by reaction 2, resulting in a higher yield. Thus the Kobayashi model is capable of explaining the observed dependence of yield on the heating rate [13,6,16,20] as well as on temperature.

3.3.2 Ubhayakar et al.

Ubhayakar et al. [29] performed devolatilization experiments in hot combustion gases with temperatures from 1800K to 2250K, which is the temperature range that would require a two reaction model. The model used was in fact the two reaction model presented by Kobayashi with some modifications. Ubhayakar assumed that the stoichiometric mass constants were equal to x/x_n where x_n is equal to the (H/C) ratio of volatile n, $n=1,2$ and x is equal to the

(H/C) ratio of the coal. As the coal particles were entrained in hot combustion gases, the model used by Ubhayakar incorporates the two reaction model followed by the cracking of the volatiles. The parameters for the two reaction model were fitted using the data provided by Kimber and Gray [16] and Badzioch and Hawksley [15].

From the determination of the stoichiometric constants it appeared that the high temperature process led to higher yields of lower (H/C) volatiles and lower char than the lower temperature process. These observations are derived from the values of α_n :

$$\alpha_1 = 0.3 = x/x_1 \rightarrow x_1 = .194$$

$$\alpha_2 = 0.8 = x/x_2 \rightarrow x_2 = .07275$$

The lower char yield is backed by experimental results [10,15,16] finding increased weight loss with increased temperature. However, as the (H/C) ratios of the volatiles released were unrecorded by Badzioch and Hawksley [15] and Kimber and Gray [16], these results could not be verified. Also, using two sets of experimental data to fit the parameters of the model to be used to fit additional parameters to a third set of data is not advisable as the conditions in the different furnaces can result in very different devolatilization behaviour and therefore parameter estimates are obviously in question.

3.3.3 Jamaluddin et al.

The coal in the experiments of Jamaluddin et al. [13] was devolatilized over a temperature range of 800-1400C, which also supports the use of a two reaction model. Jamaluddin [13] also used the Kobayashi model; however, some slight modifications were made. The low temperature kinetic rate constants were taken as those determined by Badzioch and Hawksley [15] while the high temperature constants were set to those as determined by Ubhayakar et al. [29]. The low temperature mass stoichiometric constant was taken as the proximate analysis volatile matter, which is the definition of α_1 originally given by Kobayashi. However

α_2 was determined from the measured pyrolysis data and was defined by:

$$\alpha_2 = QV_o \quad (3.19)$$

where $Q = V^*/(V_o - V_r)$ as defined by Badzioch and Hawksley [15]. As a result, at high temperatures with $k_2 \gg k_1$, the model would reduce down to:

$$V = QV_o(1 - \exp(-k_2t)) \quad (3.20)$$

This model has the same form as the model introduced by Badzioch and Hawksley [15] for low temperature ($< 1273K$) devolatilization, if at the high temperatures the correction factor, C , for the asymptotic weight loss were to be set to zero. The model was found to be accurate for the high volatile bituminous coal but to overpredict the weight loss for the medium volatile coal by up to five percent. One should note that using rate parameters determined by other researchers could compromise the values of α_1 and α_2 determined by fitting the model to the data.

3.3.4 Suzuki et al.

Suzuki et al. [33] performed devolatilization experiments with combustion air as the secondary gas stream with a temperature range up to 1483K. However the furnace had recirculating flow and therefore the temperature-time history of the coal particles is uncertain. Suzuki also used the Kobayashi model; however, α_1 was selected to provide agreement between the experimental data and the predictions while holding all other parameters constant. The values of α_1 were then correlated with the (H/C) ratio and the proximate volatile matter of the coal to provide a means of estimating α_1 . Suzuki found that the extent of devolatilization through the first reaction, α_1 , increases with an increase of the proximate volatile matter and (H/C) ratio of the coal. However, one should note that fixing the other parameters may fix the behaviour of α_1 : i.e. if the values of the other parameters were changed one might find that the behavior of α_1 was changed as well.

3.3.5 Baxter et al.

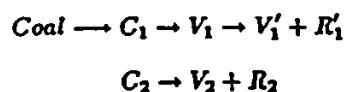
Baxter et al. [34] used statistical routines to fit the parameters of the parallel reaction model to the data obtained by Kobayashi [1]. The temperature, velocity and radiation conditions inside Kobayashi's furnace were calculated with a numerical model of the flow, and were then utilized to determine the temperature of the particle as a function of time. However, the results of this analysis are questionable: at a furnace temperature of 2100K, the particle model developed by Baxter predicts a plateau in the temperature profile at 1400K which is said to be a result of the high rate of mass transfer due to devolatilization of the coal particle. In view of the low value of heat of pyrolysis, it seems unreasonable that the mass flow from the coal particle would maintain the coal particle's temperature 700K below the ambient temperature and still maintain a high rate of mass release. Another difficulty with this model prediction is that it indicates that there is in fact no high temperature devolatilization and would bring to question the temperature profiles of the devolatilizing coal particle at lower temperatures as predicted by this model. The reason for these problems appears to be an incorrect particle energy balance: the enthalpy of the escaping devolatilization gases was included in the energy balance, which can be shown to be in error when the first law of thermodynamics is applied to the pyrolyzing coal particle (Appendix A).

Other researchers [31,35] also have employed the Kobayashi model, using the values of α and k as determined by Kobayashi. As previously stated, Kobayashi expended little effort in optimizing the parameters for the best fit, moreover; his values are specific to his two test coals, so that using his constants without further testing or modifications is not advisable.

3.4 Two component model

The two component model differs from the two competitive reaction model in that instead of having two reactions that come into play at different temperatures, it is assumed that the coal consists of two components. These two components of the coal pyrolyze by independent,

first order reactions which have substantially different rate constants. The mechanism is as follows:



where the first reaction includes a secondary cracking reaction. This model can be simplified by neglecting the secondary cracking stage.

3.4.1 Nsakala et al.

Nsakala [4] studied the kinetics of lignite pyrolysis at 1081K in a drop tube furnace. The model used to describe the devolatilization was the two component hypothesis without the secondary cracking. The evidence cited by Nsakala that dictated the need for this type of model was a 'break' in the weight loss behavior, figure 4, that occurred when the residence time was increased; this was seen to be characteristic of two independent parallel reactions having substantially different rate constants. However, this 'break' could be the result of the weight loss approaching the asymptotic weight loss.

This model requires that the initial concentrations of each component, the proportionality constant, γ , between V_2 and R_2 plus the rate constants to be determined. Nsakala found that the asymptotic weight loss was not a function of temperature, rather

$$V^\infty = C_1 + C_2/(1 + \gamma) \quad (3.21)$$

The number of parameters to be estimated as well as the asymptotic weight loss not being temperature dependent make this model quite undesirable.

3.5 Multiple Parallel Reaction Mechanism

An alternative model to the two parallel competing reaction model is the multiple parallel reaction model. The premise of this model is that the devolatilization of the coal is a complex phenomenon that should be modelled as a large number of independent parallel reactions. The problem is simplified if it is assumed that the pre-exponentials for each reaction are the same and the reaction rates only differ in activation energies. It is further simplified by assuming that the number of reactions is large enough to permit E to be expressed as a continuous distribution function.

Anthony et al. [5,6] generalized this model to allow for non-isothermal processes. This model was also adapted and modified by several researchers [11,21,36,37].

3.5.1 Anthony and Howard

Anthony and Howard [5,6] performed devolatilization experiments in the temperature range of 673-1373K which is within the single low temperature reaction range. The as yet unreleased volatile fraction for a particular reaction i of the multiple parallel reactions is:

$$V_i^* - V_i = V_i^* \exp\left(-\int_0^t k dt\right) \quad (3.22)$$

V_i^* is a differential part of the total yield V^* and may be written:

$$V_i^* = dV^* \quad (3.23)$$

$$= V^* f(E) dE \quad (3.24)$$

with

$$\int_0^\infty f(E) dE = 1 \quad (3.25)$$

Integrating equation 3.22 over all values of E using equation 3.24 yields;

$$(V^* - V)/V^* = \int_{-\infty}^{\infty} \exp\left(-\int_0^t k dt\right) f(E) dE \quad (3.26)$$

Anthony and Howard stated that there is negligible numerical effect of altering the lower limit on the left integral from 0 to $-\infty$. The distribution function, $f(E)$, is assumed to be Gaussian with a mean activation energy E_0 and standard deviation σ :

$$f(E) = [\sigma(2\pi)^{0.5}]^{-1} \exp[-(E - E_0)^2/2\sigma^2] \quad (3.27)$$

The model has the $\int_0^t k dt$ term to account for non-isothermal processes.

One difficulty with this model is that it does not predict the variation of yield with temperature at higher temperatures. This can be illustrated by assuming an isothermal process, for which, equation 3.26 becomes:

$$(V^* - V)/V^* = \int_{-\infty}^{\infty} \exp(-kt) f(E) dE \quad (3.28)$$

as $t \rightarrow \infty$,

$$(V^* - V)/V^* = \int_{-\infty}^{\infty} f(E) dE = 0 \quad (3.29)$$

which shows that the asymptotic weight loss is a constant and equal to V^* and therefore independent of temperature. Anthony and Howard state that this model can give the impression of an asymptote being reached by a low temperature decomposition when it is compared with one at high temperatures, but this really amounts to a misinterpretation of the results. The behavior of this model can be illustrated by assuming a uniform rather than a Gaussian distribution of activation energy:

$$\int_{E_a}^{E_b} f(E) dE = 1 \rightarrow f(E) = 1/(E_b - E_a) \quad (3.30)$$

Substituting equation 3.30 into the isothermal equation 3.28, the resulting equation is:

$$V = V^* [1 - RT/(E_b - E_a) [E_1(k_0 t Z_b) - E_1(k_0 t Z_a)]] \quad (3.31)$$

where $E_1(x)$ is the exponential integral:

$$E_1(x) = \int_x^{\infty} \frac{\exp(-t)}{t} dt$$

$$Z_i = \exp(-E_i/RT)$$

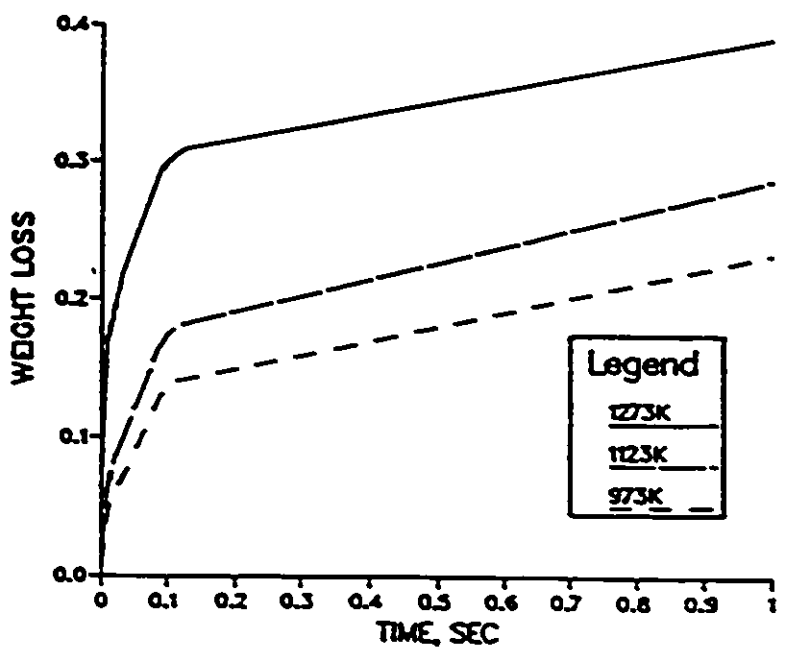
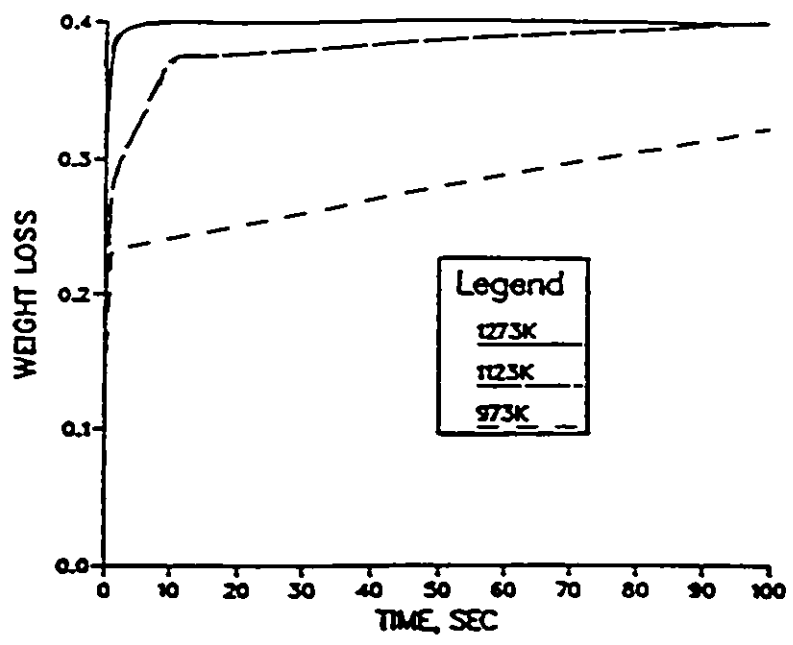


Figure 5: Weight loss versus residence time as predicted by Anthony and Howard [5,6] model for various temperatures

Figure 5 is a graph of the resulting weight loss. It could appear that the low temperature devolatilization had reached an asymptote although in reality it had not. Thus this model does not describe the variation of the asymptotic weight loss with temperature as the Kobayashi model does. A further problem with this model is that k_0 and E are correlated [6,37], since a higher value of k_0 tends to shift the distribution to higher activation energies.

3.5.2 Hashimoto et al.

Hashimoto et al. [37] also used the multiple parallel reaction model to model the thermal regeneration of activated carbons used in wastewater treatment with a temperature range up to 1173K. Hashimoto used Anthony and Howard's non-isothermal model with a modification to correct the dependence of the distribution curve of E on the value of k_0 . This weak point was corrected by approximating k_0 as a function of E :

$$k_0 = \phi \exp(\beta E) \quad (3.32)$$

This modification increases the number of parameters required to be fitted by two and solves the problem of the correlation between k_0 and E . However, this model still has the problem of the ultimate yield not being a function of temperature.

3.5.3 Solomon et al.

Solomon et al. [21] performed pyrolysis experiments in an entrained flow reactor which was designed to operate up to a maximum temperature of 1923K. The model used to describe the pyrolysis of coal was Anthony and Howard's model with a Gaussian distribution for the activation energy. The model, however, was used to describe individual species evolution rather than pyrolysis of the coal as a whole. Solomon justified using a distribution function for the activation energy of individual species by the fact that the quantity of each gas species depends upon the functional group distribution in the original coal. Solomon also

hypothesizes that the functional groups decompose at rates which are insensitive to coal rank to form light gas species. It is for this reason that the model was fitted to the pyrolysis of a lignite in an entrained flow reactor and then applied to a bituminous coal pyrolyzed in a heated grid to test its generality. One difficulty that can be pointed out in this method is that the lignite was only heated to a single temperature (1373 K) while the temperature range of the bituminous coal tests was 673-2073 K. There was a problem in the collection of the tar and soot and therefore substantial scatter existed in the data.

The fit of the model to either coal's devolatilization products is not very good [21]. This might be due to the fact that the parameters were fitted using the functional groups present in the coal. The functional group composition of the coal was then required to be found and the kinetic rate constants of these groups then formed the distribution functions of E. This complicated modeling has a lot of room for error, owing to the many parameters involved.

3.5.4 Suuberg et al.

Suuberg et al. [11] investigated the kinetics of lignite pyrolysis using a heated grid with a constant heating rate and a maximum temperature of 1273K. Suuberg was investigating the applicability of the multiple parallel reaction model to the devolatilization of a lignite by modeling the appearance of several products. Many products are not adequately modeled by a single reaction [11,38] but in fact are the result of different reactions in different temperature intervals. Figure 6 also shows how the various individual reactions form a smooth total weight loss curve. In spite of this evidence, which supports the use of the competitive two reaction model with temperature dependent ultimate yield, Suuberg supports the use of the parallel multiple reaction model, since the distribution function of E is similar to those obtained based on weight loss data [5,6]. Suuberg states that the kinetic parameters obtained by the parallel multiple reaction model are overall properties, in spite of the fact that the species are involved as a result of some combination of two reactions.

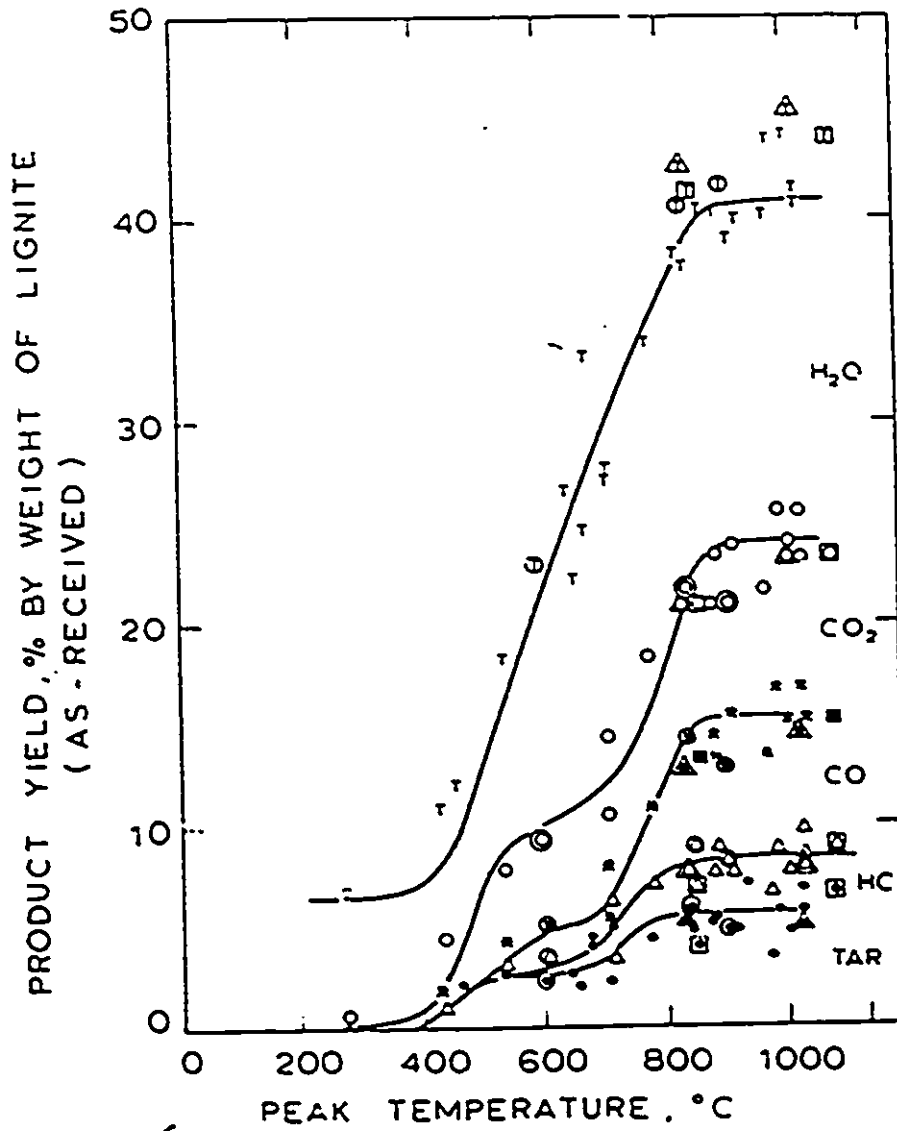


Figure 6: Pyrolysis product composition from lignite coal heated to different peak temperatures

3.5.5 Rizvi

Rizvi [36] modeled the combustion of pulverized coal particles in swirling flow combustors. Rizvi evaluated the performance of the first order reaction, evaporation, two competing reaction and multiple parallel reaction models by comparing the flame behavior that results from the models to the actual flame behavior. Rizvi found that satisfactory predictions of the flame behavior were obtained when either the evaporation or multiple parallel reaction models were utilized while both the two competing reaction and Badzioch and Hawksley's single first order reaction models were found to be less successful. However, it must be stressed that all reaction constants used came from the literature and no attempt was made to fit them for the particular coal being used. Optimization of the constants would probably make all these models more accurate and would certainly be required for a meaningful test. These findings can be seen to be quite questionable, for the two 'acceptable' models are at opposite ends of the spectrum: i.e. one is a purely physical model while the other represents a large number of independent parallel reactions. Another problem with this conclusion is that the analysis is based upon the turbulent flame behavior where any number of unknown factors might come into play apart from the devolatilization process itself.

3.5.6 Sprouse et al.

Sprouse et al. [39] fitted Anthony and Howard's multiple parallel reaction model as well as Kobayashi's two reaction model to the high temperature lignite devolatilization data supplied by Kobayashi [1]. Sprouse performed a non-linear least squares curve-fitting routine on Kobayashi's data, since there was some question whether the Anthony and Howard model, which was previously only applied to low temperature ($< 1200K$) pyrolysis, could adequately handle high temperature devolatilization. Sprouse fitted both models to the Kobayashi data and found that the standard deviation of the Anthony and Howard model was 4.6% while it was 6.1% for the Kobayashi model. This small difference in the standard deviations of the two models is not significant, especially when the char combustion is

the rate controlling step for the complete combustion process. Sprouse also compared the abilities of the two different models to adequately fit devolatilization data by applying the models to the devolatilization of coal during an ASTM test. Although Sprouse found that Anthony and Howard's model described the ASTM devolatilization more accurately than the Kobayashi model, this test cannot be considered a good test due to the long residence time, during which secondary reactions have ample opportunity to effect the devolatilization results.

Sprouse points out that the Anthony and Howard model fits the high temperature data while using fewer parameters. However, k_0 and E are correlated [6,37] and therefore the equation suggested by Hashimoto [37] to correct this model weakness should be added which in turn raised the number of parameters to be fitted. Also, as discussed on page 41, the multiple parallel reaction model only appears to model the change in ultimate yield with temperature, and actually gives a constant ultimate yield.

Sprouse also questions the validity of the Kobayashi model since it cannot predict that a coal heated at low temperature will always devolatilize further when the temperature is raised, while the Anthony and Howard model can predict this behavior. However, a model should suit the purposes of the researcher: since in coal combustion the coal is consumed and therefore any question of reheating to a higher temperature is eliminated, this argument against the Kobayashi model can be considered unimportant for the present purposes.

3.6 Conclusions

The models presented in the literature have been examined and analyzed for their suitability and accuracy in describing the devolatilization of coal. The utility of the evaporation model is confined to the correlation of weight loss data over very narrow ranges of conditions; it is unsuitable as a general model. The one reaction models appear to be suitable for low temperature (below 1300K) pyrolysis and either did not describe the temperature

dependence of the ultimate yield or used some sort of empirical correction [15,19]. The two component hypothesis [4] complicated the pyrolysis model and yet did not address the problems stated above. The multiple parallel reaction model was only used to fit low temperature devolatilization and did not describe the temperature dependence of the ultimate yield at high temperatures. In the form suggested by Anthony and Howard [5,6] a numerical integration of the probability function is required, while other multiple parallel reaction schemes are too complex for the inclusion in a complete model of coal combustion in a furnace.

However, the two competing reaction model illustrated the temperature dependence of the asymptotic weight loss. It is flexible, in that at low temperatures this model reduces down into the simpler one reaction which was found to be acceptable at lower temperatures. This is also the only model which will predict a dependence of the weight loss on the heating rate or temperature history. It is for these reasons that the two competing reaction model has been selected as the best model for the purposes of the present work.

Table 2: Parameter estimates determined by Kobayashi

reaction	k_0	E
low	2E5	25
high	1.3E7	40

Chapter 4

Reactor Model Program

The entrained flow reactor has been designed to provide data under conditions where the particle temperature-time history may be determined and where the heating rate and reaction conditions match a pulverized coal combustor. A particle heating program written by Flaxman [7] models the furnace flow fields as well as the particle motion and heating. This program was modified with the addition of a devolatilization model. The coal loadings are usually kept small to prevent secondary cracking reactions and therefore the effect of the coal particles on the gas velocity and temperature fields is neglected [7,13]. The temperature and velocity fields inside the reactor are determined by numerically solving all fundamental governing equations of energy, momentum and conservation of mass using finite difference techniques. The temperature and velocity fields of the furnace are then used to calculate the coal particle temperature and velocity by numerical solution of the differential equations of particle motion and heating.

As many different designs of entrained flow reactors exist, each with its own geometry, gas flows and particle feed rates, the particle heating program was designed to be flexible so that different furnaces could be modelled by making simple adjustments inside the program. The flexibility of the program is in part achieved by dividing the flow field area into small

control volumes with varying sizes which form a grid pattern. The grid spacing was chosen so that there are many points in the region of large gradients and fewer points as the gradients become smaller. A sample grid for the EMR reactor is shown in figure 7. The nodes for the grid are placed such that the control volume boundaries lie exactly halfway between the adjacent nodes. The nodes can then be adjusted to model the dimensions of the desired entrained flow reactor, for example the Kobayashi furnace [1], with dimensions as shown in table 3.

4.1 Method of Integration

The original particle heating program assumed that the particles do not react chemically. This program was modified by adding the two competitive reaction model selected for coal devolatilization:

$$V = \int_0^t (\alpha_1 k_1 + \alpha_2 k_2) \exp\left(\int_0^t -(k_1 + k_2) dt\right) dt \quad (4.1)$$

As equation 4.1 can not be easily integrated analytically, different methods of numerical integration were investigated to select the simplest method, with regard to consumption of computer time, which can still accurately perform the integration. The accuracy of the methods of integration was tested by making weight loss predictions for a single first order devolatilization reaction in a particle undergoing heating according to:

$$T = Z(1 - \exp(-\beta t)) + T_0 \quad (4.2)$$

where:

- $\beta = 12k/(\rho c_p d^2)$
- Z is the difference between the final equilibrium temperature and the initial temperature, T_0 .

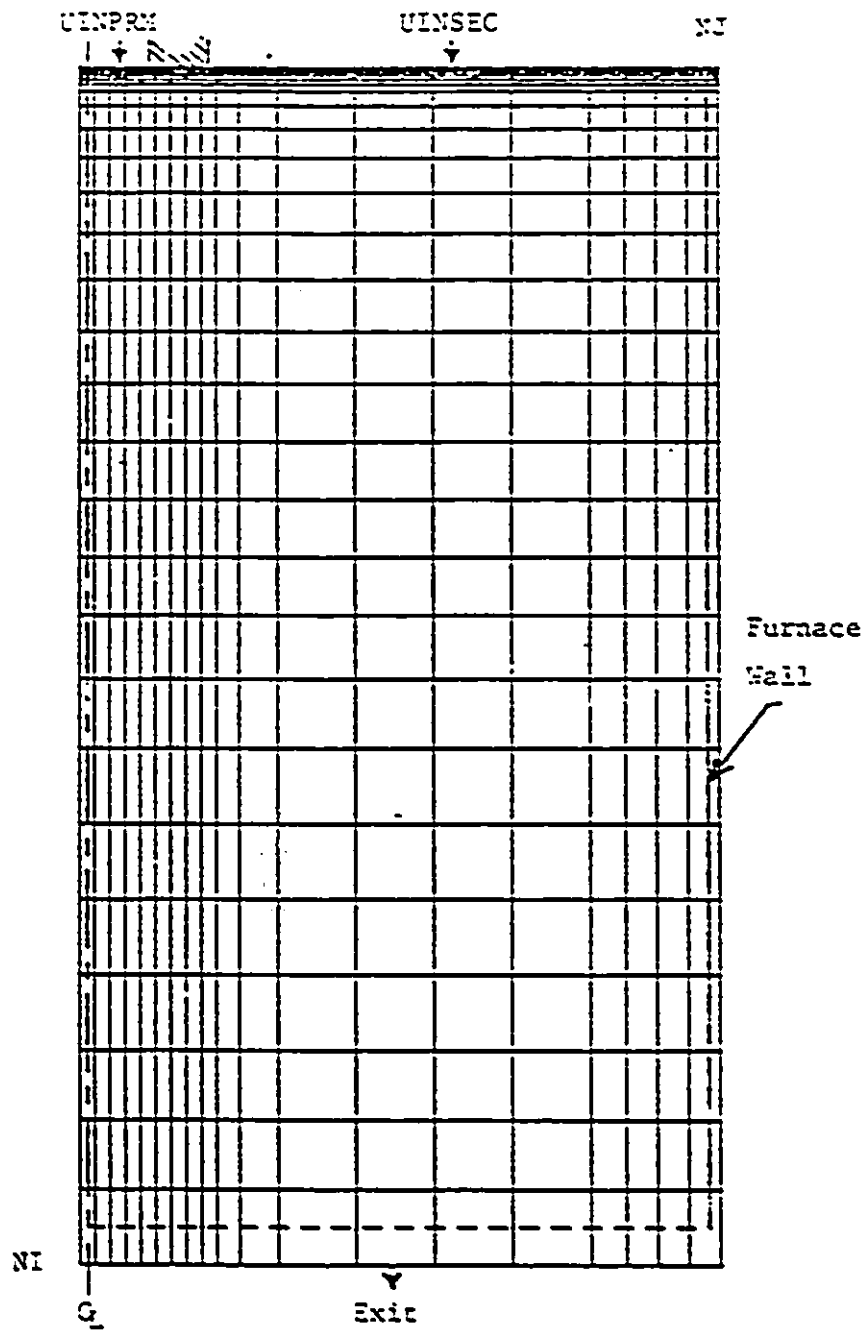


Figure 7: Sample Grid for Laminar Flow Furnace [7]

and comparing these to the analytical solution for this problem. Although the total amount of work involved is not significantly changed, a simpler method with a small step length gives similar accuracy to a more complex method with a larger step length [40]. As the particle heating program already is limited to small step sizes (maximum time step is 5 ms) in the prediction of the particle temperature and velocity, the simpler methods of numerical integration were that investigated are:

- summation - the integration is performed by assuming that the level of the ordinate is constant throughout the step:

$$I = y_1 \cdot (x_2 - x_1) \quad (4.3)$$

where the subscripts 1 and 2 refer to the beginning and end of the integration step respectively.

- trapezoid rule - in trapezoid rule, the value of the integral is the arithmetic average of the two ordinates multiplied by the distance between them:

$$I = \frac{1}{2}(y_1 + y_2)(x_2 - x_1) \quad (4.4)$$

- Simpson's rule - Simpson's rule for three points is based on fitting a quadratic to three equally spaced data points. The resulting equation is:

$$I = \frac{1}{6}(y_1 + 4y_2 + y_3)2h \quad (4.5)$$

In the particle heating program, the maximum temperature step was limited to 5 K, and therefore during particle heatup the magnitude of the time step can vary. This eliminates Simpson's rule, as this method requires equal spacing between the three points used in each integration step.

The exact solution of the first order reaction equation for the weight loss of a particle undergoing exponential heating with a time step of 5 ms is shown in figure 8 with

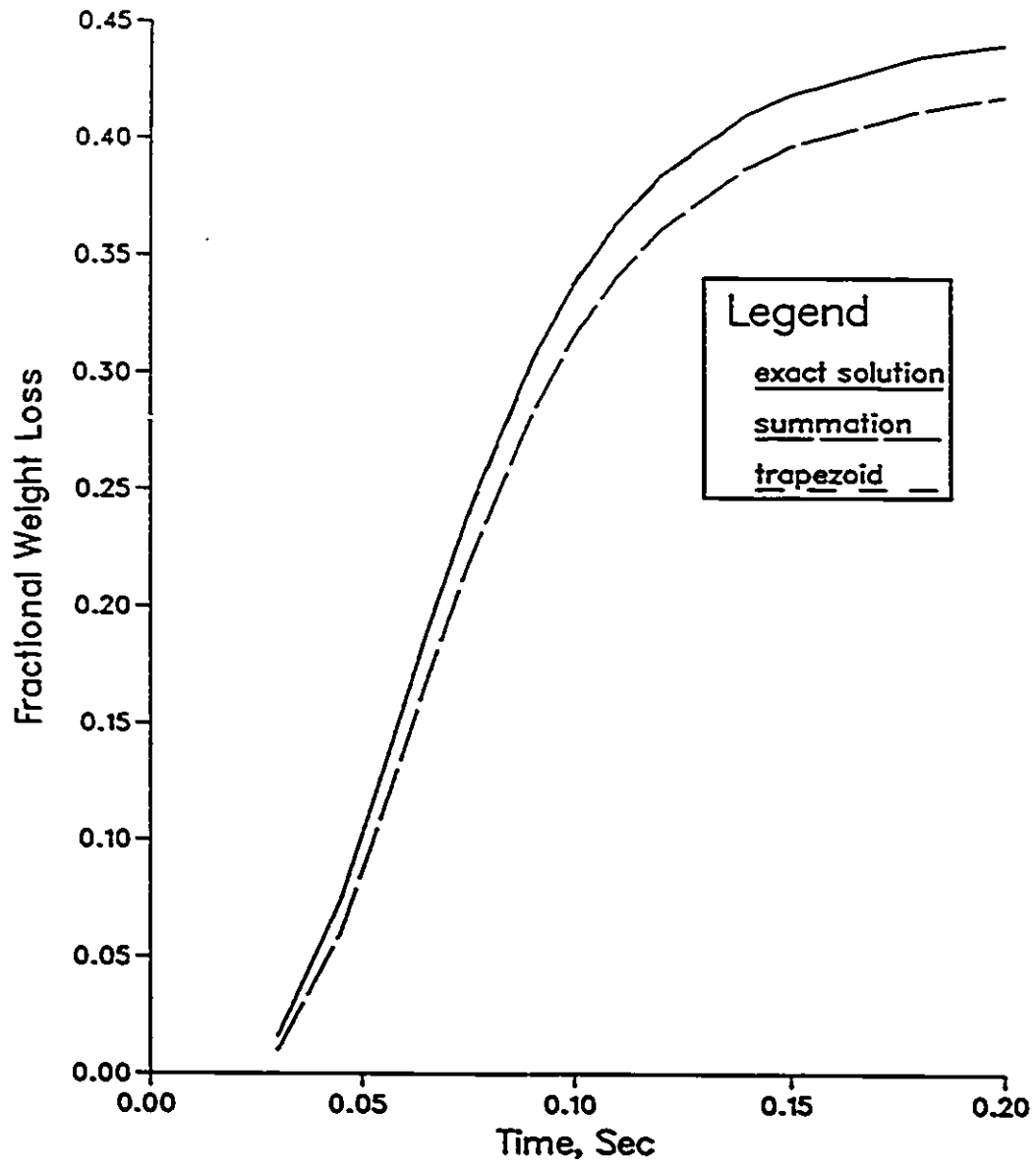


Figure 8: Weight Loss Versus Time for Particle Undergoing Exponential Heating

the predictions of the equation numerically integrated using either the summation or the trapezoidal rule. The results suggest that although the method of summation is inaccurate, the trapezoid rule has sufficient accuracy to very closely approximate the exact solution. The accuracy of the method of numerical integration will have even more importance with the two competing reaction model, equation 4.1, which requires two integrations to be performed in order to solve the equation.

4.2 Effects of mass transfer

The particle heating program solves for the particle velocity and temperature as it passes through the furnace flow field. The acceleration of the particle is given by:

$$\frac{du_p}{dt} = g - \frac{3c_d\rho}{4\rho_p d_p} (u_p - u) |u_p - u| \quad (4.6)$$

For small Reynolds numbers, this equation can be linearized as:

$$\frac{du_p}{dt} = g - A(u_p - u) \quad (4.7)$$

where

$$A = \frac{18\mu}{\rho_p d_p^2} (1 + 0.15 Re_o^{0.687})$$

$$Re = \frac{\rho |u_p - u| d_p}{\mu}$$

The bracketed term in A is a correction to Stokes' law for $Re > 1$. With a small time step, Δt , u and Re can be assumed to be constant and this equation can be integrated directly over Δt since A is a constant:

$$u_p = u - \frac{1}{A} [(g - A(u_{p0} - u))e^{-A\Delta t} - g] \quad (4.8)$$

where u_{p0} is the particle velocity at the beginning of Δt . The original expression for particle heat transfer was:

$$\frac{dT}{dt} = \frac{6}{\rho_p c_{pp} d_p} (q_{rad} - q_{conv}) \quad (4.9)$$

As stated earlier, the value of Δt must be selected so that u , Re , and the gas temperature can be assumed constant. Equation 4.9 can also be integrated analytically in a fashion similar to equation 4.6 if these values are assumed constant over the time step, Δt . The value of Δt was selected by arbitrarily choosing a maximum temperature step, ΔT_{max} , of 5K and therefore

$$\Delta t \approx \frac{\rho_p c_{pp} d_p \Delta T_{max}}{6(q_{rado} - q_{convo})} \quad (4.10)$$

where q_{rado} and q_{convo} are from the previous time step. This results in a small time step initially where the heating is rapid, which gradually increases. A maximum time step of 5 ms was chosen to ensure the gas velocity is nearly constant over the time step.

When the devolatilization model was added to the particle heating program, several modifications were incorporated. Corrections to the convective heat transfer coefficient and drag coefficient are required to allow for the effects of mass transfer from the pyrolyzing coal particle. This can be corrected for by means of the transfer number, B , which is defined as:

$$B = (Y_o - Y_\infty)/(1 - Y_o) \quad (4.11)$$

where Y_o and Y_∞ are the particle surface and ambient mass fractions of volatiles respectively. From simple droplet evaporation theory, this is related to the volatiles mass flux G by:

$$B = \exp(r_o G / \rho D) - 1 \quad (4.12)$$

where r_o is the particle radius, G the mass flux of volatiles, ρ the gas density and D the diffusion coefficient. The drag coefficient is then [41]:

$$c_d = c_{do}/(1 + B) \quad (4.13)$$

where c_{do} is the drag coefficient of the non-pyrolyzing coal particle:

$$c_{do} = \frac{24}{Re} (1 + 0.15 Re^{0.687}) \quad (4.14)$$

$$Re = \frac{\rho |u_p - u| d_p}{\mu}$$

The net effect is that the drag coefficient is decreased by the transfer because the boundary layer thickness is increased, lowering the skin friction, and the wake region is filled, leading to a reduction in form drag. The heat transfer coefficient becomes [41]:

$$h = h_o \ln(1 + B)/B \quad (4.15)$$

where h_o refers to the convective heat transfer coefficient in the absence of mass transfer [24]:

$$h = [2.0 + (0.4Re^{0.5} + 0.6Re^{0.66})(Pr^{0.25})(\frac{\mu}{\mu_p})^{0.25}] \frac{\mu c_p}{Pr d_p} \quad (4.16)$$

At small mass transfer rates, equation 4.15 reduces to h being equal to h_o , since $\ln(1 + B) \sim B$ for small B . Mass transfer decreases the values of the convective heat transfer coefficient, again because of the increased thickness of the boundary layer. The thermal conductivity of the gas in equation 4.16 is substituted using the definition of the Prandtl number:

$$Pr = \frac{c_p \mu}{k} \quad (4.17)$$

so that

$$k = \frac{c_p \mu}{Pr} \quad (4.18)$$

where the heat capacity of the gas is estimated using correlations from Reid, Prausnitz, and Sherwood [42], and the gas viscosity is fitted by the Sutherland equation [17]:

$$\mu = \frac{BT^{1.5}}{T + S}$$

where B and S are constants. The mass transfer from a devolatilizing coal particle (using parameter estimates determined by Kobayashi [1]) can be seen in figure 9 to have a negligible effect on the particle temperature.

The original particle energy balance was modified by including the heat of pyrolysis term:

$$\frac{dT}{dt} = \frac{6}{\rho_p c_{pp} d_p} [q_{rad} - q_{conv} - GH_r] \quad (4.19)$$

where G is the instantaneous mass flux from the particle surface and is equal to:

$$G = (\Delta V \cdot \rho_p \cdot V_p)/(A_o \cdot \Delta t)$$

where:

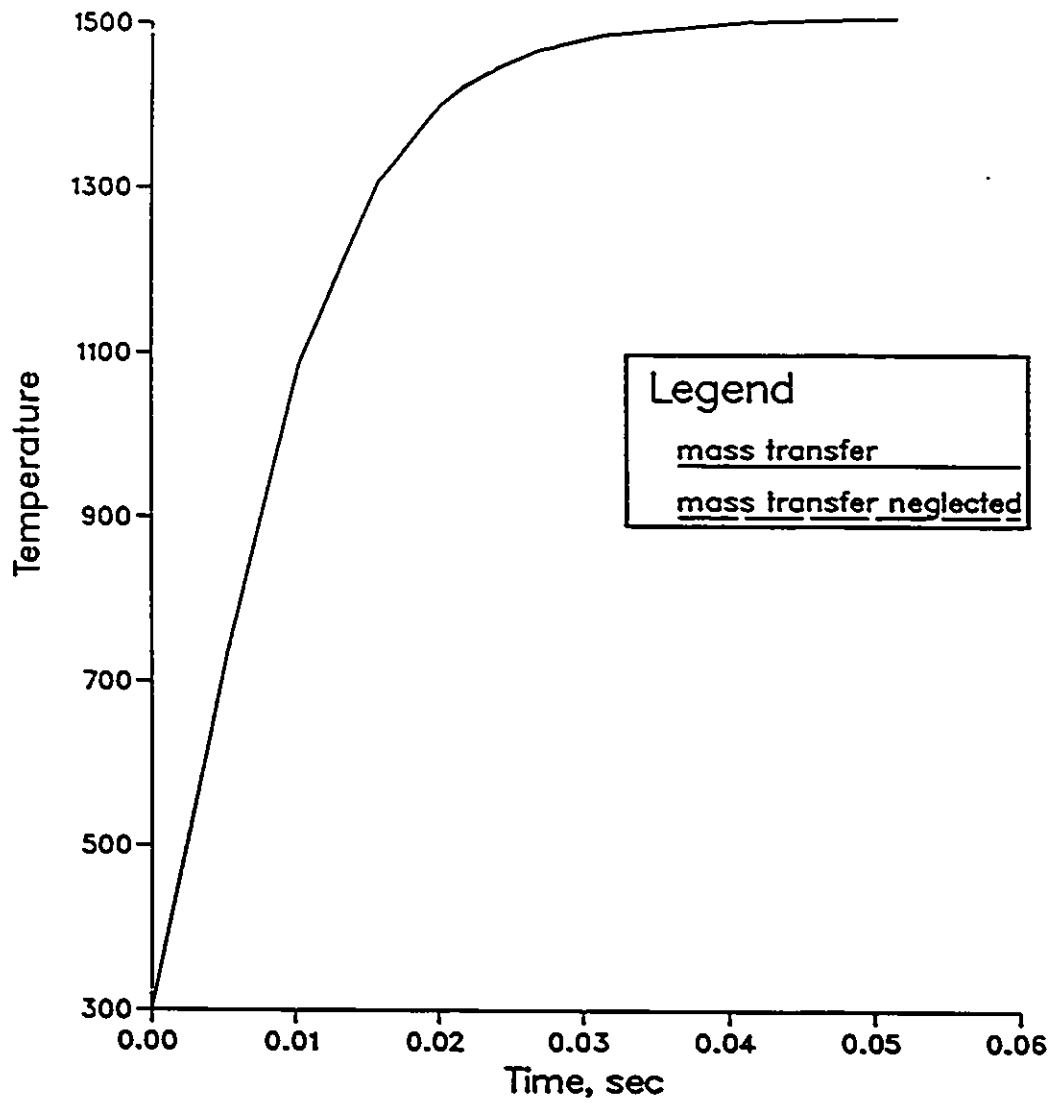


Figure 9: Effects of Mass Transfer on a Devolatilizing Coal Particle

- ΔV - the change in weight loss during the time step
- V_p - the particle volume
- A_s - the particle surface area

4.3 Physical properties of coal

Modeling of coal pyrolysis requires data for physical properties of coal such as the specific heat, density and emissivity. There is little variation in the estimates of the coal emissivity which is generally listed [24,25] as:

$$\epsilon = 0.8 \quad (4.20)$$

Unfortunately, there is a basic lack of specific heat and density data, so estimates of these properties of coal have been used in this study. These estimates for a substance like coal, which changes both chemically and physically when heated, are questionable. The estimates of these properties are even questionable for unheated coal because of the difficulty in accounting for the strong effects of coal rank, mineral matter and moisture content. The method of selection of estimates by other experimenters will be reviewed.

4.3.1 Specific heat

Merrick [8] found that the specific heat of coal usually increases with temperature and volatile matter. The specific heat of coal and coke was modelled based on atoms oscillating in the solid matrix. It was postulated that as the coal devolatilizes, the loss of hydrogen content results in the specific heat approaching the lower curve for coke. Figure 10 also shows that the specific heat generally could be considered to remain constant at a value of 2000 J/kg K in the temperature range of interest. However, it should be noted that this model predicts the specific heat for coals heated at lower heating rates and lower temperatures than a coal particle would experience upon entering a combustor. The dependence of the

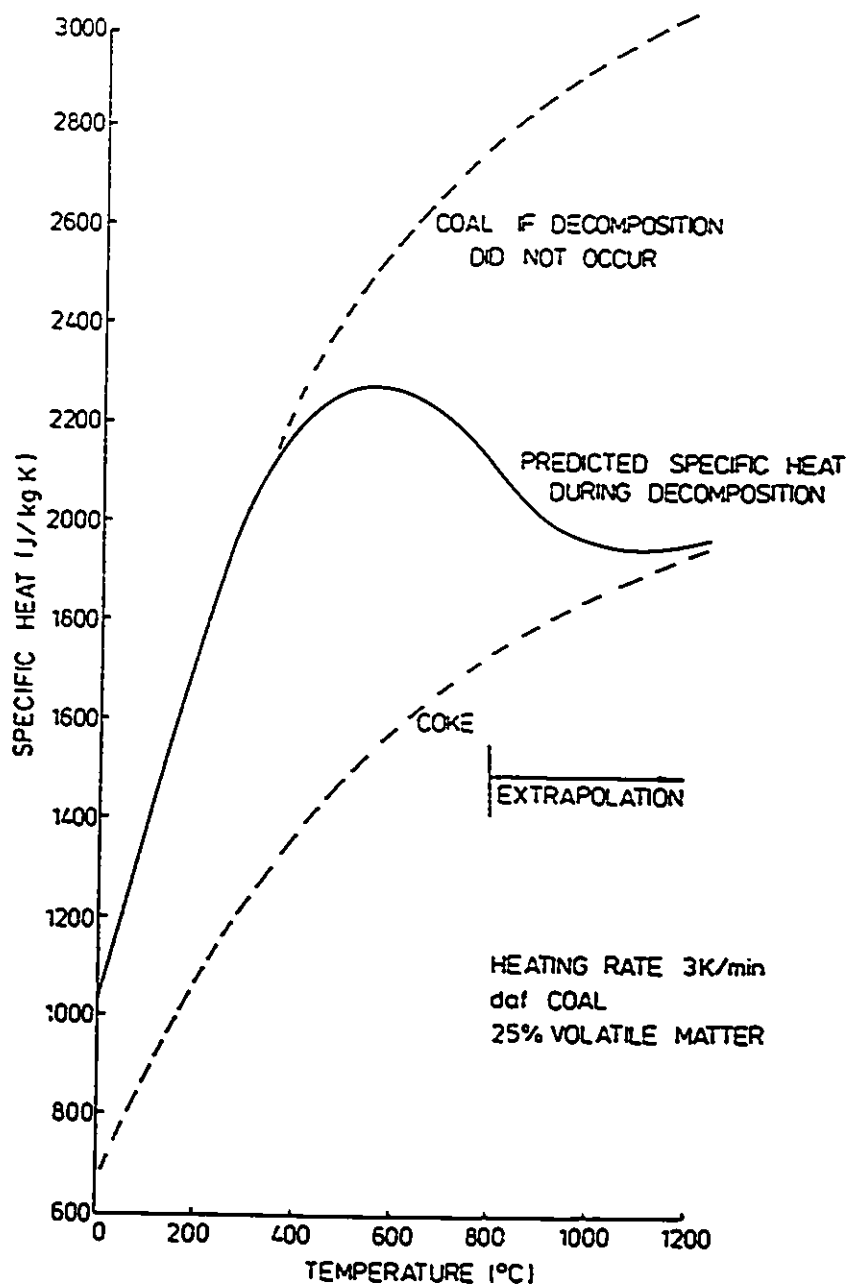


Figure 10: Predictions of the Specific Heat of Coal and Coke [8]

specific heat on devolatilization would suggest that specific heat could also depend on the heating history. Merrick stated that this comparatively high specific heat included the endothermic heat of pyrolysis.

Kobayashi [1] found that the specific heat of raw coal increases with increasing volatile matter and moisture content but decreases with increasing ash content. Coals with volatile matter in the range of forty percent were found to have specific heats around 1255 J/kg K. The specific heat was also found to be affected by the physical and chemical changes of the coal during heating. It was found that for a given heating rate, the position of the specific heat maximum is displaced towards higher temperatures as the volatile matter of the coal decreases. Chars produced from coals with volatile matter in the range of thirty to forty percent would be expected to have a specific heat value of 1380 J/kg K.

Eisermann et al. [43] presented a method of estimating the specific heat of coal and char. This method is based on the summation of specific heats weighed by the respective mass fractions of the different components: moisture, primary volatile matter, secondary volatile matter, fixed carbon, and ash. The evaluation of the original fraction of volatile matter in the coal or char is found by a correlation which utilizes the composition of the coal or char as determined by ultimate analysis. The secondary volatile matter is taken to be ten percent if the total volatile matter content is greater than ten percent and equals the total volatile matter if the amount is less than or equal to ten percent. The primary volatile matter is taken to be the amount in excess of ten percent. It should be noted that this seemingly arbitrary categorization of the volatile matters, as well as the evaluation of the amount of original volatile matter, is highly questionable. The specific heat of each component is then estimated using correlations with the devolatilization temperature as the only variable. The specific heat of coal and char is determined by a weighted summation of the different components. The difference between the specific heats of coal and char is determined mainly by their different compositions. There are two main problems with this method: first, the correlations that determine the specific heat of each component are based solely on temperature and therefore are highly specific; secondly, the use of broad categories

as 'primary volatile matter' results in the model not being able to account for the variations in composition of these mixtures [38].

The majority of researchers did not list the physical properties used for coal. Of the researchers that did, the estimate that was used in calculations was merely stated with little or no discussion. The specific heat estimates used by these researchers [44,20,45,28] varied from 1255-4187 J/kg K.

The specific heat of coal is not well documented and there is much uncertainty in the values listed, particularly as it is difficult experimentally to separate the specific heat and the heat of pyrolysis. These two must be separated, however, since the devolatilization process depends on the temperature and heating history. Hence Merrick's data [8] is unusable. As Kobayashi's devolatilization data was to be used in determining rate constant estimates, it was decided that to be consistent it would be best to use the specific heat estimate for char listed by Kobayashi (1380 J/kg K), as it is also an 'intermediate' value of all the specific heat estimates listed. A realistic value could be expected to lie between the specific heat of pure carbon (750 J/(kg K) at room temperature [25]) and those of typical liquid hydrocarbons (roughly 2000 J/(kg K)); this rules out the larger values reported in the literature.

4.4 Heat of Pyrolysis

A complete energy balance on a devolatilizing coal particle must include the endothermic heat of coal devolatilization. Heats of reaction in the range of $10^5 - 10^6$ J/kg are not unreasonable when considering thermal bond breaking processes such as:



However, the heat of pyrolysis, which theoretically could be calculated from the heats of formation of reactants and products, is in practice unknown.

Maloney and Jenkins [20] listed the heat of reaction to be in the range of 2.1E5 to

4.2E5 J/kg coal. Stickler et al. [45] included the heat of pyrolysis for each reaction in a two competitive reaction scheme as 1.675E6 and 8.37E5 J/kg for the low and high temperature reactions respectively. Tsai and Scaroni [46] predicted a temperature drop of 5-25 K for a heat of pyrolysis of 1.67E6 J/kg. It should be noted that these researchers listed the values of the heat of pyrolysis with little or no discussion. For the sake of comparison, the heat of combustion of coal ranges from 20E6 to 35 E6 J/kg and a typical hydrocarbon from 40E6 to 45E6 J/kg.

Mahajan et al. [23] tested the heat of pyrolysis at temperatures up to 853K using a thermal analytical technique called differential scanning calorimetry, in which the heat flow between the sample and reference material is measured. The heat of pyrolysis varied from -1.2E5 to 2.8E5 J/kg and was an irregular function of carbon content that had a maximum in exothermicity and endothermicity around 71% and 81% carbon respectively. It should be noted that there was some question about the results, since after correction for weight changes, the exothermic effects observed in uncorrected curves became either entirely or partly endothermic.

Freihant [9] tested the effect of the heat of reaction, which was varied from 0-4.2E6 J/kg, upon the predicted temperature internal profiles of a 100 μm particle. From figure 11, it can be seen that the maximum temperature difference predicted inside the particle is 150K.

This survey shows that there is wide disagreement as to the value of the heat of pyrolysis: it is very difficult to measure, and will almost certainly vary with coal rank and ultimate yield. In performing measurements of the heat of pyrolysis, it is easy to confuse it with evaporation of moisture or the variation of specific heat with temperature. In view of this, an intermediate value of the heat of pyrolysis, 8.37E5 J/kg, was arbitrarily selected for the model. The sensitivity of the model to the value chosen was tested by making sample calculations for the Kobayashi furnace [1]. The heat of pyrolysis can be seen in figure 12 to have but a slight effect upon the particle temperature: the comparison of the temperature variation due to the heat of pyrolysis to the weight loss versus time history

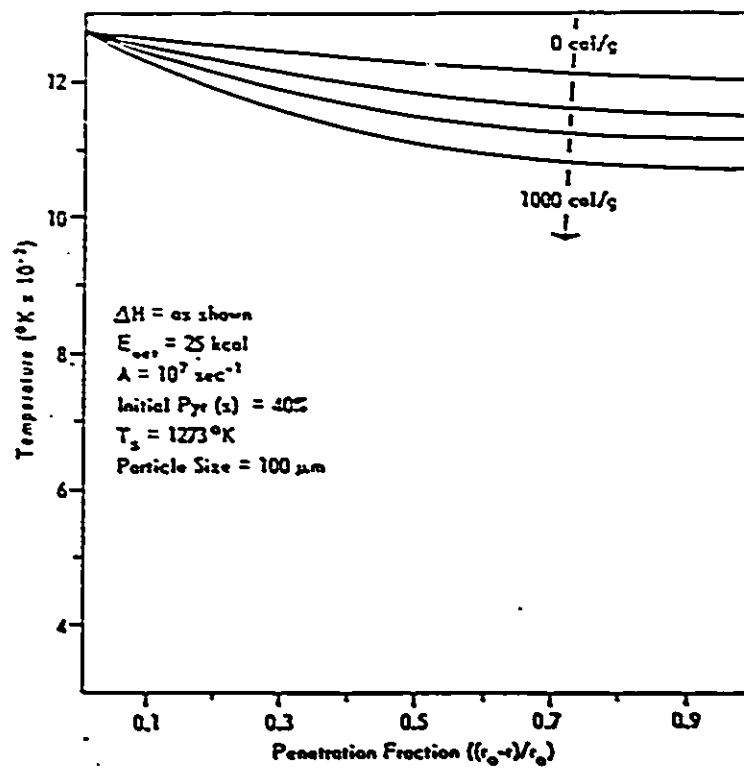


Figure 11: Effect of Heat of Reaction on Internal Temperature Profile [9]

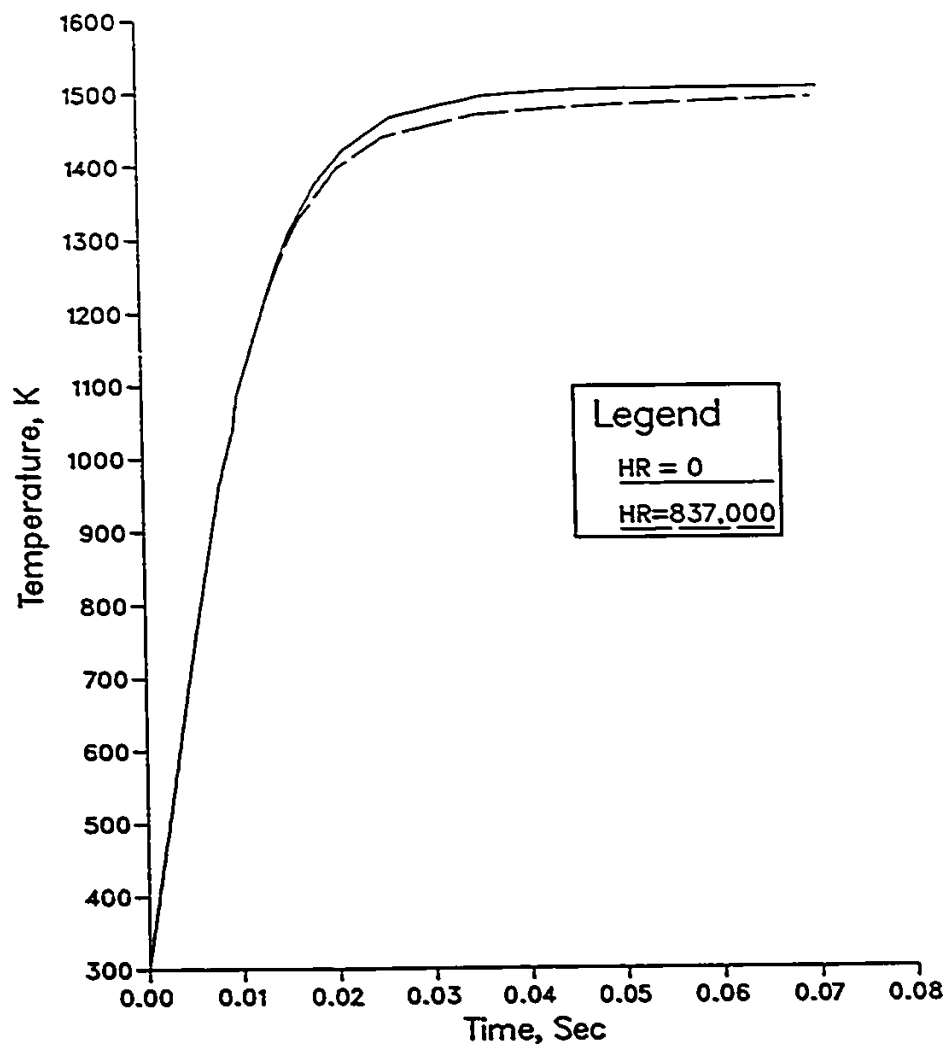


Figure 12: Effect of heat of pyrolysis on particle temperature

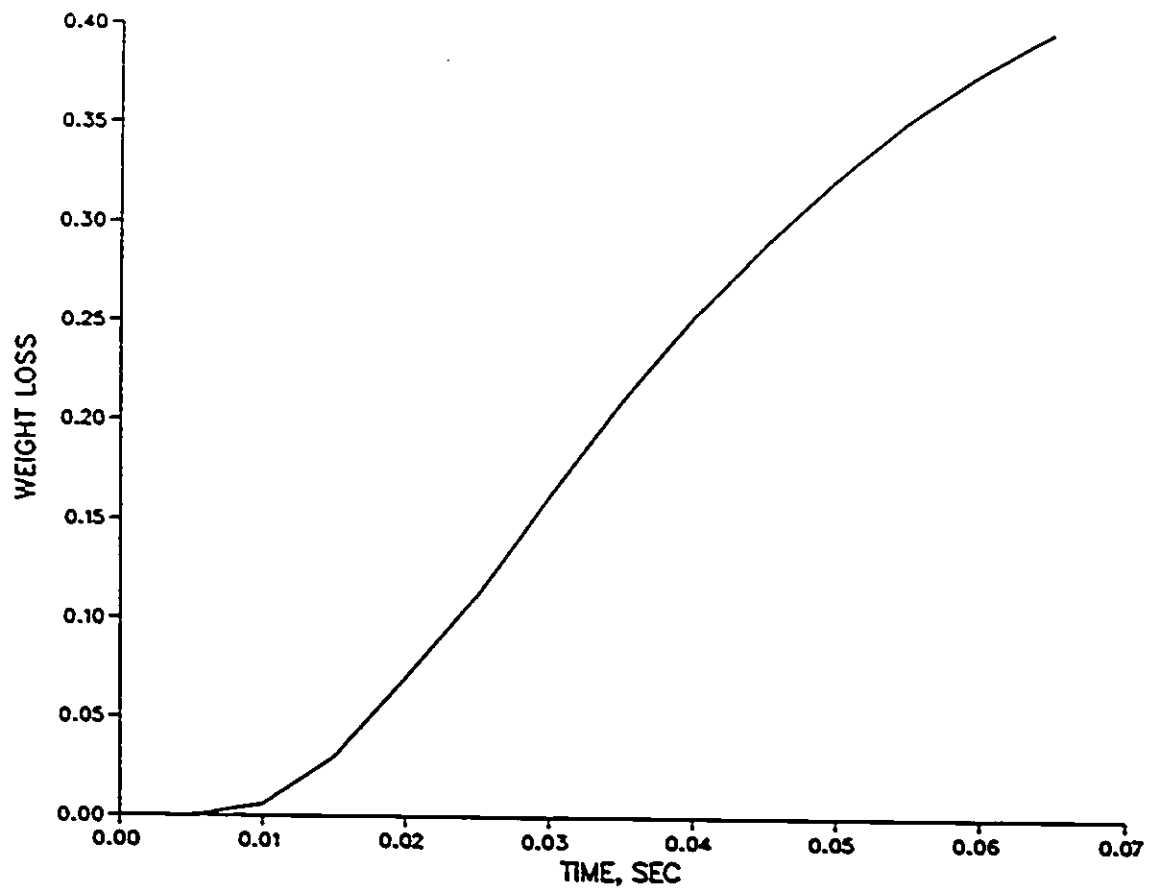


Figure 13: Weight Loss Versus Time for particle in 1510K furnace

shown in figure 13 shows that the effect on the particle temperature becomes the most significant, as expected, in the later stages of the devolatilization once a significant portion of the particle has devolatilized. These results suggest that little attention needs to be devoted to accurate evaluation of the heat of pyrolysis.

4.4.1 Density and Diameter Behavior

Coal undergoes considerable physical change upon heating. One of these changes is swelling, which is of particular interest as it could result in clogging of experimental or industrial equipment. Researchers have identified two different types of behavior during devolatilization:

- particle diameter remains relatively constant but density decreases as devolatilization proceeds. This behavior has been verified by visual observation of lignite coal particles after devolatilization experiments [1,4,27,47].
- particle diameter increases and density decreases as well. This behavior also has been substantiated by visual observation [15,27,47,48,49,50,51] of bituminous coals.

The ASTM free swelling index measures the tendency of coal to swell when burned or gasified in a fixed or fluidized bed; however, it is not recommended as a method of determining the expansion of coal in coke ovens [14]. Swelling coals are generally medium to high volatile bituminous coals which become plastic on heating.

Constant particle diameter

The changing density of a constant volume particle can be calculated as:

$$\rho = \rho_o MAFR(1 - V) + (1 - MAFR)\rho_o \quad (4.21)$$

where

- MAFR represents the moisture and ash free fraction of the coal
- ρ_o is the original density of the coal particle
- V is the fractional weight loss of coal on a moisture and ash free basis

The second term corresponds to the ash in the coal particle which is assumed to remain constant. The first term corresponds to the devolatilizing mass of coal. Equation 4.21 can be further reduced to:

$$\rho = \rho_o(1 - MAFR \cdot V) \quad (4.22)$$

Changing particle diameter and density

Several researchers [48,36] have addressed the problem of changing particle diameter by using a swelling factor. Coal particles have been observed to swell by as little as ten percent to as much as ten times the original particle diameter. A suggested model for changing particle diameter [48,36] is as follows:

$$d = d_p(1 + (S_{sw} - 1)(1 - X_v)) \quad (4.23)$$

where

- d_p - original particle diameter
- S_{sw} - ratio of swelled particle diameter to original diameter
- X_v - fraction of volatiles not yet released

One serious problem with this method is that it requires an estimate of the ultimate yield, which however is a function of temperature and heating history and is not known until the devolatilization is complete. An alternative method of predicting the particle diameter would therefore be desirable, but no other expression has been devised as yet.

The density of the particle is linked with the changing particle diameter by the following equation:

$$\rho = \rho_0(1 - MAFR \cdot V) \cdot \frac{d_p^3}{d^3} \quad (4.24)$$

where

- d_p - initial particle diameter
- d - current particle diameter

Calculations in appendix B show that if the particle diameter increases, the heat transfer by convection increases as d/d_p , while the heat transfer by radiation could increase as $(d/d_p)^2$. Although Kobayashi [1] did not record the diameter of the devolatilizing coal particles during the devolatilization experiments, additional experiments were conducted in which the changing diameter of the coal undergoing pyrolysis was recorded. The determination of the particle temperature at the point of the last observation at which there is minimal particle size change indicates that the particle is essentially heated up to furnace temperature before any significant particle size change occurs, thereby minimizing any change in heat transfer due to particle size. The effect of particle size on particle motion is also checked in appendix B, which indicates that there is no significant change in velocity associated with the increased size of the particle. Because of this, and because of the problems associated with modelling the swelling of the particles, only the constant particle diameter equation has been incorporated into the computer program in the present work. Although the particles in this study reached furnace temperature before significant swelling occurred, this might not be true for other furnaces and the change in heat transfer rates could seriously effect the accuracy of the particle heating program and therefore this problem should be investigated and a more acceptable equation to describe changing particle diameter should be developed.

Table 3: Kobayashi Furnace Dimensions

	size, inches
burner	.047 ID 3/16 OD
reactor tube	2 ID

Chapter 5

Fitting Routine

A part of the object of this study is devising a procedure for fitting devolatilization reaction constants to experimental data. This chapter describes a trial fitting procedure, which in the following chapter will be applied to the data of Kobayashi [1] to test its utility. Future work with this procedure may result in further modifications; in particular, experience may allow for elimination of some of the steps used to get initial estimates of the parameters.

The two reaction model:

$$V = \int_0^t (\alpha_1 k_1 + \alpha_2 k_2) c dt \quad (5.1)$$

where

$$c = \exp \int_0^t -(k_1 + k_2) dt$$

is to be fitted to the experimental data with the following parameters to be estimated for each of the reactions:

- α_i - the ultimate yield
- k_{oi} - the pre-exponential constant in the Arrhenius rate expression

- E_i - the activation energy of each reaction path

A two part procedure was required for fitting. The model is intrinsically nonlinear and therefore a non-linear regression routine is required. However, as the convergence of the non-linear routine to a solution proved to be greatly dependent upon the quality of the initial estimates, an approximate model using isothermal devolatilization and linear regression was first used to get initial estimates. The first part therefore assumed that devolatilization occurred isothermally, while the second part incorporated the full heating history of the particle and therefore involved non-isothermal devolatilization. Each part of the analysis had several steps which will be listed in full.

5.1 Isothermal fitting procedure

The isothermal analysis was performed by assuming the particle temperature was constant and equal to that of the furnace. The heating histories of the particles were examined and any data obtained at a temperature deviating from the furnace temperature by more than about twenty percent were omitted from this section of the analysis. The isothermal fitting of the data was performed using SAS [52], which is an acronym for Statistical Analysis System. The first SAS procedure used is the REG procedure which is used to fit least squares estimates to linear regression models. Least squares estimates of the parameters of non-linear models are produced using the SAS procedure called NLIN. Non-linear models are more difficult to specify and estimate than linear models, for linear models require simply the independent and dependent variables to be listed, while for non-linear models one must write the regression expression, guess starting values and specify derivatives of the model with respect to the parameters.

The isothermal fitting procedure is broken down into several steps to produce initial estimates for the non-isothermal fitting procedure. In the first step, the single first order

reaction model

$$V = \alpha_1(1 - \exp(-kt)) \quad (5.2)$$

$$k = k_o \exp E/RT$$

with the parameters α_1 , the ultimate yield at temperature T , and k , the reaction rate constant, for all of the temperature runs was fitted to the isothermal weight loss data using NLIN. The process of selecting starting values for the parameter estimates that are required by NLIN is simplified since α , the ultimate yield, can only logically vary between 0 and 1.

The second stage of the isothermal fitting routine is to produce initial estimates of the pre-exponential constants and activation energies of each reaction. With estimates of k at several different temperature levels, the Arrhenius equation is linearized to the form

$$\ln k = \ln k_o - E/RT \quad (5.3)$$

This linearized equation is fitted to the data with the SAS linear regression procedure called REG by fitting $\ln k$ versus $1/T$. In the use of least squares, one of the assumptions made about the pure error of the data is that its variance is constant over the region of the operating variables used to collect the data. The logarithmic transformation used to convert the rate expression from a non-linear to a linear expression can lead to a violation of this assumption. Therefore, this procedure is used to get initial estimates of k_o and E from the slope and intercept of the fitted line, which are then to be used in the non-linear fitting routine. This leads to the third step of the isothermal fitting routine in which the reaction rate constants, k_o and E , are fitted non-linearly

$$k = k_o \exp E/RT \quad (5.4)$$

with the linear estimates input as the required initial estimates. The last step in the isothermal fitting is fitting

$$V = \alpha(1 - \exp(-k_o \exp(-E/RT)t)) \quad (5.5)$$

non-linearly using the isothermal data. The value of α was set to the least squares estimate found during the first step of the fitting routine. This step is important, for the parameter estimates determined in this step are not dependent on the values of k produced in step one as the parameter estimates found in the previous two steps are. The results of the non-linear fitting of the rate constant parameters are used as initial estimates of the parameters for the non-isothermal fitting routine. Although not all the values of the parameter estimates from this step are required as initial estimates of the parameters in the non-isothermal procedure, they are all included to verify that this procedure converges to a single solution regardless of the initial starting values.

5.2 Non-isothermal fitting procedure

The second part of the fitting procedure incorporates the full heating history of a particle at a given furnace temperature. The full heating history of the particle is important to the devolatilization process, since the longer the heat-up time is the greater the effect the first reaction has on the pyrolysis of a particle heated to elevated temperatures. The fitting routine used in this procedure is an IMSL routine [53] called ZXSSQ. IMSL is a system of Fortran subroutines for mathematics and statistics, in which ZXSSQ is a derivative-free routine that finds the local minimum of the sum of squares of non-linear equations. One of the major advantages to ZXSSQ is that it eliminates the need for explicit derivatives. This is a very important consideration since the full model:

$$V = \int_0^t (\alpha_1 k_1 + \alpha_2 k_2) \exp\left(\int_0^t -(k_1 + k_2) dt\right) dt \quad (5.6)$$

cannot be easily integrated analytically. As the pyrolysis is non-isothermal, the temperature change with time must be incorporated into the integral. An examination of a typical temperature-time profile, figure 14, shows that the best function to describe its behavior is an exponential function as used by Badzioch and Hawksley [15]. However the first integration results in exponential integrals which in turn need to be integrated. These problems

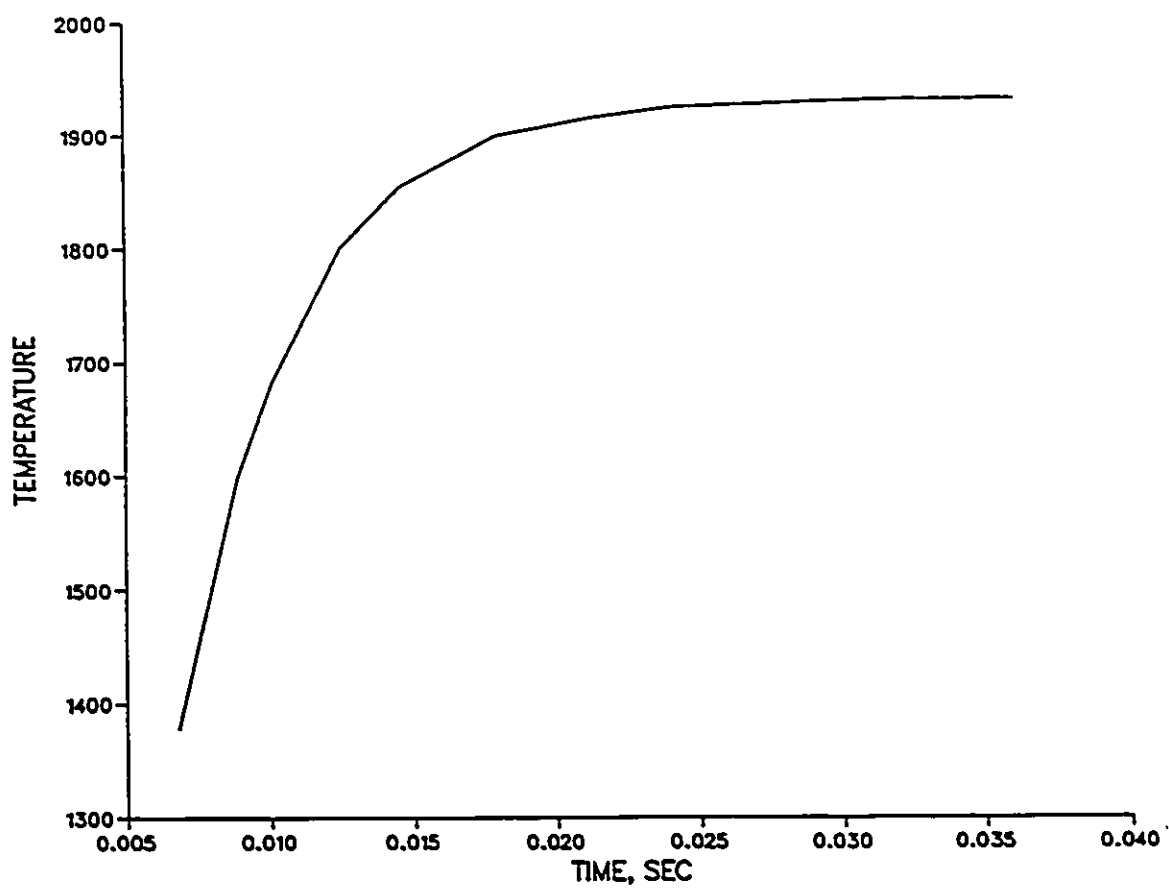


Figure 14: Typical Temperature-time History of a Coal Particle in a Laminar Flow Furnace